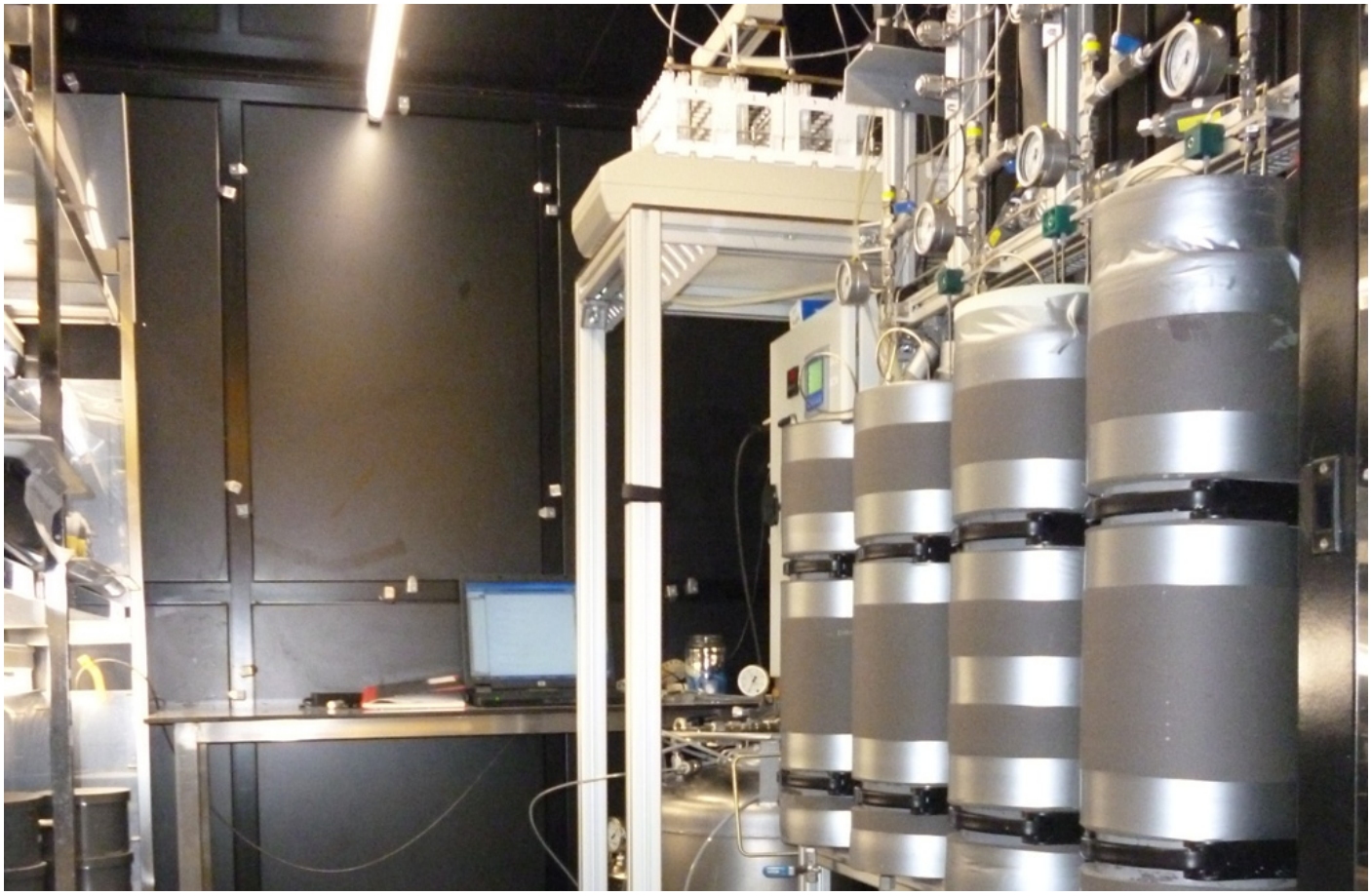

Hydrochemical changes in aquifer thermal energy storage systems investigated with anoxic column experiments

January 2013
BTO 2013.002

KWR Watercycle Research Institute

BTO

KWR Watercycle Research Institute

Hydrochemical changes in aquifer thermal energy storage systems investigated with anoxic column experiments

January 2013
BTO 2013.002

© 2013 KWR
All rights reserved. No part of this book may be reproduced, stored in a database or retrieval system, or published, in any form or in any way, electronically, mechanically, by print, photoprint, microfilm or any other means without prior written permission from the publisher.

Postbus 1072 3430 BB Nieuwegein The Netherlands P +31 30 606 95 11 F +31 30 606 11 65E info@kwrwater.nl

Colofon

Title
Hydrochemical changes in aquifer thermal energy storage systems investigated with anoxic column experiments

Project number
B111680

Research programme
BTO Source risk management

Project manager
Dr. G. v.d. Berg

Client
CvO

Quality Assurance
Prof. dr. Pieter. J. Stuyfzand[1,2], dr. Boris van Breukelen[2], dr. Paul van der Wielen[1] (chapter 5.3.5)

Author
Matthijs Bonte Msc[1]

[1] KWR Watercycle Research Institute
[2] VU University Amsterdam

Sent to
This report has been distributed among BTO-participants and is publicly available.

Voorwoord

Dit rapport is het resultaat van circa twee jaar werk waarbij een anoxische kolomproefinstallatie is gebouwd en gebruikt voor de experimenten. Dit bleek een uitdagende klus en een groot aantal mensen is hierbij betrokken geweest. De volgende collega's en stagiaires wil ik bedanken voor hun inzet tijdens de bouw van de opstelling en uitvoeren van experimenten: Julia Claas en Valentina Chacon, beide afstudeerders van de VU, voor hulp bij de experimenten. Rob Stoevelaar, Harry van Weegen en Sidney Meijerink (VU en KWR werkplaatsen) voor het geweldige werk dat zij geleverd hebben om de installatie te bouwen. John Visser (VU Lab) en Rudo Verweij (VU, voor het mogen gebruiken van een klimaatkamer).

Matthijs Bonte

Samenvatting

Achtergrond
De toepassing van warmte-/koudeopslag (WKO) groeit de laatste jaren sterk. WKO systemen zijn tegenwoordig een standaard onderdeel bij realisatie van kantoren en toepassing in woningbouw begint ook toe te nemen. De systemen worden soms geplaatst in dezelfde watervoerende lagen waaruit grondwater wordt onttrokken voor de productie van drinkwater. De drinkwatersector maakt zich om deze reden zorgen over de mogelijke gevolgen van WKO op de kwaliteit van haar grondstof. Om deze reden is binnen het bedrijfstakonderzoek (BTO) in 2009 een onderzoek gestart naar de effecten van WKO. Het BTO onderzoek is gestart met een inventarisatie van de mogelijke risico's van WKO systemen voor drinkwaterproductie (BTO 2009.030(s) "Hoe combineren we drinkwater met bodemenergiesystemen") en de evaluatie van de waterkwaliteitmonitoringsdata van een WKO systeem in Eindhoven (BTO 2009.045(s) Evaluation of the monitoring data of the aquifer thermal energy storage system at High Tech Campus Eindhoven).

De resultaten van het laatstgenoemde rapport laten zien dat de grondwaterkwaliteit wordt beïnvloed door opmenging van grondwater afkomstig van verschillende dieptes met een verschil in waterkwaliteit. Naast de monitoring in Eindhoven, is tevens het WKO systeem van het RIVM in Bilthoven gedurende 2 jaar gemonitord en de voorlopige data laten zien dat hieruit hetzelfde beeld volgt. Wat tevens bij deze twee locaties opviel was dat het thermische effect ter plaatse van monitoringsbuizen zeer gering was (grootteorde enkele graden), wat het lastig maakt om uitspraken te doen over de waterkwaliteitsinvloed van WKO over het gehele thans toegestane temperatuurbereik tot 25°C. Om deze redenen is besloten om het veldwerk uit te breiden met laboratoriumonderzoek waarbij sedimenten met grondwater worden doorspoeld onder verschillende temperaturen en verblijftijden. De sedimenten zijn afkomstig van dezelfde geologische formaties als waar de putten van de onderzochte WKO systemen in zijn afgesteld zodat een vergelijking met velddata mogelijk is.

Het doel van kolomproeven is het in beeld brengen van de veranderingen in waterkwaliteit en geochemie die sec het gevolg zijn van een temperatuursvariatie in het watervoerende pakket.

Methode
Figuur S-1 laat de kolomproevenopstelling zien die gebouwd is voor de experimenten. Het influent wordt bewaard in een RVS drukvat dat onder een N_2/CO_2 atmosfeer staat. Het influent is grondwater bemonsterd uit een peilbuis afgesteld in een boorgat waar ook sedimenten voor de proef zijn verzameld. Het influent wordt gefiltreerd over een 0,5 µm filter en met vier pompjes door de sedimentkernen geperst. De sedimentkernen worden op een temperatuur gehouden van 5°C (koude bel), 11°C (referentie), 25°C (maximum toelaatbaar voor een warme bel) en 60°C (hoge temperatuur opslag alleen in pilotsetting toegestaan). Het effluent van de vier kernen wordt wederom gefiltreerd over 0,5 µm en middels een fractieverzamelaar worden monsters op vooraf geprogrammeerde tijdstippen genomen. De proeven zijn uitgevoerd op drie sedimentmonsters, allen afkomstig van de Sterksel formatie. Drie soorten proeven zijn uitgevoerd:

- Met een verblijftijd van één dag waarbij het sediment 25 keer is doorspoeld (sedimenten A,B&C)
- Een proef waarbij de verblijftijd stapsgewijs toenam van 1 tot 35 dagen (sedimenten B&C)
- Een proef met een verblijftijd van 5 dagen en één doorspoeling waarbij de temperatuur met stapjes van vijf graden is gevarieerd (sediment C).

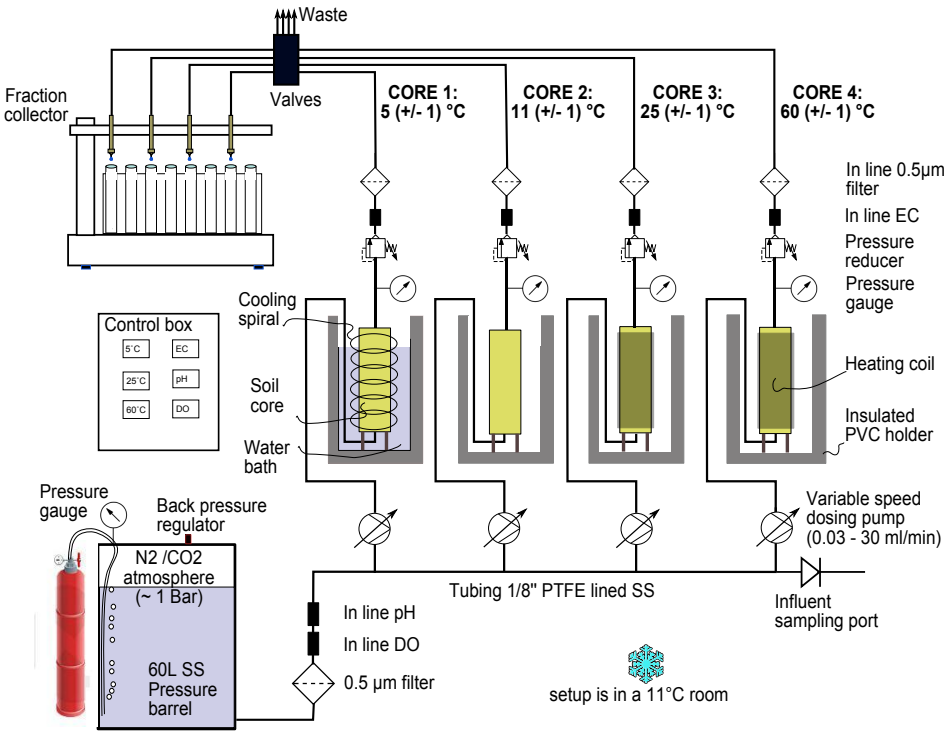

Figuur S-1: Schematische weergave kolomproefopstelling

Resultaten kolomproeven met 1 dag verblijftijd

Een selectie van resultaten van de laboratoriumexperimenten voor sediment C is weergegeven in figuur S-2. Hierin is te zien dat bij 5 en 25°C weinig verschillen in waterkwaliteit worden waargenomen ten opzichte van de referentie (11°C). Een uitzondering is het gedrag bij arseen, dat bij 25°C een toename van onder de detectielimiet (d.l. = ca. 1µg/l voor As) tot circa 15 µg/l liet zien in sediment B en circa 40 µg/l bij sediment C (de drinkwaternorm is 10µg/l). Ook bij sediment A was een relatie zichtbaar met temperatuur, maar lagen de concentraties in absolute zin dicht bij de detectiegrens. Bij 60°C is te zien dat de arseenconcentratie verder oploopt terwijl bij 5°C juist de laagste arseenconcentraties worden gemeten.

De toename van As is vermoedelijk een gevolg van desorptie van arseen van ijzeroxiden. Uit laboratoriumonderzoek beschreven in de literatuur aan pure vaste fase ijzeroxiden blijkt de evenwichtsreactie tussen vrij en gebonden arseen temperatuurafhankelijk [1]: Arseen wordt met toenemende temperatuur minder preferent gebonden dan andere metalen. Het voorkomen van ijzeroxiden wordt bevestigd geochemische analyses en door de geologische beschrijving door TNO van deze formatie. Andere stoffen die sterk binden aan ijzeroxiden zijn boor en kiezelzuur, en ook voor deze stoffen is een temperatuurafhankelijkheid te zien in het uitlooggedrag. De sterke positieve correlatie tussen kiezelzuur en kalium wijst er echter op dat oplossen van silicaten(K-veldspaat) ook plaatsvindt.

Bij sedimenten A en C wijzen de toenemende alkaliniteit en Ca concentratie op het oplossen van calciet. Bij sediment B is dit alleen bij 5°C en is er bij 11 en 25°C geen duidelijke verandering in Ca en alkaliniteit waarneembaar. Bij 60°C is in sediment B een afname zichtbaar in alkaliniteit en Ca wat op neerslag van calciet wijst. Dit is opvallend omdat het influent water onderverzadigd is ten opzichte van calciet, zowel bij 11 als 60°C. Mogelijk slaat een ijzer carbonaat, zoals sideriet of ankeriet neer. Voor deze mineralen wordt bij 60°C door het hoge Fe gehalte wel een oververzadiging berekend. Aanvullende aanwijzingen hiervoor zijn: 1) Uit XRD analyses blijkt dat ankeriet in het oorspronkelijke sediment aanwezig is, waardoor het als entmateriaal kan dienen, 2) bij lage temperaturen is neerslag van sideriet vaak erg traag, veel trager dan calciet, maar bij hogere temperaturen wordt neerslag van ijzercarbonaten juist sneller dan pure calciet [2], en 3) bij eerdere kolomproeven in de jaren 90 gefocust op kalkneerslag bij WKO werd gevonden dat mineraalneerslag zich beperkte tot ijzer-mangaan-fosfaat carbonaten en dat de neerslag vrijwel stopte zodra al het Fe was neergeslagen [3].

Bij 60°C wijzen de verhoogde dissolved organic carbon (DOC) gehaltes erop dat sedimentair organisch materiaal (SOM) versneld wordt afgebroken en desorbeert van ijzeroxiden. Bij 25°C is de gemiddelde effluent concentratie in de drie experimenten licht verhoogd ten opzichte van de influent concentratie, maar het verschil is statistisch niet significant.

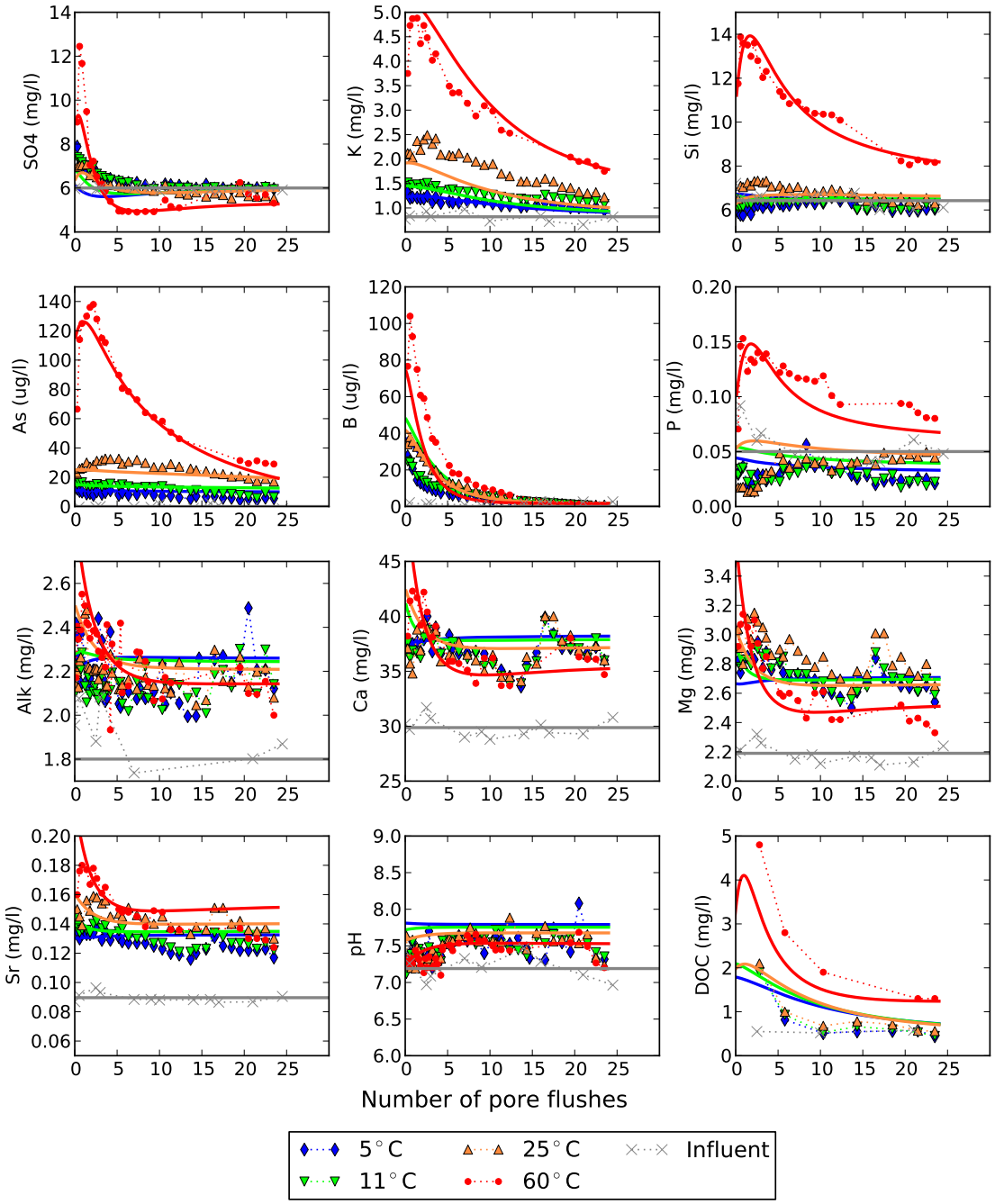

Figuur S-2: Effluent data en modelsimulaties voor een selectie van waterkwaliteitsparameters bij 1 dag verblijftijd en toenemend aantal doorspoelingen. De punten geven de waarnemingen weer, de lijnen geven modelberekeningen weer met het hydrochemische model PHREEQC.

Modellering met PHREEQC

De kolomproef met sediment C is gemodelleerd met het hydrochemische model PHREEQC [4] om te controleren of de waargenomen waterkwaliteitsveranderingen door de genoemde processen kunnen zijn veroorzaakt. Om het model te ijken zijn parameters gevarieerd waarvoor geen (literatuur)waarden bekend of waarvoor de bandbreedte in literatuur groot is. Het ijken van het model is uitgevoerd door PHREEQC te koppelen aan het parameterschattingsprogramma PEST [5]. De volgende processen zijn meegnomen in het model:

- Evenwicht met een carbonaat solid solution bestaande uit calciet, dolomiet en strontianiet. Hiermee worden de verhoogde concentraties van Ca, Mg, Sr de alkaliniteit en pH gemodelleerd. De fracties calciet, dolomiet en strontianiet zijn gevarieerd om het model te ijken.

- Kinetische oplossing van K-veldspaat om de verhoogde concentraties K en Si bij 25°C en 60°C te verklaren. Om het model te ijken is het reactieve mineraaloppervlak gevarieerd.
- Kinetische sulfaatreductie is gesimuleerd om de verlaagde concentraties SO_4 bij 60°C te verklaren. Om het model te ijken is de reactiesnelheid en de activeringsenergie gevarieerd.
- Cation uitwisseling waarmee de uitwisseling van Ca, Mg, K, Fe, NH_4 en Sr met kleideeltjes en organisch materiaal is gesimuleerd. De reactie-enthalpiën van de cationreacties zijn gevarieerd om het model te ijken.
- *Surface complexation* is gebruikt om desorptie van As, B, Mo, DOC en P van ijzer oxiden te simuleren. Om het model te ijken zijn de evenwichtsconstanten en reactie-enthalpiën en het aantal sorptieplaatsen gevarieerd.

De gesimuleerde effluentconcentraties zijn weergegeven in figuur S-2. De fit tussen gemeten en gesimuleerde concentraties is redelijk te noemen. Voor stoffen waarvoor grote verschillen bij de verschillende temperaturen zijn gemeten, zijn deze redelijk goed te verklaren met bovengenoemde processen. Naast het schatten van parameters, is PEST ook gebruikt om de 95% betrouwbaarheidsinterval van parameters in te bepalen en de correlatie tussen verschillende ijkparameters. Hieruit komt naar voren dat een aantal parameters sterk aan elkaar is gecorreleerd en daardoor een groot betrouwbaarheidsinterval heeft. Voorbeelden zijn de parameters van de individuele cation uitwisselingsreacties en enkele parameters voor de gemodelleerde *surface complexation* (bijvoorbeeld Mo, DOC en Si). Voor desorptie van arseen en boor zijn reactie-enthalpieën bepaald van respectievelijk -40±12.5kJ/mol en -19.2±13.1kJ/mol.

Resultaten kolomproeven met toenemende verblijftijd

Figuur S-3 toont een selectie van de resultaten van de analyses bij toenemende verblijftijden. Te zien is dat DOC in de warmste kolom verder oploopt maar in de overige kolommen nagenoeg constant blijft. Uitzondering is de 25°C kolom in experiment C waarbij ook een lichte toename in DOC waargenomen wordt. Verder is te zien dat bij vrijwel alle kolommen sulfaatgehalten met toenemende verblijftijd teruglopen: dit duidt op sulfaatreductie. De sulfaatreductiesnelheid neemt toe met toenemende temperatuur. Bij 5 en 11°C is het proces in experiment B zeer langzaam, terwijl bij experiment C wel een duidelijke teruggang in sulfaatgehalten te zien is.

Het sedimentair organisch stof (SOM) wordt bij door enzymen in oplossing (hydrolyse) waarna het door micro-organismen wordt gebruikt als koolstofbron. De accumulatie van DOC bij 60°C wijst erop dat de tweede stap bij hogere temperaturen maatgevend is terwijl bij 25°C de tweede stap maatgevend is. Dit wordt in de literatuur ook beschreven voor temperatuurafhankelijkheid van sulfaatreductie in mariene sedimenten [1-3]. Het verschil in sulfaatreductie en DOC productie tussen experiment B en C is waarschijnlijk een gevolg van de afbreekbaarheid van het SOM. Bij experiment C is dit blijkbaar beter afbreekbaar. Het optreden van de versnelde sulfaatreductie en het daaraan gekoppelde verbruik van SOM is een belangrijke waarneming in relatie tot drinkwater. SOM is belangrijk omdat organische verontreinigingen hier sterk aan binden en het dus een bijdrage levert aan het reinigend vermogen van de ondergrond.

Daarnaast kan een accumulatie van DOC tot verkleuring van het grondwater leiden (wat ook zichtbaar was) en kan complexen vormen met vrijgemaakte zware metalen waardoor deze in oplossing blijven.

Fe^{2+} neemt in de 5 en 11°C kolommen bij experiment B toe wat op reductie van ijzer(hydr)oxiden duidt. Bij sediment C is geen toename in Fe^{2+} te zien, wat kan betekenen dat ijzer reductie hier niet plaatsvindt, of dat het wel plaatsvindt maar dat het gevormde Fe^{2+} reageert met sulfiden gevormd tijdens sulfaatreductie en neerslaat als pyriet. Pyriet kan mogelijk arseen vastleggen, maar hier is in de data geen duidelijk beeld over naar voren gekomen.

Tijdens experiment C is tevens opgelost methaan gemeten in het effluent. Hieruit blijkt dat alleen bij 25°C methanogene redoxcondities ontstaan. Het is opvallend dat bij 60°C blijkbaar wel versnelde sulfaatreductie plaatsvindt maar geen methaanvorming.

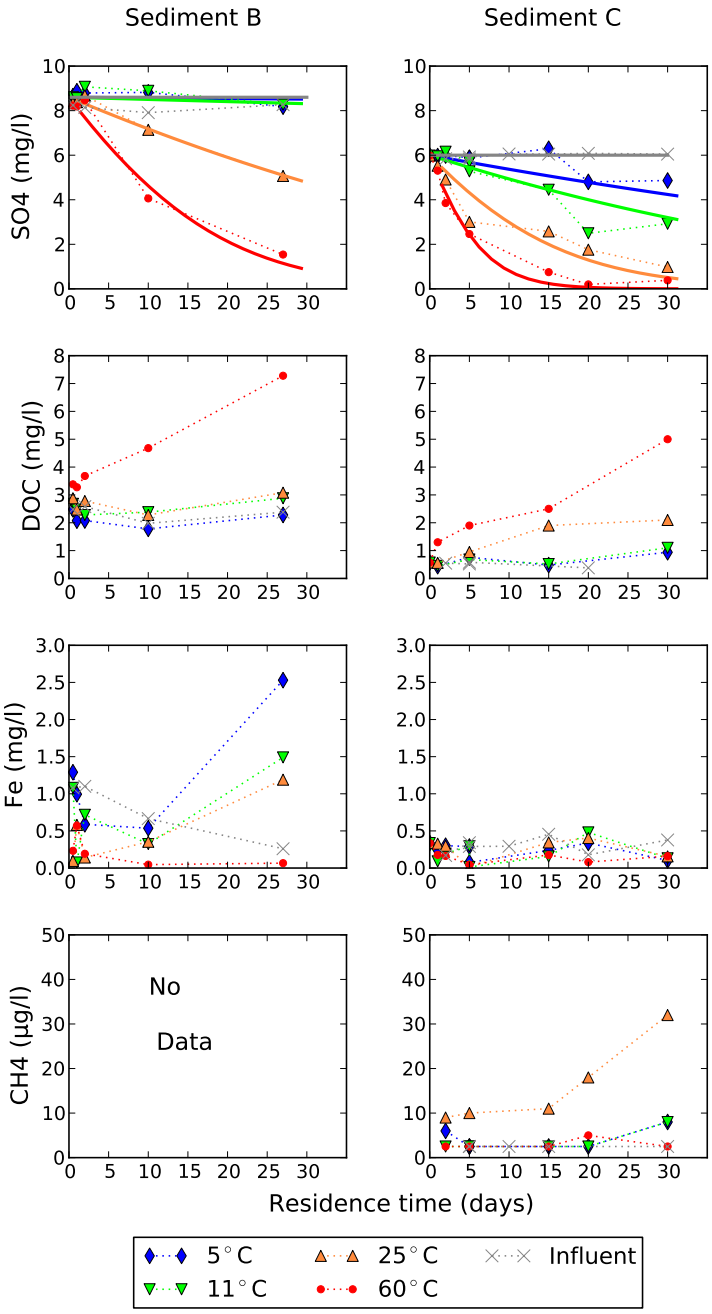

Figuur S-3: Analyseresultaten met toenemende verblijftijd. De punten en gestippelde lijnen geven de meetdata weer, voor SO4 zijn tevens de resultaten weergegeven van SO4 concentraties op basis van een Monod sulfaatreductie model (gesimuleerd met PHREEQC/PEST).

Resultaten getrapte temperatuurproeven

Figuur S-4 tonen de resultaten van de proeven waarbij de temperatuur met stappen van 5 °C is verhoogd tussen 5°C en 80°C. De resultaten laten zien dat twee minima in sulfaatconcentratie worden waargenomen: nabij 40°C en 70°C, wat duidt op maxima in sulfaatreductiesnelheid. De data duiden op het opkomen van een thermofiele sulfaatreducerende microbiologische populatie, iets wat eerder is beschreven voor arctische mariene sedimenten [6, 7] maar nog niet voor sedimenten uit watervoerende pakketten. Op basis van de temperatuursafhankelijkheid van sulfaatreductie (zowel figuur S-3 als S-4) wordt een activeringsenergie gevonden van 44 tot 134 kJ/mol voor temperaturen tot 40 °C, daarboven wordt 88kJ/mol gevonden.

De DOC concentraties lopen vrijwel lineair op met toenemende temperatuur. De afwezigheid van een duidelijk optimum duidt erop dat dit bij hogere temperaturen een a-biotisch proces is. Iets wat

op basis van andere data eerder is beschreven door Brons e.a. [8]. Voor DOC mobilisatie wordt een activeringsenergie gevonden van 33 kJ/mol. Het is verder opvallend dat bij temperaturen tot 40°C wel productie van methaan wordt waargenomen, maar in het warmere bereik niet. Een mogelijke verklaring is dat sulfaatreduceerders sporen kunnen vormen en zo in sluimerende toestand wel aanwezig kunnen zijn, maar methaanproducerende archaea hebben deze capaciteit niet.

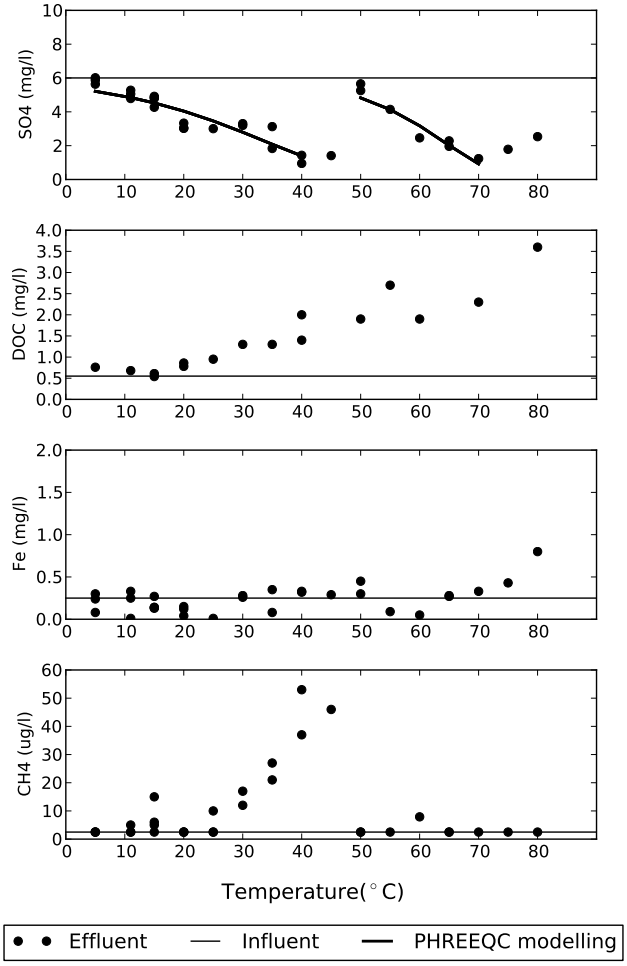

Figure S-4 Waarnemingen van sulfaat, DOC, Fe en methaan tijdens de getrapte temperatuurproef.

Microbiologische waarnemingen

Naast de chemische analyses, zijn ook microbiologische analyses uitgevoerd tijdens de proeven met sedimenten B en C om te bekijken in hoeverre de microbiologische populatie wijzigt. Hierbij is de microbiologische populatie in beeld gebracht met T-RFLP analyse op zowel in- als effluent water, en het zand uit de kolom (Figuur S-5). Analyse op effluent is uitgevoerd bij een verblijftijd van het water in de kolom van 15 dagen en 40 dagen. Analyse op zand is uitgevoerd na een totale incubatietijd van circa 3 maanden (onder verschillende waterverblijftijden). Figuur S-5 toont de resultaten van deze analyses als bandenpatronen en een dendrogram die de gelijkenis tussen verschillende monsters inzichtelijk maakt. De resultaten laten zien dat de bacteriële populatie bij 60°C bij sediment B sterk afwijkt van de bacteriële populaties bij de overige temperaturen. De bacteriële populaties bij de overige temperaturen lijken op elkaar, maar er is mogelijk wel een tendens van koud naar warm in de samenstelling van de bacteriepopulaties. Bij sediment C wordt geen duidelijke unieke temperatuurcluster waargenomen, terwijl dit voor 60°C wel te verwachten is. Mogelijk komt dit doordat bij sediment C een hogere dispersie in de kolom aanwezig is, waardoor bemonsterd effluent onvoldoende incubatietijd heeft ondergaan en de samenstelling van de bacteriepopulatie veel gelijkenis heeft met de samenstelling van de bacteriepopulatie in het influent.

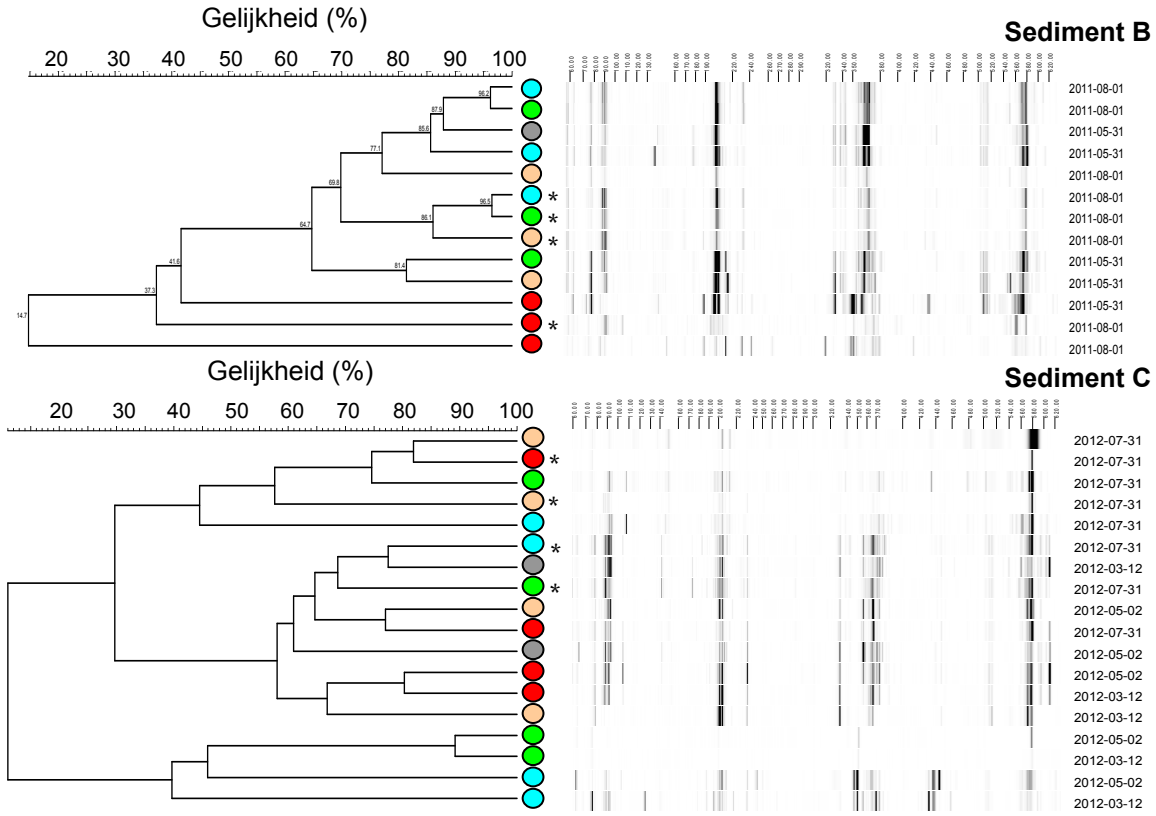

Figuur S-5 Resultaten TRFLP fingerprinting. De bolletjes voor de labels geven de verschillende temperaturen weer : ● *Influent (11°C);* ● *: 5°C kolom;* ● *11°C kolom;* ● *25°C kolom;* ● *60°C kolom. Analyses zijn uitgevoerd op water en sediment (laatste aangegeven met *).*

Conclusie

De resultaten van de kolomexperimenten laten zien dat bij afkoeling van grondwater van 11°C naar 5°C geen effecten op waterkwaliteit worden gemeten. Bij opwarming van 11°C naar 25°C wordt een verhoogde mobiliteit van arseen waargenomen en neemt de snelheid waarmee sulfaatreductie in sedimenten plaatsvindt toe. Bij nog hogere temperaturen (60°C) worden verhoogde concentraties DOC uitgespoeld, dit laatste kan tot verkleuring van water leiden, en worden verhoogde concentraties P, K, Si, As, Mo, V en F gemeten. Bij 60°C wordt tevens een sterke verandering in de samenstelling van de microbiologische populatie waargenomen. De achterliggende chemische processen zijn vermoedelijk desorptie van ijzeroxiden (As, P, K, Si, Mo, DOC en V), oplossen van K-veldspaat (Si, K, Li) en afbraak van sedimentair organisch materiaal (DOC en P).

De mobiliteit van arseen is een punt dat aandacht vereist. Maar of dit onder veldomstandigheden tot problemen kan leiden hangt van een aantal zaken af. Ten eerste hoeveel arseen er van nature in het sediment aanwezig is en in welke vorm: alleen arseen dat aan reactieve oppervlakken is gesorbeerd (met name ijzeroxiden) mobiliseert bij een temperatuurverhoging. Vermoedelijk zal arseen dat is opgenomen in de kristalstructuur van mineralen (bijvoorbeeld pyriet) niet vrijkomen. Ten tweede hangt het af van de temperatuurdynamiek van het WKO systeem. Maar weinig WKO systemen werken op de maximaal toelaatbare temperatuur. Daarnaast is sorptie een reversibel proces en is te verwachten dat bij afkoeling arseen weer kan resorberen.

Referenties

1. Kersten, M. and N. Vlasova, *Arsenite adsorption on goethite at elevated temperatures.* Applied Geochemistry, 2009. **24**(1): p. 32-43.
2. Johnson, M.L., *Ferrous carbonate precipitation kinetics: A temperature ramped approach*, 1991, Rice University: Houston. p. 139.

3. Griffioen, J. and C.A.J. Appelo, *Nature and extent of carbonate precipitation during aquifer thermal energy storage.* Applied Geochemistry, 1993. **8**(2): p. 161-176.
4. Parkhurst, D.L. and C.A.J. Appelo, *User's guide to PHREEQC (version 2)--A computer program for speciation, batch-reaction, one-dimensional transport, and inverse geochemical calculations*, 1999, U.S. Geological Survey p. 312 p.
5. Doherty, J., *PEST, Model-Independent Parameter Estimation. User Manual: 5th Edition*, 2010. p. 336.
6. Isaksen, M. F.; Bak, F.; Jørgensen, B. B., Thermophilic sulfate-reducing bacteria in cold marine sediment. FEMS Microbiol. Ecol. 1994, 14, (1), 1-8.
7. Hubert, C.; Arnosti, C.; Bruchert, V.; Loy, A.; Vandieken, V.; Jorgensen, B. B., Thermophilic anaerobes in Arctic marine sediments induced to mineralize complex organic matter at high temperature. Environmental Microbiology 2010, 12, (4), 1089-1104.
8. Brons, H. J.; Griffioen, J.; Appelo, C. A. J.; Zehnder, A. J. B., (Bio)geochemical reactions in aquifer material from a thermal energy storage site. Water Research 1991, 25, (6), 729-736.

Contents

Voorwoord **1**

Samenvatting **3**

Contents **11**

1 Introduction **13**

2 Materials and methods **15**

2.1 Sediments collection,characterisation, and geochemical analyses 15

2.2 Influent water collection and characterisation 18

2.3 Experimental setup 19

2.4 Hydrochemical analyses 21

2.5 Data analysis 21

3 Experiments with 1-day residence time **23**

3.1 General patterns and results 23

3.2 Dissolution and precipitation of carbonates 25

3.3 Dissolution of silicates 27

3.4 Interaction with sedimentary organic matter (SOM) 31

3.5 Mobilisation of arsenic and other trace compounds 31

3.6 Operational and environmental implications for ATES systems 37

4 Hydrochemical modelling of 1 day residence time experiments **39**

4.1 Hydrochemical model description 39

4.2 Results and discussion 45

5 Prolongued incubation time experiments **51**

5.1 Introduction and objective 51

5.2 Redox geochemistry, Monod kinetics and temperature dependance 51

5.3 Results and discussion 53
5.3.1 Experiments with increasing residence time 53
5.3.2 Experiments with temperature ramping 55
5.3.3 Rates and activation energies for sulfate reduction 57
5.3.4 Activation energy of organic carbon mobilisation 59
5.3.5 Changes in microbiological population and activity 60

5.4 Conclusions 62

6 Conclusions **63**

7 References **65**

© KWR

I	**Bore logs for Helvoit and Scherpenzeel and detailed geochemical results**	**73**
II	**Photo impression of experimental setup**	**83**
III	**Analyses of the breakthrough curves**	**87**
IV	**Chemical analyses in- and effluent – TABLES**	**89**
V	**Chemical analyses in- and effluent – GRAPHS**	**107**
VI	**Statistical analyses**	**121**
VII	**Detailed description of carbonate solid solution precipitation**	**125**

1 Introduction

Shallow geothermal systems including aquifer thermal energy storage (ATES) or open loop ground source heat pumps use groundwater to store or harvest energy for heating or cooling purposes. Worldwide interest for these systems is rapidly increasing in response to the growing demand for a more sustainable way of acclimatizing the built environment. Over the last decade, the number of ATES systems in the Netherlands has grown rapidly: from around 100 in the year 2000 to more than 1000 in 2010. Also in other regions around the world, use of aquifers for heating and cooling purposes is growing. Examples include China [4], Korea [5], the United States [6] and other European countries like Germany, Switzerland, Austria, Sweden, Denmark, Norway, France [7].

In the Netherlands, most shallow geothermal systems operate at a relatively small temperature ranging to several degrees above and below the natural groundwater temperature. The maximum allowable injection temperature is set in provincial regulations and ranges between 25 and 30 °C [8]. Interest for medium and high temperature shallow geothermal systems, between 40 to 80°C is growing and societal pressure is increasing to allow those operations as well. Operating at a higher temperature level makes ATES systems suitable for storage of industrial waste heat, which can increase the viability of waste heat re-use projects.

Shallow geothermal systems in the Netherlands operate in the same aquifers used for the production of drinking water. And the rapid growth has led to an increasing number of sites where shallow geothermal systems are planned or built near or even within the groundwater protection zones of groundwater pumping stations used for public water supply. This leads to questions by regulators regarding the risks of ATES on water quality in aquifers used for public water supply, in the Netherlands and abroad [9, 10].

Most published research on ATES systems, however, focuses on operational aspects, such as their scaling in relation to mineral precipitation occurring in high temperature systems (>40°C), and is based on either laboratory experiments [11], chemical equilibrium modeling [12], or a combination of both [13]. Also, a number of papers published in the 80s and 90s describe pilot tests of ATES systems [14-16]. The results of these studies show, for example, that precipitation of iron-carbonates can form a problem for ATES depending on aquifer geochemistry. Brons et al. [17] found mobilization of sedimentary organic carbon with increasing temperature. In none of these studies, trace elements and heavy metals were included. Microbiological research on ATES showed that although no evidence is observed for growth of pathogens [18], or increasing cell counts [19], a considerable change in the microbiological community composition may occur [20-22].

Our previous research at an ATES site in Eindhoven (the Netherlands) at a low temperature ATES system (<25°C) located around 570 m from a public drinking water supply well field showed that the groundwater circulation by the ATES system can impact chemical groundwater quality by introducing shallow groundwater with a different chemical composition at greater depth [23]. The effect of mixing of different water qualities masks potential temperature driven water quality effects at these ATES systems. Discrimination of mixing effects from temperature driven effects is important for policy makers, regulators and ATES designers who wish to determine the maximum allowable infiltration temperature in an ATES system. Both from an environmental (effects on other groundwater users) and operational (prevention of clogging or corrosion) point of view.

In order to get a good understanding of temperature driven hydrochemical changes in aquifers used for drinking water production, we carried out anoxic column experiments at 5, 11, 25, and 60°C. This study extends the earlier mentioned studies because we analyzed a much broader suite of chemical elements, including major ions, trace metals, nutrients, and organic carbon. The results of this study provide an overview of which naturally occurring elements can be expected to be mobilized during ATES operation and provides guidelines for monitoring near shallow geothermal systems (both ATES systems and ground source heat pumps).

2 Materials and methods

2.1 Sediments collection,characterisation, and geochemical analyses

Sediments and water used in the column experiments were collected from two locations: Two samples (sediment sample A and B) were collected at Helvoirt and a third sample (sediment sample C) was collected at Scherpenzeel (Figure 2-1). The collected unconsolidated anoxic sandy sediments were taken from the same geological formation (Sterksel). This formation also accommodates many ATES systems including those in the towns of Eindhoven and Bilthoven, locations where we also performed research but reported elsewhere [23]. The formation is also widely used for drinking water production. Bore logs for the two bore holes are included in Appendix I.

The sediment samples were collected using either Ackerman cores (40 cm long, 6.7 cm diameter stainless steel (SS304)), or 1 m long, 0.1 m diameter PVC cores from boreholes drilled with the percussion drilling method. The drilling contractor was instructed to use a minimum amount of working water to avoid contamination and working water was sparged with N_2 gas before use to make it anoxic. Samples A and B were stored in a glovebox under nitrogen atmosphere to keep anoxic conditions at around 20°C. Samples A and B were stored for around 3 and 6 months, respectively, until use.Sample C was stored for 2 months at 4°C in a second PVC liner filled with water sparged with N_2 gas and spiked with an anti-oxidant ($NaHSO_3$) in order to avoid permanent gas use in the glovebox. Note that freezing of the samples was intendedly not done as this lowers the microbiological activity [24].

A combination of geochemical analyses was used to characterize the sediment (Table 2-1): 1) Major oxides were determined using $LiBO_2$ fusion followed by X-Ray fluorescence (XRF) analysis; 2) Rare earth and refractory elements were determined by inductively coupled plasma mass spectrometry (ICP-MS) following a lithium metaborate / tetraborate fusion and nitric acid digestion; 3) Grain size distribution was determined using laser grain size analyses; 4) reactive organic carbon, black carbon, and total carbonate content were assumed to equal loss on ignition at 330°C, 550°C, and 1000°C, respectively, by thermogravimetry (TGA); 4) Total sulfur by combustion followed by gas chromatography; 5) Major mineral phases by recording X-Ray powder diffraction (XRD) patterns on a subsample having a density >2.66 g/cm^3 and < 2.64 g/cm^3. The latter was done to remove quartz (density >2.66 g/cm^3), which is the dominant mineral phase, and to increase the detection limit for other mineral phases. XRD patterns were analyzed using the ICDD pdf4 database.

The measured geochemical parameters are used to calculate a number of relevant additional reactive capacity properties: pyrite content, non-pyrite reactive iron (ironoxides), and the cation exchange capacity (CEC) based on empirical relations derived for Dutch sediments (including the geological formations used here) reported in [25].

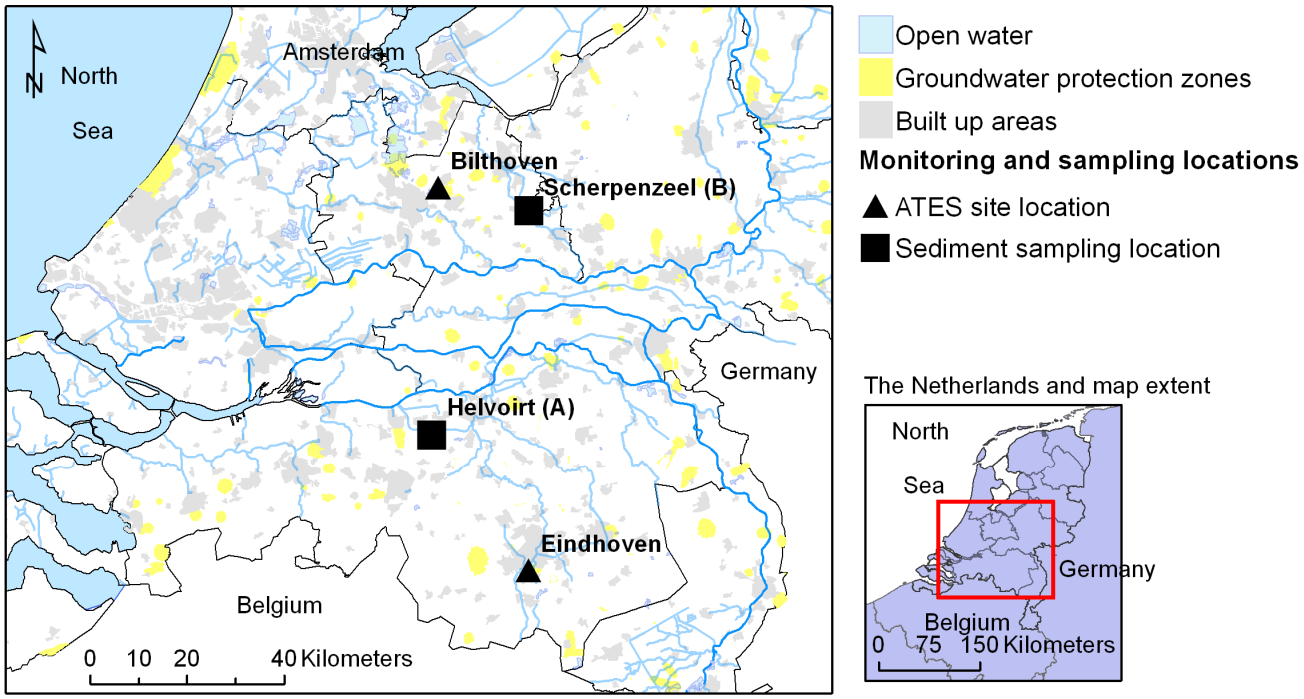

Figure 2-1 Sediment sampling locations and ATES pilot sites.

Table 2-1 Geochemical and hydraulic characteristics of sediments used in column experiments

			Sediment A	Sediment B	Sediment C
Location			Helvoirt	Helvoirt	Scherpenzeel
Sampling depth (m-surface level)			44-46	32-34	34-36
Measured parameters	**Method**	**Unit**			
Reactive organic matter (LOI330)	TGA	%d.w.	0.24	0.15	0.06
'Black carbon' (LOI550)		%d.w.	0.76	0.48	0.14
Carbonate content (LOI 1000)		%d.w.	6.00	0.54	0.74
Clay content (<8 µm)	Laser grain size analyses	%d.w.	3.76	2.21	1.34
Median grain size (d_{50})		µm	187	244	310
Uniformity coefficient (U, d_{60} /d_{10})			3.83	2.44	2.05
S	CS LECO autoanalyzer	%d.w.	0.10	0.03	0.05
Fe_2O_3	XRF	%d.w.	1.36	1.02	0.59
MnO		%d.w.	0.04	0.02	0.02
Al_2O_3		%d.w.	4.04	4.55	3.36
CaO		%d.w.	3.02	0.95	0.39
MgO		%d.w.	0.72	0.58	0.22
Cr_2O_3		%d.w.	0.037	0.028	0.001
SiO_2		%d.w.	85.4	86.0	92.5
As	$LiBO_2$ fusion followed by HNO_3 digestion and ICP-MS	ppm	5.7	2.9	3.7
Ni		ppm	11.1	12.9	7.4
Pb		ppm	32.1	21.1	3.2
Cu		ppm	11.0	8.7	2.9
Sr		ppm	93.1	63.3	43.6
Al	Oxalic acid extraction	mg.kg d.w.	n/a	90	182
Fe			n/a	457	1063
Mn			n/a	6	37
P			n/a	27	33
Si			n/a	25	99
Minerals present (qualitative)					
Quartz	XRD	Present?	Yes	Yes	Yes
Clinochlore		Present?	Yes	Yes	Yes
Muscovite		Present?	Yes	Yes	
Mica group		Present?	Yes	Yes	
Ferrian clinozoisite		Present?			Yes
Albite		Present?	Yes	Yes	Yes
Orthoclase		Present?	Yes	Yes	Yes
Dolomite		Present?	Yes	Yes	Yes
Ankerite $CaMg_{0.32}Fe_{0.68}(CO_3)_2$		Present?		Yes	
Calcite, magnesium ($Mg_{0.03}Ca_{0.97}(CO_3)$)		Present?	Yes	Yes	Yes
Calculated parameters	**Equation or method**	**Unit**			
Bulk density, ρ_b	Weight / volume	g/cm^3	1.94	1.94	2.12
Porosity, n	$n = (\rho_{bulk} - \rho_{H2O})/ (\rho_{solid} - \rho_{H2O})$		0.43	0.43	0.32
Dispersivity, λ with s.e.	CXTFIT [26]	cm	8.04(0.78)	3.43(0.83)	13.3 (0.1)
Cation exchange capacity, CEC	$CEC_{meq/kg}$=4Clay + 12.5 OM [27]	meq/kg	24.5	14.8	7.1
	$CEC_{meq/l} = \rho_b\ CEC_{meq/kg} / n$	meq/l	111	67	42
Pyrite	$0.5*S*M_{FeS2}/M_S$ [25]	%d.w.	0.19	0.06	0.09
Fe in pyrite	$0.5*S*M_{Fe}/M_S$ [25]	%d.w.	0.09	0.03	0.04
Reactive Fe (not in pyrite)	$2*M_{Fe}/M_{Fe2O3}*(Fe_2O_3-(0.225*Al_2O_3-0.91\%)) - 0.5*S*M_{Fe}/M_S$ [25]	%d.w.	0.87	0.61	0.48
Reactive Fe		%d.w.	0.87	0.61	0.48

2.2 Influent water collection and characterisation

Groundwater collected from a monitoring filter, placed in the borehole that the sediment samples were collected from, was used as influent. The depth of the filter corresponded within 5 m from the depth that the sediment was collected from. Groundwater was collected in a stainless steel 60 l pressure barrel using a submersible sampling pump at 20 m below the water table. Prior to sampling, the pressure barrel was first depressurised to 0.4 bar and then filled with pure N_2 gas to 1 bar pressure for three consecutive times. The monitoring well was purged at around 1 m^3/hour for 30 minutes prior to sampling while assuring that electrical conductivity (EC), pH, temperature and dissolved oxygen (DO) were sufficiently stable. Groundwater was filtered in-line with a 0.45 µm filter. The influent barrel was filled completely, thereby removing the complete gas filled head space with a adjustable pressure relieve valve. Collected influent was chemically characterised over the running time of the experiment using a variety of analytical techniques (refer to section 2.4). Results are summarised in Table 2-2 showing for each influent parameter the mean concentration (µ) and the standard deviation of the analyses (σ). The partial CO_2 pressure ($P_{CO2}(g)$), redox potential (pe), and charge balance were calculated with PHREEQC [28].

Table 2-2 Chemical characteristics of the influent water showing mean concentrations and standard deviations in parenthesis during the experiments

Parameter	Unit	Sediment A	Sediment B	Sediment C
pH	-	7 (0.1)	6.9 (0.2)	7.3 (0.2)
EC	µS/cm	240 (5)	227 (8)	202 (5)
Alkalinity	meq/l	1.4 (0.1)	1.3 (0.1)	2 (0.2)
$P_{CO2(g)}$	Atm	0.01	0.01	0.006
pe	-	-0.4	-1.4	-1
Charge balance	%	-2.4%	+3.3%	+0.9%
Cl	mg/l	27.8 (0.8)	27.2 (1.2)	7.1 (0.2)
SO_4	mg/l	8 (0.3)	7.8 (0.2)	6 (0.1)
NO_3	mg/l	<0.25 (n/a)	<0.25 (n/a)	<0.25 (n/a)
NH_4	mg/l	0.4 (0.1)	0.5 (0.1)	0.09 (0.01)
tot-P	µg/l	12 (7)	37 (55)	65 (20)
F	µg/l	70 (23)	57 (12)	64 (6)
DOC	mg/l	2.3 (0.07)	2.0 (0.06)	0.6 (0.03)
Na	mg/l	12.0 (0.1)	13.6 (1.2)	5.6 (0.2)
K	mg/l	1.1 (0.02)	1.8 (0.6)	0.8 (0.1)
Ca	mg/l	28.2 (2)	24.3 (2.3)	29.9 (0.8)
Mg	mg/l	2.2 (0.2)	2.1 (0.3)	2.2 (0.1)
Fe	mg/l	0.3 (0.1)	6.5 (0.3)	0.3 (0.1)
Mn	mg/l	1.5 (0.01)	0.9 (0.01)	0.1 (0.01)
Si	mg/l	10.4 (0.1)	10.4 (0.4)	5.2 (0.9)
Al	µg/l	<1 (n/a)	1 (0.5)	<1 (n/a)
As	µg/l	2 (0.2)	6 (1.7)	6 (5.8)
B	µg/l	4 (0.1)	4 (1)	1 (0.4)
Ba	µg/l	10 (2)	6 (7)	16 (9)
Cd	µg/l	8 (2)	20 (1)	24 (54)
Co	µg/l	4 (1)	4 (1)	<1 (n/a)
Cr	µg/l	50 (1)	55 (2)	15 (1)
Cu	µg/l	0.1 (0.1)	<0.1 (n/a)	0.1 (0.1)
Li	µg/l	0.5 (0.1)	1.7 (0.2)	0.4 (0.4)
Ni	µg/l	0.7 (0.4)	0.7 (3.4)	3.3 (3.7)
Zn	µg/l	5.1 (0.1)	4.4 (0.1)	53.7 (5.7)

2.3 Experimental setup

Sediment cores were unpacked in a glove box under a N_2 atmosphere, mixed thoroughly for 30 minutes using stainless steel spatulas to obtain a homogeneous sample, and repacked in four 0.4 m long stainless steel cores (polished and HNO_3 washed (pacified) steel quality SS304) with an internal diameter of 0.066 m. Repacking was carried out with 0.05 m increments. After addition of each layer, the sediment was compacted to avoid the formation of preferential flow paths [29].

The cores were then placed in the experimental set-up shown in Figure 2-2. A photo impression of the setup is presented in Appendix II. The four cores were maintained at temperatures of 5, 11 25 and 60°C. The entire setup was placed in a 11°C climate room, the 5°C core was additionally cooled with a circulation cooler and the 25 and 60 °C cores were heated with heating mats (Mechaheat custom made). Influent water was kept at a constant pressure of 1 bar by means of gently flushing the influent barrel with a mixture of 99% N_2/1% CO_2. The CO_2 partial pressure (P_{CO2}) was calculated from measured pH and Alkalinity using PHREEQC [28]. Dissolved oxygen (D.O.) and pH of the influent were continually logged with an in-line sensor (Mettler Toledo Easysense pH31 and $O_2$21). An in-line EC sensor (Mettler Toledo Cond 71) was used at each effluent stream.

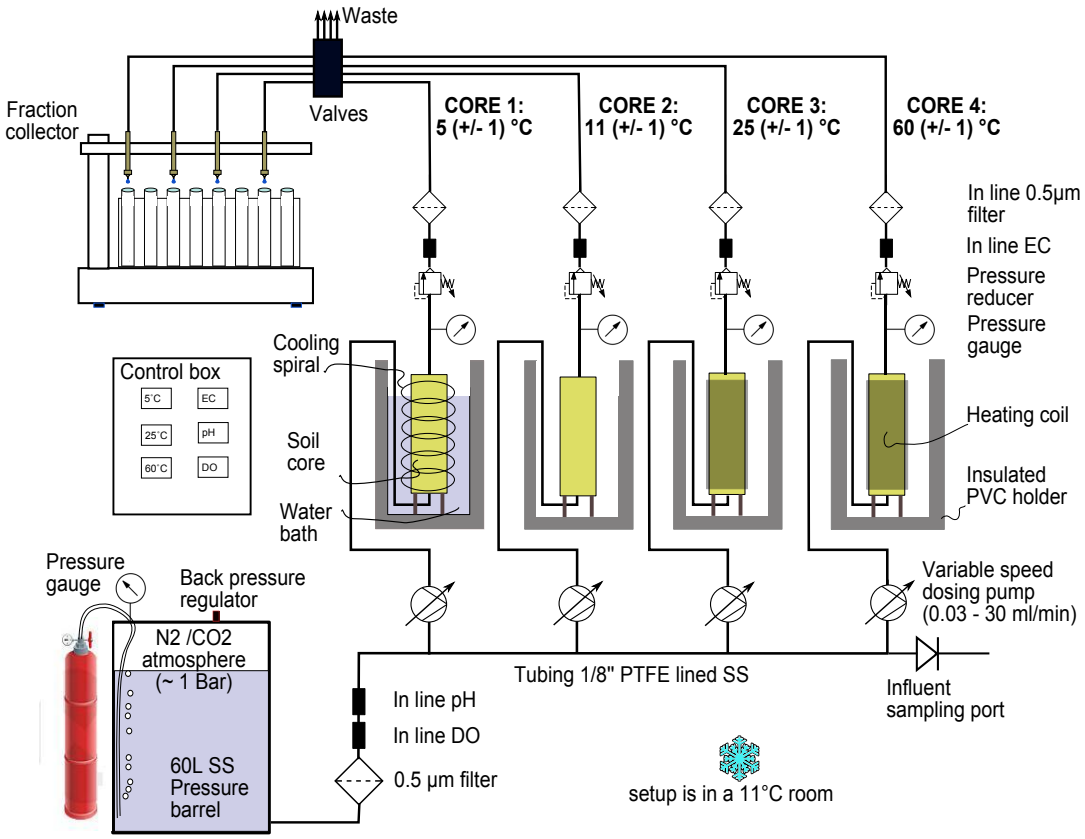

Figure 2-2 Experimental setup used for anaerobic column experiments

Three types of tests were carried out focusing on different processes (Table 2-3):
1. A constant flux test with a one day residence time focusing on relatively quick kinetically unrestricted reactions, such as cation exchange and surface complexation.
2. A flow-stop test where the column is thoroughly flushed with a relatively high flux (2 ml/min, completely flusing the column in less than 2 hours) followed by a period with no flow of variable length. This test focuses on relatively slow reactions mainly focusing on redox reactions, and
3. A test similar to the previous but with a fixed 5 days residence time while the temperatures is varied to get additional data with temperature. This test provides additional insight in the rates of various redox processes over a wide temperature range.

Prior to these three tests, a breakthrough test was carried using a conservative tracer out to determine the effective porosity and dispersivity which is used to determine the average residence time, to check that no preferential flow paths are present and in the numerical modelling. The BTT tests were analyzed with the model CXTFIT [26]. The results are shown in Table 2-1 (detailed description of method is included in Appendix III). Table 2-3 presents an overview of which test was carried out with which sediment type. One difference is noted between tests A1 and B1 on one hand and C1: During tests A1 and B1 it became obvious from the first two (A1 and B1) that pore water composition in the cores can differ greatly from influent water. To eliminate the flushing of pore water effect, and get a better view on hydrochemical changes pure resulting from temperature in the first pore flushes, the cores in experiment C1 were all first flushed at 11 °C.

Table 2-3 Types of experiments carries out showing test types and sediments used (A, B and C).

Test		Description	Processes investigated	Sediment used		
				A	B	C
0	**Breakthrough test**	Column flushed with conservative tracer. Experiment B with CaBr, experiments A & C with NaCl	Determination of porosity and dispersivity	√	√	√
1	**Leaching test:** 1 day residence time at 5ºC, 11ºC, 25ºC and 60ºC	Columns were flushed with influent at a constant flux resulting in 1 day residence for 25 pore flushes.	Investigating relatively 'quick' or kinetically unrestricted processes and leaching behavior of sediments: i.e. cation exchange, (de)sorption from oxides, carbonate interaction	√	√	√
2	**Incubation test, variable residence time:** Increasing residence time from 1 to 30 days at 5ºC, 11ºC, 25ºC and 60ºC	Columns were used as a batch reactor where water was sampled with increasing residence times	Investigating 'slow' kinetically restricted processes: i.e. redox reactions		√	√
3	**Incubation test, variable temperature:** fixed 5 day residence time temperatures: 15, 20, 25, 30, 35, 45, 55, 60, 65, 70, 75 and 80ºC	Columns were used as a batch reactor where water was sampled with increasing residence times	Extending tests 1 and 2 at multiple temperatures, but restricted for two residence times			√

Blank tests

Steel cores were used because it is essential to keep the sediment anoxic and frequently used plastics like Teflon or Polyproylene are permeable to oxygen. Stainless steel quality SS304 used here however contains Ni (8-11%) and Cr (18 and 20%) (EN standard 1.4301) and this could thus interfere with the testing results. The results of a literature review on metal release by steel by Santonen *et al*. [30] show that the results of these studies are not conclusive but do show that when preparing acidic food in new pans, some release of Cr and Ni can occur. To further determine whether these substances can interfere with the results we performed blank tests where a 8 cm long section of 1/8'' SS304 tubing was incubated with demineralised water (milli-Q) in a 12 ml PE sample vial for 5 days at room temperature and at 60ºC. The higher steel-water ratio and the longer contact time than applied in the column tests should thus give a conservative estimate of actual leaching from setup material during testing. The results show that Ni and Fe can leach in significant amounts and Mo, Cr and V show values just above the detection limit (Table 2-4).

Table 2-4Results from blank testing using SS304 tubing steel with demineralised and tap water at 20ºC and 60ºC. All values are in µg/l.

	Demineralised water			Tap water		
	Control	**20ºC**	**60ºC**	***Control***	**20ºC**	**60ºC**
Fe	<1	75	87	30	6	18
Cr	<1	<1	<1	<1	<1	<1
Ni	<1	7	8	5	3	6
Mo	<1	2	2	3	1	2
V	<1	<1	<1	4	3	2

2.4 Hydrochemical analyses

Alkalinity of in- and effluents were measured by titration with H_2SO_4 down to a pH of 4. Major cations, trace elements, and heavy metals were analysed with inductively coupled plasma optical emission spectrometry (ICP-OES, Varian 720 ES-axial), anions with ion chromatography (Dionex DX-120 IC equipped with IonPac AS14 column), NH_4 by colorimetry (Labmedics Aquakem 200), and dissolved organic carbon (DOC) was measured using high temperature catalytic oxidation (Shimadzu Model TOC-500A analyzer). Quality of the analyses was verified by calculating the electrical balance with PHREEQC.

Terminal restriction fragment length polymorphism (T-RFLP) of 16S rRNA genes and analysis of adenosine triphosphate (ATP) was used to detect changes in the microbiological population and activity. Table 2-5 summarises the analyses carried out with the different experiments. Quality of the analyses was verified by calculating the electrical balance with PHREEQC; the average ion balance error of all analyses was -0.7%; the average absolute error was 3.2%.

Table 2-5 Types of experiments carries out showing test types (1,2 or 3) and sediments used (A,B and C). Right columns give a code for each test: e.g. A1 is the 1-day residence time experiment with sediment A

Group	Elements	Method	Sediments		
			A	B	C
Main	Alkalinity + pH	Titration	√	√	√
Cations	Na, K, Ca, Mg, Fe, Al, Si, Ag, As, B, Ba, Be, Bi, Cd, Co, Cr, Cu, Eu, Ga, Ho, In, La, Li, Mo, Ni, P, Pb, Sb, Sc, Se, Sr, Th, Ti, Tl, U, V, W, Yb, Zn, Zr	ICP-OES	√	√	√
Anions	Cl, SO_4, NO_3, NO_2, Br and F	IC, Ion chormatography	√	√	√
NH4	NH4	photometric titration (Aquakem)			√
Organic carbon	DOC	High temperature catalytic oxidation	√	√	√
Biomass	ATP				√
Microbiological fingerprinting	T-RFLP			√	√

2.5 Data analysis

In order to get a comprehensive overview of the substances which show a temperature dependence in leaching behaviour, we calculated the mean leaching concentration during the testing period at 5°C, 25°C, and 60°C and compared it to the reference of 11°C (which is the in-situ temperature). The significance of the difference in average concentration was tested at 1% and 5% confidence levels with a Mann Whitney U (MWU) test. This test is comparable to the more frequently used t-test but does not require a normal distribution. Statistical calculations were performed using the SciPy module [31]
All calculations for redox speciations and saturation indices were carried out using PHREEQC [28].

3 Experiments with 1-day residence time

3.1 General patterns and results

The chemical analyses of influent and effluents for the three leaching tests with one day residence time are presented in Appendix IV (tables) and V (graphs). The statistical data of the MWU test for each substance is provided in Appendix VI which contains the relative difference between mean leaching concentration at 5, 25, and 60°C and the 11°C leaching concentration.

Table 3-1 shows which elements were significantly influenced in all three experiments based on the MWU test. Table 3-1 also shows the elements identified in the sediments by XRF and HNO_3 /ICP-MS. This comparison shows that most heavy metals and trace elements that are not mobilized by increased temperatures are actually present in the sediment. Figure 3-1 presents the effluent graphs from experiment C for substances which show a statistical significant deviation from the effluent at the reference temperature (natural background temperature).

In all experiments at all temperatures an increase in alkalinity, Ca and Mg was observed pointing to the dissolution of carbonate minerals (Fig. 3-1). This aspect is further elaborated in the next section. The comparison of the 5°C effluent to the 11°C effluent shows there are no substances which show a significant difference in mean effluent concentration in all three tested sediments. A number of substances shows significant differences in one or two of three experiments. For example: Li showed a significant decrease at 5°C in experiments A and C whereas K showed a decrease at 5°C compared to 11°C in all three experiments but the difference was only significant in experiment C.

The 25°C effluent shows a significant increase in As concentrations compared to the 11°C for all three sediments. Looking at the individual experiments, it can be seen that in experiment B, the effluent's electrical conductivity at 25°C is significantly lower than in the 11°C effluent. This is the consequence of reduced concentrations of HCO_3, Ca, Mg and Sr implying carbonate mineral precipitation.
At 60°C, quite a number of substances show concentrations which are significantly higher than concentrations in the 11°C effluent: pH, F, DOC, P, K, Si, Mo and V. All substances show especially large differences between 11 and 60°C experiments during the initial pore flushes, becoming less with increasing pore flushes. This is clearly visible in Figure 3-1 which also shows that concentrations of substances like DOC, Si, K decrease less rapid than As and Mo. In all three sediments, the 60°C effluent showed a clear increase in B concentration during the first 5 pore flushes. During the remaining pore flushes, effluent concentrations from the 60°C column

A noteworthy differences in effluents between the different testing temperatures which was not observed in all three sediments is that in the 60°C effluents of sediments A and B higher concentrations of Be and Cr were measured. The sediment content of Cr_2O_3 of sediments A and B (respectively 0.037% and 0.028%) is also considerably higher than in sediment C (0.001%) indicating that if Cr is present in the sediment it may be leached out by a temperature increase. For Be the differences between the different sediments was less pronounced: <1ppm, <1ppm and 2ppm in sediments A, B and C, respectively, but here the detection limit of Be is relatively high potentially masking differences in geochemistry. It is interesting to note that all trace elements (As, B, Mo, Cr and V) behave as oxyanions in water.

In the following we discuss the main processes and mineral interactions due to temperature perturbations. We distinguish the carbonate minerals, silicate minerals, organic carbon, and trace metals in this description.

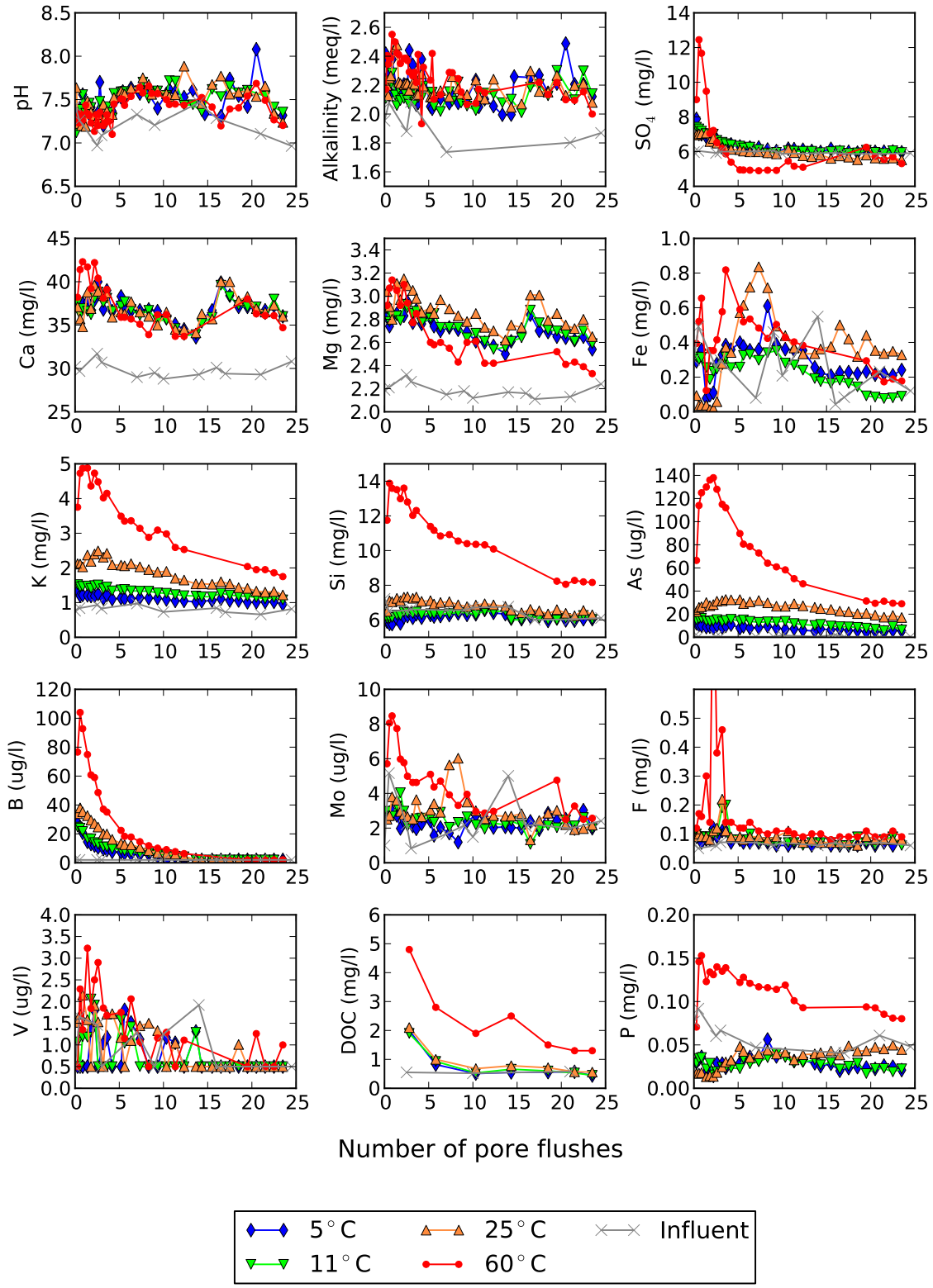

Figure 3-1 A selection of effluent graphs for main cations and anions, trace elements, and nutrients for sediment C. Results for the 60°C column between pore flushes 13 and 19 are not shown because of sampling errors.

Table 3-1 Summary of leaching behaviour of the 5ºC, 25ºC and 60ºC columns compared to the reference column of 11ºC during 1 day residence time with indication of availability of substances in sediment. The detection limit of the different elements are included in Appendix VI (aqueous) and Appendix I (geochemical)

Leaching behavior	**Geochemical**	**Temperature level**		
		5ºC	**25ºC**	**60ºC**
Substances significantly thermally influenced (p<0.01) in **all three** experiments,	Substance present in sediment		As	pH, DOC, P K, Si, As, Mo, V
	Not analysed			F
Leaching behavior **not** significantly influenced by temperature in **all three** experiments	Substance present in sediment	Alkalinity, SO_4, Na, Mg, Sr, Ca, Fe, Mn, Al, Ba, Be, Co, Cr, Cu, Eu, Ho, Ni, Li, Pb, Sb, Sc, Yb, Zn		
	Substance below detection limit in sediment	Ag, Bi, Cd		
	Not analysed	Br, Cl, B, Tl		
Substance **below detection limit** in reference and testing temperature	Substance present in sediment	Ga, La, Th		
	Substance below detection limit in sediment	Bi, Se		

3.2 Dissolution and precipitation of carbonates

Dissolution of pure calcite is given by the following reaction equation [32]:

$$CaCO_3 + CO_2 + H_2O \leftrightarrow Ca^{2+} + 2HCO_3^- \quad (3\text{-}1)$$

which shows that HCO_3^- and Ca molar concentrations in water undergoing either precipitation or dissolution of calcite are correlated by a factor 2. The relation is shown in Figure 3-2 by the line with a slope of 2 along with observed Ca versus alkalinity (alkalinity is at neutral pH approximately equal to HCO_3^-). Effluents of experiments A and C were characterized by increasing Ca and alkalinity concentrations along the calcite dissolution-precipitation line. The dissolution of calcite is also reflected in the pH increase varying between 0.2 and 0.4 (Figure 3-1) caused by the consumption of carbonic acid. In experiment B, however, decreasing Ca and alkalinity concentrations point to calcite precipitation, especially in the 60ºC effluent. This is remarkable considering the small differences in the influents' Ca , alkalinity, and pH between influents used for experiments A and B. PHREEQC [28] was used to calculate saturation indices (SIs) of influent water for the main carbonate minerals for the three experiments as a function of temperature (Figure 3-3). The calculated SIs show that influents of all three experiments are sub-saturated with respect to calcite ($CaCO_3$), dolomite ($CaMg(CO_3)_2$), and rhodochrosite ($MnCO_3$) over the full temperature testing range. Only the influent of experiment B shows a supersaturation with respect to siderite at temperatures above 40ºC. When calculating SIs with respect to siderite using PHREEQC, it is noted that there are considerable differences between the different databases included with PHREEQC. To illustrate this variation, Figure 3-3 also shows the SI based on the Minteq.v4 database, as well as the results when using the thermodynamic data from a recent study on temperature dependence of siderite [33]. The differences in SIs for siderite as resulting from the use of different databases is quite remarkable: In experiment B, no precipitation of siderite would be expected at 60ºC based on calculations using the Minteq.v4 database, whereas the calculations based on the other two sets of thermodynamic data show the occurrence of a considerable super-saturation.

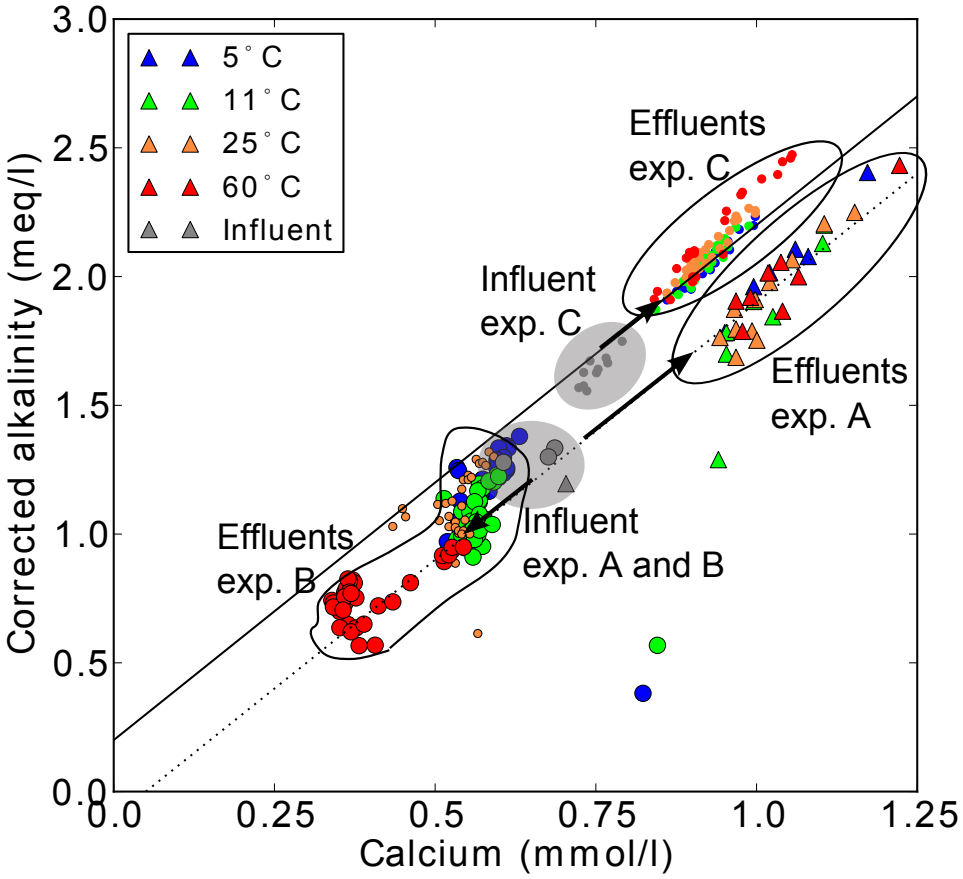

Figure 3-2 Relationship between Ca and alkalinity as an indication of calcite dissolution/precipitation. Lines show the stochiometric ratio of Ca and alkalinity changes according to reaction 3-1. Note that most 11 °C experiment B sample markers for are behind the 25 °C and not visible in the plot.

Obviously, precipitation of pure phase siderite would not result in decreasing Ca concentrations. Precipitation of a solid solution of siderite and calcite, however, would remove both Ca and Fe from the solution and can explain the observed changes in water quality. The formation of a Fe, Ca carbonate was also shown in high temperature (90°C) column experiments conducted by Griffioen and Appelo [11]. The difference with these experiments is, however, that for the current experiments the solution is sub-saturated with respect to pure calcite, whereas in the experiments of Griffioen and Appelo [11] the influent became increasingly oversaturated with higher temperature. In order to explore whether precipitation of a solid solution of siderite and calcite can explain the observations, the saturation constant and precipitation kinetics are investigated in further detail in Appendix VII.

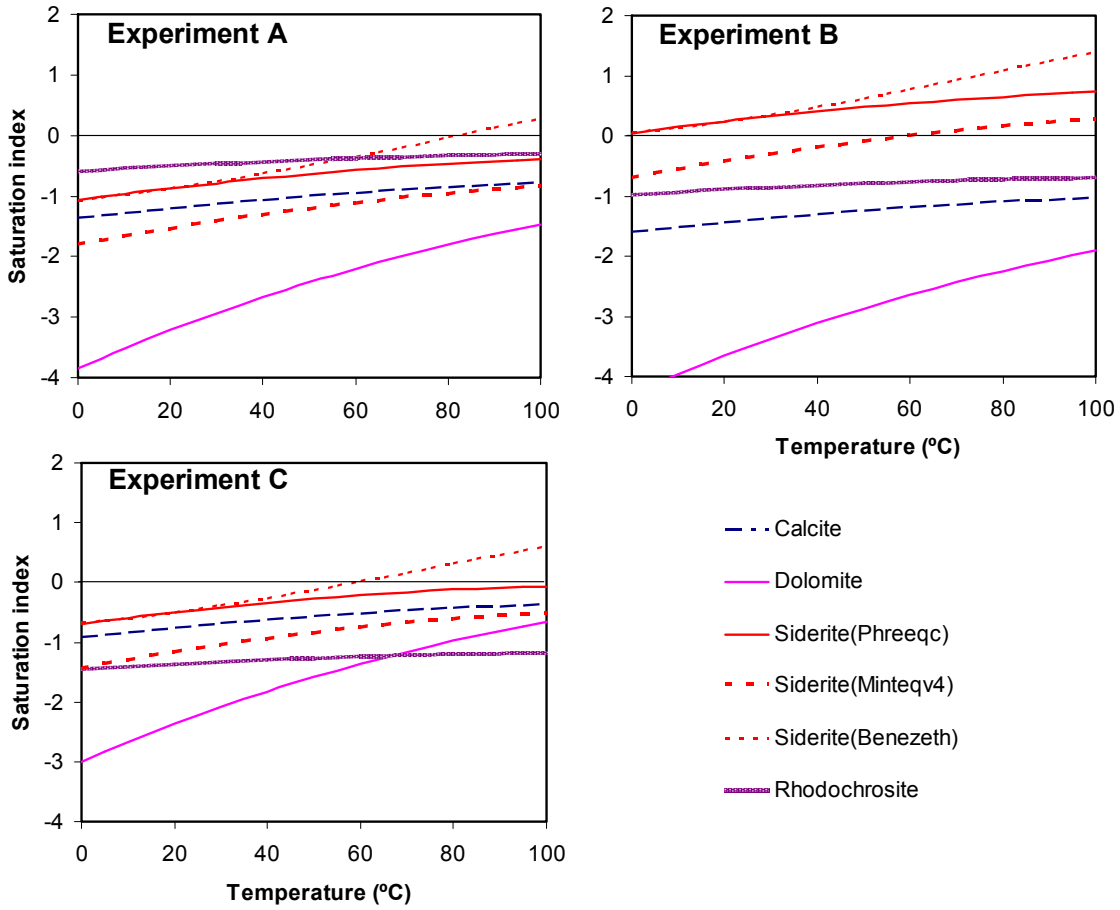

Figure 3-3 Saturation indices of several carbonate minerals as a function of temperature for the three used influent waters calculated using PHREEQC. For siderite, saturations indices were calculated using three sets of thermodynamic data: Siderite (PHREEQC) is based on the thermodynamic data contained in the PHREEQC database with a logK = -10.89 and ΔH=-2.48kcal; Siderite (Minteqv4) is based on the Minteq.v4 thermodynamic data with logK = -10.24 and ΔH=-16kJ, Siderite (Benezeth) is based on thermodynamic data from [33] who provide LogK=a+b(T/K) + c(T/K)$^{-1}$+d log(T/K) with a =175.56, b=0.0139, c=-675.483 and d=-67.898.

3.3 Dissolution of silicates

The second group of minerals that is discussed, is composed of silicates. In all 60ºC experiments, an increase in K and Si concentrations was observed. This can be explained by the following reactions:

- Cation exchange, where K is released with temperature increase. The exchanger selectively sorbs K at both lower temperatures and lower aqueous K concentrations [34]. Increasing temperature causes replacement of K for Ca on exchangers such as clay minerals.
- Desorption of Si from iron-oxides with increasing temperature [35]
- Dissolution of silicates such as K-feldspar or clay minerals yielding both Si and K.

The contribution of each reaction is hard to discriminate. One can get an idea of each reaction's contribution by looking at the stochiometric ratio of K and Si for each reaction and comparing this to the ratio in the effluent. Table 3.2 shows the involved reactions, the resulting stochiometric ratios and the log_K (mostly based on the PHREEQC database).

Figure 3-4 shows Si plotted against K (in mM) for sediments B and C. The Si versus K plots show a difference between experiments B and C: In experiment B, there was a decrease in Si concentration at the three lower temperatures accompanied by a relatively strong increase in K. From the reactions shown in Table 3.5, only sorption of Si by iron(hydr)oxides can explain this decrease. Sorption of Si can be caused by a lower Si concentration in the pore water than the used influent. According to Kersten *et al.* [35] sorption of Si to iron(hydro)xides is an exothermic process, which implies that at higher temperatures Si sorption to iron(hydro)xides is less strong. This may explain why at the higher temperatures, no decrease of Si is observed. The potential sorption of Si makes it hard to identify the

process responsible for the increasing K concentrations. During the initial pore flushes of experiment B, the K concentration increased with a factor of 160 to more than 8 mmol/l (300mg/l).

Table 3-2 Overview of reactions in sediments containing clay minerals, iron(hydr)oxides, and K-feldspar involving K and Si.

Reaction	Reaction	LogK, 25ºC	Si/K	Source
Cation exchange (clay minerals and organic matter)				
$KX \leftrightarrow K^+ + X^-$	(3-2)	0.7	0	[34]
Silica (de)sorption (iron(hydr)oxides)				
$\equiv FeOH + Si_4(OH)_4o \leftrightarrow \equiv FeH_3SiO_4$	(3-3)	4.28	∞	[36]
$\equiv FeOH + Si_4(OH)_4^o \leftrightarrow \equiv FeOSi(OH)_3$	(3-4)	3.62	∞	[37]
$2\equiv FeOH^{-0.5} + Si_4(OH)_4^0 \leftrightarrow \equiv (FeO)_2^{-1+\Delta z}{}_2Si(OH)_2^{\Delta z\beta+} + 2H_2O$	(3-5)	4.60	∞	[35]
(In)congruent mica dissolution or alteration				
Muscovite to gibbsite $KAl_3Si3O_{10}(OH)_2 + 9H_2O + H^+ \rightarrow K^+ + 3H_4SiO4^o + 3Al(OH)_3$	(3-6)	-11.63	3	
Muscovite to kaolinite $2KAl_3Si_3O_{10}(OH)_2 + 3H_2O + 2H^+ \rightarrow 2K^+ + 3Al_2Si_2O_5(OH)_4$	(3-7)	3.1	∞	
Illite dissolution $K_{0.6}Mg_{0.25}Al_{2.3}Si_{3.5}O_{10}(OH)_2 + 11.2H_2O \rightarrow 0.6K^+ + 0.25Mg^{+2} + 2.3Al(OH)^{4-} + 3.5H_4SiO4 + 1.2H^+$		-40.27	5.8	
(In)congruent K-feldspar dissolution				
K-feldspar to muscovite $3KAlSi_3O_8 + 12H_2O + 2H^+ \rightarrow 2K^+ + 6H_4SiO_4^o + KAl_3Si_3O_{10}(OH)_2$	(3-8)	-10.34	3	
Hydrolysis of K-feldspar to form kaolinite $2KAlSi_3O_8 + 2H^+ + 9\ H_2O \rightarrow Si_2Al_2O_5(OH)_4 + 2K^+ + 4Si(OH)_4$	(3-9)	-3.96	2	
Congruent dissolution of K-feldspar $KAlSi_3O_8 + 8\ H_2O \rightarrow K^+ + Al(OH)_4^- + 3H_4SiO_4^o$	(3-10)	-20.573	3	

The Si and K concentrations of the 25ºC and 60ºC effluents from sediment C show a high correlation suggesting either K containing mica (muscovite) or feldspar dissolution. Calculated SIs show that at both 11 and 60ºC influents are supersaturated with respect to muscovite. Influent at 11ºC is supersaturated with respect to illite but under-saturated (SI_{illite} = -4.5) at 60ºC. Dissolution of illite would however yield a much higher Si:K ratio than observed here.

The Si:K ratio of 2.5 in the 60ºC sediment is between the values expected for the reaction equations for K-feldspar hydrolysis and congruent dissolution. The $SI_{K\text{-}feldspar}$ points to sub-saturation at both 11 and 60ºC (respectively -1.6 and -4.6) which is remarkable as it would imply that at ambient conditions K and Si concentrations are not in equilibrium with K-feldspar. This would be expected as this mineral is present in the aquifer. A possible explanation for this discrepancy can be found in the SEM analyses of the sediment which showed that a large fraction of the K-feldspar found in the sediment is partly covered with a mixture of clay minerals such as kaolinite and gibbsite. In the pre-testing SEM photographs (Figure 3-5), it was observed that the larger grains (both quartz and feldspar) present in the sediment were almost completely covered with weathering products. This implies that the reactive surface is strongly limited thereby minimizing field weathering rates. This process is quite widely described in literature for K-feldspar [38], anorthite [39], and biotite [40]. Flushing of the sediments during column testing invokes displacement of especially the finer particles and re-exposed fresh mineral surfaces. This enables dissolution which was not observed under ambient field conditions. This suggests that this process is a laboratory artifact, which is however not the case as argued in the following. ATES wells will locally invoke an increased flow velocity which decreases linearly with the distance squared. In order to estimate the size of this influenced area, we can compare the Darcy flow velocity (in our case 0.4m/day, based on a column length of 0.4 m and a residence time of 1 day) with field flow velocities. The circular area near a well with capacity Q (m^3/hour) and screen height (H, m), where a certain flow velocity (v, m/hour) is exceeded, has a radius of:

$$r = \sqrt{\frac{Q}{Hv\pi}} \qquad (3\text{-}11)$$

It is assumed that aquifer and lab column porosity are identical. For a typical ATES well, for example of the RIVM set in the same geological formation used here, having a capacity of Q = 100 m^3/hour set in a

H=50 m thick aquifer, the Darcy velocity experienced in our column experiments (v=0.4m/day) will be exceeded up to 6.2 m distance from the well. Thus, part of the driver of K-feldspar dissolution can also be expected near pumping wells used for ATES. This velocity is far greater than the ambient groundwater velocity at this site, which is around 10 m/year (0.03m/day).

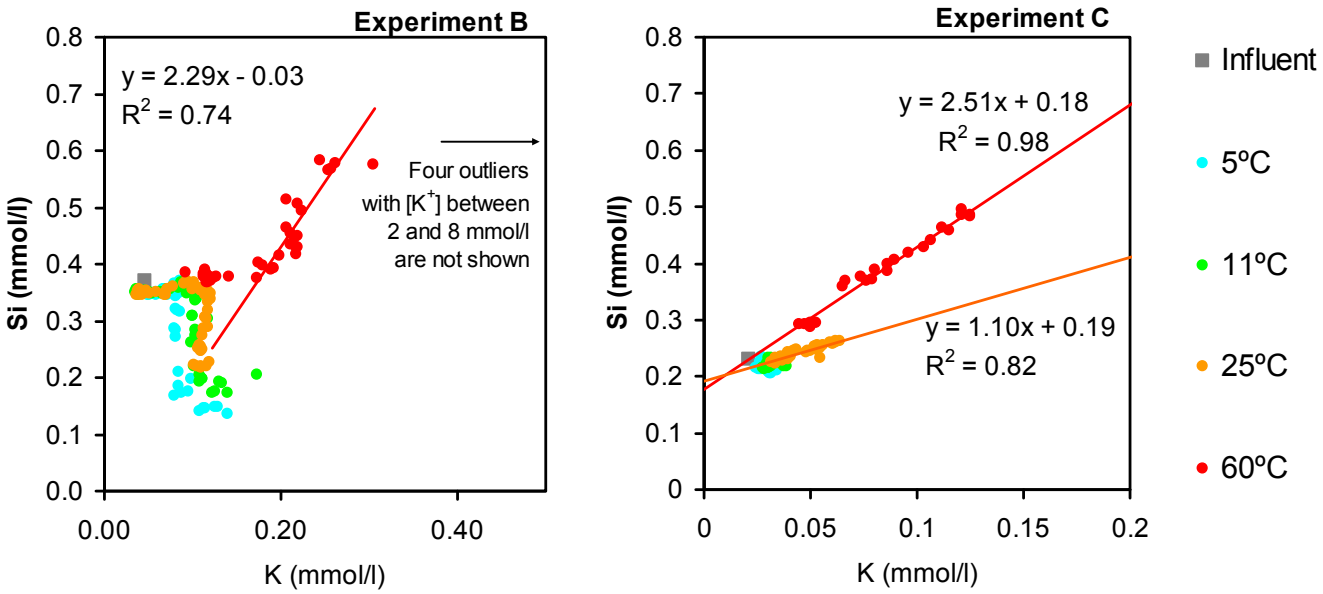

Figure 3-4 Relationship between Si and K molal concentrations in sediments B and C. Data of sediment A shows a similar pattern to that of sediment B. Regression lines are drawn for the linear part of the 60ºC data of sediment B and both the 25 ºC and 60 ºC data of sediment C.

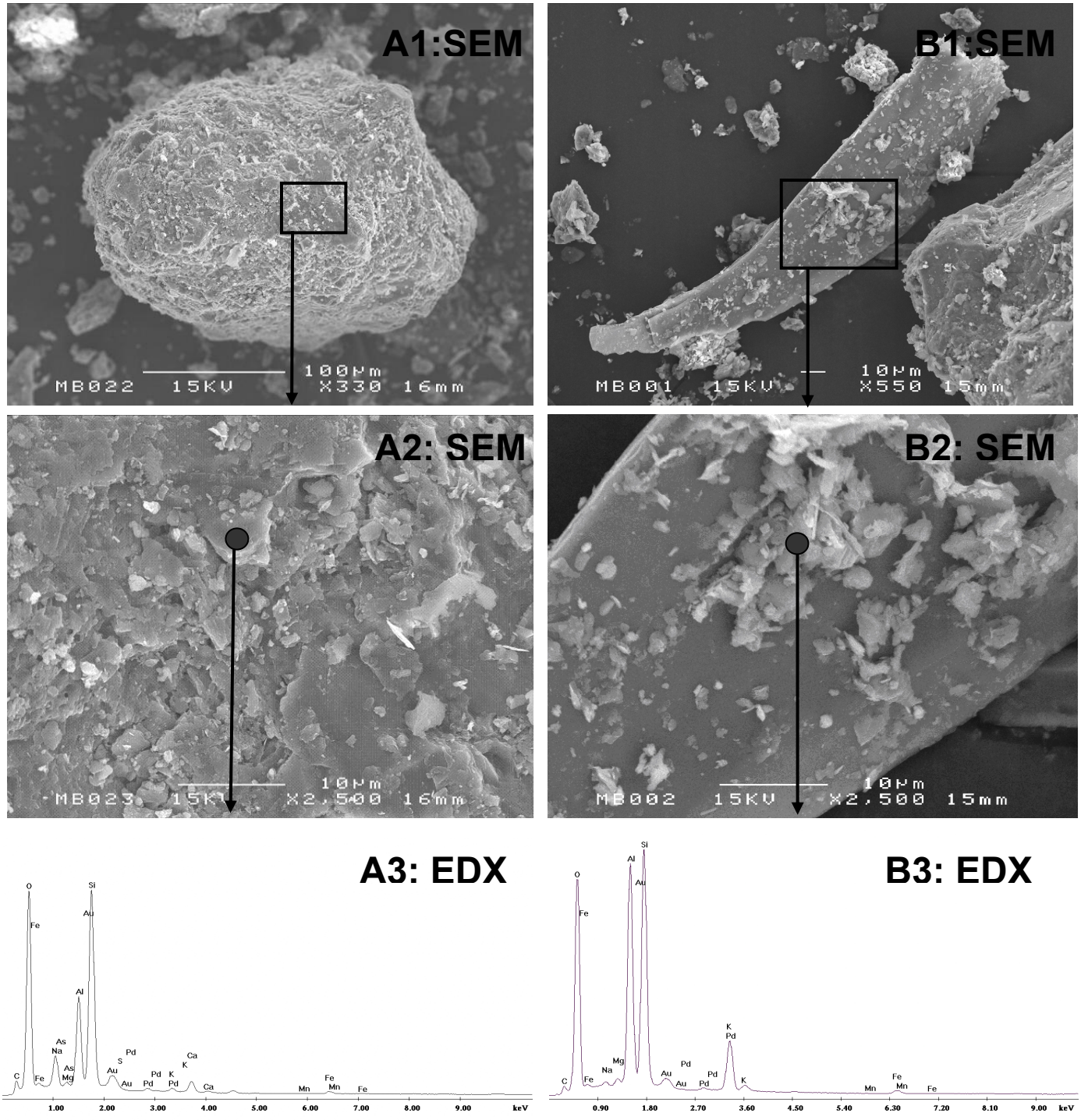

Figure 3-5 Left: Pre-testing SEM image of a grain (mother material cannot be identified due to weathering layer) completely covered with clay particles as shown by close up (A2) and EDX (A3). Right: Post-testing SEM image of K-feldspar grain from 60°C sediment partially covered with gibbsite and kaolinite fragments and EDX scan. Both images are from sediment B.

3.4 Interaction with sedimentary organic matter (SOM)

Dissolved organic carbon (DOC) increased in the 60°C effluents of all three sediments. This was also observed in earlier column tests investigating ATES effects [17, 41]. The DOC concentration in the 60°C effluent of sediment C increased from 0.55 mg/l to maximally 4.8 mg/l. DOC in the 60°C effluents of sediments A and B increased more: from 2.4 to 8.5 mg/l and from 2.2 to 7.3 mg/l, respectively. Two mechanisms can be responsible for these increases: 1) desorption of organic acids from iron oxides [42, 43] and 2) microbial respiration of SOM [17].

A key difference between these two processes is that DOC involved in sorption generally comprises large fulvic or humic acids [42] while respiration of SOM is a stepwise transformation of SOM to volatile fatty acids such as acetate which are then consumed by sulfate reducing bacteria or methanogenic archaea generating inorganic carbon thereby increasing alkalinity and not necessarily DOC. In the second process DOC would therefore only accumulate with increasing temperature if the ratio of DOC oxidation versus DOC production rates becomes lower. These aspects are discussed further in section 5.3 in the context of the experiments with increasing residence time focusing on redox processes.

The relative contribution of the two different processes leading to DOC accumulation is hard to quantify. However, a qualitative indication can be obtained since different elution profiles can be expected: desorption will generate a peak in DOC which will gradually decrease towards the influent concentration with continuing flushing, whereas SOM derived DOC will yield a constant DOC concentration with progressive flushing (under equal residence time) assuming ample SOM in the sediment. The elution curves for sediments A and especially B (Appendix V) are characterised by a short peak (< 7 pore flushes) followed by constant increase relative to the influent DOC. In sediment C, a gradual decrease in DOC is observed up to 20 pore flushes after which DOC stabilises just above the influent DOC concentration. This suggests that in sediments A and B, the DOC increase is mostly derived from SOM, whereas in sediment C it is mostly derived from desorption. This qualitative observation is in agreement with the geochemical analyses: reactive SOM in sediment C is much smaller than that in sediments A and B, whereas iron oxide content is also lower in sediment C than in sediments A and B but to a considerable smaller extent than for the SOM difference.

3.5 Mobilisation of arsenic and other trace compounds

A number of mechanisms responsible for arsenic mobilization in aquifers are reported in the literature [44, 45] which can be divided in three main groups: 1) oxidation of pyrite, 2) reduction of Fe(III) minerals, or 3) desorption from charged surfaces such as Fe, Al, Mn-oxides.

Oxidation of As containing pyrite is often responsible for As mobilization in anoxic aquifers used for aquifer storage and recovery [46-48]. In our experiments, however, and in ATES systems in general, great care is taken to avoid the intrusion of oxygen or nitrate into the system as this would cause clogging of wells by ironhydroxide precipitation [49]. Influent DO and NO_3 were consistently below the detection limit during the experiment (DO < 0.05 mg/l and NO_3 < 0.1 mg/L). Furthermore, the effluent data shows that this mechanism is probably not responsible for the arsenic mobilization as oxidation of pyrite by either nitrate or oxygen would be accompanied by an increase of SO_4. Our data shows a constant SO_4 in effluent from the 5-25 °C columns and equal to the influent SO_4, and concentration, whereas a slight decrease was observed for the 60°C column pointing to a sulfate-reducing environment in the column which agrees with aquifer conditions. Oxidation of pyrite can thus be ruled out.

Microbiologically mediated reductive dissolution of iron (hydr)oxides could be an explanation instead. This process is held responsible for arsenic mobilization in delta areas such as Bangladesh. However, as discussed above, the redox conditions in the sediment point to sulfate reducing conditions and not ferrous iron reduction. Second, given the slow, kinetically restricted nature of this reaction, it is expected that this process would show a clear relation between Fe(II) and As concentrations with increasing residence time. However, these concentration patterns are not present in our data (results not shown). The third general explanation, desorption of arsenic, is described for both iron(hydro)xides [44, 50-52], clays [53, 54], and carbonates [55, 56]. Desorption from clay is unlikely in this case because the pH_{PZC} of clay minerals is generally far lower than the aqueous pH in our experiments and clay minerals provide sorption sites mainly for cations. Experiments with calcite and both As^{III} and As^{V} [55, 56] show that only As^{V} sorption could occur while our speciation calculations (using NO_3/NH_4 and Fe^{2+}/Fe^{3+} as redox couples) showed that As is mainly present as As^{III} in our experiments (Figure 3-6) making

desorption from carbonates unlikely. Desorption of As^{III} from iron(hydr)oxides is described with the following reactions [52, 57]:

$$\equiv FeOH + H_3AsO_3 \leftrightarrow \equiv FeH_2AsO_3 + H_2O \quad (3\text{-}15)$$

$$\equiv FeOH + H_2AsO_3^- \leftrightarrow \equiv FeHAsO_3^- + H_2O \quad (3\text{-}16)$$

Desorption from iron(hydr)oxides with temperature can be driven by a number of processes: First and most prominent is the temperature induced change in sorption equilibrium constant for reactions 3-15 and 3-16. Kersten *et al.* [51] showed in laboratory experiments with synthetic goethite that arsenite sorption to goethite is an exothermic process. Another process could be the release of anions which compete with As for sorption sites [58] such as PO_4 or SiO_2 (CO_3 is also often mentioned as a competitor for As but the alkalinity is not different at the four tested temperatures). As discussed earlier, P is present in SOM and will be mobilized upon SOM decomposition as PO_4 together with DOC and NH_4. However, as shown above, the P increase that can be attributed to SOM mineralization (0.006-0.01 mg/l) is only a fraction of the total P-increase (0.05 to 0.1 mg/l as shown in Figure 3-1). This implies that sorption of PO_4 itself to iron-oxides is probably temperature dependent as well.

Mo, V and B also behave as oxyanions like As and together with fluoride engage in surface complexation with iron(hydr)oxides [57]. Although leaching of these elements only shows a significant temperature dependence at 60°C it is likely that for those elements desorption from ironoxides is also responsible for their mobilizationa main controlling reaction. Summarising, the increased concentrations of As, B, Mo and P are likely due to temperature induced desorption from ironoxides.

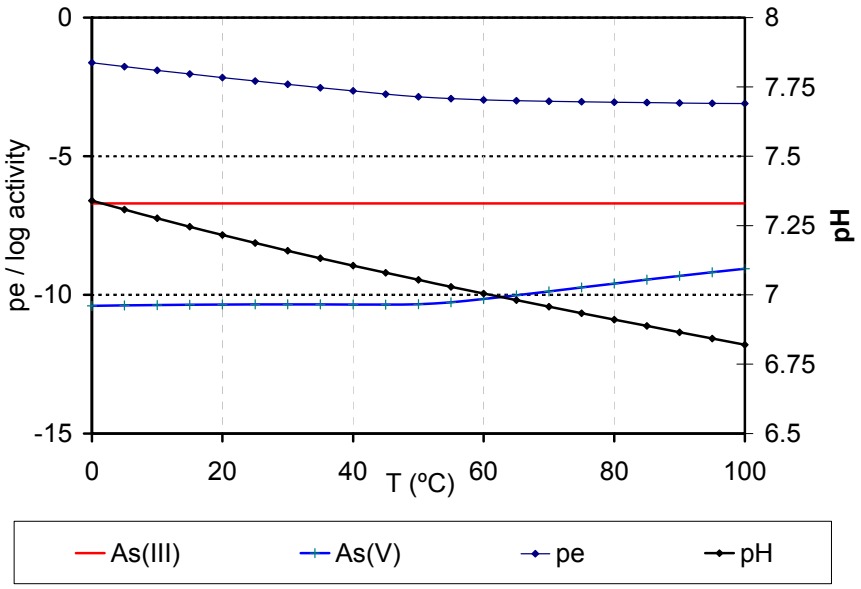

Figure 3-6 Arsenic redox state, pe and pH for influent of sediment C as a function of temperature, determined with PHREEQC[28].

Sorption isotherms

In order to further quantify the desorption behavior of As with increasing temperature it is useful to derive the sorption isotherms for each testing temperature. Column experiments are well suited to determine the sorption isotherm and thermodynamic parameters for the sorbent [59-61]. The solid-solution ratio of columns is more representative for aquifer conditions than in batch experiments and changing the flow velocity allows for determination of kinetic parameters [59]. Using the results of column experiments, however, also presents some difficulties, the most prominent one is correcting for hydrodynamic dispersion. Some authors have developed analytical or numerical solutions, e.g. [61, 62], which are especially useful when the dispersive breakthrough of a solute cannot be ignored. The effect of dispersion is especially important for solutes which have a moderate to low retardation (for example like K in cation exchange) which show a complete breakthrough within several pore flushes [61]. In the

current case, As shows a relatively large retardation because after 25 pore flushes, the effluent concentration is still well above the influent concentration (Figure 3-1). The sorption isotherm data can be constructed by calculating the sorbed amount of As from the effluent observation data. We use a simplified version of the concept developed by Griffioen *et al.* [61] where we ignore the effect of dispersion of the effluent curve. In the next chapter, we use PHREEQC modeling to simulate As release in the column including dispersion.

To determine the sorption isotherms, we first calculate the initial amount of sorbed arsenic, S_0 (mg As/kg dry weight) by integrating the surface of the arsenic leaching curve at 60°C using:

$$S_0 = \frac{-qC_0}{am} \tag{3-17}$$

where C_0 and a are the intercept and slope from a plot of ln[C] versus the number of pore and m is the amount of sorbent, which we assume is equal to the weight of reactive Fe (g). This extrapolation assumes that sorption behaves linearly over the observed concentration range and that the initial sorbed concentration is equal for all temperatures. An alternative is to determinate the amount of sorbed arsenic with an complete wet chemical extraction method, for example an extraction using PO_4 [63]. Next, we calculate for each aqueous observation data point the matching sorbed concentration, using:

$$S_i = (S_{i-1} - q\Delta tC_i)/m \tag{3-18}$$

Where S_i is sorbed As concentration (µg/kg) at sampling point i, corresponding to the aqueous concentration C_i (µg/l), Δt is the length of the time period between sampling point i and the previous sampling point (i-1), q is the flow rate of column test (l/day). The results of the constructed isotherm using equations (3-17) and (3-18) are shown in Figure 3-7. It is noted that the 11°C data for sediment B is not shown because construction of the isotherm was not possible due to much scatter; for sediment A a sorption isotherm is not calculated because at 5°C and 11°C As concentrations remained below the detection limit. The experimental data were fitted using both Freundlich (3-19) and Langmuir (3-20) isotherms, commonly used for As sorption [64, 65];

$$S = K_F C^{1/n} \tag{3-19}$$

$$S = S_{\max}\frac{CK_L}{1+K_L C} \tag{3-20}$$

where S is the mass of arsenic sorbed (µg/g), C is the equilibrium arsenic concentration (µg/l), K_F is the Freundlich constant indicative of the adsorption capacity (l/kg), and n is a fitting constant (dimensionless) indicative of the sorption intensity, K_L is the Langmuir constant and S_{max} is the maximum sorption capacity (µg/g). At low aqueous concentrations, $S_{max}K_L$ is equal to the initial slope of the sorption isotherm and often used as the distribution coefficient, K_d.

The Freundlich isotherm can be linearised by plotting C and Q on a logarithmic scale. The slope and intercept of the regression line are equal to the parameters n and K, respectively. The Langmuir parameters can be estimated by plotting S/C versus S. However, it can be expected that S_{max} will not change due to temperature changes (it may over longer time periods due to increasing crystallinity). We therefore fitted Langmuir curves for the different temperatures assuming a constant S_{max} by minimizing the normalised root mean squared error (NRMSE) between the S_i value calculated with 3-18 and that calculated with 3-20. The NRMSE is calculated with:

$$NMRMSE = 100\%\frac{\sqrt{(S_{isotherm} - S_{observed})^2/n}}{(S_{\max} - S_{\min})} \tag{3-21}$$

The fitted Freundlich and Langmuir isotherms are also shown in Figure 3-7, the derived sorption parameters and the NRMSE are shown in Table 3-3. The comparison of experimental data and fitted Freundlich curve shows a good agreement between model and data. The fit for the Langmuir curve is less good, especially for the 60°C data, which is due to the simple fact that this model contains less degrees of freedom. The Langmuir model is however expected to provide a more robust description of the sorption process because it can be expected that the sorption of As is maximized by the number of

sorption sites, and it is expected that this maximum of sorption sites is an intrinsic sediment property and not influenced by temperature. Only on longer time frames, it can be expected that ironoxides may become more crystalline and the number of sorption sites can decrease.

The data also show that the sorption isotherm for 5, 11 and 25°C only cover a narrow concentration spectrum. The NRMSE are only applicable within the range of measured aqueous As concentrations and use of an isotherm beyond this is prone to errors. In order to derive a complete isotherm, the sorbent should first be completely covered with As which would require a different experimental setup.

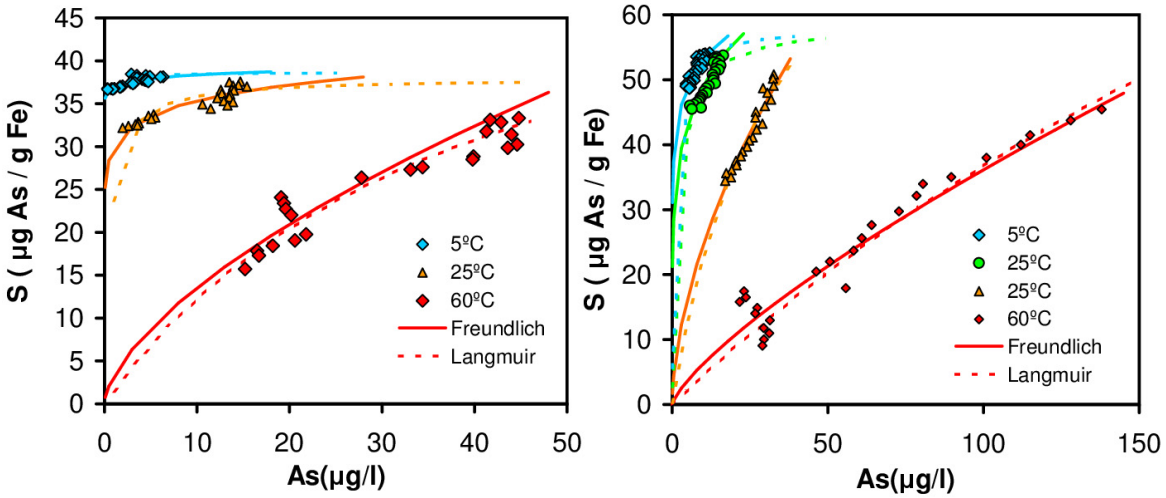

Figure 3-7 Sorption isotherms for arsenic using data from sediments B and C for temperature 5 °C(blue), 11°C (green, only sediment C), 25 °C (orange) and 60°C(red). Markers are for observed aqueous concentrations and calculated sorbed masses. The fitted Freundlich and Langmuir isotherms are shown with solid and dashed lines, respectively.

Table 3-3 Freundlich and Langmuir sorption parameters for arsenic sorption on iron oxides in sand

	Experiment B			**Experiment C**			
Freundlich parameters	**5°C**	**25°C**	**60°C**	**5°C**	**11°C**	**25°C**	**60°C**
K_F (l/g)	37.0	29.9	3.2	40.6	32.3	6.5	1.1
1/n ( )	0.02	0.07	0.63	0.12	0.18	0.58	0.76
Langmuir parameters							
K_L (l/g)	22.0	1.7	0.02	1.1	0.5	0.0	0.002
S_{max} (ug As/g $Fe_{reactive}$)	38.6	38.0	62.4	58.0	58.7	97.9	187.9

Temperature influence

Next, the impact of temperature on the sorption process was determined by calculating the change in standard Gibbs free energy (ΔG0, kJ mol-1), entropy (ΔS, kJ mol-1T-1), and the reaction enthalpy (ΔH, kJ mol-1) for the sorption reaction using the following equations [66]:

$$\Delta G_0 = -RT \ln K_d \tag{3-21}$$

$$\ln K_d = \frac{\Delta S}{R} - \frac{\Delta H}{RT} \tag{3-22}$$

where Kd is the distribution coefficient at infinite dilution, R the gas constant (8.314 J K-1 mol-1), and T the absolute temperature (Kelvin). The entropy change and enthalpy were calculated from the intercept and slope of a van 't Hoff plot (ln(Kd) versus T-1) where Kd is derived from the slope of the Freundlich (Kd,F in Eq 8) and Langmuir (Kd,L in Eq 9) isotherms at infinite dilution (or zero concentration), given by:

$$K_{d,F} = K_F / n \tag{3-23}$$

$$K_{d,L} = K_L S_{\max} \tag{3-24}$$

The entropy change and enthalpy are calculated from the intercept and slope of a van 't Hoff plot (ln(K) versus T^{-1}, shown in Figure 3-8). The results of the calculations are shown in Table 3-4. The negative ΔH indicates sorption is exothermic and the sorption capacity decreases with increasing temperature causing the increased As concentration at elevated temperatures. There is a considerable variation in enthalpies calculated for the different sediments and models. The difference between the sorption parameters for the two models is due to the fact that the sorption parameters Freundlich and Langmuir models have a very different definition. This implies that using a ΔH for sorption also depends strongly on the selected model.

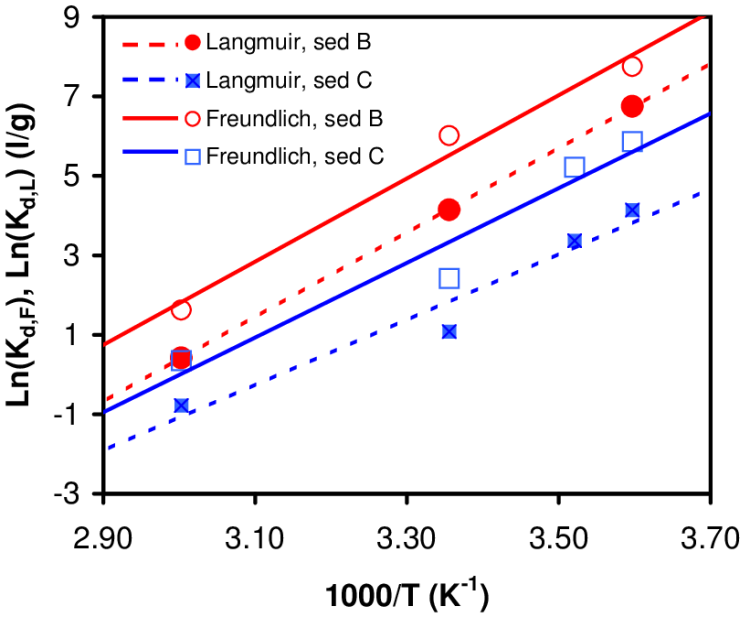

Figure 3-8 Van 't Hoff plots: ln(K) versus 1000/T for experimental data of arsenic from sediment B (red diamonds) and C (black and grey squares) using Freundlich sorption isotherms (solid symbols) Langmuir isotherms (open symbols). Regression lines are shown for Freundlich (dashed lines) and Langmuir (solid lines). Data from sediment A are not shown as arsenic concentrations were below detection limit at 5 and 11°C.

Table 3-4 Thermodynamic parameters Gibbs energy, change in entropy and change in enthalpy for arsenite sorption on sediments of sediments B and C.

Sorption model	Experiment B			Experiment C			
	5ºC	25ºC	60ºC	5ºC	11ºC	25ºC	60ºC
Freundlich							
Ln ($K_{d,F}$)	3.6	3.4	1.2	3.7	3.5	1.9	0.1
ΔG_0 (kJ mol^{-1})	-8.3	-8.4	-3.2	-8.6	-8.2	-4.6	-0.2
ΔS (J K^{-1} mol^{-1})	-29.6±4.8			-28.1±5.5			
ΔH (kJ mol^{-1})	-87.1±12			-77.9±13.5			
R^2	0.98			0.94			
Langmuir							
Ln ($K_{d,L}$)	3.1	0.5	-3.7	0.1	-0.7	-3.5	-6.0
ΔG_0 (kJ mol^{-1})	-15.6	-10.3	-1.2	-9.6	-7.9	-2.7	2.2
ΔS (J K^{-1} mol^{-1})	-31.6±0.2			-25.8±4.6			
ΔH (kJ mol^{-1})	-88.5±0.5			-68.6±11.4			
R^2	1.00			0.99			

In order to compare the thermodynamic data of As sorption to iron(hydr)oxides derived here, Table 3-5 presents a compilation of data derived from the literature. Included here are iron(hydr)oxides but also some clay minerals and carbonates for comparison. The data shows that As sorption is generally an exothermic process confirming our findings. However, the data for akageneite (a type of ironoxide) shows endothermic sorption behavior. The spread in ΔH values for the iron-oxides for As^{III} is quite large: -161.8 to -26 kJ/mol, with our ΔH values being at the higher end . The large range is probably due to 1) sedimentary differences, the type of ironoxide used (degree of crystallinity or aging), the As concentration levels, and 2) the method applied to calculate ΔH: some authors use fitting parameters derived from sorption isotherms (e.g. [64]), while others use a surface complexation model (e.g. [51]). These differences are also present in our data.

Table 3-5 Apparent thermodynamic parameters for arsenic sorption onto different types of sorbents

Main minerals	Arsenic redox state	Temperature range	ΔS (kJ mol^{-1} K^{-1})	ΔH (kJ mol^{-1})	Comment	Reference
Sediment with mixture of Fe and Al oxides	III	25, 35, 45ºC	-0.342	-109.5		[50]
	V	25, 35, 45ºC	-0.159	-54.1		
Zero valent Fe	III	25, 35, 45ºC	-0.01	-11.9	Freundlich isotherm	[64]
	III	25, 35, 45ºC	-0.17	-112.41	Langmuir isotherm; Values were corrected from original published data to correct for erroneous value for gas constant used.	
Kaolinite	V	25,40,55,70ºC	-0.219	-59.52		[53]
Illite	V	25,40,55,70ºC	-0.177	-51.24		
Montmorillonite	V	25,40,55,70ºC	-0.204	-73.9		
Goethite	III	10,25,50,60ºC	+0.026	-26.0 ± 5	Sorption of As on goethite, enthalpy for an intrinsic K value for the CD music model by [67]	[51]
	III	10,25,50,60ºC	+0.015	-27.6 ± 5		
Fe-oxides	III	20,25,30ºC	-0.526	-161.8	Waste containing mainly Fe-oxides	[68]
Akaganeite	III	20,30,40ºC	n/a	+8.87		[65]
	V	20,30,40ºC	n/a	+56.43		
Mixture of Lepidocrocite, magnetite, goethite	?	?	-0.018	-34.7		[69]
Akaganeite	III	?	n/a	+20		[70]
	V	?	n/a	+8		
Siderite	V	15,25,35,45ºC	+0.11	+6.57		[71]
Fe-Al Binary Oxide	III	25,40,60ºC	-0.072	-12.64	Values for As = 10mg/l	[72]
	V	25,40,60ºC	-0.002	-24.53		

3.6 Operational and environmental implications for ATES systems

1. Operational implications

The findings of our sediments highlight the importance of considering other carbonate minerals than calcite when designing water treatment for high temperature ATES wells. Especially in groundwater with sufficiently high Fe concentrations causing the water to become supersaturated with respect to siderite at higher temperatures may cause precipitation of Fe containing carbonates can be a problem at increased temperature.

A second operational aspect is that of anaerobic corrosion due to sulfate reduction. The 60ºC data showed that sulfate reduction is occurring. This aspect is further investigated in column sediments run in batch mode reported elsewhere, but the initial findings show that this process has two distinctive temperature optima at 40 and 70ºC. Sulfate-reducing bacteria can be responsible for corrosion of metal surfaces under anaerobic conditions and were recently isolated in district heating systems causing serious corrosion and unexpected damage [73].

2. Implications for drinking water production

A number of environmental implications can be drawn from our data that are relevant for the groundwater's usability as raw water source:

First, various toxic substances are shown to be increasingly mobile under elevated temperatures (As, Mo, and V, and Be and Cr is sediments A and B). The responsible mechanism is, however, probably reversible; when the temperature is reduced it can be expected that these elements are re-sorbed. There is, however, a catch: field data show that a significant effect of ATES systems in the field is the mixing of different hydrochemical groundwater types [23]. The presence of sorbed As is likely to be limited to layers rich in iron(hydr)oxides and an increase in temperature will increase the aqueous As

concentration in these layers. Circulation of groundwater by ATES, will mobilise the heated groundwater enriched in As to layers having a lower content of iron(hydr)oxides. Even though the thermal impacts of the ATES system might dissipate when the system is de-commissioned, the effects of mobilisation and re-distribution of As and other elements will be irreversible.
A second environmental aspect is the increased DOC concentration in water. DOC can lead to discolouration of the water [74], which requires advanced energy intensive treatment processes such as ozonation [75]. In addition, the mobilisation of organic carbon leads to a reduction in SOM which in turn is a very important factor in immobilisation of organic pollutants [32]. Also, the humic substances can form complexes with trace elements, causing them to remain mobile and not become resorbed with decreasing temperature outside the direct zone of influence of the ATES system [32].

4 Hydrochemical modelling of 1 day residence time experiments

In the previous chapter we described the data of the column leaching experiments and provided a qualitative interpretation of the data obtained. In doing so, we developed a conceptual model. In the following, we test the validity of this conceptual model by hydrochemical modelling of the column experiment. Modelling potentially allows for a more quantitative derivation of ΔH_r values for the surface complexation reactions in the Dzombek and Morel database for As, B, PO_4, and SO_4 accounting for competitive sorption (this is ignored when using van 't Hoff plots).

4.1 Hydrochemical model description

Modelling framework, initial and boundary conditions
We used the modelling code PHREEQC version 2.18 [28] to simulate the inferred governing hydrochemical processes using the advection-dispersion-reaction equation. A combination of the Minteq.v4 database for aqueous speciation and the standard PHREEQC database for the description of cation-exchange and silicate minerals dissolution was used.

The sediment column was represented by 10 cells of 0.04 m length. The time and space discretisation of the multi-cell model was based on the condition that the cell size should be smaller than the twice the dispersivity ($\Delta x \leq 2\alpha_L$). It is further noted that Phreeqc automatically prevents any numerical dispersion in the way dispersion is simulated by the code. The tracer test showed that α_L is around 10 cm. Therefore, a cell size of 4 cm was selected, and a time step (i.e., residence time in a cell) of 24 h×60 min.×60 s/10 cells = 8640 s.

A constant flux of influent was applied at the inlet of the series of cells with a freely draining outlet cell. Each cell of the either one or twenty cell model contained reactive mineral phases. A 2^{nd} / 11^{th} cell was added to represent the sampling point which was kept at room temperature (20 °C) and did not contain any solid reactants. The applied room temperature for the sampling cell corrects for the temperature dependence of pH in the effluent (pH was measured at room temperature). The initial conditions in the sediment column for the reactive surfaces (minerals, cation-exchanger, iron-oxide surface) were set by first applying equilibrium between those phases and the initial aqueous solution at 11ºC (in-situ groundwater temperature). Because the initial pore water chemistry was not analysed, it was assumed equal to the average effluent composition as observed for the first three pore flushes from the 11ºC column. Table 4.1 presents an overview of the initial pore water concentration and the influent concentrations used in the model. It is noted that Fe is sampled after filtration over 0.45µm and considered to be Fe(II). In order to constrain the model's redox conditions, a very low Fe(III) concentration was entered which was not measured.

Table 4.1 Initial pore water and influent composition used for the PHREEQC simulations. All values are in mg/l, except when stated otherwise.

Element or parameter	Influent	Initial pore water
Temp	11	11
pH	7.2	7.2
Alkalinity (meq/l)	1.8	1.8
F	0.06	0.1
Cl	7.14	7.16
Br	0.04	0.03
SO_4	6	6
NH_4	0.087	0.087
NO_3	1E-09	1E-09
P	0.05	0.05
Doc	1.3	1.3
Na	5.57	6.6
K	0.82	1.42
Si	6.42	6.42
Ca	29.85	37.15
Mg	2.19	2.82
Sr	0.0896	0.0896
Fe(II)	0.26	0.28
Fe(III)	1E-09	1E-09
Mn	0.0769	0.0618
Al	0.015	0.0337
As	1.00E-06	0.0145
B	0.0017	0.05
Mo	0.002	0.002

Simulated processes

Based on the description in the previous chapter, we included the following hydrochemical processes: equilibrium calcite dissolution and gibbsite precipitation, kinetic K-feldspar dissolution, cation-exchange, surface complexation to iron-oxides, and kinetically-controlled sulfate-reduction coupled to oxidation of sedimentary organic matter (SOM). For calcite dissolution, cation-exchange, and K-feldspar dissolution, both the equilibrium constant (log10 of the equilibrium constant K, or -pK) and reaction enthalpy (ΔH_r in kJ/mol) are available in the combined Phreeqc/Minteq.v4 database allowing for temperature compensation according to the Van 't Hoff equation [32]:

$$\frac{\log K_{T_1}}{\log K_{T_2}} = \frac{-\Delta H_r}{2.303R}\left(\frac{1}{T_1} - \frac{1}{T_2}\right) \tag{4-1}$$

where K_{T1} and K_{T2} are the equilibrium constants at temperatures T_1 and T_2 (K), respectively, and R is the molecular gas constant (8.314 J K^{-1} mol^{-1}). However, reaction enthalpy data for surface complexation reactions with iron-oxides are absent in the combined Phreeqc/Minteq.v4 database. Therefore, reaction enthalpies were adopted from the constructed van 't Hoff plots (derived in the previous chapter).
The temperature dependence for each kinetic reaction was described with the Arrhenius equation [76]:

$$\ln\left(\frac{r_{T1}}{r_{T2}}\right) = \frac{-E_a}{R}\left(\frac{1}{T_1} - \frac{1}{T_2}\right) \tag{4-2}$$

where E_a is the activation energy (kJ mol^{-1}). Table 4-2 presents an overview of all included reactions and reaction related model parameters. In the following we discuss the different processes included in more detail.

Carbonate and gibbsite equilibria
Thermal gravimetric analysis (TGA) showed that the sediments contained ±0.5% d.w. carbonate. XRD analyses provided more detail to the mineralogy showing the presence of dolomite and Mg-calcite. Based on leaching pattern, and XRF results, it is further assumed that the carbonate contains a trace of Sr. To simulate the dissolution of an impure Ca-carbonate with traces of Mg and Sr, we simulated a carbonate solid solution and optimised for fractions of calcite, dolomite, and strontianite (respectively $CaCO_3$, $CaMg(CO_3)_2$, and $SrCO_3$). Dissolution of silicates can cause super saturation with respect to gibbsite which is found to readily precipitate during these reactions. In the PHREEQC model, an equilibrium (SI=0) was therefore imposed with respect to gibbsite.

Kinetic dissolution of K-feldspar
The PHREEQC database contains a rate equation describing the kinetic dissolution of K-feldspar based on Sverdrup [77] which we used as a starting point. A commonly observed feature for silicate weathering is that the weathering rate declines with progress of weathering [78, 79] caused by either: 1) incongruent dissolution and the formation of a altered layer [80, 81], or 2) precipitation of secondary minerals such as gibbsite and kaolinite on the surface of the primary dissolving minerals [82]. These processes are not included in the Svedrup rate equation. The decreasing K and Si production with increasing pore flushes observed in our experiments also point to a decreasing dissolution rate with time. Therefore, we combined the rate equation of Sverdrup [77] (equation 4-4) with an empirical relation based on a power law as used by White and Brantley [78] (equation 4-3) to describe the dissolution rate as a function of time:

$$R(t) = R_0 / t^m \quad \text{with:} \tag{4-3}$$

$$R_0 = \frac{A_{BET}}{V} k_{sum} = \frac{A_{BET}}{V} (k_{H^+} a_{H^+}^{n_{H^+}} + k_{H_2O} + k_{OH^-} a_{OH^-}^{n_{OH^-}} + k_{CO_2} P_{CO_2}^{n_{CO_2}} + k_{DOC} a_{DOC}^{n_{DOC}}) \tag{4-4}$$

Where R(t) is the dissolution rate in mol/l after t years and m is the power exponent. Note that t is not necessarily the age of the sediment but the time between R(t) and R_0. White and Brantley [78] found an average m value of 0.61 based on a large number of weathering experiments, and we adopted this value as an initial estimate and optimised it during model calibration. R_0 is the initial dissolution rate at t = 0 years in mol/l day for a fresh mineral (the meaning of 'fresh' is further discussed below, A_{BET} is the reactive mineral surface area (m^2) in contact with a volume V of water (l), and in parentheses are the individual contributions to the overall rate (k_{sum}) of protons, pure water, hydroxide ions, dissolved CO_2 gas, and dissolved organic carbon (DOC), described with a species specific rate constant (k) multiplied with the activity of the reacting species (a). The temperature dependence of each of the individual rate components was described with the Arrhenius equation [77]. Table 4-2 shows the values of each of the parameters in the rate equation 4-2 and the activation energies based on the results of several laboratory experiments conducted by Sverdrup [77]. The E_a values contained in the standard PHREEQC database are taken from a study on albite weathering presented in the same Sverdrup publication [77].

Table 4.2 Parameters used in kinetic modelling of K-feldspar dissolution. pk (-log(k)) and n values are defined for 25°C. Ea = activation energies. Values for OH^-, CO_2, and DOC were set equal to those for albite dissolution as observed by Sverdrup [77].

	pk (keq m^{-2} s^{-1})	n	Ea (kJ/mol)
H^+	12.5	0.5	60.0
H_2O	15.3	1	35.0
OH^-	14.2	0.3	32.1
CO_2	14.6	14.6	59.3
DOC	13.9	0.4	24.0

The water volume, V, (l) in contact with feldspar within the sediment (kg) is calculated with:

$$V = \frac{M_t n}{\rho_{solid,total}(1-n)} \tag{4-5}$$

where M_t is the total mass of dry sediment (usually taken as 1 kg), and $\rho_{solid,total}$ is the average dry density of all solids. A porosity of 0.32 and solid grain density of 2.65 kg/dm^3 (taken equal to the specific density of quartz) yield V = 0.18 dm^3/kg.
The initial reactive surface area of the mineral under consideration usually is determined in laboratory experiments with gas adsorption, a so called 'BET' measurement [83]. For natural or mixed sediments like the sediments used here, this method was not feasible. An indication of the initial reactive surface area was achieved from the geometric surface area, A_{geo}[77]:

$$A_{BET} = A_{geo}\lambda = \frac{6M_i}{\rho_{solid,i}\phi}\bar{d}\lambda \qquad (4\text{-}6)$$

where M_i is the mass of mineral i involved (kg) which has to be related to the volume of water in contact with this mineral, ρ_{solid} is the dry density of the mineral (ranging between 2.55 to 2.76 kg/dm^3; taken as ρ=2.65 kg/dm^3), ϕ is the sphericity of the grains (ranging between 0.85 to 0.9 [77], taken as 0.87), d is the average grain size (310 µm based on the median grain size shown in Table 2-1), and λ (surface roughness) is defined as the ratio between the BET surface area and the geometric surface area [84]. λ unfortunately is very poorly constrained but generally increases with age, ranging from λ=1 for synthetic freshly prepared minerals to around λ=400 for field minerals deposited >10^6 years ago [78]. This parameter was allowed to vary allowing for model calibration. An initial value of λ=40 was applied.

Kinetic sulfate-reduction
The reduced sulfate concentrations between outlet and inlet at 60°C are inferred to be the result of sulfate-reduction coupled to the oxidation of sedimentary organic material (SOM). The complete oxidation of SOM by sulfate takes place according to the following reaction:

$$2CH_2O + SO_4^{2-} \rightarrow 2HCO_3^- + H_2S$$

The kinetics of this reaction is commonly described with the following rate equation based on Monod kinetics [32, 85-87]:

$$r_{SOM} = r_{\max}\frac{m_{SO_4}}{k_{SO_4} + m_{SO_4}}$$

where r_{SOM} is the rate with which SOM is oxidized (mol/s which is equal to half the rate of SO_4 being reduced), r_{max} is the maximum rate constant [s^{-1}] and k_{SO4} is the half saturation constant of sulfate [mol/l]. Initial estimates for r_{max} and k_{SO4} are 10^{-13} [s^{-1}] and 10^{-4} [mol/l], respectively, based on Parkhurst and Appelo [28]. The E_a values were derived from running the experiments in "batch" mode to achieve longer residence times to enable a more accurate determination of those activation energies (reported elsewhere [88]).
The overall reaction does not consider the production of DOC which is actually produced as an intermediate product during sulfate reduction involving a number of steps [89]: 1) macromolecules present in SOM such as proteins, lipids, and polysaccharids are hydrolysed by hydrolytic bacteria to [32] monomers and polymers like amino acids, sugars and long-chain fatty acids, 2) the short chained monomers are further mineralised and fermented by fermentative bacteria into fermentation products such as volatile fatty acids (VFA) including acetate and butyrate, and 3) in the presence of sulfate, sulfate reducing bacteria will consume these VFAs and produce sulphide and CO_2 (which will react with water and dissociate into HCO_3-). In general, there is a close coupling between these three reactions and the intermediate products (which together with present humic and fulvic acids are analysed as the sum parameter DOC) are typically low in concentration. With increasing temperature up to 40°C, however, a decoupling is observed between biogenic hydrolysis, fermentation, and sulfate reduction steps leading to an accumulation of DOC [2]. Robador [2] concludes that it is unclear whether the decoupling of the rates of hydrolysis and SR is due to DOC becoming more refractory or due to limitations in the growth of sulfate reducing biomass.

Cation-exchange
Cation-exchange including Na, K, Ca, Mg, Fe, and Sr exchange were simulated as equilibrium reactions using exchange half-reactions based on the Gaines-Thomas convention [90]. The half-reactions are defined with logK values (called exchange coefficients) related to the reference half reaction, $Na^+ + X^-$ = NaX (logK=0). Initial values for those exchange coefficients and their enthalpies were taken from the

PHREEQC database and further optimised during model calibration. We assumed that within the 1 day of residence time, the aqueous solution and exchanger were in local equilibrium. This assumption is based on various studies on the kinetics of cation-exchange processes showing that equilibrium is achieved within several hours [91-93] and in agreement with the residence time applied in other studies where equilibrium for cation-exchange was assumed, e.g., 36 hours by DeSutter, et al. [94] which they note was more time than required to reach equilibrium for thin soil slices, 13.8 hours by Griffioen and Appelo [11] for aquifer sediments in a column of 136 mm length, and 6 to 24 hours by Bond and Phillips [95]. The exchanger content was estimated with an empirical regression equation [27] and expressed in meq/l pore water by multiplying the result with the ratio of bulk density and porosity:

$$CEC = \frac{\rho_b}{n}(4x\%clay + 12.5x\%SOM)$$

Where CEC is the cation exchange capacity (meq/l), ρ_b is the bulk density (kg/dm^3), n is the porosity (dimensionless), %clay is the percentage of clay (determined with laser grain size analyses) and %SOM is the organic matter content (determined with TGA).

Surface complexation of trace elements on iron oxides

Decreasing sorption with elevated temperature of iron(hydr)oxides for trace metals was found to result in the mobilization of trace elements including B, As, P and Mo. The content of the pool of reactive Fe-oxides in the sediments was determined with an oxalic acid extraction (Table 2-1), but no information is available on the variation in crystallinity of the present Fe-phases. Given the sulfate-reducing conditions (as shown by the lower SO_4 concentration in the outlet at higher temperature), the presence of ferrihydrite is unlikely as type of iron oxide as it is generally used as oxidiser prior to sulfate [96]. The reactive iron is, therefore, likely to be present in a relatively crystalline form, e.g., goethite. Although iron oxides were not identified by XRD analysis, the Sterksel formation is reported to have high concentrations of iron oxides [97] resulting in red to brown sediment color.

Calculations of surface complexation of trace elements on iron-oxides were performed with PHREEQC using the electrostatic diffuse double layer model of Dzombek and Morel (D&M) [57]. Although this model was initially developed for ferrihydrite, the model concept has successfully been applied to goethite [52]. The logK values describing the sorption equilibrium are fairly similar for goethite and ferrihydrite and the main difference between the two Fe phases is the specific surface area which is generally around a factor 10 smaller for goethite than for ferrihydrite. We used the following properties for goethite in the surface complexation model: surface area A_{Fe}=60m^2/g (based on reported values for goethite and hematite in [52]) and 14 g goethite/l (based on Fe from oxalic acid extraction), and optimised the model on the number of weak sorption sites /mol (N_w) while keeping the number of strong sorption sites constant at 1/40th of the weak sites (as defined in the original D&M database). Consistent with the D&M database, sorption of anions only takes place on weak sites, whereas cations sorb on both weak and strong sites. We only modified parameters for the weak sites, and strong sites are used as defined in the D&M database.

Equilibrium constants for protonation of the surface and for a large number of oxyanions and metals are included in the D&M model and present in the Minteq.v4 database used by Phreeqc. In order to describe the sorption behaviour of trace metals like As, B, and Mo adequately, we have expanded the D&M database with sorption equations for silica (based on [36, 37]), carbonate (present in the PHREEQC data and based on [98]), and DOC (based on [43]). These elements are present in relatively high concentrations compared with trace elements such as B and As and compete for sorption sites.

Shown in Table 4-3 are the reactions included that were found to play a substantial role in trace element sorption. For several species a number of dissociation reactions is present in the D&M database, but depending on pH and pe, only one reaction is often dominant in determining the sorbed concentrations. Therefore, we could limit the number of sorption reactions because the pH was buffered due to the presence of calcite and pe was not observed to change much. During model calibration, we optimised the pK and ΔH values for this selection of governing sorption reactions. Note the original D&M model only contains pK values, ΔH values were, therefore, optimised. Initial estimates for ΔH values were obtained from the literature for surface protonation, Si, and B as shown in Table 4-3, for As sorption, ΔH was based on the value estimated with the Van 't Hoff plot in the previous section.

Table 4.3: Reactions and parameters included in the PHREEQC-PEST model with initial and optimised parameter values. Calculated 95% uncertainty limits are shown in parenthesis; n.o. = not optimised.

Reaction	logK[1]		ΔH (kJ/mol)[1]		Other (optimized) Parameters
	Initial	optimized	Initial	optimized	
Equilibrium) calcite dissolution and gibbsite precipitation					
$(Ca_x,Mg_y,Sr_z)CO_3 + CO_2 + H2O \leftrightarrow xCa^{2+} + yMg^{2+} + zSr^{2+} + 2HCO_3^-$ Based on end members:					x = 0.89 (0.04) y = 0.10 (0.01) z = 0.01, n.o.
Calcite	-8.5	n.o.	-9.6	n.o.	
Dolomite	-17.1	n.o.	-39.4	n.o.	
Strontianite	-9.3	n.o.	-1.7	n.o.	
$Al(OH)_3 + 3\ H^+ \leftrightarrow Al^{3+} + 3\ H_2O$	8.11	n.o.	-95.4	n.o.	
Kinetic K-Feldspar dissolution					
$KAlSi_3O_8 + 8\ H_2O \rightarrow K^+ + Al(OH)_4^- + 3H_4SiO_4^o$	-20.6	n.o.	128.95	n.o.	
Rate equation: $R(t) = R_0 / t^m$ with: $R_0 = \frac{A_{BET}}{V} k_{sum}$ $A_{BET} = A_{geo}\lambda = \frac{6M_i}{\rho_{solid,i}\phi}\bar{d}\lambda$					A_{geo} = 71 dm^2 V = 0.18 dm^3/kg λ = 38.0 (3.3) m=0.70 (0.08) (E_a for individual parameters are not optimized)
Cation exchange					
CEC (X)					X = 0.047 meq/l
$K^+ + X^- \leftrightarrow KX$	0.7	0.8 (0.6)	-4.3	-6.3 (2.9)	
$Ca^{2+} + 2X^- \leftrightarrow CaX2$	0.8	0.1 (0.7)	7.2	8.0 (3.5)	
$Mg^{2+} + 2X^- \leftrightarrow MgX2$	0.6	0.2 (2.7)	7.4	7.8 (3.5)	
$Sr^{2+} + 2X^- \leftrightarrow SrX2$	0.91	0.7 (3.5)	5.5	5.5 (3.6)	
Kinetic sulfate-reduction:					
$2CH_2O + SO_4^{2-} \rightarrow 2HCO_3^- + H_2S$ Rate equation: $r_{SOM} = r_{\max}\frac{m_{SO_4}}{k_{SO_4} + m_{SO_4}}$					r_{max} = 3 x 10^{-11} day^{-1} k_{SO4} = 9.6 mg/l E_a = 60 kJ/mol
Surface complexation to weak sites of goethite					
Surface complexation constants:					A_{Fe} = 60 m^2/g N_w = 0.009 (0.003) mol/l $N_s = N_w/40$ W = 14 g/l
$\equiv FeOH + H^+ \leftrightarrow \equiv FeOH^{2+}$	7.29	n.o.	-47.3[2]	n.o.	
$\equiv FeOH \leftrightarrow \equiv FeO^- + H^+$	8.93	n.o.	54.0[2]	n.o.	
$\equiv FeOH + H_4SiO_4 \leftrightarrow \equiv FeH_3SiO_4 + H_2O$	3.6[3]	4.7 (0.4)	-43.7[3]	-11.1 (34)	
$\equiv FeOH + H_3AsO_3 \leftrightarrow \equiv FeH_2AsO_3 + H_2O$	5.42[4]	5.9 (0.4)	-80[5]	-47.5 (33.5)	
$\equiv FeOH + MoO_4^{2-} + H^+ \leftrightarrow \equiv FeMoO_4^- + H_2O$	9.5	14.6 (0.7)	-80[6]	-65.9 (69.4)	
$\equiv FeOH + H_3BO_3 \leftrightarrow \equiv FeH_2BO_3 + H_2O$	0.62	4.6 (0.3)	-13.8[7]	-24.9 (33.9)	
$\equiv FeOH + CO_3^{2-} + 2H^+ \leftrightarrow \equiv FeHCO_3 + H_2O$	20.4[8]	n.o.	-80[6]	-87.4 (48.8)	
$\equiv FeOH + DOC^- \leftrightarrow \equiv FeOHDOC^-$	10.3[9]	8 (3.55)	-80[6]	n/a (∞)	
$\equiv FeOH + DOC^- + H^+ \leftrightarrow \equiv FeDOC + H_2O$	2.41[9]	7 (0.63)	-80[6]	-27.7 (69.8)	
$\equiv FeOH + PO_4^{3-} + H^+ \leftrightarrow \equiv FePO_4^{2-} + H_2O$	17.72	23.5 (1.2)	-80[6]	-48.5 (107.6)	
$\equiv FeOH + PO_4^{3-} + 2H^+ \leftrightarrow \equiv FeHPO4^- + H_2O$	25.39	28.7 (0.8)	-80[6]	-41.6 (57.7)	
$\equiv FeOH + PO_4^{3-} + 3H^+ \leftrightarrow \equiv FeH_2PO4 + H_2O$	31.29	30 (2)	-80[6]	-361 (146)	
$\equiv FeOH + Ca^{2+} \leftrightarrow \equiv FeOCa^+ + H^+$	-5.85	n.o.	35[10]	22 (173)	
$\equiv FeOH + Mg^{2+} \leftrightarrow \equiv FeOMg^+ + H^+$	-4.6	n.o.	80[10]	40.2 (71.7)	

Notes:
1:All values are derived from PHREEQC database, unless stated otherwise
2: Based on [99]
3: Based on [36, 37]
4: Value for goethite, 2pK model [52]
5: Value from van 't Hoff plot, previous chapter
6: No value available, assumed equal to As
7: Value for hydrous Al-oxide from [100]
8: Value from [98]
9: Value for 2,3 DHBA (a NOM analogue organic acid) sorption on goethite [43]
10: Value for ferrihydrite from [101]

Model optimization
The non-linear parameter estimation program PEST [102] was used to constrain parameters for which none or only few literature values were available. PEST minimises the sum of the squared differences between observed and modelled hydrochemical data using the Gauss-Marquardt-Levenberg method. The squared differences for each observation group (i.e., all observations of pH, alkalinity, SO_4, K, Ca, Mg, Sr, Fe, Mn, Si, As, B, Mo, P, and DOC) are given a weight defined by the inverse of the observed average concentration in the observation group according to the method described by Dai and Samper [103]:

$$w_i = \frac{1}{E_i \sigma_i}$$

where E_i and σ_i are the analytical error and standard deviation of the observations for species i, respectively. Initial runs of PEST with the applied procedure showed that parameters were very poorly constrained leading to very large 95% confidence intervals (CI) for the parameters involved. In order to adequately include literature based initial estimates for certain parameters we included prior information in the model for the cation-exchange logK and ΔH values, and the logK values for surface complexation. The use of prior information is included in the objective function that PEST minimizes and limits the uncertainty for the parameter values found [103]. PEST was also used to calculate the correlation between model parameters, which can be used to test the models' solution uniqueness.

4.2 Results and discussion

Model calibration and simulation results
Figure 4-1 show the simulated and observed pH, alkalinity, SO_4, K, Ca, Mg, Sr, Si, As, B, P, and DOC concentrations. The model matches overall concentration patterns for most species well. The simulated Ca, Mg, Sr, and alkalinity match the general increased concentration levels observed for the effluent, suggesting that the dissolution of a carbonate solid solution is an adequate explanation. The model could not reproduce the subtle concentration variations among the different temperatures and with time. The similarity between the effluent concentrations of these species at the different temperatures shows that the under-saturation of the influent with respect to carbonates is the main driver for dissolution.

Overall, the resemblance between observed and simulated K and Si concentrations support the hypothesis that K-feldspar dissolution is responsible for the enrichment of these solutes. In contrast to the species involved in carbonate dissolution, K and Si concentrations show substantial differences between the different testing temperatures. The 60°C effluent is strongly enriched in Si and K, whereas the 25 °C column shows a much smaller enrichment in K. The 5 and 11°C effluents have K and Si concentrations which are nearly identical to the influent concentrations.

The species that are controlled by surface complexation, including As, B, Mo, and P, show a reasonable resemblance between observed and simulated concentrations. All species show gradually decreasing concentration levels which can be explained by as follows: The model first equilibrates the reactive surface (the iron oxide) with the initial pore water composition at 11°C. Upon a temperature increase, the equilibrium constant and intrinsic sorption capacity decrease for sorption reactions with a negative enthalpy (exothermic sorption) and increase for those complexation reactions with a positive enthalpy. For example, Ca and Mg. This causes the aqueous concentration for a species with an negative surface complexation enthalpy such as As and B to increase and its sorbed concentration to decrease. PHREEQC calculates the sorbed and aqueous concentrations at equilibrium for the given temperature. With progressing pore flushes, the sorbed concentration for these oxyanions gradually decreases as the previously sorbed species is flushes out. Species that have a surface complexation reaction with a high log_k (and are thus strongly sorbed), show a strong retardation in the column and it takes a large number of pore flushes to reach the influent concentration, whereas species that have a low equilibrium constant (e.g., B) reach influent concentration levels within a few pore flushes.

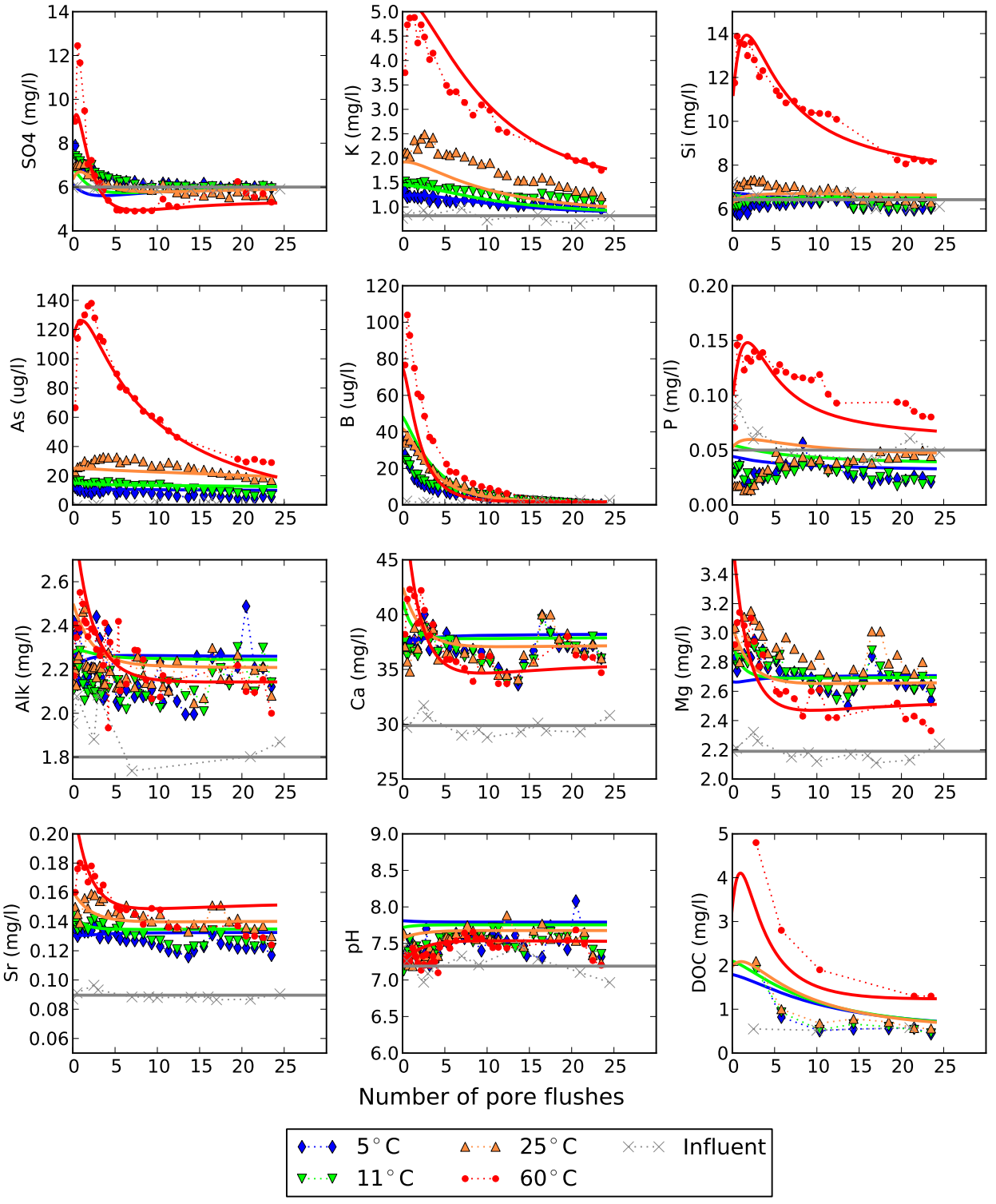

Figure 4-1 Model simulation of experiment C of elements related to silicate and carbonate dissolution, sulphate reduction and surface complexation. Observations are represented by dots, simulations are shown by lines in same colours as the corresponding dots.

Optimised parameters and solution uniqueness

The optimised parameter values are shown in Table 4.3 with the 95% confidence intervals (CI) which give an indication of their accuracy. The model solutions' uniqueness is further explored with the correlation matrix presented in Table 4.4.

The logK values for Ca and K cation exchange are within the literature ranges compiled by Karlsen, et al. [104]: For K-exchange a range was found of $logK_{Na/K}$ = 0.15 to 2.6 (our logK=0.8±0. 6), for Ca a range was found of $logK_{Na/Ca}$ of 0.29-2.44 (our logK = 0.1±0.7), and for $logK_{Na/Mg}$ a range was documented of 0.16-1.62 (our logK=0.2±2.7). For all exchange coefficients, the calculated CI is large compared to their optimised values. This large uncertainty results from other processes also influencing K, Ca, and Mg concentrations (carbonate and K-feldspar dissolution). Note the CEC is kept constant in the optimisation. Allowing a variation in this parameter (which was estimated with an empirical relation) would further increase the CI.

Values of ΔH for cation exchange are less frequently reported in literature than the equilibrium constants. The PHREEQC database, however, does contain for all cation exchange reactions enthalpies which were used as initial values derived from a number of studies [34, 105, 106]. Appel, et al. [107] report a quite large range of values for $\Delta H_{Ca/K}$ compiled from literature from -3.3 to -16.3 kJ/mol showing that estimates reported in literature can vary considerably.

The optimised logK values for surface complexation are generally not far off the initial values derived from the PHREEQC database based on the D&M database with the exception of logK values for Mo and B. For these species, it is noted that inspection of the sorption data and fitted models in the original work by Dzombak and Morel [57] shows that the sorption edges are predicted well for acidic pH values when the sorbed fraction > 10%. At neutral pH, the sorbed fraction is less and the simulated pH sorption edges for B and As generally under estimate the observation data. Because our experiments are performed only at neutral pH, the equilibrium constants for surface complexation are increased during model calibration to compensate for the mismatch between observed and predicted sorption in the original data. This however implies that the values that we report here are likely to overestimate the extent of sorption at more acidic pH values.

The found ΔH values show that sorption of oxyanions to iron oxide is exothermic with ΔH values ranging from -11.1 to -87.4 kJ/mol. Similar to the parameters found for cation exchange, the CI for most enthalpies is large compared to the optimised parameters. The poor parameter constraint is due to the high correlation between the different enthalpies (Table 4.3) which is caused by the nature of sorption. Sorption onto iron oxides is a competitive process implying that optimised logK values of different trace metals in mixed solutions are related to each other. For example, if sorption of one species is given a larger log_k, it means that other species will sorb less. The selectivity of a given species therefore depends on its own K value and the K values of the competing species. This results in a high correlation and large uncertainty of all K values.

Table 4.4 Selection of the correlation matrix for the parameters associated with surface complexation. R^2 values > 0.5 are shaded.

	ΔH_{As}	ΔH_{B}	ΔH_{PO4-1}	ΔH_{PO4-2}	ΔH_{Si}	ΔH_{SO4}	ΔH_{DOC-1}	ΔH_{Mo}	ΔH_{Ca}	$LogK_{As}$	$LogK_{SO4}$	$LogK_{B}$	$LogK_{Si}$	$LogK_{PO4}$	$LogK_{PO4-2}$	$LogK_{PO4-3}$	$LogK_{DOC-2}$	$LogK_{DOC-2}$	$LogK_{Mo}$	Nw
ΔH_{As}	1.00	0.97	0.88	0.96	0.95	0.03	0.88	0.85	0.02	-0.14	0.00	-0.16	-0.08	-0.34	-0.15	-0.47	-0.35	0.00	-0.31	-0.11
ΔH_{B}		1.00	0.86	0.95	0.93	0.02	0.86	0.84	0.02	-0.15	0.00	-0.14	-0.09	-0.35	-0.19	-0.47	-0.36	0.00	-0.32	-0.14
ΔH_{PO4-1}			1.00	0.90	0.84	0.04	0.81	0.78	-0.07	-0.07	0.00	-0.06	-0.03	-0.04	-0.15	-0.59	-0.20	0.00	-0.16	-0.12
ΔH_{PO4-2}				1.00	0.91	0.00	0.89	0.86	-0.10	-0.15	0.00	-0.16	-0.08	-0.32	-0.25	-0.49	-0.36	0.00	-0.31	-0.20
ΔH_{Si}					1.00	0.01	0.83	0.82	-0.02	-0.14	0.00	-0.16	-0.22	-0.31	-0.06	-0.39	-0.32	0.00	-0.27	-0.08
ΔH_{SO4}						1.00	0.04	0.04	-0.13	-0.03	0.00	-0.04	0.02	-0.04	0.13	-0.11	0.00	0.00	0.01	0.13
ΔH_{DOC-1}							1.00	0.79	-0.08	-0.25	0.00	-0.27	-0.19	-0.31	-0.12	-0.46	-0.24	0.00	-0.33	0.04
ΔH_{Mo}								1.00	-0.20	-0.22	0.00	-0.24	-0.16	-0.41	-0.13	-0.40	-0.38	0.00	-0.19	-0.06
ΔH_{Ca}									1.00	-0.12	0.00	-0.10	-0.09	0.08	-0.47	-0.29	-0.14	0.00	-0.25	-0.11
$LogK_{As}$										1.00	0.00	0.98	0.84	0.70	0.42	0.37	0.83	0.00	0.83	-0.53
$LogK_{SO4}$											1.00	0.00	0.00	0.00	0.00	0.00	0.00	0.00	0.00	0.00
$LogK_{B}$												1.00	0.83	0.71	0.37	0.34	0.81	0.00	0.83	-0.56
$LogK_{Si}$													1.00	0.55	0.26	0.24	0.65	0.00	0.67	-0.44
$LogK_{PO4}$														1.00	0.34	0.17	0.83	0.00	0.73	-0.13
$LogK_{PO4-2}$															1.00	0.60	0.60	0.00	0.56	0.47
$LogK_{PO4-3}$																1.00	0.45	0.00	0.44	0.16
$LogK_{DOC-2}$																	1.00	0.00	0.83	-0.12
$LogK_{DOC-2}$																		1.00	0.00	0.00
$LogK_{Mo}$																			1.00	-0.23
Nw																				1.00

Changes in composition of reactive surfaces

In order to explore the geochemical changes occurring during the column experiments, PHREEQC was used to calculate the composition of i) the cation exchange complex and ii) the iron oxide sorption sites complex (Figure 4-2).

Major shifts in the cation exchanger composition affect Ca which is already the dominant species sorbed at 11°C but becomes even more dominant at 60°C. Combining the ΔH values for the half exchange reactions of K and Ca according to Hess' law shows that K-Ca exchange is the most exothermic one of all cation exchange combinations (Table 4-2). But although between 5 and 25°C a decreasing K fraction is calculated, as is expected from its exothermic nature, at 60 °C the K fraction is nearly the same as the initial fraction. This is due to the enhanced release of K from K-feldspar dissolution increasing its aqueous concentration and thereby also increasing the sorbed K fraction.

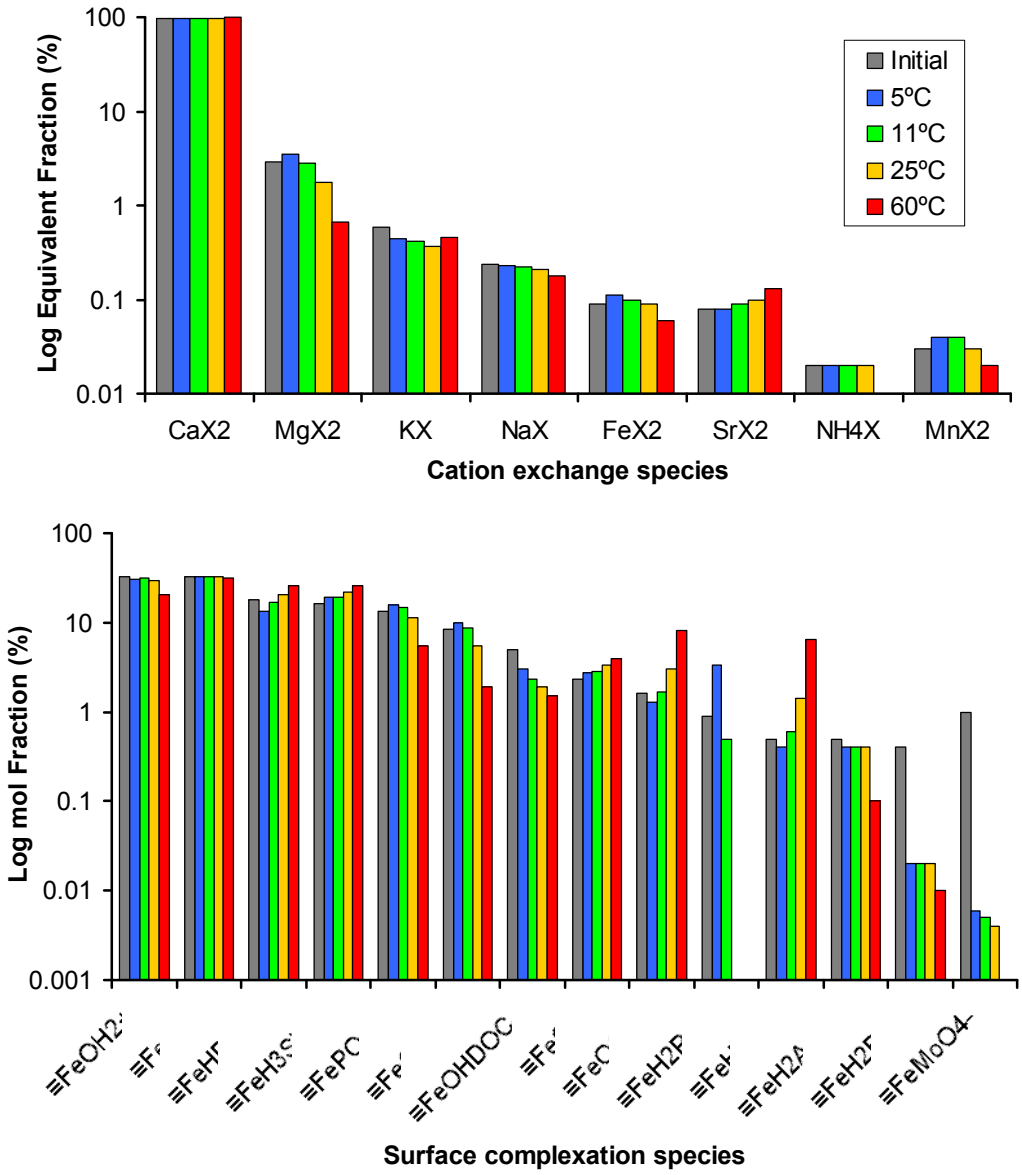

Figure 4-2 Simulated composition of the cation exchanger and surface complexation surface before the experiment starts and at the end of the experiment (following 25 pore flushes) for 5 °C, 11 °C, 25 °C, and 60°. Total sorbed P is represented by ≡Fe-P

The changes in the surface complexation sorption complex show that the release of As, B, Mo, and P with increasing temperature is compensated by an uptake of primarily Ca^{2+}, $H4SiO4^{0}$ and CO_3^{2-}. Note that for P sorption there is a shift between the different P-species sorbed, but overall there is a small

relative decrease in the fraction sorbed leading to considerable effects to P in solution (total sorbed is indicated separately). The increase in sorption of the cations with increasing temperature resulting of automatic model calibration are consistent with the findings of Trivedi and Axe [101] who show that the adsorption enthalpy is a function of the structural parameters and charge of the sorbing ion:

$$\Delta H = f\left(Nx\frac{Z^2}{R_H} \right)$$

where N is the hydration number, Z is the valence of the ion and R_H is the radius of the hydrated ion. Neutral oxyanions like $B(OH)_3$ and $As(OH)_3$ have no net charge, and it is unclear how this relation should be applied to them. It is however obvious from the that negative species like MoO_4^{2-} and PO_4^{3-} will have a negative and cations a positive ΔH.

This suggests that metals (such as Pb, Co, Zn, and Ni) are preferentially sorbed upon a temperature increase. No consistent decrease for these parameters with increasing temperature was observed in all of the three tested sediments, which was the case for arsenic. This is however likely due to the fact that these elements are initially present in concentrations near or below the detection limit and a further decrease is not significant. In the influent used with sediment B, concentrations of Co, Ni, Zn, and Pb were above the detection limit (not the case for experiment C). The 60°C effluent of sediment B did show a reduction in these species compared the lower temperatures confirming this hypothesis (Figure 4-3). Mann Whitney-U testing confirms that the 60°C effluents for sediment B has significantly lower concentrations in Cd, Pb, Zn, and Ni than the 11°C effluents ($P<0.01$). This difference between sorption behavior of metals and oxy-anions is an interesting topic for further investigations. The performance of water treatment using iron oxides (or other reactive surfaces) or in-situ groundwater remediation could be optimized by temperature control.

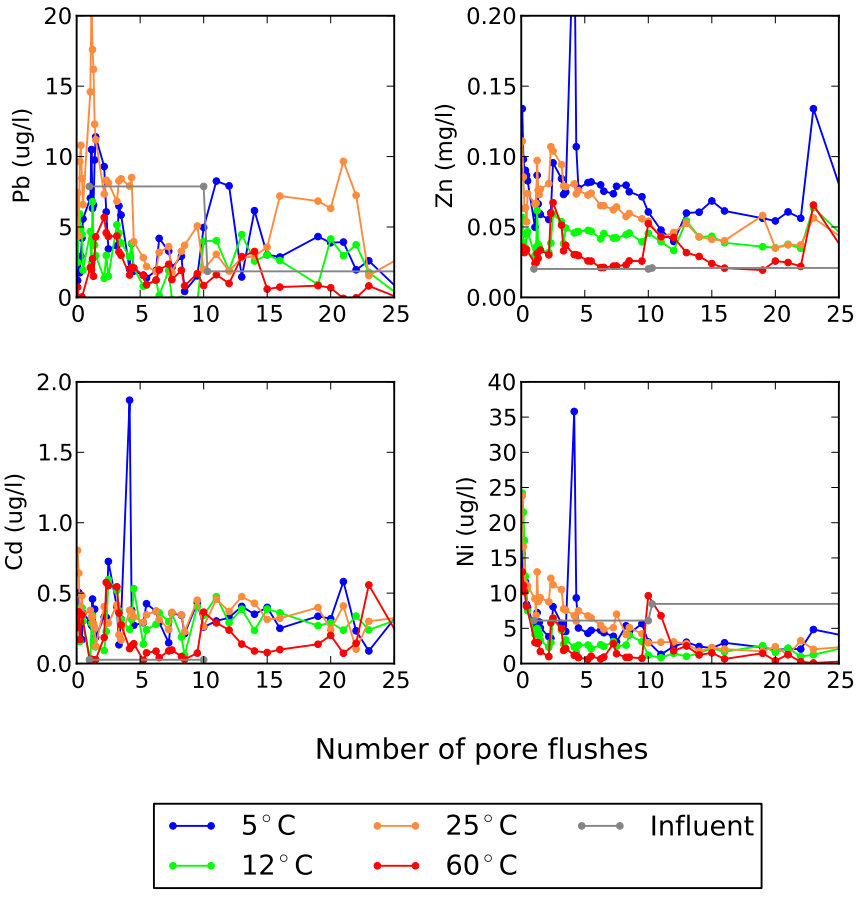

Figure 4-3 Concentrations of heavy metals Pb, Zn, Cd, and Ni measured during the experiments with sediment B.

5 Prolongued incubation time experiments

5.1 Introduction and objective

As discussed in chapter 1, most published research on ATES systems focuses on inorganic operational aspects, such as their scaling in relation to mineral precipitation occurring in high temperature systems (>40°C). Studies focusing on impacts of ATES on organic geochemistry and microbiological functioning are fewer. Brons *et al.* [17] and Jesuβek *et al.* [41] both report increased concentrations of dissolved organic carbon with increasing temperature in laboratory experiments. In a second study, Jesuβek *et al.* [108] added acetate to the incubated sediments and showed that sulfate reduction could take place at 10, 25, 40 and 70°C, thus far beyond the in-situ temperature. A shift in the microbiological community composition related to temperature was also observed by Brielmann *et al* [20] in an actual field ATES site resulting in temperature variations between 8.5 and 17.8°C, but the temperature and microbiological changes were of similar magnitude as those caused by a nearby infiltrating river.

Impacts on organic geochemistry and the microbiological functioning are relevant for groundwater quality and drinking water production for a number of reasons, both positive and negative: 1) Respiration of SOM and increasing concentrations of DOC can cause colour issues with water. 2) The removal of SOM can deplete soils from its contaminant buffering capacity. 3) On the other hand, the increased temperature may enhance biodegradation and remove contaminants more quickly than at natural conditions. These processes are also relevant for operating an ATES system: sulfate reducing bacteria can cause corrosion to, and subsequent failure of ferrous metals, and to a lesser degree to stainless steel [109]. Corrosion damage to district heating infrastructure by sulfate reducing organisms was recently reported [73].

The aim of the experiments with longer residence time reported in this chapter is to investigate the influence of temperature (5-80°C) on redox hydrochemistry and associated microbiological changes of anoxic (primarily sulfate reducing) sediments. The novelty of this study compared to the earlier mentioned research is that we: 1) incubated anoxic aquifer sediments that were not exposed to oxygen, (freeze) drying, or frozen (the latter two are often used to prevent oxidation, but can impact on the microbiological community); 2) did not add acetate to force sulfate reduction or other redox reactions, which makes the experiments more representative for natural aquifer conditions where SOM is slowly mineralised through a sequence of hydrolysis, fermentation, and oxidation; 3) use the SO_4 reduction rate as a proxy for microbial activity and organic matter mineralisation combined with TRFLP fingerprinting to map the changes in microbiological diversity.

5.2 Redox geochemistry, Monod kinetics and temperature dependance

The sediments used here were taken from an anoxic, sulfate reducing aquifer. Iron reducing and methanogenic conditions were observed at other locations in the same geological formation, for example in Eindhoven [110] , but not at the site itself. Groundwater at depths where ATES systems are realised generally lack dissolved oxygen and nitrate (some exceptions are found in ice pushed areas in the Netherlands), so that redox reactions with these oxidants are not described here. Generally SOM oxidation by iron reduction (Eq. 5-1), sulfate reduction (SR, Eq. 5-2), and SOM fermentation coupled to methane production (Eq. 5-3) can be described with the following set of reaction equations and Gibbs free energies derived from [111]:

$$(CH_2O)_{106}(NH_3)_{16}(H_3PO_4) + 424FeOOH + 848H^+ \rightarrow 424Fe^{2+} + 106CO_2 + 16NH_3 + H_3PO_4 + 742H_2O \qquad \Delta G^0 = -1330\,kJ/mol \qquad (5\text{-}1)$$

$$(CH_2O)_{106}(NH_3)_{16}(H_3PO_4) + 53SO_4^{2-} \rightarrow 106CO_2 + 16NH_3 + 53S^{2-} + H_3PO_4 + 106H_2O \qquad \Delta G^0 = -380\,kJ/mol \qquad (5\text{-}2)$$

$$(CH_2O)_{106}(NH_3)_{16}(H_3PO_4) \rightarrow 53CO_2 + 53CH_4 + 16NH_3 + H_3PO_4 \qquad \Delta G^0 = -350 kJ/mol \qquad (5\text{-}3)$$

where ΔG^0 is the Gibbs free energy, or the energy yield of the reaction, based on CH_2O representing organic matter with oxidation state of glucose, standard conditions (1 atm, 1 mol concentrations) and a pH of 7, as reported by [111]. A more negative ΔG^0 value means more energy can be gained from a reduction reaction by microorganisms. Oxidation of SOM coupled with iron reduction (here as goethite) yields more energy than that coupled to SR and methane production. This difference in energy yields causes the typical redox zonation observed in groundwater where SOM oxidation takes place using the oxidant which generates the highest energy yield, or $O_2 > NO_3^- > Fe^{3+} > SO_4$ followed by direct SOM fermentation [32]. This is a generalisation because the actual energy yield also depends on the actual concentrations, pH, and temperature of the redox reaction [96]. And in the case of iron reduction, also on the crystallinity of the iron minerals: oxidation of goethite yields less energy than ferrihydrite [96] causing the latter iron minerals to be stable under sulfate reducing conditions whereas ferrihydrite is generally very reactive.

All these reactions are biologically catalysed; the abiotic, purely chemical reaction rate in sterile conditions is orders of magnitude lower than the biomediated reaction rates [32]. Biogenic turnover of organic carbon in either SR or methane formation is a three-step process (figure 5-1, reprinted from [89]): 1) macromolecules present in sedimentary organic matter (SOM) such as proteins, lipids and polysaccharides are hydrolysed by hydrolytic bacteria to monomers like amino acids, sugars and long-chain fatty acids, 2) the monomers are fermented by fermentative bacteria into fermentation products such as volatile fatty acids (VFA) including acetate and butyrate, and 3) in the presence of sulfate, sulfate reducing bacteria will consume these VFAs and produce sulphide and CO_2 (which will dissociate into HCO_3), and in the absence of SO_4, the VFAs are consumed by methanogens producing methane. In general, the production rate of fermentation products is overall rate limiting and the concentration of VFA will be very low.

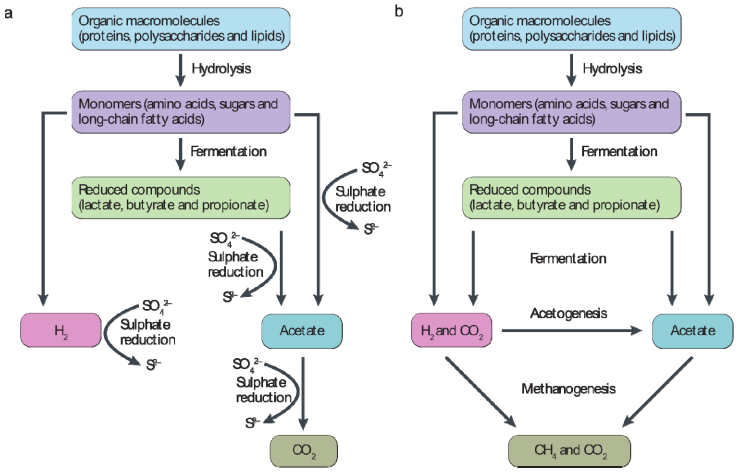

Figure 5-1 Flow diagram of organic carbon mineralization in the presence of sulfate by sulfate reducing bacteria (a, left) and in the absence of sulfate by methanogens (b, right) (from [89]).

The overall rate of SR is kinetically controlled and can be described with a Monod type expression rate [112, 113]:

$$r = r_{\max} \frac{m_{SO_4}}{k_{SO_4} + m_{SO_4}} \qquad (5\text{-}1)$$

Here, r is the rate with which sulfate is reduced (SRR in M/s), which -- in absence of other oxidants such as nitrate or oxygen -- equals the rate (both expressed in electron equivalents) at which SOM is being oxidized, r_{max} is the maximum rate constant [M/s], and k_{SO_4} is the half saturation constant [mol/l]. Initial estimates for r_{max} and k_{SO_4} are 10^{-13} [M/s] and 10^{-4} [mol/l] based on Parkhurst and Appelo, 1999 [28]. The temperature dependence of the redox reaction can be expressed using the Arrhenius equation which

shows that a linear relation exists between the natural logarithm of the reduction rate and the inverse of temperature eg [76]:

$$\ln(r) = \ln(A) + \left(\frac{-E_a}{R} \frac{1}{T} \right) \quad (5\text{-}2)$$

Where E_a is the activation energy (J mol^{-1}), R is the molecular gas constant (8.314 J K^{-1} mol^{-1}), T is the absolute temperature (K), and A is a constant. A commonly used parameter to express the temperature dependence is the Q_{10} which increase in reaction rate for a 10K increase in temperature [76]:

$$Q_{10} = \exp\left[\frac{E_a 10}{RT(T+10)} \right] \quad (5\text{-}3)$$

The results of the experiments were analysed using equations (5-1), (5-2) and (5-3) in order to derive values for r_{max}, E_a, and Q_{10} which are in combination with the microbiological data related to temperature. Modelling of SO_4 concentrations with the Monod rate equation was done using PHREEQC [28]. The reaction rate and activation energy were determined by minimising the difference between observed and simulated SO_4 concentrations using PEST [102]. We assumed a constant half saturation concentration of 10 mg/l. The activation energy was also determined for the DOC mobilisation. Based on the observed linear DOC increase with residence time observed in the data (Figure 5-2, discussed below), a zero order degradation rate is assumed and the activation energy is determined from the slope of an Arrhenius plot and Equation 5-2.

5.3 Results and discussion

5.3.1 Experiments with increasing residence time

Figure 5-2 shows the observed SO_4, DOC, Fe, and CH_4 concentrations as a function of residence time for sediments B and C. Methane was only measured during the experiment with sediment C.

The results in figure 5.2 show that during the experiment with sediment B at 5°C and 11°C, sulfate concentrations remained close to the influent concentration, implying that the SR rate is very low. The 25°C and 60°C effluents of sediment B show a clear decrease in sulfate concentrations with increasing residence time pointing to sulfate reducing conditions at both temperatures. For sediment C, decreasing SO_4 concentrations are observed with increasing residence times for all four temperatures. It is noted that saturation states of various sulfate salts calculated with PHREEQC (Table 5.1), all point to strong sub-saturation. This indicates that precipitation of sulfate salts is unlikely to explain the decreasing SO_4 concentrations making SR the most viable explanation for the reduced concentrations.

In the experiment with sediment B, DOC concentrations increased in the 60°C effluent with increasing residence time, whereas it remained similar to the influent concentration for the other three temperatures. In the experiment with sediment C, an increase in DOC production was observed at both 25°C and 60°C. DOC production progressed quite linearly with time. DOC accumulation with temperature increase in aquifer sediments was also observed by Brons, et al. [17] and more recently by Jesußek, et al. [41], and also in the 1-day residence time column experiments described in Chapter 3. In the 1-day residence time experiments, it was inferred that DOC production at elevated temperature was the result of both desorption from oxide mineral surfaces and hydrolysis of SOM to DOM. The steady increase in DOC concentration with residence time of several weeks observed here, suggests that the DOC accumulation is the result of transformation of SOM to DOC, and not to desorption. Desorption of DOC to equilibrium conditions is reported as a process that takes place on a time scale of hours to days [42, 114] and not weeks as observed here. Furthermore, the desorption rate decreases as it reaches equilibrium and does not steadily increase as observed here. It is however noted that there are not many studies on the desorption kinetics of DOC in sediments.

Oxidation of SOM by either sulfate comprises a number of steps and intermediate products such as VFA which make up the DOC. At in-situ temperatures, the intermediate products are generally kept at low concentrations, which is consistent with the observations presented for sediment C where SR is occurring at both 5°C and 11°C, but no increase in DOC is observed. Only if the hydrolysis rate exceeds the reduction steps, an increase in DOC is expected. Robador et al. [2] and Weston and Joye [3] observed such a decoupling between the different steps when marine sediments were incubated above their ambient temperature, leading to an accumulation of DOC. Brons et al. [17] using both sterilised and natural sediments in their experiments, however, concluded that the production of DOC at temperatures

above 30°C becomes an abiotic process and should be viewed as purely chemical hydrolysis of SOM. This distinction cannot be made from the data here.

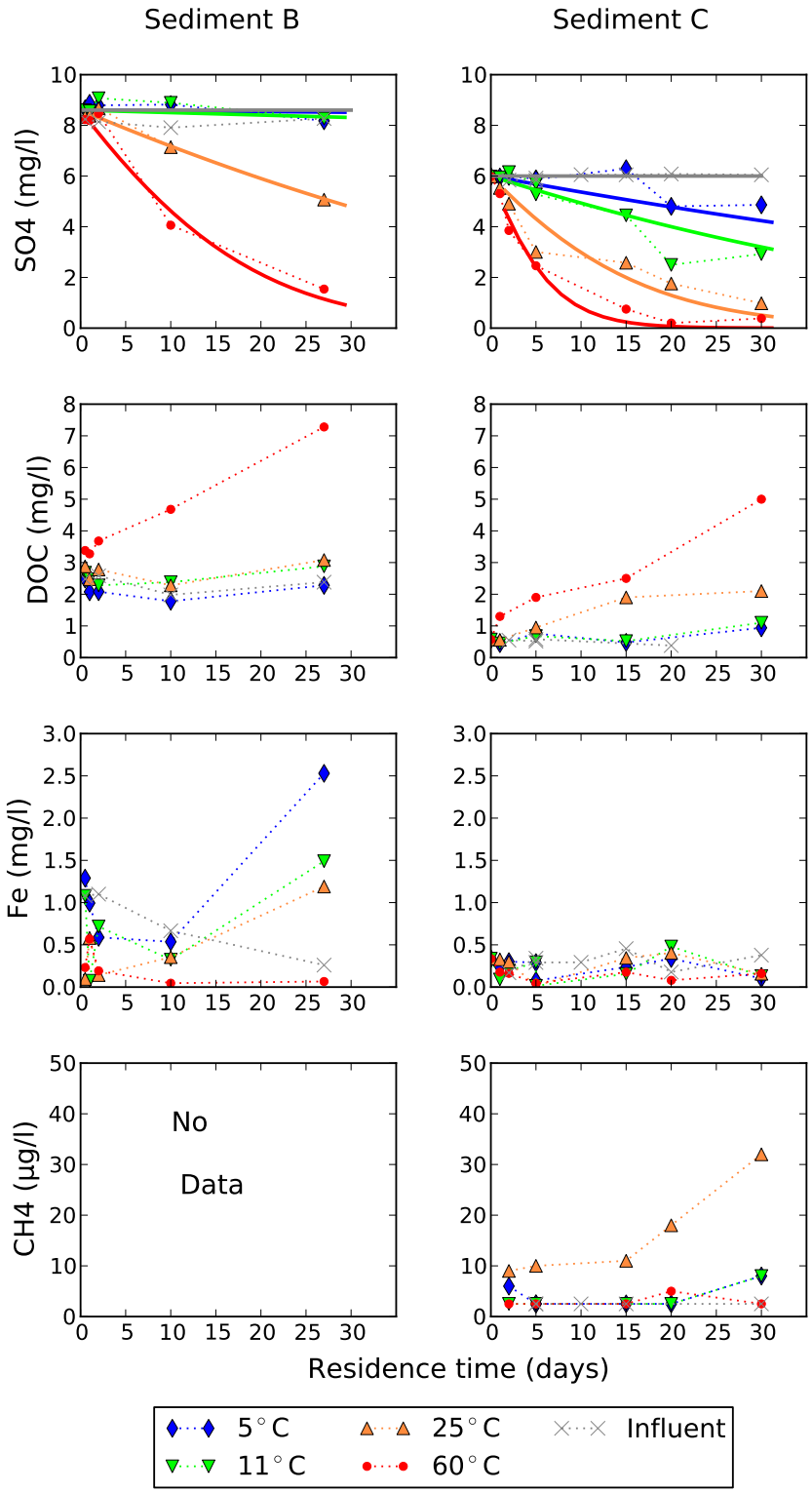

Figure 5-2 Observed concentrations of SO_4, DOC, Fe, and CH_4 (points and dashed lines) for effluents of sediments B and C as a function of residence time. SO_4 was also simulated with a Monod SO_4 reduction equation (solid lines)

Table 5-1 Saturation states of sulfate salts with respect to influent at 60°C, calculated with PHREEQC

Names	Influent used with sediment B	Influent used with sediment C
$Al_4(OH)10SO_4$	-10.12	-16.63
$AlOHSO_4$	-6.49	-9.56
Alunite ($KAl_3(SO_4)2(OH)_6$)	-4.39	-11.23
Anhydrite ($CaSO_4$)	-3.16	-3.16
Celestite ($SrSO_4$)	-3.78	-3.91
Epsomite ($MgSO_4:7H_2O$)	-6.41	-6.69
$Fe_2(SO_4)_3$	-45.36	-49.03
Gypsum ($CaSO_4:2H_2O$)	-3.06	-3.06
H-Jarosite ($(H_3O)Fe_3(SO_4)2(OH)_6$)	-21.1	-21.77
Na-Jarosite ($NaFe_3(SO_4)_2(OH)_6$)	-20.19	-20.43
Thenardite (Na_2SO_4)	-10.76	-11.83

The increasing Fe^{2+} concentration in the 5°C effluent of sediment B and to a lesser degree the 11 and 25°C effluents points to iron-reducing conditions. In the effluents of sediments C and that of the 60°C of sediment B, no increase in Fe^{2+} concentration is observed. This difference could be due to: 1) iron reduction is absent in sediment C due to the presence of more crystalline iron phases (e.g. goethite or hematite) in sediment C compared to sediment B, or 2) iron reduction is occurring but produced iron reacts with produced sulfide to form FeS or pyrite. During the late time data of sediment C's 60°C effluent, when SO_4 is nearly reduced to 0 mg/l, no increase is observed in Fe concentrations. This suggests that the first explanation is most viable for sediment C. FeS or pyrite require HS produced by sulfate reduction. If all sulfate is reduced, no more HS can be formed and Fe can no longer react to form Fe or pyrite.

For sediment B, SO_4 concentrations are still decreasing at the end of the experiment at 25 and 60°C, so here masking of iron reduction could also be an explanation. It is interesting to note that the data suggests that in sediment B, both sulfate and iron reducing conditions occurs simultaneously. This is contrary to the common observation that different redox zones are mutually exclusive. The concomitant occurrence of redox processes is however also observed in natural sediments by Jakobsen and Postma [115] who explain it by other processes (other than the terminal electron-accepting processes) in the system limiting the overall rate of organic matter oxidation. In the case of Jakobsen and Postma [115], dissolution of calcite increased the pH, lowering the energy yield of iron reduction which caused more favourable conditions for sulfate reduction. The effect of pH on redox reaction energy yield with iron reduction and sulfate reduction can also be seen from equations 5-1 and 5-2. Iron reduction consumes H^+ which implies that an increase in pH reduces the energy yield.

Only during the experiment with sediment C, methane was measured in effluents. The data shows that only in the 25°C effluent methane was measured in significant amounts. Methane in the 25°C effluent increased especially after 15 days, when nearly all SO_4 is removed.

5.3.2 Experiments with temperature ramping

Figure 5-3 presents the results of the experiments where the temperature is increased with 5°C increments for a 5 day incubation of sediment C. The reduced SO_4 concentrations compared to influent point to SR occurring at all temperatures, except 5°C. Over this temperature range (5-80 °C), two distinctive minima in SO_4 concentrations are observed at T_{opt} = 40 and T_{opt} = 70°C suggesting that these are temperature optima for distinct sulfate reducing bacterial populations. Between 45 and 50°C, SO_4 concentrations are very close to the influent concentrations, suggesting low SR activity which could be explained by a transition from mesophilic to thermophilic activity.

The emergence of a thermophilic bacterial community, far beyond the in-situ conditions has been reported before, mainly in marine cold sediments [116-120]. Using incubation experiments on arctic marine sediments Hubert, et al. [118] found two distinct SRR peaks at 32 and 56°C which occur at lower levels than the peaks found in this study. The in-situ temperature of those marine sediments was however also around 10°C lower than that at the present site. In terrestrial aquifer sediments, the emergence of thermophilic SR conditions are reported by Jesußek, et al. [108] who used sediments from

an oxic environment while tap water spiked with acetate was used as influent. The latter experiments were carried out at four temperature steps (10, 25, 50 and 70ºC) which did not allow derivation of a $T_{opt.}$

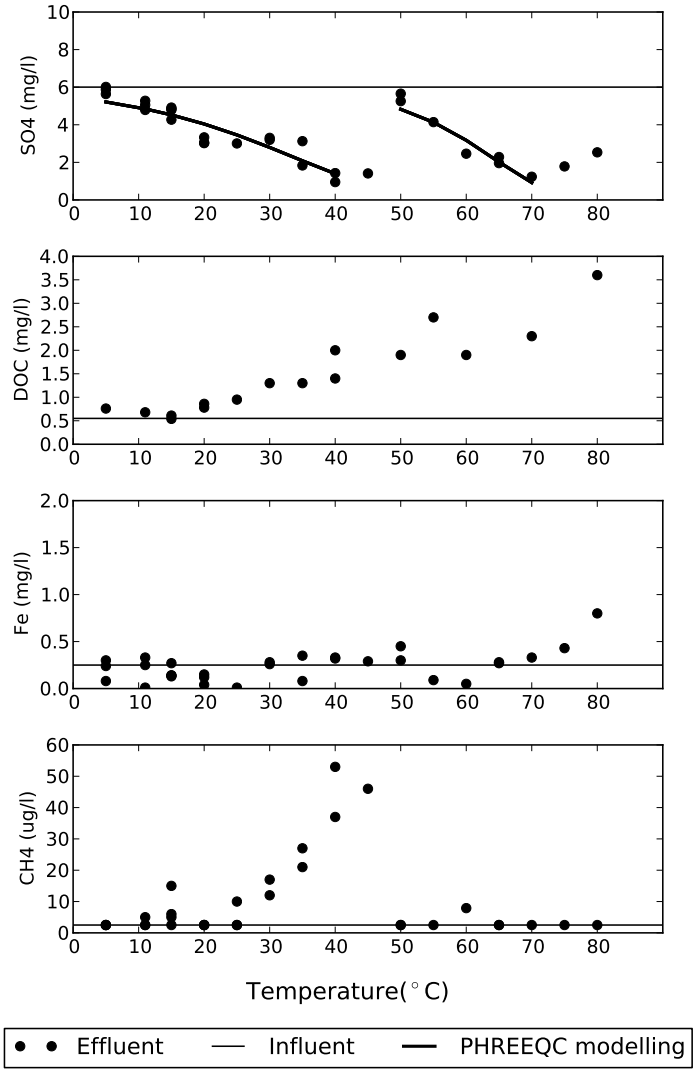

Figure 5-3 Observed concentrations of SO_4, DOC, Fe and CH_4 (points and dashed lines) for effluent with 5 day residence time at different temperatures. Also shown are the influent concentrations and the SO_4 simulated concentrations with PHREEQC

The DOC concentrations measured in effluents up to 15ºC are close to the influent concentration. Beyond 20ºC, a gradual increase in DOC is observed from 0.5 mg/l in influent to 3.6 mg/l at 80ºC. A key observation made from the generally steadily increasing DOC concentration pattern is that the data lack the presence of distinct minima as observed for sulfate. In the previous section, the decoupling between the reaction rates of the different steps involved in microbial respiration of SOM with increasing temperature was described as a cause for accumulation of DOC. The fact, that SR shows two clear temperature optima while DOC accumulation shows a fairly linear increase with temperature, suggests that the mobilization of DOC behaves like a chemical (abiotic) reaction, without a clear microbiologically set temperature niche. The conversion of SOM to monomers (which are measured with DOC) as shown in Figure 5-1 involves enzymes generated by the sulfate reducing organisms which catalyse the hydrolysis step. Wallenstein [121] describes that these enzymes are denaturated at temperatures far beyond their in-situ temperature. This makes it unlikely that biotic enzyme stimulated hydrolysis is responsible for the DOC production over the entire temperature range. As described earlier, Brons, et al. [17] attributed the DOC mobilisation beyond 55ºC to chemical mineralization which is supported by our

data. In a more recent study on DOC leaching from unsaturated soils, both sterilised and non-sterilised, Xu and Saiers [122] found an increase in DOC leaching from the sterilised soil supporting the hypothesis that the increased concentration of DOC was abiotic. Xu and Saiers [122] attributed the DOC mobilisation to desorption from soil particles and not as a result of SOM mineralisation.

The iron data in Figure 5-3 show no clear indications of iron reducing conditions over the temperature range. Methane production was greatest between 25°C and 40°C corresponding to the first region of maximum SRR. It is interesting that at the higher temperatures, no significant methane production is observed. Degassing could be an explanation for this, but at all temperatures, the methane concentrations remained well below the solubility as reported by Duan and Mao [123], ranging between 2470 and 250 µmol/l in pure water at 1 bar pressure for 0 and 60°C, respectively. The solubility decreases somewhat with increasing mineralization of the water but solubility is still well above the values measured here. An alternative explanation is that while thermophilic sulfate reducing bacteria are capable of spore formation, which were found in marine cold water sediments (e.g. [117, 119, 124]), methane producing archaea do not form spores.

5.3.3 Rates and activation energies for sulfate reduction

The data were further analysed to derive the kinetic parameters and activation energies. In Figures 5-2 and 5-3, the simulated SO_4 concentrations based on the optimised parameters for the Monod and Arrhenius equations (equations 5-1 and 5-2) are shown. Table 5-2 presents the optimised kinetic parameters, including the in-situ reduction rate ($r_{in\text{-}situ}$ in M/s) derived for the in-situ temperature ($T_{in\text{-}situ}$ in °C), the optimum rate (r_{opt} in M/s) and the corresponding optimum temperature (T_{opt} in °C), the temperature above which SR stops (T_{max} in °C), the derived activation energy and Q_{10} factor. Also shown is the 95% confidence interval calculated by PEST. For the increasing residence time data, only data for the lower three temperature steps are used as it can be seen from the temperature ramping data that the 5, 11, 25 and 60°C data are not on the same slope. For the temperature ramping experiment, two sets of maximum reduction rate and activation energy are determined based on the temperature ranges 5-40°C and 50-70°C.

In-situ SRR of $2.6x10^{-12}$ to $1.4x10^{-11}$ M/s at 11°C, and E_a values of 134±250 and 59±27 kJ/mol are found from the increasing residence time experiments on sediments B and C, respectively. The relatively large confidence interval for E_a of sediment B is the result of negligible SRR at 5 and 11°C. In sediment C, sulfate concentrations are decreasing more rapidly with progressive incubation time resulting in a much smaller confidence interval.

From the ramping experiment on sediment C, maximum SRR at optimum temperatures are derived of $8.7\pm2.3x10^{-10}$ and $9.9\pm2.2x10^{-10}$ M/s at 40°C and 70°C. Activation energies for the low and high temperature ranges are 44±20 and 88±47 kJ/mol, respectively. The resulting Q_{10} for the lower temperature range in sediment C is 2.4 for the increasing residence time experiment and 1.9 for the temperature ramping experiment, both near the Q_{10} of 2 generally expected for microbial processes. In sediment B, a higher activation energy and Q_{10} are found. The lower SRR for sediment B indicates the SOM is more recalcitrant than that in sediment C. This agrees with the conceptual model for temperature dependence of SOM turnover by Davidson and Janssens [125] in which recalcitrant soil organic matter results in low SOM breakdown rates and higher activation energies and Q_{10} values.

Also shown in Table 5-2 is a compilation of SR kinetic and thermodynamic data derived from literature for marine, aquifer, and geothermal sediments. Data on SR for aquifer sediments are few: Jakobsen and Postma [126] performed in-situ measurements on SRR and compared the results to values found in literature for sediments of different ages. The data shows that the oldest sediments yield the lowest rates, with the limitation made by Jakobsen and Postma [126] that diagenetic history and nature of organic matter will also play a role. The sediments we used are of the fluvial Sterksel formation, deposited during the later part of the Early Pleistocene and the Middle Pleistocene [97]. The SRR for sediment B ($2.6x10^{-12}$ M/s) falls within the range reported for Pleistocene sediments ($4.1x10^{-13}$ to $1.2x10^{-11}$ M/s) while that of sediment C ($1.4x10^{-11}$ M/s) is just above the range. This could be attributed to the fact that the SRR by Jakobsen and Postma [126] are based on field estimates, which generally yield lower values than laboratory estimates. Homogenization of the sediment is known to enhance the availability of organic carbon and increase SRR [127]. Hansen, et al. [127] found that SRR determined in homogenized samples is between 1.1 and 3.2 times higher than that determined in undisturbed cores.

Table 5-2 Results of kinetic and thermodynamic sulfate reduction parameters derived with PHREEQC/PEST for fluvial Pleistocene sand. Shown are derived best fit values and the standard errors (±). Also shown are values reported in literature for marine and aquifer sediments. If two samples are available, the range is shown. With more samples the average and standard deviation are shown.

Sediment type or experiment	$T_{in\text{-}situ}$ (ºC)	T_{opt} (ºC)	T_{max} (ºC)	$r_{in\text{-}situ}$[5] (M/s)	r_{opt}[5] (M/s)	E_a (kJ/mol)	Q_{10}	Source
Our experiments								
A. Increasing residence time								
Sediment B (5-25ºC)	11	n.a.	n.a.	$2.6x10^{-12}$	n.a.	134±250	7.0	
Sediment C (5-25ºC)	11	n.a.	n.a.	$1.4x10^{-11}$	n.a.	59±27	2.4	
B. Temperature ramping								
Sediment C (5-40ºC)	11	40	47	n.a.	$8.7±2.3x10^{-10}$	44±20	1.9	
Sediment C (50-70ºC)	11	70	>80	n.a.	$9.9±2.2x10^{-10}$	88±47	3.6	
Literature values for aquifer sediments								
Rømø aquifer, Holocene sediment				$1.6 - 140x10^{-12}$				[126]
Tuse Næs, Pleistocene sediment				$5 - 12 x10^{-12}$				
Data compilation of others:								
Cretaceous rock				$2.2 - 48x10^{-16}$				
Tertiary rock				$3.2x10^{-15}$				
Cretaceous rock				$6.3x10^{-15}$				
Pleistocene sediment				$4.4x10^{-13}$				
Pleistocene sediment				$4.1x10^{-13}$				
Pleistocene sediment				$7.3x10^{-13}$				
Reactive permeable aquifer barrier				$1.3x10^{-9}$		40	1.8	[85]
Literature values for marine and estuarine sediments (all Holocene)								
Arctic sediments, n=10	3.2	22.6	33	$2.3±3.1x10^{-10}$	$1.5±1.7x10^{-9}$	34±11	2.5±0.4	[76]
Estuarine sediments, moderate climate, n=6	3-27			$4.5±4.1x10^{-9}$	$7.2±7.4x10^{-9}$	51±19	2.3±0.6	[128]
Marine sediments Arctic	2	22-32	40	$0.9-5.1x10^{-10}$	$1.3x10^{-8}$	50	2.1	[129]
Moderate climate	3-20	30-36	>40	$0.2-7.6 x10^{-10}$	$3.1x10^{-8}$	81	3.2	
Literature values for geothermal sediments								
Hydrothermal vent sediment at : $2.2 x10^{7}$ Pa (in situ) (73-100ºC)	80	100	105	$1.5x10^{-8}$	$1.3x10^{-7}$	115[1]	5.3	[130]
$4.5 x10^{7}$ Pa (73-95ºC)	80	95	105		$1.6x10^{-7}$	96[1]	4.0	
Yellowstone geothermal Park: Obsidian pool, 35, 65, 85ºC	85			$2.9 x10^{-10}$		17	1.2	[131]
Black sediment pool, 30, 40, 70ºC	70			$4.9 x10^{-9}$		38	1.5	
Mushroom spring, 30, 60, 70ºC	60			$6.4 x10^{-9}$		119	3.8	
Guaymas Basin hydrothermal vent: sample A (53-63ºC)	25	63	67		$3.2 x10^{-9}$	254[2]	40	[132]
sample B (70-77ºC)	70	77	83		$1.9 x10^{-9}$	334[2]	127	
sample C (60-83ºC)	75	83	90		$6.9 x10^{-9}$	102[2]	4.4	
Literature values for incubated experiments at both low and high temperatures								
Marine Arctic sediment: Psychrotolerant range (0-22ºC)	-2 - +4	22	32	$1 – 15 x10^{-10}$	$1.4x10^{-9}$	71[3]	2.8	[117, 118]
Thermophilic range (47-56ºC)	-2 - +4	56	64	$1 – 15 x10^{-10}$	$8x10^{-8}$	98[3]	4.1	
Marine moderate sediment Mesophilic range (0-40ºC)	0-15	31	40	$5.8 x10^{-10}$	$5.8x10^{-9}$	75[4]	3.0	[119]
Thermophilic range (45-58ºC)	0-15	58	65		$5.1x10^{-9}$	199[4]	17.9	
Geothermal lacustrine sediment: Mesophilic range (20-50ºC)	60-101	45			$1.2 x10^{-9}$			[133]
Thermophilic range(50-82ºC)	60-101	65	82		$1.2 x10^{-9}$	114	3.3	

Note: 1. Calculated with SRR and temperatures shown in Table 1 in [130]. 2. Based on SRR and temperatures shown in Figure 6 in [130]. 3. Based on SRR and temperatures shown in Figure 1 in [118]. 4. 3. Based on SRR and temperatures shown in Figure 1B in [119]. 5. Marine SRR are often reported in nmol/cm^3 /day determined by ^{35}S radiotracer method where SR is determined per cm3 sediment. These values are converted to a SR in M/s using the published porosity for the sediment used. If no porosity is given, a porosity of 0.5 was assumed.

Only one study was found that contained an estimate of the SR activation energy for aquifer sediments [85]. This study however describes a reactive barrier consisting of organic matter derived from municipal waste and cannot be regarded as representative for groundwater conditions. The derived SRR is two orders of magnitude higher than found in our experiments. The activation energy of 40 kJ/mol is however not far from our derived value.

Because data on activation energies in aquifer sediments are few, we included a number of studies on marine (generally cold water) sediments in Table 5-2 which contain activation energies. The SRR for aquifer sediments are generally lower than those observed in marine sediments, which is likely the result of the fact that all marine sediments are generally collected within a few centimetres depth and are much younger than aquifer sediments. Two studies contain estimates of activation energies. The studies by Sawicka, et al. [76] and Marvin-DiPasquale and Capone [128] yielded E_a vales of 34±11 kJ/mol and 51±19 kJ/mol, respectively (the range presents the 95% confidence interval of 10 values). These values are in the same order of magnitude as observed for the low temperature range in sediment C.

A number of studies on SRR in geothermal sediments is shown Table 5-2 which generally yield high SRR and high E_a values. The SRR for these sediments is comparable to those observed in the arctic sediments. The E_a values for most studies are above 100 kJ/mol, with the exception of the results for Obsidian and Black Sediment Pools by Roychoudhury [131]. These E_a estimates can however be biased by the fact that the SRR was measured at only three temperatures. The lower of these temperatures is a rate probably representative of mesophilic SR organisms, while the higher temperature SR are likely to be representative for thermophilic organisms.

The last three SR studies shown in Table 5-2 involve incubation of sediments at temperatures far beyond their in-situ temperature. Both Hubert, et al. [118] and Isaksen, et al. [119] report SRR over a very wide temperature range and detect two SRR peaks. The data in the publications were used to derive activation energies. Like in our data, the SRR at T_{opt} for the two temperature ranges are quite similar, but E_a for the thermophilic range is higher than for the colder range. The study Elsgaard, et al. [133] was opposite to our experiment and that of Hubert, et al. [118] in the sense that mesophilic SR was induced in thermophilic sediments at a much lower temperature than in-situ conditions. This study only reported an E_a for the thermophilic range.

In conclusion, the results from our experiments and their comparison with the review presented in Table 5-2 show that the activation energies for experiments < 45°C ranges between 35 and 80 kJ/mol (ignoring our own E_a for sediment B because of its high confidence interval). Thermophilic sulfate reduction always has a higher activation energy, generally >100kJ/mol. A possible explanation for this phenomenon is that there is a fundamental trade-off in biochemical processes between the enzyme stability and activity [134]. The catalytic capacity of enzymes depends on their molecular flexibility which determines their capacity to bind and catalyse substrates [135]. Enzymes produced by thermophilic SR organisms require a higher thermostability making them less flexible and less efficient catalysts to hydrolyse and ferment SOM. This in turn results in higher E_a values for thermophilic enzymes compared to mesophilic enzymes.

5.3.4 Activation energy of organic carbon mobilisation

The temperature ramping experiment allows for the derivation of the activation energy of this process. We assume a zero order degradation of SOM. The rate of this is derived from the 5 day residence time experiments. The activation energy is subsequently derived from the slope of an Arrhenius plot and Equation 5-2. The results of this analysis are presented in Table 5-3, together with the results from other studies. It is noted that Brons, et al. [17] reported a very low E_a of 0.36 to 0.86 kJ/mol, which results in a Q_{10} of nearly 1. Translating the DOC concentrations measured in influent and effluents reported in Table 1 of Brons, et al. [17] to DOC respiration rates, and determining the Arrhenius slope of this yields E_a values similar to the other values.

The value reported by Xu and Saiers [122] is derived for temperature dependence of DOC leaching during column experiments with unsaturated sand samples. The E_a value shown in Table 5-3 for Jesußek, et al. [41] is derived by use of the DOC mobilisation rates described in the text of this paper. Overall, the similarity in derived E_a values between the studies is striking. Except for the peat value reported by Brons, et al. [17], the values found show a narrow range of 32.9 and 37.3 kJ/mol. The similarity in values, irrespective of redox and saturation conditions, supports the hypothesis that DOC mobilisation is a pure chemical process.

Table 5-3 Thermodynamic parameters for DOC mobilization derived from our temperature ramping data, and a comparison to values reported in literature and values calculated from data reported in other studies.

Experiment and material	Method	E_a (kJ/mol)	Q_{10} (11ºC to 21 ºC)	Source
Our data	Calculated from temperature ramping experiment	32.9	1.61	
Anoxic and oxic sand and peat samples for ATES research	Written in text	0.36 - 0.86	1.005-1.013	[17]
	Based on DOC production rate in sand sample Table 1 of this study	35.3	1.67	
	Based on DOC production rate in peat sample Table 1 of this study	52.4	2.14	
Unsaturated column studies	Derived with modelling	34.0	1.64	[122]
Oxic sand samples for ATES research	Calculated from DOC mobilization rates in text	37.3	1.72	[41]

5.3.5 Changes in microbiological population and activity

Terminal restriction fragment length polymorphism (T-RFLP) of 16S rRNA genes and analysis of adenosine triphosphate (ATP) were used to detect changes in the microbial population and activity.

Figure 5-4 shows the results of the T-RFLP performed on in- and effluent and sand samples of sediment B. The dendrogram of the T-RFLP patterns of sediment B shows that the T-RFLP pattern of the 60ºC samples cluster in a group that has a low similarity (5% to 40%) to the T-RFLP patterns of the other samples. The T-RFLP patterns from the remaining samples (from 5, 11 and 25ºC effluents, and influent) have a similarity between 65 and 97%. The T-RFLP patterns of the 60ºC samples have a lower number of bands than the T-RFLP patterns of the lower temperature samples and bands are present at different locations. The T-RFLP patterns of sediment C were different from sediment B, since no distinct temperature group is present in the samples of sediment C. It is possible that the results of these analyses were biased by a relatively large dispersion in the columns of this sediment (13 cm) compared to sediment B (3.4 cm) which, combined with relative large sample volume requirement, resulted in a fraction of water that did not undergo sufficient incubation time in the effluent. This was not a problem in the chemical analyses because these samples were taken prior to the microbiological samples and sampling volumes for chemical analyses were a factor 20 smaller. The only samples that appear distinctively different for the sediment C experiment are the 5ºC and 11ºC samples collected in March and May. However, the cluster for the 11ºC samples appears to be biased by the DNA yield reflected in the low visibility of bands. This may have also influenced the top four samples shown for sediment C.

The ATP measurements for effluent samples showed a large variation between the different sampling rounds, resulting in the high standard deviation (Table 5-5). Subsequently, no significant differences were present between ATP measurements of 11ºC (reference) compared to the other three testing temperatures in the experiment with sediment C (T-test, lowest P = 0.32 for 60ºC). Sediment B and C both did show an interesting pattern where total ATP was highest in 11ºC samples, which is remarkable given the low sulfate reduction rate at this temperature compared to the 25ºC and 60ºC columns. Also free ATP was measured, which gives an indication of ATP not contained in cells or generated by died cells. The highest concentration of free ATP was observed in the influent, which might have been caused by starvation of microorganisms during storage of the influent in a stainless steel barrel. In all effluent, free ATP was less than 7% of the total ATP, indicating that (micro)biological populations in the columns are active and not dead. Even at 60°C, the percentage of free ATP was low, which indicates that an active thermophilic microbial population has developed in this column.

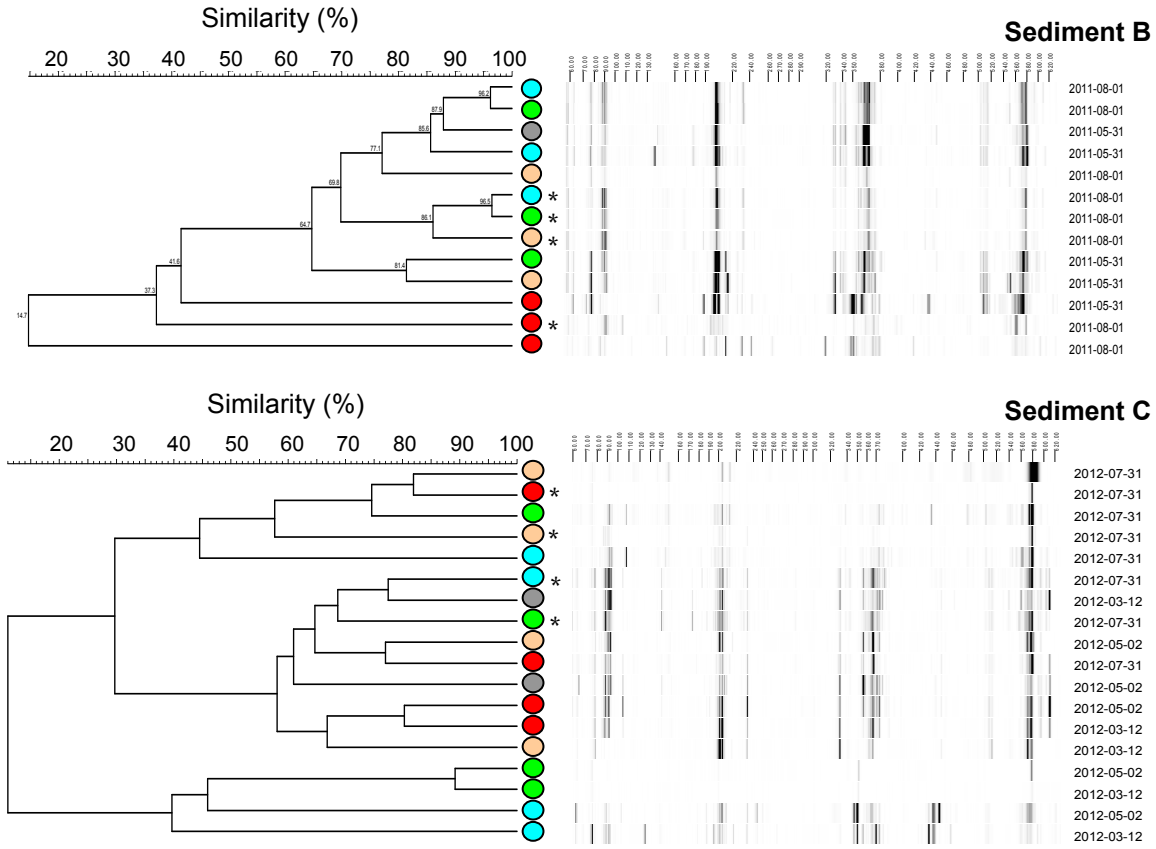

*Figure 5-4 Results of the T-RFLP scans on sediment B (top) and C (bottom). The colour markers behind the different samples show the testing temperatures: ● Influent (11°C); ● : 5°C column; ● 11°C column; ● 25°C column ; ● 60°C Column. Analyses are carried out on effluent and sediment (the latter highlighted with a * behind the sample marker)*

Table 5-4 ATP data for in- and effluents during incubation tests. Shown are number of samples (n), average ATP (μ) and standard deviation (σ)

	ATP (ng/l)			Free ATP (ng/l)		
Sediment B	**n**	**μ**	**σ**	**n**	**μ**	**σ**
5ºC	1	924	n/a	n/a		
11ºC	1	1006	n/a	n/a		
25ºC	1	742	n/a	n/a		
60ºC	1	308	n/a	n/a		
Sediment C						
Influent	5	37	17	3	6.3	3.3
5ºC	8	60	66	6	3.7	1.8
11ºC	8	76	65	6	2.0	0.3
25ºC	8	64	43	6	3.6	1.8
60ºC	8	49	36	6	2.7	2.3

5.4 Conclusions

1. Subjecting aquifer sediments to temperatures far beyond the in-situ temperature resulted in the emergence of thermophilic sulfate reducing conditions. TRFLP scans show a distinctively different microbiological population in one of the sediments. The derived sulfate reduction rates for mesophilic and thermophilic conditions are of similar order of magnitude.
2. The derived activation energies for SR at temperatures below 50°C ranges between 44±20 and 134±250 kJ/mol. Activation energies from our experiments and those derived from a literature review shows that thermophilic sulfate reduction generally has a higher activation energy, generally > 80 kJ/mol. The reason behind this difference could be a trade-off between enzyme stability and activity. Thermostable enzymes are less flexible making them less efficient catalysts yielding higher activation energies.
3. The temperature dependence of DOC production shows a distinctively different pattern compared to sulfate reduction. It is hypothesized that DOC production is purely chemical and not biologically mediated. The E_a derived from our data is around 33 kJ/mol; a review of literature values results in a range of 33 to 37 kJ/mol for sandy sediments.
4. No methane production was observed in the thermophilic temperature range. This is probable due to the absence of spore formation of methane producing archaea.

6 Conclusions

The experiments reported here show that water quality is not affected when these anoxic aquifer sediments are subjected to lower (5°C) than in-situ temperature (11°C). At the currently allowed maximum hot well temperature (25°C), As concentrations were significantly higher than under ambient conditions. At 60 °C, significant effects were observed for pH, DOC, P, K, Si, As, Mo, V, and F following 1 day residence time. Consequently, these elements should be considered for water quality monitoring programs of ATES projects. Arsenic behaviour was most alarming because it exceeded the drinking water guideline of 10 µg/l in two of the three tested sediments at 25°C and in all sediments at 60°C.

No consistent significant temperature effects were observed for Na, Mg, Sr, Ca, Fe, Mn, Al, Ba, Co, Cr, Cu, Eu, Ho, Ni, Pb, Sb, Sc, Yb, Zn, Ga, and La, all of which were present in the sediment as shown by XRF analyses. These results highlight the need for careful evaluation of hydrogeochemical conditions when situating ATES systems in aquifers used for drinking water production.

It is hypothesized that these temperature induced chemical effects are caused by a combination of processes: The (in)congruent dissolution of silicates (K-feldspar) is most likely responsible for the increased levels of K and Si. The increasing DOC at 60 °C is both due to desorption and SOM mineralisation. Desorption from iron oxides is believed to be responsible for increasing concentrations of As, B, Mo, V, and Be. The validity of this hypothesis was tested using geochemical modeling using PHREEQC The overall patterns in chemical water quality could well be simulated with the model which confirms that these processes may be held responsible for the observed water quality changes.

In experiments with longer residence times, temperature had a clear impact on SO_4 reduction rate with maximum rates observed at 40 and 70°C. Subjecting aquifer sediments to temperatures far beyond the in-situ temperature thus resulted in the emergence of thermophilic sulfate reducing conditions. The derived sulfate reduction rates for mesophilic and thermophilic conditions are of similar order of magnitude. At the lower sulfate reduction temperature optimum, also a peak in methane production was observed, while this was absent beyond 45°C. The production rate of DOC increased over the entire temperature range without any clear temperature optimum. T-RFLP analysis of the bacterial populations shows a distinctively different bacterial population at 60°C in one of the sediments confirming the emergence of a thermophilic population. This was also confirmed by free and total ATP analyses which show that a living microbiological population was present at all four temperatures.

7 References

1. Arnosti, C.; Jørgensen, B. B.; Sagemann, J.; Thamdrup, B., Temperature dependence of microbial degradation of organic matter in marine sediments: polysaccharide hydrolysis, oxygen consumption, and sulfate reduction. *Marine Ecology Progress Series* **1998,** *165*, 59-70.
2. Robador, A.; Bruchert, V.; Steen, A. D.; Arnosti, C., Temperature induced decoupling of enzymatic hydrolysis and carbon remineralization in long-term incubations of Arctic and temperate sediments. *Geochimica et Cosmochimica Acta* **2011,** *74*, (8), 2316-2326.
3. Weston, N. B.; Joye, S. B., Temperature-driven decoupling of key phases of organic matter degradation in marine sediments. *Proceedings of the National Academy of Sciences of the United States of America* **2005,** *102*, (47), 17036-17040.
4. Yang, W.; Zhou, J.; Xu, W.; Zhang, G. Q., Current status of ground-source heat pumps in China. *Energy Policy* **2010,** *38*, (1), 323-332.
5. Lee, J. Y., Current status of ground source heat pumps in Korea. *Renewable & Sustainable Energy Reviews* **2009,** *13*, (6-7), 1560-1568.
6. Lienau, P. J., Geothermal heat pump performance and utility programs in the United States. *Energy Sources* **1997,** *19*, (1), 1-8.
7. Sanner, B.; Karytsas, C.; Mendrinos, D.; Rybach, L., Current status of ground source heat pumps and underground thermal energy storage in Europe. *Geothermics* **2003,** *32*, (4-6), 579-588.
8. Bonte, M.; Van Den Berg, G.; Wezel, A. M., Underground thermal energy storage in relation to groundwater protection (in Dutch). *Bodem* **2008,** *5/2008*, 22-26.
9. Bonte, M.; P. J. Stuyfzand, A. H., and P. Van Beelen., Underground thermal energy storage: environmental risks and policy developments in the Netherlands and European Union. . *Ecology and Society* **2011,** *16*, (1), 22.
10. Haehnlein, S.; Bayer, P.; Blum, P., International legal status of the use of shallow geothermal energy. *Renewable & Sustainable Energy Reviews* **2010,** *14*, (9), 2611-2625.
11. Griffioen, J.; Appelo, C. A. J., Nature and extent of carbonate precipitation during aquifer thermal energy storage. *Applied Geochemistry* **1993,** *8*, (2), 161-176.
12. Palmer, C. D.; Cherry, J. A., Geochemical reactions associated with low-temperature thermal energy storage in aquifers. *Can. Geotech. J.* **1984,** *21*, (3), 13.
13. Arning, E.; Kölling, M.; Schulz, H. D.; Panteleit, B.; Reichling, J., Einfluss oberflächennaher Wärmegewinnung auf geochemische Prozesse im Grundwasserleiter. *Grundwasser* **2006,** *11*, (1), 27-39.
14. Holm, T. R.; Eisenreich, S. J.; Rosenberg, H. L.; Holm, N. P., Groundwater Geochemistry of Short-Term Aquifer Thermal Energy Storage Test Cycles. *Water Resources Research* **1987,** *23*, (6), 1005-1019.
15. Palmer, C. D.; Blowes, D. W.; Frind, E. O.; Molson, J. W., Thermal-energy storage in an unconfined aquifer: 1. Field injection experiment. *Water Resources Research* **1992,** *28*, (10), 2845-2856.
16. Molson, J. W.; Frind, E. O.; Palmer, C. D., Thermal-energy storage in an unconfined aquifer. 2. Model development, validation and application. *Water Resources Research* **1992,** *28*, (10), 2857-2867.
17. Brons, H. J.; Griffioen, J.; Appelo, C. A. J.; Zehnder, A. J. B., (Bio)geochemical reactions in aquifer material from a thermal energy storage site. *Water Research* **1991,** *25*, (6), 729-736.
18. Winters, A. L. *Summary of Research on microbiological processes*; Dept. Biological Sciences. Univ. of Alabama.: 1992; p 64.
19. Schippers, A.; Reichling, J., Laboruntersuchungen zum Einfluss von Temperaturveränderungen auf die Mikrobiologie des Untergrundes. *Grundwasser* **2006,** *11*, (1), 40-45.
20. Brielmann, H.; Griebler, C.; Schmidt, S. I.; Michel, R.; Lueders, T., Effects of thermal energy discharge on shallow groundwater ecosystems. *FEMS Microbiol. Ecol.* **2009,** *68*, (3), 273-286.
21. Sowers, L.; York, K. P.; Stiles, L. In *Impact of thermal buildup on groundwater chemistry and aquifer microbes*, Ecostock 2006, New Jersey, 2006; New Jersey, 2006.
22. Brielmann, H.; Lueders, T.; Schreglmann, K.; Ferraro, F.; Avramov, M.; Hammerl, V.; Blum, P.; Bayer, P.; Griebler, C., Shallow geothermal energy usage and its potential impacts on groundwater ecosystems (Oberflächennahe Geothermie und ihre potenziellen Auswirkungen auf Grundwasserökosysteme). *Grundwasser* **2011**, 1-15.

23. Bonte, M.; Stuyfzand, P. J.; Van Den Berg, G., The effects of aquifer thermal energy storage on groundwater quality and the consequences for drinking water production: A case study from the Netherlands. *Water Science and Technology* **2011,** *63*, (9), 1922-1931.
24. Castro, H.; Queirolo, M.; Quevedo, M.; Muxí, L., Preservation methods for the storage of anaerobic sludges. *Biotechnology Letters* **2002,** *24*, (4), 329-333.
25. Griffioen, J.; Klein, J.; van Gaans, P. F. M., Reaction capacity characterization of shallow sedimentary deposits in geologically different regions of the Netherlands. *Journal of Contaminant Hydrology* **2012,** *127*, (1–4), 30-46.
26. Toride, N.; Leij, F. J.; van Genuchten, M. T. *TheCXTFIT Code for Estimating Transport Parameters from Laboratory or Field Tracer Experiments Version 2.0*; U. S. SALINITY LABORATORY: RIVERSIDE, CALIFORNIA, 1995; p 131.
27. van Helvoort, P.-J.; Griffioen, J.; Hartog, N., Characterization of the reactivity of riverine heterogeneous sediments using a facies-based approach; the Rhine-Meuse delta (The Netherlands). *Applied Geochemistry* **2007,** *22*, (12), 2735-2757.
28. Parkhurst, D. L.; Appelo, C. A. J. *User's guide to PHREEQC (version 2)--A computer program for speciation, batch-reaction, one-dimensional transport, and inverse geochemical calculations*; U.S. Geological Survey 1999; p 312 p.
29. Rinck-Pfeiffer, S.; Ragusa, S.; Sztajnbok, P.; Vandevelde, T., Interrelationships between biological, chemical, and physical processes as an analog to clogging in aquifer storage and recovery (ASR) wells. *Water Research* **2000,** *34*, (7), 2110-2118.
30. Santonen, T.; Stockmann-Juvala, H.; Zitting, A. *Review on toxicity of stainless steel*; Finnish institute of occupational health: 2010; p 87.
31. Anonymous *SciPy Reference Guide Release 0.11.0.dev-659017f*; 2012; p 969.
32. Appelo, C. A. J.; Postma, D., *Geochemistry, groundwater and pollution, second edition*. A.A. Balkema: Leiden, 2005; p 649.
33. Benezeth, P.; Dandurand, J. L.; Harrichoury, J. C., Solubility product of siderite (FeCO3) as a function of temperature (25-250°C). *Chemical Geology* **2009,** *265*, (1-2), 3-12.
34. Jardine, P. M.; Sparks, D. L., Potassium-Calcium Exchange in a Multireactive Soil System: II. Thermodynamics. *Soil Sci. Soc. Am. J.* **1984,** *48*, (1), 45-50.
35. Kersten, M.; Vlasova, N., Silicate adsorption by goethite at elevated temperatures. *Chemical Geology* **2009,** *262*, (3–4), 336-343.
36. Swedlund, P. J.; Webster, J. G., Adsorption and polymerisation of silicic acid on ferrihydrite, and its effect on arsenic adsorption. *Water Research* **1999,** *33*, (16), 3413-3422.
37. Hansen, H. C. B.; Wetche, T. P.; Raulund-Rasmussen, K.; Borggaard, O. K., Stability constants for silicate adsorbed to ferrihydrite. *Clay Minerals* **1994,** *29*, (3), 341-350.
38. Nugent, M. A.; Brantley, S. L.; Pantano, C. G.; Maurice, P. A., The influence of natural mineral coatings on feldspar weathering. *Nature* **1998,** *395*, (6702), 588-591.
39. Murakami, T.; Kogure, T.; Kadohara, H.; Ohnuki, T., Formation of secondary minerals and its effect on anorthite dissolution. *American Mineralogist* **1998,** *83*, (11-12), 1209-1219.
40. Murakami, T.; Utsunomiya, S.; Yokoyama, T.; Kasama, T., Biotite dissolution processes and mechanisms in the laboratory and in nature: Early stage weathering environment and vermiculitization. *American Mineralogist* **2003,** *88*, (2-3), 377-386.
41. Jesußek, A.; Grandel, S.; Dahmke, A., Impacts of subsurface heat storage on aquifer hydrogeochemistry. *Environ. Earth Sci.* **2012**, 1-14.
42. Filius, J. D.; Lumsdon, D. G.; Meeussen, J. C. L.; Hiemstra, T.; Van Riemsdijk, W. H., Adsorption of fulvic acid on goethite. *Geochimica et Cosmochimica Acta* **2000,** *64*, (1), 51-60.
43. Evanko, C. R.; Dzombak, D. A., Influence of Structural Features on Sorption of NOM-Analogue Organic Acids to Goethite. *Environmental Science & Technology* **1998,** *32*, (19), 2846-2855.
44. Smedley, P. L.; Kinniburgh, D. G., A review of the source, behaviour and distribution of arsenic in natural waters. *Applied Geochemistry* **2002,** *17*, (5), 517-568.
45. Stuyfzand, P. J., P. van Rossum and I. Mendizabal In *Does arsenic, in groundwater of the compound Rhine-Meuse-Scheldt-Ems delta, mencase drinking water supply in the Netherlands?*, Arsenic in groundwater, A world problem, Utrecht, 2006; Appelo, C. A. J., Ed. Unesco, WMO, Deltares & IGRAC: Utrecht, 2006; pp 102-125.

46. Jones, G. W.; Pichler, T., Relationship between Pyrite Stability and Arsenic Mobility During Aquifer Storage and Recovery in Southwest Central Florida. *Environmental Science & Technology* **2007,** *41*, (3), 723-730.
47. Wallis, I.; Prommer, H.; Pichler, T.; Post, V.; B. Norton, S.; Annable, M. D.; Simmons, C. T., Process-Based Reactive Transport Model To Quantify Arsenic Mobility during Aquifer Storage and Recovery of Potable Water. *Environmental Science & Technology* **2011,** *45*, (16), 6924-6931.
48. Vanderzalm, J. L.; Dillon, P. J.; Barry, K. E.; Miotlinski, K.; Kirby, J. K.; Le Gal La Salle, C., Arsenic mobility and impact on recovered water quality during aquifer storage and recovery using reclaimed water in a carbonate aquifer. *Applied Geochemistry* **2011,** *26*, (12), 1946-1955.
49. Van Beek, C. G. E. M., *Cause and Prevention of Clogging of Wells Abstracting Groundwater from Unconsolidated Aquifers*. IWA Publishing: London, 2011.
50. Maji, S. K., A. Pal, T. Pal, A Adak., Adsorption thermodynamics of arsenic on laterite soil. *J. Surface. Sci. Technol.* **2007,** *22*, (3-4), 161-176.
51. Kersten, M.; Vlasova, N., Arsenite adsorption on goethite at elevated temperatures. *Applied Geochemistry* **2009,** *24*, (1), 32-43.
52. Dixit, S.; Hering, J. G., Comparison of Arsenic(V) and Arsenic(III) Sorption onto Iron Oxide Minerals: Implications for Arsenic Mobility. *Environmental Science & Technology* **2003,** *37*, (18), 4182-4189.
53. Mohapatra, D.; Mishra, D.; Chaudhury, G.; Das, R., Arsenic adsorption mechanism on clay minerals and its dependence on temperature. *Korean Journal of Chemical Engineering* **2007,** *24*, (3), 426-430.
54. Lin, Z.; Puls, R. W., Adsorption, desorption and oxidation of arsenic affected by clay minerals and aging process. *Environmental Geology* **2000,** *39*, (7), 753-759.
55. Sø, H. U.; Postma, D.; Jakobsen, R.; Larsen, F., Competitive adsorption of arsenate and phosphate onto calcite; experimental results and modeling with CCM and CD-MUSIC. *Geochimica et Cosmochimica Acta* **2012,** *93*, (0), 1-13.
56. Sø, H. U.; Postma, D.; Jakobsen, R.; Larsen, F., Sorption and desorption of arsenate and arsenite on calcite. *Geochimica et Cosmochimica Acta* **2008,** *72*, (24), 5871-5884.
57. Dzombak, D. A.; Morel, F. M. M., *Surface Complexation Modeling: Hydrous Ferric Oxide*. John Wiley & Sons: New York, 1990.
58. van Halem, D.; Moed, D. H.; Verberk, J. Q. J. C.; Amy, G. L.; van Dijk, J. C., Cation exchange during subsurface iron removal. *Water Research* **2012,** *46*, (2), 307-315.
59. Limousin, G.; Gaudet, J. P.; Charlet, L.; Szenknect, S.; Barthès, V.; Krimissa, M., Sorption isotherms: A review on physical bases, modeling and measurement. *Applied Geochemistry* **2007,** *22*, (2), 249-275.
60. Seidel-Morgenstern, A., Experimental determination of single solute and competitive adsorption isotherms. *Journal of Chromatography A* **2004,** *1037*, (1–2), 255-272.
61. Griffioen, J.; Appelo, C. A. J.; Van Veldhuizen, M., Practice of chromatography: deriving isotherms from elution curves. *Soil Science Society of America Journal* **1992,** *56*, (5), 1429-1437.
62. Schweich, D.; Sardin, M.; Gaudet, J.-P., Measurement of a Cation Exchange Isotherm from Elution Curves Obtained in a Soil Column: Preliminary Results1. *Soil Sci. Soc. Am. J.* **1983,** *47*, (1), 32-37.
63. Keon, N. E.; Swartz, C. H.; Brabander, D. J.; Harvey, C.; Hemond, H. F., Validation of an Arsenic Sequential Extraction Method for Evaluating Mobility in Sediments. *Environmental Science & Technology* **2001,** *35*, (13), 2778-2784.
64. Kanel, S. R.; Manning, B.; Charlet, L.; Choi, H., Removal of Arsenic(III) from Groundwater by Nanoscale Zero-Valent Iron. *Environmental Science & Technology* **2005,** *39*, (5), 1291-1298.
65. Banerjee, K.; Amy, G. L.; Prevost, M.; Nour, S.; Jekel, M.; Gallagher, P. M.; Blumenschein, C. D., Kinetic and thermodynamic aspects of adsorption of arsenic onto granular ferric hydroxide (GFH). *Water Research* **2008,** *42*, (13), 3371-3378.
66. Stumm, W.; Morgan, J., *Aquatic chemistry: Chemical equilibria and rates in natural waters (3rd edition)* John Wiley & Sons: New York, 1995.
67. Riemsdijk, W. H. v.; Hiemstra, T., Chapter 8 The CD-MUSIC model as a framework for interpreting ion adsorption on metal (hydr) oxide surfaces. In *Interface Science and Technology*, Johannes, L., Ed. Elsevier: 2006; Vol. Volume 11, pp 251-268.
68. Negrea, A.; Lupa, L.; Ciopec, M.; Lazau, R.; Muntean, C.; Negrea, P., Adsorption of As(III) Ions onto Iron-containing Waste Sludge. *Adsorption Science & Technology* **2010,** *28*, (6), 467-484.
69. Parga, J. R., V. Vasquez, V. and H. Moreno, Thermodynamic studies on the arsenic adsorption on iron species generated by electrocoagulation. *Journal of Metallurgy* **2009,** *2009*.

70. Deliyanni, E. A., and N.K. Lazaridis In *Sorption of arsenites and arsenates onto surfactant mediated akaganeite*, 9th International conference on Environmental Science and Technology, Rhode Island, Greece, 2005; Rhode Island, Greece, 2005.
71. Guo, H.; Li, Y.; Zhao, K., Arsenate removal from aqueous solution using synthetic siderite. *Journal of Hazardous Materials* **2010,** *176*, (1–3), 174-180.
72. Hong, H.-J.; Yang, J.-S.; Kim, B.-K.; Yang, J.-W., Arsenic Removal Behavior by Fe-Al Binary Oxide: Thermodynamic and Kinetic Study. *Separation Science and Technology* **2011,** *46*, 2531-2538.
73. Abildgaard, L.; Nielsen, M. B.; Kjeldsen, K. U.; Ingvorsen, K., Desulfovibrio alkalitolerans sp. nov., a novel alkalitolerant, sulphate-reducing bacterium isolated from district heating water. *International Journal of Systematic and Evolutionary Microbiology* **2006,** *56*, (5), 1019-1024.
74. Wallage, Z. E.; Holden, J.; McDonald, A. T., Drain blocking: An effective treatment for reducing dissolved organic carbon loss and water discolouration in a drained peatland. *Science of The Total Environment* **2006,** *367*, (2–3), 811-821.
75. Rittmann, B. E.; Stilwell, D.; Garside, J. C.; Amy, G. L.; Spangenberg, C.; Kalinsky, A.; Akiyoshi, E., Treatment of a colored groundwater by ozone-biofiltration: pilot studies and modeling interpretation. *Water Research* **2002,** *36*, (13), 3387-3397.
76. Sawicka, J. E.; Jørgensen, B. B.; Brüchert, V., Temperature characteristics of bacterial sulfate reduction in continental shelf and slope sediments. *Biogeosciences Discuss.* **2012,** *9*, (1), 673-700.
77. Sverdrup, H. U., *The kinetics of base cation release due to chemical weathering*. Lund University Press: Lund, 1990.
78. White, A. F.; Brantley, S. L., The effect of time on the weathering of silicate minerals: why do weathering rates differ in the laboratory and field? *Chemical Geology* **2003,** *202*, (3–4), 479-506.
79. Ganor, J.; Lu, P.; Zheng, Z.; Zhu, C., Bridging the gap between laboratory measurements and field estimations of silicate weathering using simple calculations. *Environmental Geology* **2007,** *53*, (3), 599-610.
80. Weissbart, E. J.; Rimstidt, J. D., Wollastonite: Incongruent dissolution and leached layer formation. *Geochimica et Cosmochimica Acta* **2000,** *64*, (23), 4007-4016.
81. Schott, J.; Pokrovsky, O. S.; Spalla, O.; Devreux, F.; Gloter, A.; Mielczarski, J. A., Formation, growth and transformation of leached layers during silicate minerals dissolution: The example of wollastonite. *Geochimica et Cosmochimica Acta*, (0).
82. Murakami, T.; Kogure, T., Kadohara, Hiroyuki, Ohnuki, Toshihiko, Formation of secondary minerals and its effect on anorthite dissolution. *American Mineralogist* **1998** *83*.
83. Brunauer, S.; Emmett, P. H.; Teller, E., Adsorption of gases in multimolecular layers. *Journal of the American Chemical Society* **1938,** *60*, (2), 309-319.
84. Helgeson, H. C., Kinetics of mass transfer among silicates and aqueous solutions. *Geochimica et Cosmochimica Acta* **1971,** *35*, (5), 421-469.
85. Benner, S. G.; Blowes, D. W.; Ptacek, C. J.; Mayer, K. U., Rates of sulfate reduction and metal sulfide precipitation in a permeable reactive barrier. *Applied Geochemistry* **2002,** *17*, (3), 301-320.
86. Tarpgaard, I. H.; Røy, H.; Jørgensen, B. B., Concurrent low- and high-affinity sulfate reduction kinetics in marine sediment. *Geochimica et Cosmochimica Acta* **2011,** *75*, (11), 2997-3010.
87. Pallud, C.; Meile, C.; Laverman, A. M.; Abell, J.; Van Cappellen, P., The use of flow-through sediment reactors in biogeochemical kinetics: Methodology and examples of applications. *Marine Chemistry* **2007,** *106*, (1–2), 256-271.
88. Bonte M, v. B. B., Stuyfzand, P.J., Biochemical impacts of shallow geothermal applications in anoxic aquifers. *Biogeochemistry* **in prep**.
89. Muyzer, G.; Stams, A. J. M., The ecology and biotechnology of sulphate-reducing bacteria. *Nature Reviews Microbiology* **2008,** *6*, (6), 441-454.
90. Appelo, C. A. J., Cation and proton exchange, pH variations, and carbonate reactions in a freshening aquifer. *Water Resour. Res.* **1994,** *30*, (10), 2793-2805.
91. Jardine, P. M.; Sparks, D. L., Potassium-Calcium Exchange in a Multireactive Soil System: I. Kinetics. *Soil Sci. Soc. Am. J.* **1984,** *48*, (1), 39-45.
92. Sawhney, B. L., Kinetics of Cesium Sorption by Clay Minerals1. *Soil Sci. Soc. Am. J.* **1966,** *30*, (5), 565-569.
93. Sparks, D. L.; Jardine, P. M., Comparison of Kinetic Equations to Describe Potassium-Calcium Exchange in Pure and in Mixed Systems. *Soil Science* **1984,** *138*, (2), 115-122.

94. DeSutter, T. M.; Pierzynski, G. M.; Baker, L. R., Flow-Through and Batch Methods for Determining Calcium-Magnesium and Magnesium-Calcium Selectivity Contribution no. 04-251-J from the Kansas Agric. Exp. Stn., Manhattan, KS. *Soil Sci. Soc. Am. J.* **2006,** *70*, (2), 550-554.
95. Bond, W. J.; Phillips, I. R., Cation Exchange Isotherms Obtained with Batch and Miscible-Displacement Techniques. *Soil Sci. Soc. Am. J.* **1990,** *54*, (3), 722-728.
96. LaRowe, D. E.; Van Cappellen, P., Degradation of natural organic matter: A thermodynamic analysis. *Geochimica et Cosmochimica Acta* **2011,** *75*, (8), 2030-2042.
97. Westerhoff, W. E. *Description of the lithostratigraphical unit: Sterksel formation (in Dutch)*; TNO-NITG: Maart 2003, 2003; p 6.
98. Appelo, C. A. J.; Van Der Weiden, M. J. J.; Tournassat, C.; Charlet, L., Surface Complexation of Ferrous Iron and Carbonate on Ferrihydrite and the Mobilization of Arsenic. *Environmental Science & Technology* **2002,** *36*, (14), 3096-3103.
99. Sverjensky, D. A.; Sahai, N., Theoretical prediction of single-site enthalpies of surface protonation for oxides and silicates in water. *Geochimica et Cosmochimica Acta* **1998,** *62*, (23–24), 3703-3716.
100. De Bussetti, S. G.; Ferreiro, E. A.; Helmy, A. K., Sorption of boron by hydrous Al-oxide. *Clays and Clay Minerals* **1995,** *43*, (1), 58-62.
101. Trivedi, P.; Axe, L., Modeling Cd and Zn Sorption to Hydrous Metal Oxides. *Environmental Science & Technology* **2000,** *34*, (11), 2215-2223.
102. Doherty, J. *PEST, Model-Independent Parameter Estimation. User Manual: 5th Edition*; 2010; p 336.
103. Dai, Z.; Samper, J., Inverse problem of multicomponent reactive chemical transport in porous media: Formulation and applications. *Water Resour. Res.* **2004,** *40*, (7), W07407.
104. Karlsen, R. H.; Smits, F. J. C.; Stuyfzand, P. J.; Olsthoorn, T. N.; van Breukelen, B. M., A post audit and inverse modeling in reactive transport: 50 years of artificial recharge in the Amsterdam Water Supply Dunes. *Journal of Hydrology* **2012,** *454–455*, (0), 7-25.
105. Laudelout, H.; van Bladel, R.; Bolt, G. H.; Page, A. L., Thermodynamics of heterovalent cation exchange reactions in a montmorillonite clay. *Transactions of the Faraday Society* **1968,** *64*, 1477-1488.
106. Van Bladel, R.; Gheyi, H. R., Thermodynamic Study of Calcium-Sodium and Calcium-Magnesium Exchange in Calcareous Soils1. *Soil Sci. Soc. Am. J.* **1980,** *44*, (5), 938-942.
107. Appel, C.; Rhue, D.; Ma, L.; Reve, B., Heats of K/Ca and K/Pb exchange in two tropical soils as measured by flow calorimetry. *Soil Science* **2002,** *167*, (12), 773-781.
108. Jesußek, A.; Köber, R.; Grandel, S.; Dahmke, A., Aquifer heat storage: sulphate reduction with acetate at increased temperatures. *Environ. Earth Sci.* **2012**, 1-9.
109. Brons, H. J.; Zehnder, A. J. B., *Biochemical aspects of aquifer thermal energy storage*. TNO: The Hague, 1990; p 73-81.
110. Bonte, M.; Stuyfzand, P. J.; van den Berg, G. A.; Hijnen, W., Effects of aquifer thermal energy storage on groundwater quality and the consequences for drinking water production: a case study from the Netherlands. *Water Science & Technology* **2011,** *63*, (9), 1922-1931.
111. Froelich, P. N.; Klinkhammer, G. P.; Bender, M. L.; Luedtke, N. A.; Heath, G. R.; Cullen, D.; Dauphin, P.; Hammond, D.; Hartman, B.; Maynard, V., Early oxidation of organic matter in pelagic sediments of the eastern equatorial Atlantic: suboxic diagenesis. *Geochimica et Cosmochimica Acta* **1979,** *43*, (7), 1075-1090.
112. Van Cappellen, P.; Gaillard, J.-F., Biogeochemical dynamics in aquatic sediments. *Reviews in Mineralogy and Geochemistry* **1996,** *34*, (1), 335-376.
113. Sharma, L.; Greskowiak, J.; Ray, C.; Eckert, P.; Prommer, H., Elucidating temperature effects on seasonal variations of biogeochemical turnover rates during riverbank filtration. *Journal of Hydrology* **2012,** *428-429*, 104-115.
114. Ding, C.; Yang, X.; Liu, W.; Chang, Y.; Shang, C., Removal of natural organic matter using surfactant-modified iron oxide-coated sand. *Journal of Hazardous Materials* **2010,** *174*, (1–3), 567-572.
115. Jakobsen, R.; Postma, D., Redox zoning, rates of sulfate reduction and interactions with Fe-reduction and methanogenesis in a shallow sandy aquifer, Rømø, Denmark. *Geochimica et Cosmochimica Acta* **1999,** *63*, (1), 137-151.
116. McBee, R. H.; McBee, V. H., The incidence of thermophilic bacteria in arctiv soils and waters. *Journal of Bacteriology* **1956,** *71*, (2), 182-185.
117. Hubert, C.; Arnosti, C.; Bruchert, V.; Loy, A.; Vandieken, V.; Jorgensen, B. B., Thermophilic anaerobes in Arctic marine sediments induced to mineralize complex organic matter at high temperature. *Environmental Microbiology* **2010,** *12*, (4), 1089-1104.

118. Hubert, C.; Loy, A.; Nickel, M.; Arnosti, C.; Baranyi, C.; Brüchert, V.; Ferdelman, T.; Finster, K.; Christensen, F. M.; Rosa de Rezende, J.; Vandieken, V.; Jørgensen, B. B., A Constant Flux of Diverse Thermophilic Bacteria into the Cold Arctic Seabed. *Science* **2009,** *325*, (5947), 1541-1544.
119. Isaksen, M. F.; Bak, F.; Jørgensen, B. B., Thermophilic sulfate-reducing bacteria in cold marine sediment. *FEMS Microbiol. Ecol.* **1994,** *14*, (1), 1-8.
120. Bae, S. S.; Lee, J.-H.; Kim, S.-J., Bacillus alveayuensis sp. nov., a thermophilic bacterium isolated from deep-sea sediments of the Ayu Trough. *International Journal of Systematic and Evolutionary Microbiology* **2005,** *55*, (3), 1211-1215.
121. Wallenstein, M., S. Allison, J. Ernakovich, J. M. Steinweg, and R. Sinsabaugh., Controls on the temperature sensitivity of soil enzymes: A key driver of in-situ enzyme activity rates. In *Soil Enzymology*, Varma, G. C. S. a. A., Ed. Springer-Verlag: Berlin Heidelberg, 2011; pp 245-258.
122. Xu, N.; Saiers, J. E., Temperature and Hydrologic Controls on Dissolved Organic Matter Mobilization and Transport within a Forest Topsoil. *Environmental Science & Technology* **2010,** *44*, (14), 5423-5429.
123. Duan, Z.; Mao, S., A thermodynamic model for calculating methane solubility, density and gas phase composition of methane-bearing aqueous fluids from 273 to 523K and from 1 to 2000bar. *Geochimica et Cosmochimica Acta* **2006,** *70*, (13), 3369-3386.
124. De Rezende, J. R.; Kjeldsen, K. U.; Hubert, C. R. J.; Finster, K.; Loy, A.; Jørgensen, B. B., Dispersal of thermophilic Desulfotomaculum endospores into Baltic Sea sediments over thousands of years. *ISME Journal* **2013,** *7*, (1), 72-84.
125. Davidson, E. A.; Janssens, I. A., Temperature sensitivity of soil carbon decomposition and feedbacks to climate change. *Nature* **2006,** *440*, (7081), 165-173.
126. Jakobsen, R.; Postma, D., In situ rates of sulfate reduction in an aquifer (Rømø, Denmark) and implications for the reactivity of organic matter. *Geology* **1994,** *22*, (12), 1101-1106.
127. Hansen, J. W.; Thamdrup, B.; Jørgensen, B. B., Anoxic incubation of sediment in gas-tight plastic bags: a method for biogeochemical process studies. *Marine Ecology Progress Series* **2000,** *208*, 273-282.
128. Marvin-DiPasquale, M. C.; Capone, D. G., Benthic sulfate reduction along the Chesapeake Bay central channel. I. Spatial trends and controls. *Marine Ecology Progress Series* **1998,** *168*, 213-228.
129. Robador, A.; Brüchert, V.; Jørgensen, B. B., The impact of temperature change on the activity and community composition of sulfate-reducing bacteria in arctic versus temperate marine sediments. *Environmental Microbiology* **2009,** *11*, (7), 1692-1703.
130. Kallmeyer, J.; Boetius, A., Effects of Temperature and Pressure on Sulfate Reduction and Anaerobic Oxidation of Methane in Hydrothermal Sediments of Guaymas Basin. *Applied and Environmental Microbiology* **2004,** *70*, (2), 1231-1233.
131. Roychoudhury, A. N., Sulfate Respiration in Extreme Environments: A Kinetic Study. *Geomicrobiology Journal* **2004,** *21*, (1), 33-43.
132. Jørgensen, B. B.; Zawacki, L. X.; Jannasch, H. W., Thermophilic bacterial sulfate reduction in deep-sea sediments at the Guaymas Basin hydrothermal vent site (Gulf of California). *Deep Sea Research Part A. Oceanographic Research Papers* **1990,** *37*, (4), 695-710.
133. Elsgaard, L.; Prieur, D.; Mukwaya, G. M.; Jørgensen, B. B., Thermophilic Sulfate Reduction in Hydrothermal Sediment of Lake Tanganyika, East Africa. *Applied and Environmental Microbiology* **1994,** *60*, (5), 1473-1480.
134. D'Amico, S.; Marx, J.-C.; Gerday, C.; Feller, G., Activity-Stability Relationships in Extremophilic Enzymes. *Journal of Biological Chemistry* **2003,** *278*, (10), 7891-7896.
135. Danson, M. J.; Hough, D. W.; Russell, R. J. M.; Taylor, G. L.; Pearl, L., Enzyme thermostability and thermoactivity. *Protein engineering* **1996,** *9*, (8), 629-630.
136. Klotz, D.; Seiler, K. P.; Moser, H.; Neumaier, F., Dispersivity and velocity relationship from laboratory and field experiments. *Journal of Hydrology* **1980,** *45*, (3–4), 169-184.
137. Lippmann, F., Phase diagrams depicting the aqueous solubility of binary mineral systems. *Neues Jahrbuch fur Mineralogie Abhandlung* **1980,** *130*, (3), 243.
138. Glynn, P. D.; Reardon, E. J., Solid-solution aqueous-solution equilibria; thermodynamic theory and representation. *Am J Sci* **1990,** *290*, (2), 164-201.
139. Lippmann, F., Stable and metastable solubility diagrams for the system CaCO3-MgCO3-H2O at ordinary temperature. *Bulletin De Mineralogie* **1982,** *105*, (3), 273-279.
140. Lippmann, F., The solubility products of complex minerals, mixed crystals, and three-layer clay minerals. *Neues Jahrbuch für Mineralogie* **1977,** *130*, 243-263.

141. Prieto, M., Thermodynamics of Solid Solution-Aqueous Solution Systems. In *Thermodynamics and Kinetics of Water-Rock Interaction*, Mineralogical Soc Amer: Chantilly, 2009; Vol. 70, pp 47-85.
142. Glynn, P., Solid-Solution Solubilities and Thermodynamics: Sulfates, Carbonates and Halides. *Reviews in Mineralogy and Geochemistry* **2000,** *40*, (1), 481-511.
143. Hildebrand, J. H., *Solubility of non-electrolytes*. Reinhold Pub. Corp: New York, 1936.
144. Thompson Jr, J. B.; Waldbaum, D. R., Analysis of the two-phase region halite-sylvite in the system NaClî— ¸KCl. *Geochimica et Cosmochimica Acta* **1969,** *33*, (6), 671-690.
145. Romanek, C. S.; Jiménez-López, C.; Navarro, A. R.; Sánchez-Román, M.; Sahai, N.; Coleman, M., Inorganic synthesis of Fe–Ca–Mg carbonates at low temperature. *Geochimica et Cosmochimica Acta* **2009,** *73*, (18), 5361-5376.
146. Jensen, D. L.; Boddum, J. K.; Tjell, J. C.; Christensen, T. H., The solubility of rhodochrosite (MnCO3) and siderite (FeCO3) in anaerobic aquatic environments. *Applied Geochemistry* **2002,** *17*, (4), 503-511.
147. Tomson, M. B.; Johnson, M. L. In *How Ferrous Carbonate Kinetics Impacts Oilfield Corrosion*, SPE International Symposium on Oilfield Chemistry, Anaheim, California, 20-22 February 1991, 1991; Anaheim, California, 1991.
148. Snoeyink, V. L.; Wagner, I., *Internal corrosion of water distribution systems*. American Water Works Association & DVGW-TEW: 1996.
149. Golubev, S. V.; Benezeth, P.; Schott, J.; Dandurand, J. L.; Castillo, A., Siderite dissolution kinetics in acidic aqueous solutions from 25 to 100°C and 0 to 50bar atm pCO2. *Chemical Geology* **2009,** *265*, (1-2), 13-19.
150. Johnson, M. L. Ferrous carbonate precipitation kinetics: A temperature ramped approach. Rice University, Houston, 1991.
151. Kazmierczak, T. F.; Tomson, M. B.; Nancollas, G. H., Crystal growth of calcium carbonate. A controlled composition kinetic study. *The Journal of Physical Chemistry* **1982,** *86*, (1), 103-107.

I Bore logs for Helvoit and Scherpenzeel and detailed geochemical results

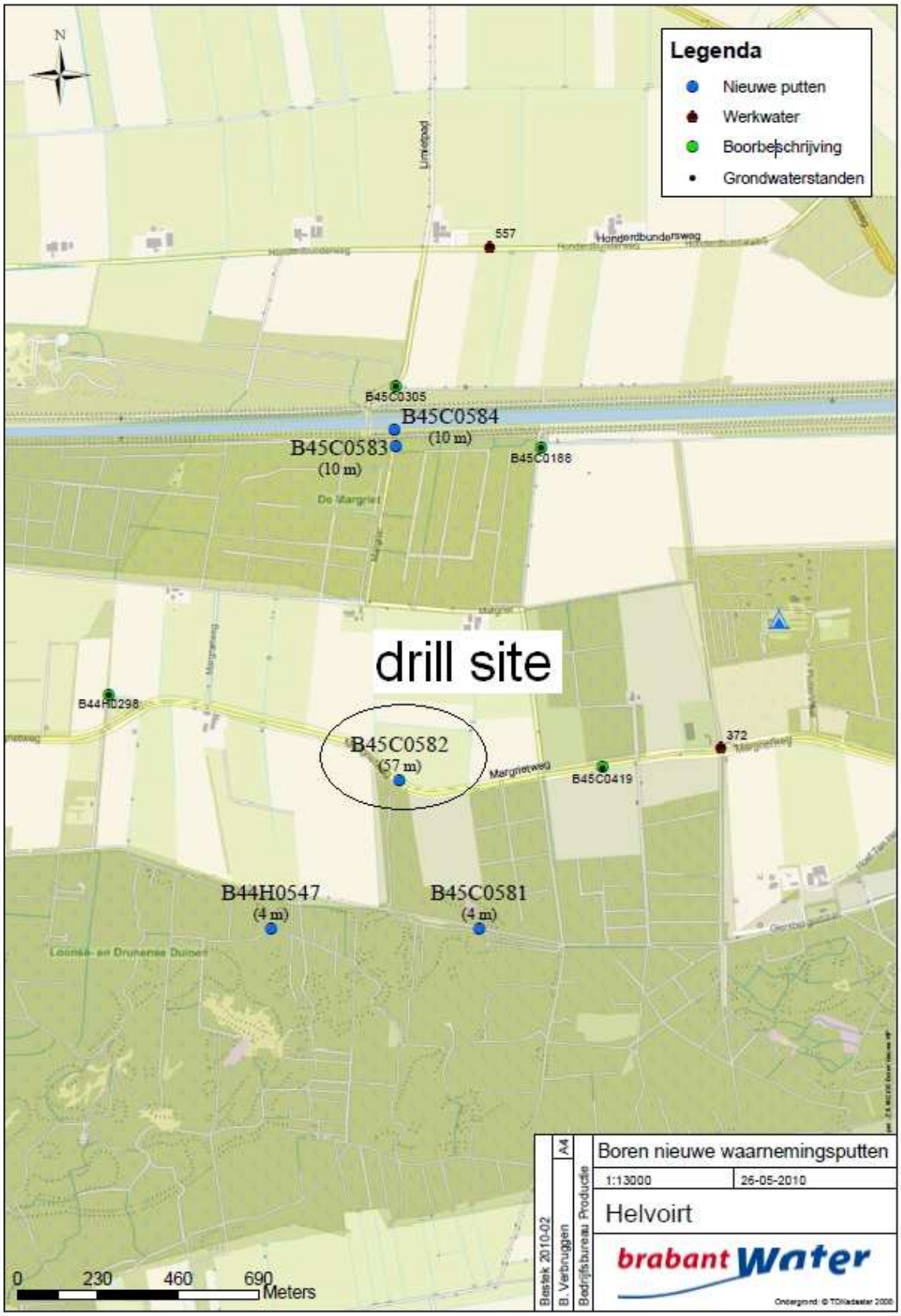

brabant Water

BOORSTAAT

Locatie:	Helvoirt	**Diam. 1 [mm]:**	
BW nr.:		**Diam. 2 [mm]:**	
TNO nr.:	B45C0582	**Diam. 3 [mm]:**	
x-coord. [m]:	140302	**Datum:**	
y-coord. [m]:	407890	**Boorfirma:**	Geotron
MV [m+NAP]:		**Type Boring:**	
Diepte [m-MV]:	57	**Boorgatmeting:**	

O.K. laag [m-MV]	grond-soort	omschrijving	homogeen/ heterogeen	korrelgr. [µ]
0.55	zand	bruin, matig grof, organisch		220
1.50	zand	geel grijs, matig grof, zwak siltig, licht organisch		220
5.00	zand	bruin grijs, matig grof, zwak siltig, licht organisch		250
5.40	veen	bruin		-
7.50	zand	bruin, matig grof, sterk slitg, matig organisch, enkel grintje		230
12.90	zand	licht bruin, matig grof, zwak siltig, enkel grintje, hout resten		280
13.40	klei	licht grijs, siltig zeer fijn		
14.20	zand	licht grijs, matig grof, sterk siltig		230
17.80	zand	licht grijs, matig grof, matig siltig, zwak organisch, hout restjes		300
20.00	zand	licht grijs, zeer grof, zwak grind houdend		380
23.10	zand	licht grijs, zeer grof, zwak grind houdend, hout resjes		320
23.60	zand	licht grijs, uiterst grof, matig grind, hout restjes, leem bolletjes		450
26.00	zand	licht grijs, uiterst grof, matig grind, hout restjes		450
28.50	zand	licht grijs, zeer grof, matig silt,matig silt lensjes		330
31.50	zand	licht grijs, matig grof, zwak siltig, hout restjes		300
32.00	zand	licht grijs, zeer grof, hout restjes	**Experiment B**	320
35.10	zand	licht grijs, zeer grof, enkel grindje		350
38.50	zand	licht grijs, matig grof, sterk siltig, klei lensjes		280
40.40	zand	licht grijs, matig grof, sterk klei houdend, matig silt		250
41.00	zand	licht grijs, matig grof, matig siltig, klei laagjes		250
42.30	zand	licht grijs, matig grof, sterk klei en siltig houdend, klei laagjes		250
42.70	zand	licht grijs, matig grof, zwak siltig, hout restjes		300
43.80	zand	licht grijs, matig grof, matig silt en klei houdend	**Experiment A**	250
44.50	zand	licht grijs, zeer grof, enkele grintjes, hout restjes		380
47.00	zand	licht grijs, uiterst grof, zwak grind houdend		620
48.40	zand	licht grijs, uiterst grof, matig grind houdend, klei lensjes		620
49.50	zand	licht grijs, zeer grof, zwak silt en grind houdend		320
53.00	zand	licht grijs, zeer grof, zwak silt en grind houdend, klei stenen, hout restjes		310
54.00	zand	licht grijs, uiterst grof, sterk fijn grind, zwak siltig, hout restjes		620
57.00	zand	licht grijs, uiterst grof,sterk grind houdend, humeus resten		830

Raadgevend Ingenieursbureau
Wiertsema & Partners B.V.
Feithspark 6 9356 BZ Tolbert
Postbus 27 9356 ZG Tolbert
Tel. (0594) 51 68 64
Fax (0594) 51 64 79
E-mail: info@wiertsema.nl
Internet: www.wiertsema.nl

Wiertsema & Partners

RAADGEVEND INGENIEURS

Resultaten grondmechanische boring

ten behoeve van het inrichten van een hydrologisch waarnemingsmeetnet Woudenberg e.o. te Woudenberg

Opdrachtnummer
VN-54917-6

Opdrachtgever
Vitens B.V.
Postbus 1090
8200 BB Lelystad

Datum rapport
15 februari 2012

Rapportnummer:	R18050
Status:	Definitief
Opgesteld door:	T. Aans
Vrijgegeven door:	A. Palsma
Handtekening:	

54917-6 R18050 Resultaten grondmechanische boring.pdf

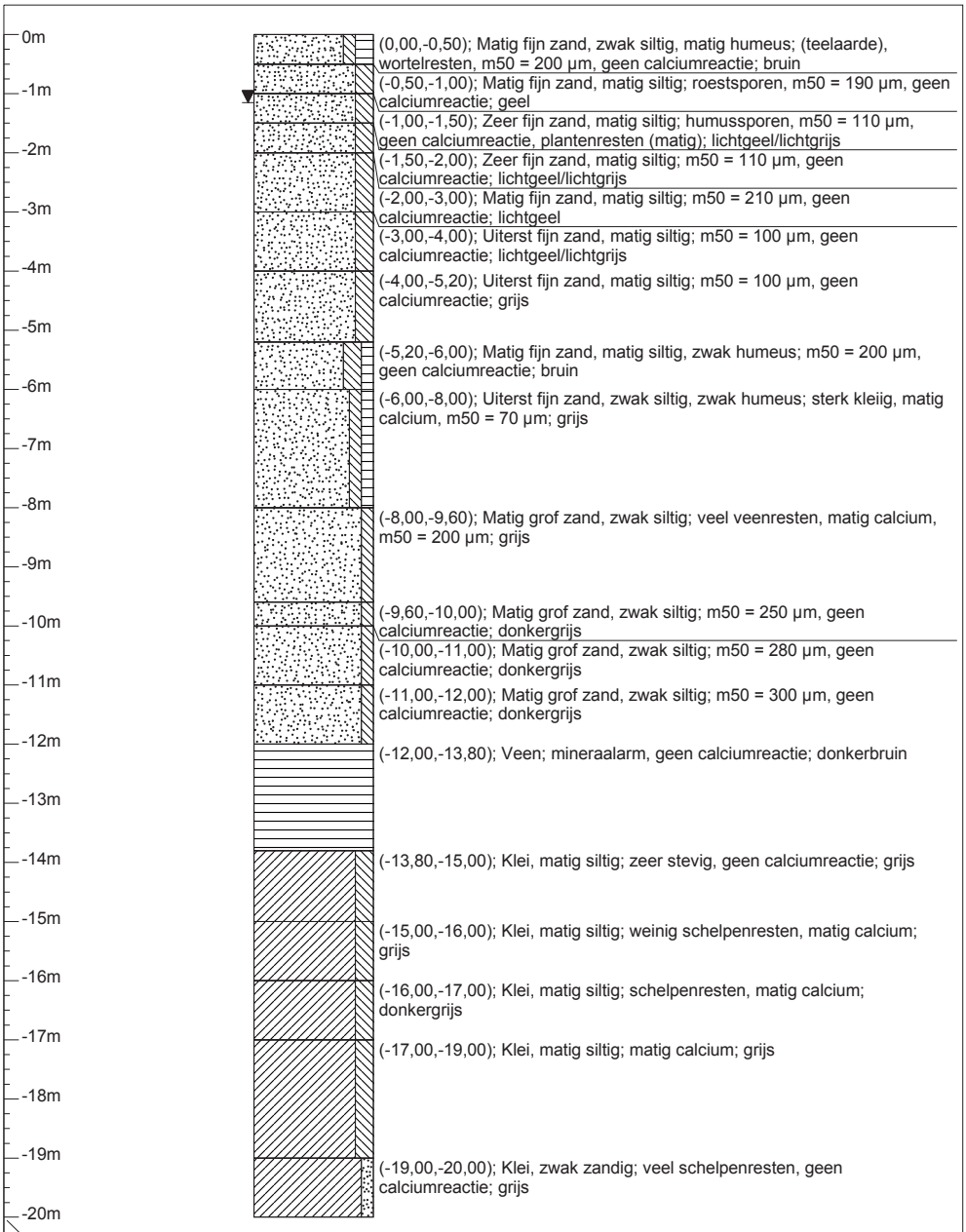

	Project/Plaats	Woudenberg	Datum	16-1-2012	Ons kenmerk	VN-54917-6
	Opdrachtgever		X-coordinaat	160.274 m	Uw kenmerk	
	Boormethode	Pulsboring	Y-coordinaat	454.374 m	Boornummer	
	Boormeester	HV/HH	KM		Boring F-2	
Getekend conform NEN 5104						

Wiertsema & Partners
RAADGEVEND INGENIEURS

kwaliteitswaarborg bodembeheer SIKB

AKKOORD UITV

54917-6 R18050 Resultaten grondmechanische boring.pdf

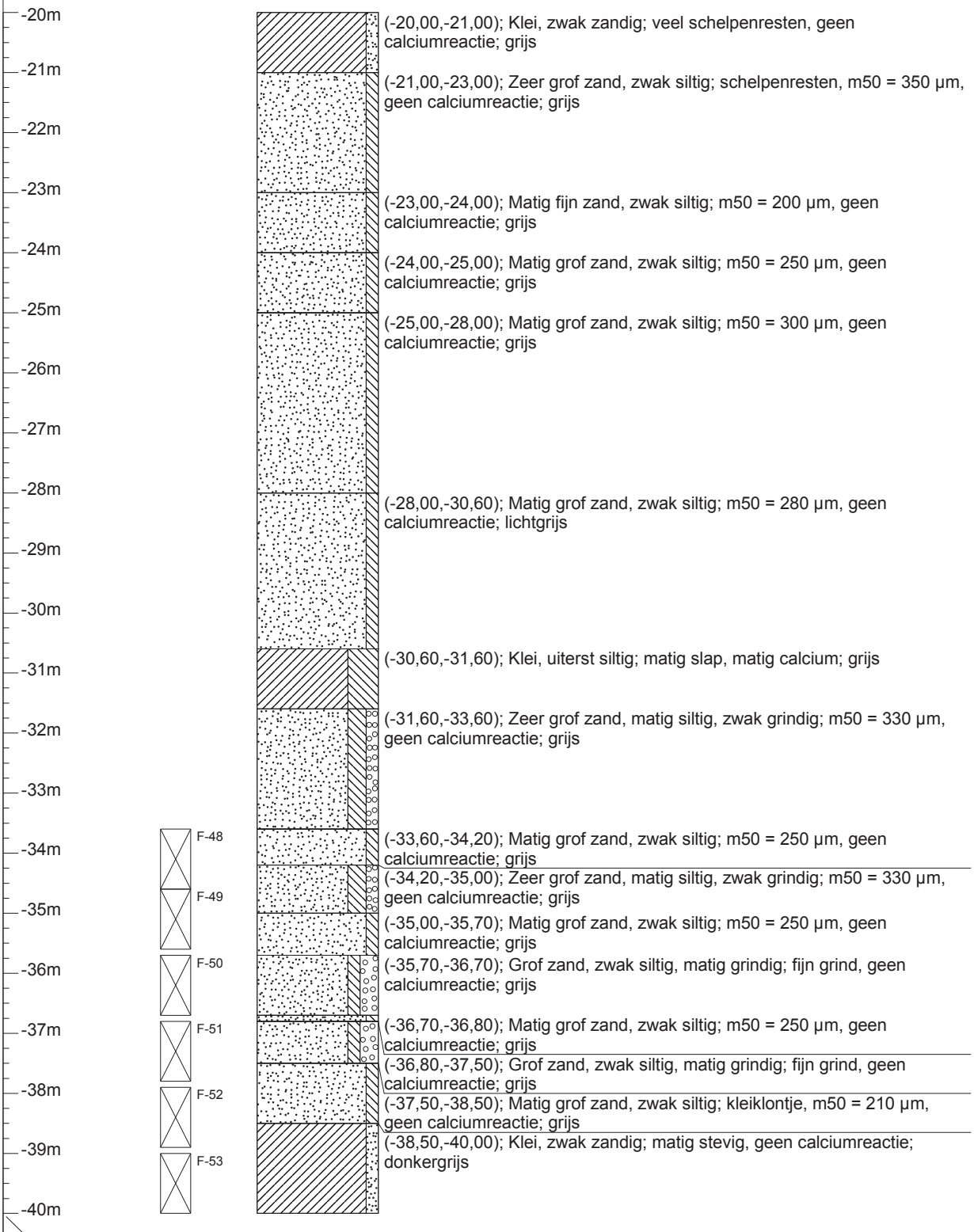

	Project/Plaats	Woudenberg	Datum	16-1-2012	Ons kenmerk	VN-54917-6
	Opdrachtgever		X-coordinaat	160.274 m	Uw kenmerk	
	Boormethode	Pulsboring	Y-coordinaat	454.374 m	Boornummer	
	Boormeester	HV/HH	KM		Boring F-2	
Getekend conform NEN 5104						

Wiertsema & Partners
RAADGEVEND INGENIEURS

kwaliteitswaarborg bodembeheer SIKB

AKKOORD UITV

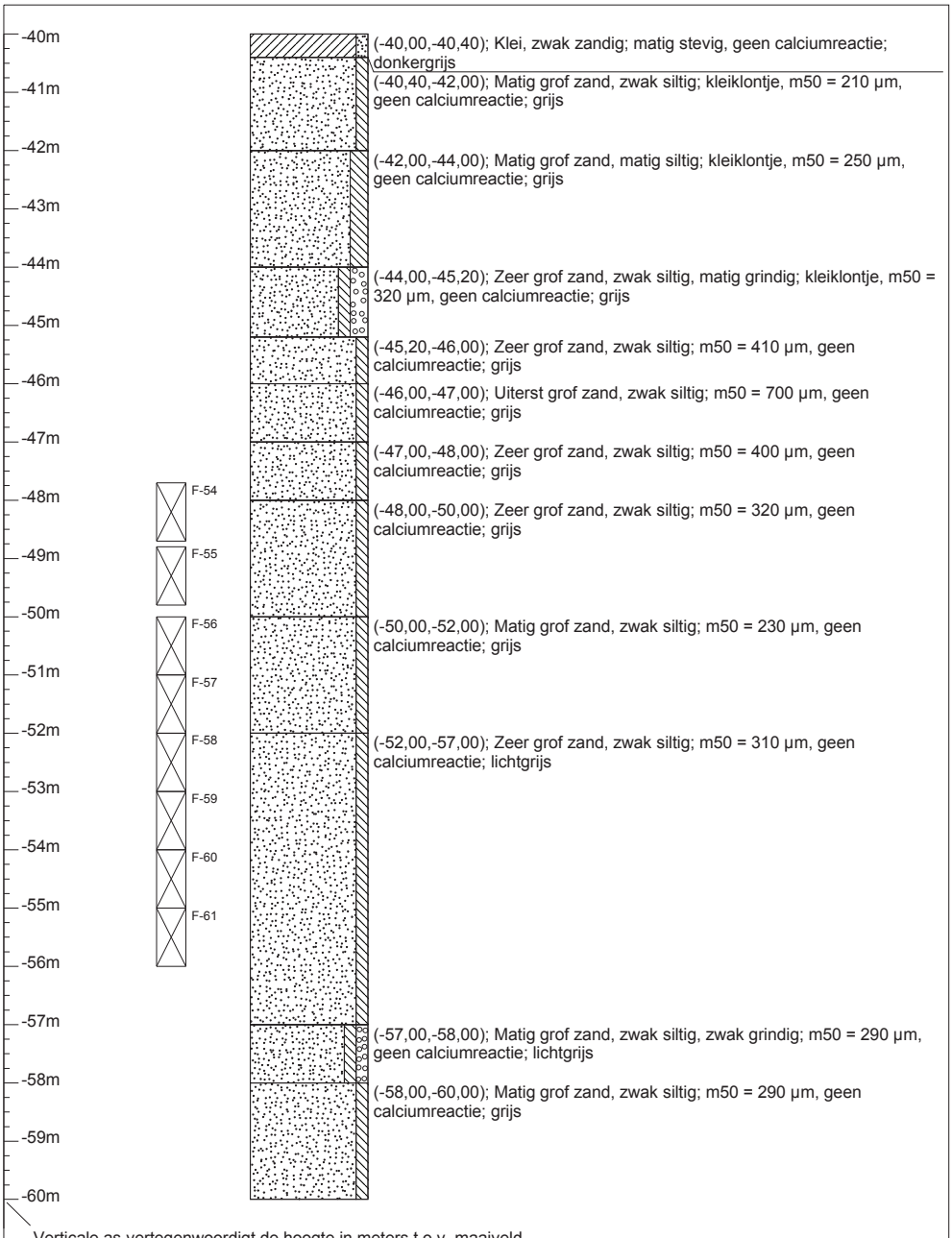

	Project/Plaats	Woudenberg	Datum	16-1-2012	Ons kenmerk	VN-54917-6
	Opdrachtgever		X-coordinaat	160.274 m	Uw kenmerk	
	Boormethode	Pulsboring	Y-coordinaat	454.374 m	Boornummer	
	Boormeester	HV/HH	KM		Boring F-2	
Getekend conform NEN 5104						

Wiertsema & Partners
RAADGEVEND INGENIEURS

kwaliteitswaarborg bodembeheer SIKB

AKKOORD UITV

54917-6 R18050 Resultaten grondmechanische boring.pdf

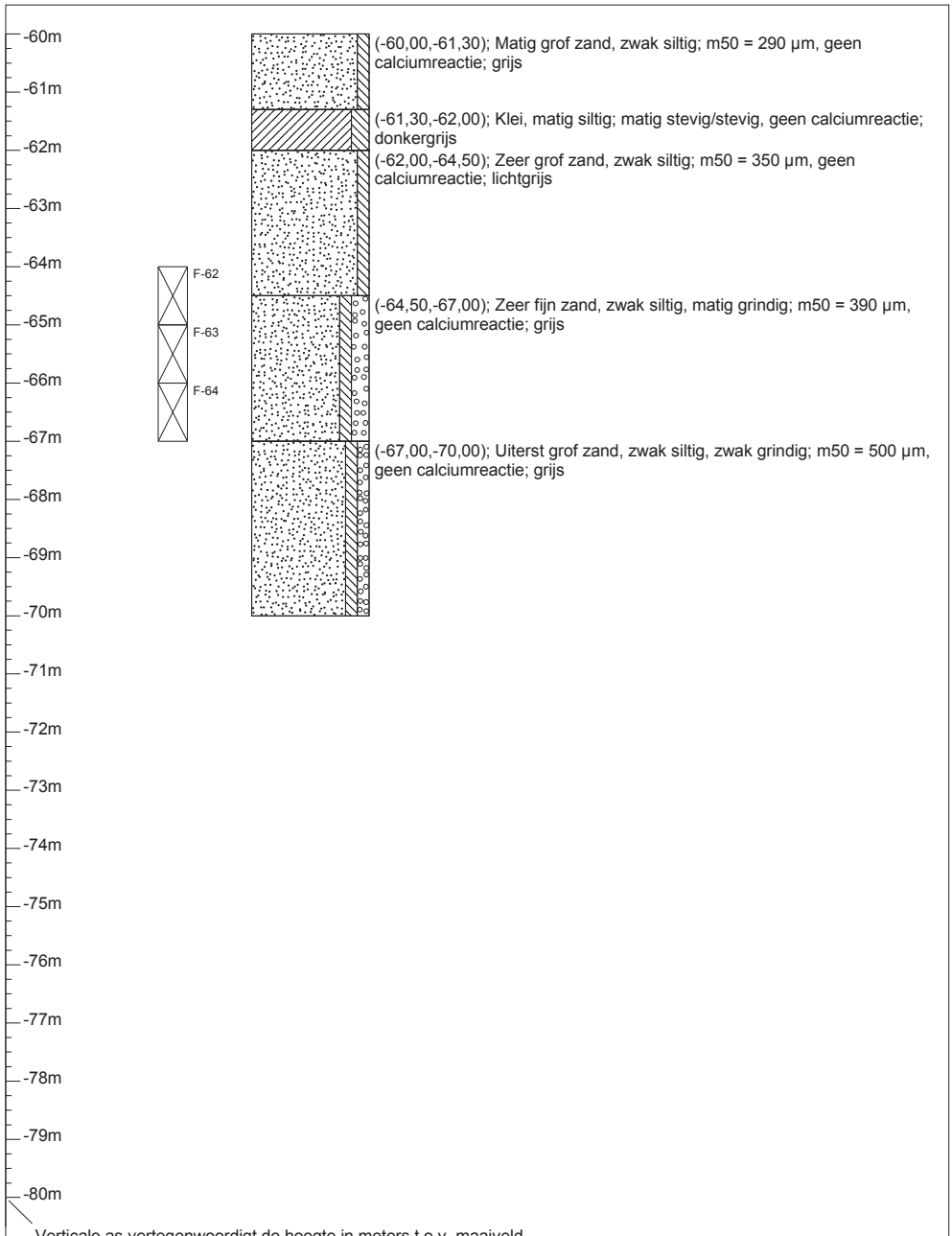

	Project/Plaats	Woudenberg	Datum	16-1-2012	Ons kenmerk	VN-54917-6
	Opdrachtgever		X-coordinaat	160.274 m	Uw kenmerk	
	Boormethode	Pulsboring	Y-coordinaat	454.374 m	Boornummer	
	Boormeester	HV/HH	KM		Boring F-2	
Getekend conform NEN 5104						

Wiertsema & Partners
RAADGEVEND INGENIEURS

kwaliteitswaarborg bodembeheer SIKB

AKKOORD UITV

54917-6 R18050 Resultaten grondmechanische boring.pdf

II Photo impression of experimental setup

Drilling at Helvoirt

Collection of sediment core at Helvoirt

Influent water collection at Scherpenzeel

Impression of column setup in a 11°C room

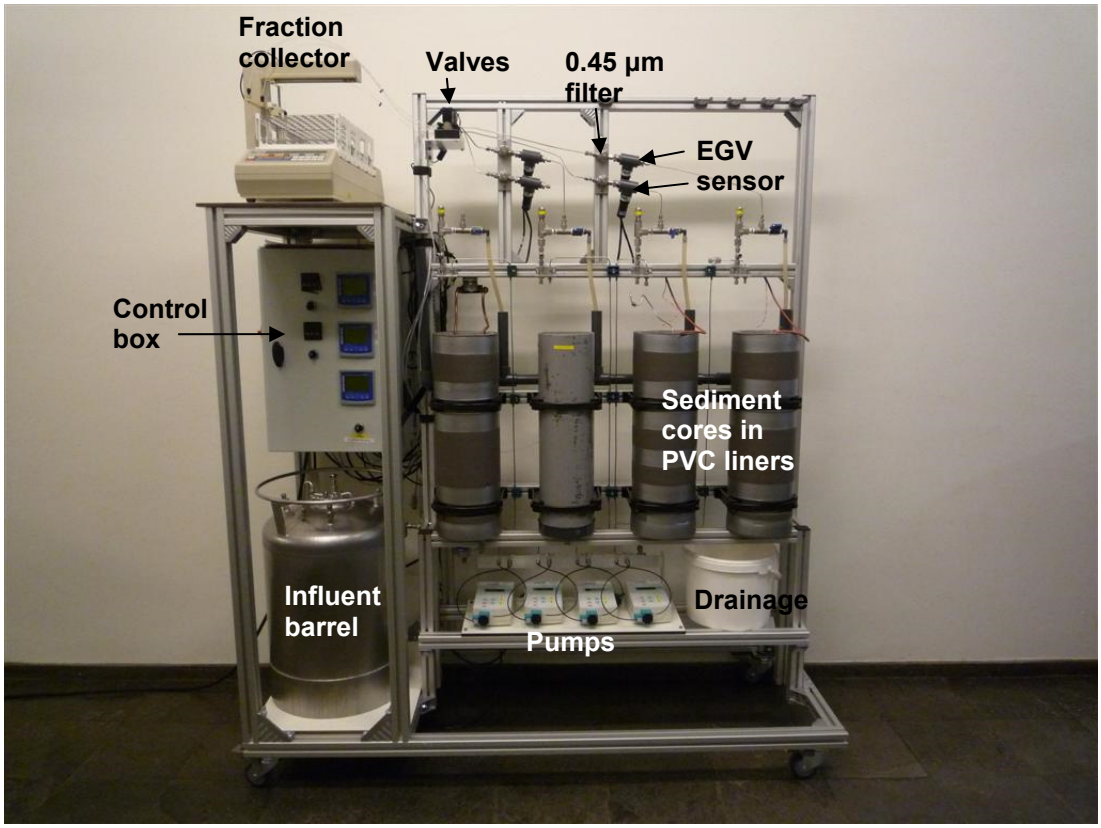

Front view of setup outside of room

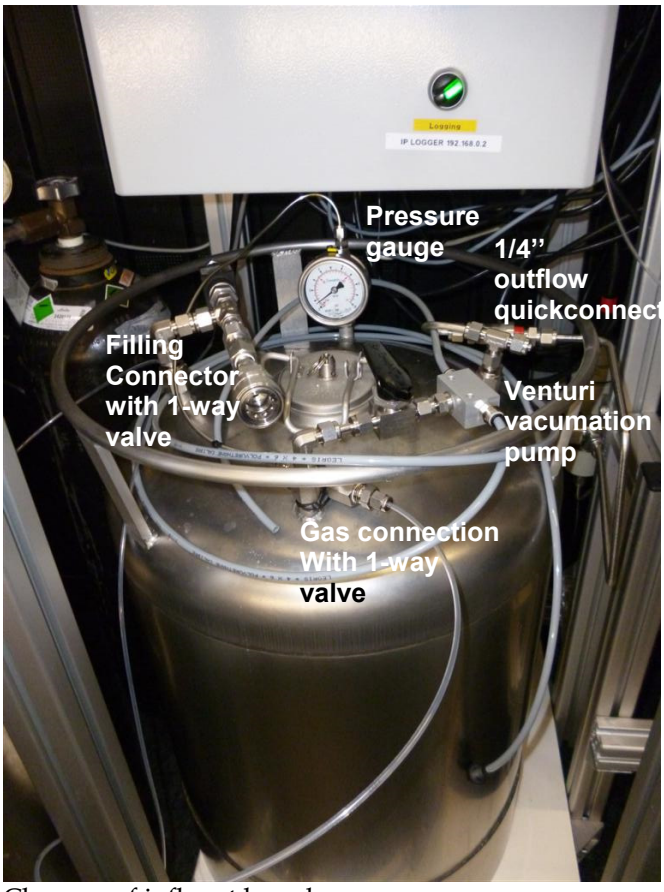

Close up of influent barrel

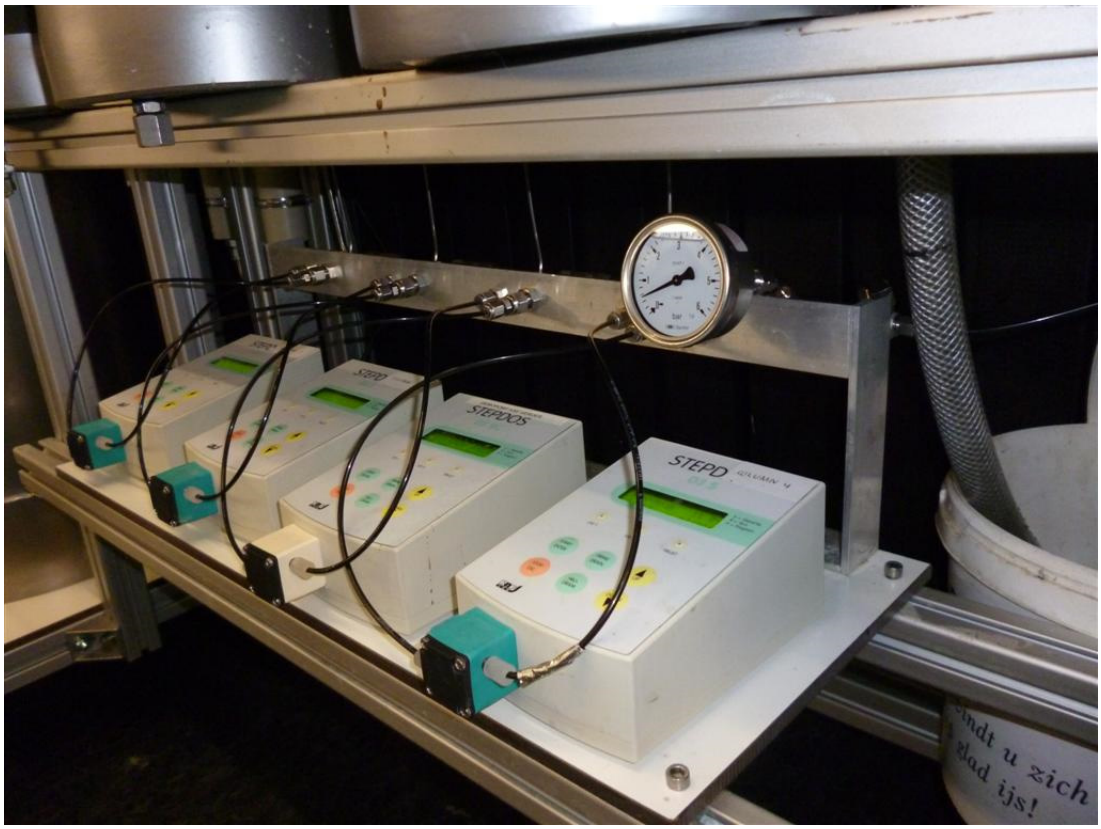

Close up of pumps

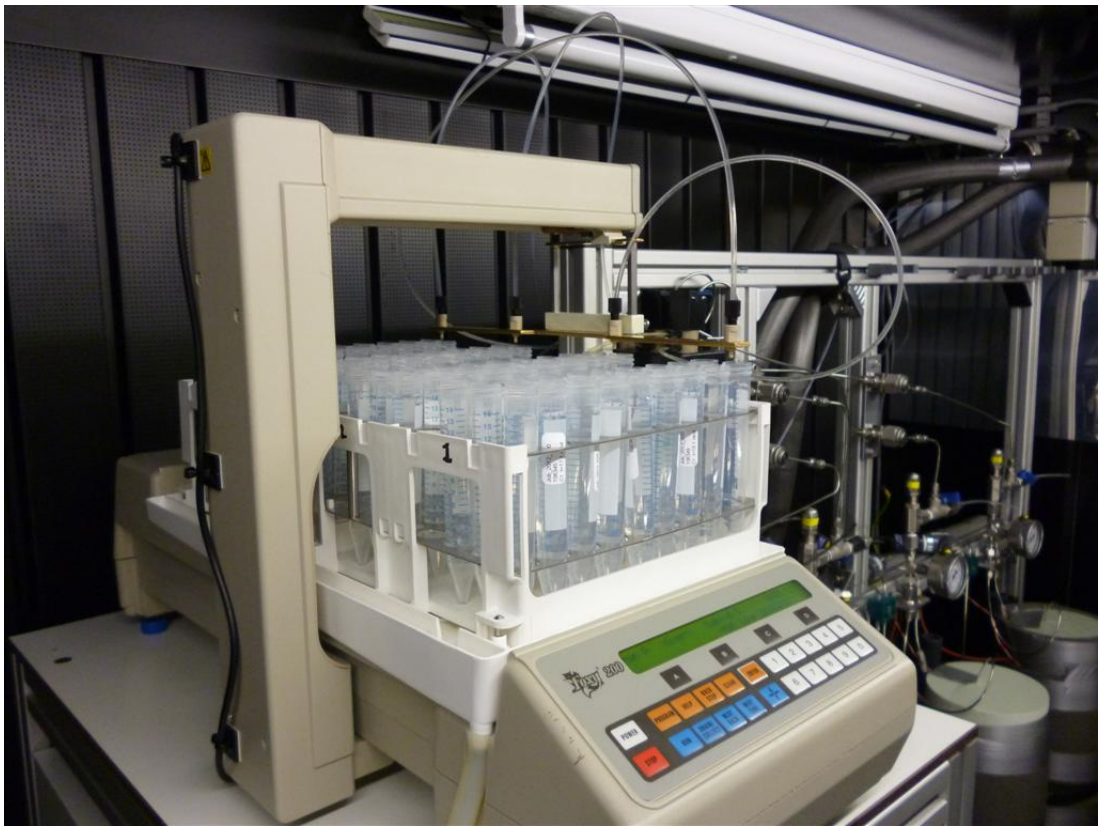
Close up of sample collector

III Analyses of the breakthrough curves

Analyses of breakthrough test

The results of the breakthrough tests were analysed using the analytical model CXTFIT [1]. This model is based on the advection-dispersion equation and estimates the main transport parameters by fitting the experimental data using a nonlinear least-squares parameter optimization method [1]. Assuming the tracer (NAME) is fully conservative, we used the model to calculate dispersivity and effective porosity. The porosity (n) can be checked with the porosity calculated from the bulk density (ρ_b) :

$$n = \frac{\rho_b - \rho_s}{\rho_w - \rho_s} \qquad \text{(III-1)}$$

Where ρ_s is the solid grain density which is assumed to be equal to 2.65 g/cm^3 considering that quartz is the main mineral present. The accuracy of the fit is described with the correlation coefficient (R^2) and the standard error defined by:

$$SE = \left[\sum (C_m - C_c)^2 / (n-2)\right]^{1/2} \qquad \text{(III-2)}$$

Results

Figure *1* and Table 1 present the results of the breakthrough tests (BTT) of the three experiments each having four columns and the derived porosity (n) and dispersivity (λ in cm), respectively. Also shown in Table 3-1 are the porosities calculated from the bulk density (Eq III-1), R^2 and the SE.
The porosities calculated from the BTT are generally lower than derived from the bulk density. The BTT porosity is likely to be more representative of the effective porosity, whereas the bulk density derived porosity is representative of the water content (which equals the effective porosity, stagnant zones and structurally bound water). It is also interesting to note that the BTT porosities generally decrease with increasing temperature (except for experiment C at 5ºC). This might be due to swelling of clay particles reducing the effective porosity or to degassing where gas pockets are formed.

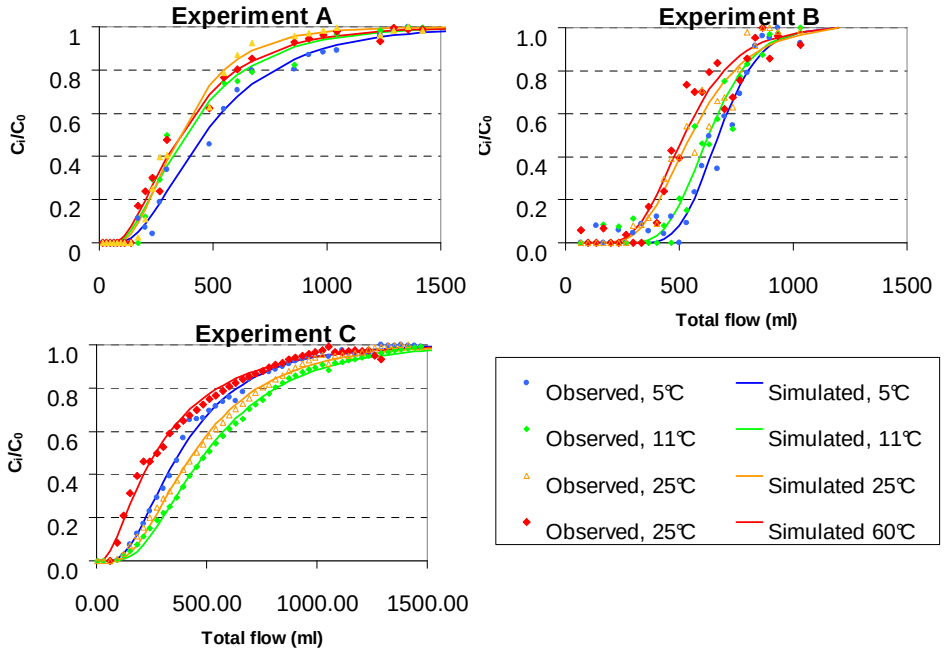

Figure 1 Results from breakthrough tests at three experiments. Solid lines are CXTFIT model results to determine dispersivity, points are observations. Red is 60°C, orange 25°C, green 11°C and blue 5°C.

The estimated dispersivities range between 1.42 and 9.26 cm, the overall average is 5.2 cm. For column experiments, Appelo and Postma [2] relate the expected dispersivity to the grain size (the 10% sieve passing) according to:

$$\lambda = 3.5\ d_{10} \qquad \text{(III-3)}$$

based on this relation, and the d10 values listed in Table 1, the dispersivity should be less than 0.1 cm which is more than an order of magnitude smaller than found here. This relation, however, disregards to consider the heterogeneity of the sediment. Klotz *et al* [3] found dispersivity values ranging between 0.2 to 23.5 cm depending on both grain size and heterogeneity as expressed by the uniformity coefficient (U, the ratio of 60% and 10% sieve passing). Another study by Perfect *et al*[4] found λ to range between 0.1 and 19 cm with most values between 4 and 7 cm. Results in this study depended on again on sediment texture where finer sediments generally yielded higher dispersivities. From Table 3-1 it can be seen that the largest dispersivities are found in experiment C. Comparing the dispersivities found here with dispersivities reported by Klotz *et al* [3] for sands with similar d_{50} and U-values (ranging between 1.0 to 2.6 cm) shows our quite high λ values are representative for the sand used and probably not the result of preferential flow paths.

Table 1 Summarised results from simulated breakthrough tests: dispersivities and porosities determined with CXTFIT, compared with the porosity calculated from bulk weights

Column	R^2	Dispersion coefficient, D (cm^2/min)	SE	Dispersivity, λ (cm)	s.d.	Effective porosity from breakthrough test (n_{eff})	Total porosity by weight, (n_{total})
Sediment A							
5ºC	0.99	0.17	0.001	7.99	0.03	0.38	n/a
11ºC	0.99	0.23	0.033	8.87	1.28	0.31	n/a
25ºC	0.99	0.16	0.019	6.06	0.70	0.29	n/a
60ºC	0.99	0.25	0.031	9.26	1.11	0.29	n/a
average	0.99	0.20	0.02	8.04	0.78	0.32	
Sediment B							
5ºC	0.96	0.21	0.046	1.42	0.31	0.41	0.38
11ºC	0.96	0.35	0.081	2.05	0.48	0.36	0.44
25ºC	0.95	1.01	0.230	5.05	1.15	0.30	0.41
60ºC	0.94	1.13	0.300	5.21	1.38	0.28	0.48
average	0.95	0.67	0.16	3.43	0.83	0.34	0.43
Sediment C							
5ºC	0.9956	3.76	0.041	10.4	0.11	0.14	0.28
11ºC	0.9995	2.53	0.010	9.2	0.04	0.18	0.31
25ºC	0.9980	3.03	0.019	9.8	0.06	0.16	0.33
60ºC	0.9896	13.01	0.099	23.8	0.18	0.09	0.34
average	1.00	5.58	0.000	13.3	0.10	0.14	0.32

References

1. Toride, N.; Leij, F. J.; van Genuchten, M. T. *TheCXTFIT Code for Estimating Transport Parameters from Laboratory or Field Tracer Experiments Version 2.0*; U. S. SALINITY LABORATORY: RIVERSIDE, CALIFORNIA, 1995; p 131.
2. Appelo, C. A. J.; Postma, D., *Geochemistry, groundwater and pollution, second edition*. A.A. Balkema: Leiden, 2005; p 649.
3. Klotz, D.; Seiler, K. P.; Moser, H.; Neumaier, F., Dispersivity and velocity relationship from laboratory and field experiments. *Journal of Hydrology* **1980,** *45*, (3–4), 169-184.
4. Perfect, E.; Sukop, M. C.; Haszler, G. R., Prediction of Dispersivity for Undisturbed Soil Columns from Water Retention Parameters. *Soil Sci. Soc. Am. J.* **2002,** *66*, (3), 696-701.

© KWR

IV Chemical analyses in- and effluent – TABLES

Type	Test	Day	t	hours	Pore flush	ID	VU_ID	Include Phreeqc	Temp	pH	EC	Alk (titr)	Alk (corr)	Cl	Br	NO3	NH4	SO4	F	DOC	UV	SUVA	Na	K	Ca	Mg	Fe	Mn	Si
Units									°C	-	µS/cm	(meq/l)	(meq/l)	mg/l	mg/l	mg/l	mg/l	mg/l	mg/l	mg/l			mg/l	mg/l	mg/l	mg/l	mg/l	mg/l	mg/l
DOL														0.1	0.05	0.1	0.01	0.1	0.02	0.200			0.0	0.00	0.00	0.00	0.001	0.001	0.01
A-a-Inf	A	6	24	144	6.0	A-Inf-6		0	20					28.9	0.06	1.6	0.35	8.4	0.03				12.0	1.08	28.2	2.21	0.04	1.49	10.30
A-a-Inf	A	9	24	216	9.0	A-Inf-9		1	20	6.9		1.37	1.20	27.8	0.03	1.3	0.40	8.1	0.07	2.4			11.9	1.05	28.2	2.21	0.61	1.50	10.40
A-a-Inf_av	A	-9999	-9999	-9999	-1.0	A-Inf_av		1	20	6.9	240	1.37	1.16	28.4	0.05	1.4	0.30	8.3	0.05	2.40			12.0	1.07	28.2	2.21	0.33	1.50	10.35
A-Sfdev	n/a	2.12									n/a			0.76	0.03	0.19	0.10	0.23	0.03	n/a			0.07	0.02	0.00	0.00	0.00	0.01	0.07
A-a-Field	A	-9999	-9999	-9999	A-f5			0	12					28.8	<0.05	<0.05		8.3	0.06				11.5	0.95	22.3	1.95	6.93	1.17	10.90
Ac-c1	A	1	2	2	0.1	Ac-c1-0.083		0	5		469			37.0	0.03	7.9		35.6	0.18				14.6	2.41	60.0	4.80	0.09	0.58	6.67
Ac-c1	A	1	6	6	0.3	Ac-c1-0.25		0	5		485			37.7	0.05	0.1		33.6	0.17				15.0	2.45	70.8	5.62	0.15	0.56	6.27
Ac-c1	A	1	10	10	0.4	Ac-c1-0.42		0	5		465			36.1	0.06	0.1		30.4	0.16				12.7	1.75	60.9	5.10	0.49	0.53	5.53
Ac-c1	A	1	24	24	1.0	Ac-c1-1		0	5		408			33.6	0.04	<0.05		23.0	0.16	17			12.0	1.53	53.8	4.50	0.01	0.48	5.63
Ac-c1	A	2	8	32	1.3	Ac-c1-1.33		0	5		369			31.0	0.05	0.6		16.0	0.13				11.8	1.47	49.2	4.11	0.91	0.45	6.02
Ac-c1	A	3	4	52	2.2	Ac-c1-2.17		0	5		343			28.0	0.02	0.1		11.6	0.16				11.0	1.38	44.2	3.66	0.05	0.40	5.82
Ac-c1	A	3	12	60	2.5	Ac-c1-2.5		0	5		334			28.9	0.04	0.1		11.0	0.18				11.0	1.36	42.7	3.56	0.68	0.39	6.28
Ac-c1	A	4	4	76	3.2	Ac-c1-3.17		0	5		315			27.1	0.02	<0.05		8.5	0.17				11.7	1.40	41.4	3.40	0.56	0.37	7.10
Ac-c1	A	4	12	84	3.5	Ac-c1-3.5		1	5	7.4	310	2.14	2.11	27.0	0.04	0.1		8.3	0.14				12.3	1.46	42.5	3.46	0.51	0.37	7.62
Ac-c1	A	5	6	102	4.3	Ac-c1-4.25		0	5		306			26.7	0.04	<0.05		8.1	0.14				12.0	1.33	41.3	3.33	0.31	0.36	7.94
Ac-c1	A	5	12	132	5.5	Ac-c1-5.5		0	5	7.2	306			26.7	0.02	<0.05		8.1	0.16				12.0	1.33	41.3	3.33	0.31	0.36	7.94
Ac-c1	A	5	24	120	5.0	Ac-c1-5		1	5	7.2	306	1.91	2.02	26.6	0.01	0.1		8.0	0.16	2.3			12.5	1.42	40.9	3.27	0.04	0.36	8.28
Ac-c1	A	6	12	132	5.5	Ac-c1-5.5		0	5		307			27.0	0.05	0.1		8.1	0.16				11.9	1.28	39.2	3.15	0.20	0.35	8.38
Ac-c1	A	7	6	150	6.3	Ac-c1-6.25		0	5		308			27.1	<0.05	1.2		7.8	0.05				12.5	1.30	41.9	3.28	0.01	0.38	8.60
Ac-c1	A	7	24	168	7.0	Ac-c1-7		1	5	7.2	307	2.25	2.08	27.3	<0.05	1.1		7.9	0.08	2.4			12.9	1.40	43.3	3.36	0.02	0.39	8.69
Ac-c1	A	8	12	180	7.5	Ac-c1-7.5		0	5		297			27.3	<0.05	1.4		8.1	0.15				13.5	1.54	44.8	3.33	0.02	0.41	9.44
Ac-c1	A	10	24	240	10.0	Ac-c1-10		1	5	7.2	305	2.08	2.40	26.8	0.03	0.3		7.8	0.11	2.6			14.3	1.47	47.0	3.40	0.02	0.47	8.91
Ac-c1	A	14	24	312	13.0	Ac-c1-13		1	5	7.4	307	2.12	1.96	28.0	<0.05	0.1	0.62	8.2	0.06				12.7	1.45	39.9	3.07	1.00	0.42	8.56
Ac-c1	A	16	24	360	15.0	Ac-c1-15		1	5		302	1.86		27.1	0.06	<0.05	0.52	7.7	0.03	3.2			12.7	1.84	39.1	2.95	0.20	0.38	9.01
Ac-c1	A	18	24	408	17.0	Ac-c1-17		1	5		304	1.8		27.5	0.06	0.1		7.8	0.03				12.8	1.35	40.6	2.96	0.02	0.43	8.95
Ac-c1	A	21	24	480	20.0	Ac-c1-20		1	5	7.3	301	1.8		31.0	<0.05	2.8	0.39	7.3	0.08				12.4	1.33	37.7	2.84	0.06	0.40	8.84
Ac-c1	A	23	24	528	22.0	Ac-c1-22		1	5		296	2.35	1.78	28.5	<0.05	0.1	0.46	8.1	0.07	2.7			12.6	1.28	38.1	2.73	0.09	0.42	9.53
Ac-c2	A	1	2	2	0.1	Ac-c2-0.08		0	12		480	1.83		38.7	0.02	7.5		32.3	0.19				14.5	2.35	62.1	5.03	0.93	0.52	6.47
Ac-c2	A	1	6	6	0.3	Ac-c2-0.25		0	12		470			37.5	0.05	<0.05		29.4	0.19				14.0	2.13	61.2	5.06	1.29	0.53	6.26
Ac-c2	A	1	10	10	0.4	Ac-c2-0.42		0	12		438			35.4	0.05	0.1		25.4	0.17				13.1	1.92	57.3	4.75	1.18	0.50	5.91
Ac-c2	A	2	8	32	1.3	Ac-c2-1.33		0	12		373			30.0	0.04	0.3		14.6	0.19				12.4	1.78	50.8	4.18	0.60	0.45	6.10
Ac-c2	A	3	4	52	2.2	Ac-c2-2.17		0	12		337			28.0	0.03	0.1		10.0	0.21				11.1	1.57	42.7	3.50	1.05	0.37	6.27
Ac-c2	A	4	4	76	3.2	Ac-c2-3.17		0	12		326			26.3	0.03	<0.05		8.8	0.18				11.2	1.52	41.0	3.35	0.14	0.34	6.71
Ac-c2	A	4	12	84	3.5	Ac-c2-3.5		1	12	7.3	324	2	1.90	26.9	0.03	0.1		8.8	0.16				11.0	1.50	39.9	3.21	0.07	0.33	6.95
Ac-c2	A	5	24	120	5.0	Ac-c2-5		0	12		316			27.1	<0.05	<0.05		8.8	0.19	2.4			12.0	1.55	41.5	3.33	0.06	0.33	7.54
Ac-c2	A	6	12	132	5.5	Ac-c2-5.5		0	12		312			26.7	0.07	0.3		8.3	0.15				12.1	1.47	40.6	3.21	0.04	0.31	8.55
Ac-c2	A	7	6	150	6.3	Ac-c2-6.25		1	12	7.3	314	1.97	2.13	27.0	<0.05	1.4		8.4	0.10	2.3			13.0	1.63	44.2	3.44	0.01	0.36	8.66
Ac-c2	A	7	24	168	7.0	Ac-c2-7		0	12		314			27.0	0.04	0.1		7.9	0.10	2.3			14.6	1.80	49.8	3.84	0.02	0.36	8.80
Ac-c2	A	8	12	180	7.5	Ac-c2-7.5		0	12		312			26.4	<0.05	1.4		8.1	0.11				13.3	1.60	45.5	3.49	0.02	0.33	8.86
Ac-c2	A	9	12	204	8.5	Ac-c2-8.5		1	12	7.4	303	1.9	1.29	27.5	0.05	6.8		8.3	0.02				11.7	1.36	37.7	2.87	0.00	0.27	9.43
Ac-c2	A	10	24	240	10.0	Ac-c2-10		1	12	7.4	304	1.92	2.20	27.6	0.05	0.4		7.9	0.07	2.4			14.0	1.60	44.3	3.22	0.02	0.32	9.57
Ac-c2	A	14	24	312	13.0	Ac-c2-13		1	12	7.5	301	2.13	1.70	31.8	<0.05	<0.05	0.52	7.2	0.08	2.6			12.4	1.28	38.2	2.65	0.04	0.33	9.67
Ac-c2	A	16	24	360	15.0	Ac-c2-15		0	12		305	1.87		28.1	<0.05	1.2	0.49	8.1	0.07				13.0	2.23	39.2	2.70	0.04	0.30	9.75
Ac-c2	A	18	24	408	17.0	Ac-c2-17		1	12	7.6	308	2.14	1.84	28.5	<0.05	1.1		8.1	0.07	2.4			12.7	1.36	41.1	2.67	0.01	0.37	9.73
Ac-c2	A	21	24	480	20.0	Ac-c2-20		1	12	7.2	300	2.12	1.78	27.6	<0.05	<0.05	0.33	7.8	0.05				12.5	1.25	38.2	2.46	0.05	0.37	9.39
Ac-c2	A	25	24	576	24.0	Ac-c2-24		0	12		305	1.83		31.9	<0.05	<0.05	0.23	7.5	0.07	2.4			12.7	1.24	40.3	2.54	0.14	0.36	9.25
Ac-c3	A	1	6	6	0.3	Ac-c3-0.25		0	25		479			37.6	0.03	0.9		31.3	0.24				14.5	2.48	59.8	5.06	1.31	0.55	6.72
Ac-c3	A	1	10	10	0.4	Ac-c3-0.42		0	25		466			34.0	0.04	0.6		23.7	0.17				13.5	2.32	54.0	4.57	0.93	0.50	6.74
Ac-c3	A	1	24	24	1.0	Ac-c3-1		0	25		408			31.7	0.02	<0.05		17.6	0.23	5.9			12.6	2.44	53.8	4.49	0.83	0.50	7.03
Ac-c3	A	2	8	32	1.3	Ac-c3-1.33		0	25		372			27.6	0.06	0.2		11.2	0.22				11.8	2.30	48.4	3.99	1.15	0.44	7.25
Ac-c3	A	3	12	60	2.5	Ac-c3-2.5		0	25		320			26.3	<0.05	<0.05		7.8	0.26				10.9	1.89	38.8	3.07	0.68	0.31	7.63
Ac-c3	A	4	4	76	3.2	Ac-c3-3.17		0	25		319			26.2	0.03	0.1		8.1	0.44				12.2	2.11	42.7	3.38	0.05	0.34	7.86
Ac-c3	A	4	8	80	3.3	Ac-c3-3.33		0	25		320	2.2		25.6	0.01	2.5		7.7	0.21				11.6	2.02	40.6	3.17	0.06	0.32	8.23
Ac-c3	A	5	6	102	4.3	Ac-c3-4.25		0	25		311			27.3	0.04	0.2		8.2	0.19				12.9	2.11	45.3	3.43	0.27	0.33	8.46
Ac-c3	A	5	24	120	5.0	Ac-c3-5		1	25	7.2	308	2.03	1.98	27.1	0.01	<0.05		8.1	0.20	2.4			12.3	1.95	40.9	3.12	0.06	0.29	9.04
Ac-c3	A	6	12	132	5.5	Ac-c3-5.5		0	25		309			26.6	0.03	0.1		7.6	0.14				12.8	1.92	43.3	3.21	0.07	0.29	9.12
Ac-c3	A	7	6	150	6.3	Ac-c3-6.25		0	25		309			26.8	<0.05	0.1		7.7	0.11				12.9	1.85	44.0	3.26	0.05	0.28	9.15
Ac-c3	A	7	24	168	7.0	Ac-c3-7		1	25	7.4	307	1.99	2.25	27.6	0.05	0.9		8.0	0.18	2.6			13.5	1.88	46.2	3.40	0.04	0.29	9.53
Ac-c3	A	8	12	180	7.5	Ac-c3-7.5		1	25	7.3	306	1.97	2.21	27.0	<0.05	0.1		7.8	0.07				13.0	1.77	44.3	3.25	0.04	0.28	9.46
Ac-c3	A	9	12	204	8.5	Ac-c3-8.5		1	25	7.4	310	1.89	1.69	27.3	0.03	1.8		7.9	0.06				11.5	1.53	38.8	2.83	0.01	0.25	9.43
Ac-c3	A	10	24	240	10.0	Ac-c3-10		1	25	7.2	304	2.11	2.07	27.5	0.05	0.3		7.8	0.08	2.7			13.0	1.87	42.3	3.06	0.04	0.26	9.44
Ac-c3	A	14	24	312	13.0	Ac-c3-13		1	25	7.5	302	1.99	1.87	27.4	<0.05	<0.05	0.94	7.8	0.05	2.8			12.3	1.45	38.7	2.77	0.03	0.23	9.37
Ac-c3	A	16	24	360	15.0	Ac-c3-15		1	25	7.5	303	1.95	1.91	27.8	<0.05	<0.05	0.56	7.9	0.05				12.5	1.50	40.0	2.79	0.07	0.23	9.87
Ac-c3	A	18	24	408	17.0	Ac-c3-17		1	25	7.5	300	1.91	1.79	31.9	<0.05	<0.05	0.46	7.5	0.04	2.8			12.7	1.41	39.8	2.74	0.06	0.22	9.86
Ac-c3	A	21	24	480	20.0	Ac-c3-20		1	25	7.5	296	1.88	1.76	27.7	<0.05	<0.05	0.39	7.8	0.05	2.8			12.4	1.31	37.8	2.56	0.06	0.21	9.63
Ac-c3	A	23	24	528	22.0	Ac-c3-22		1	25	7.4	296	1.93	1.80	28.0	<0.05	0.1	0.31	7.8	0.03				12.6	1.30	38.8	2.53	0.03	0.20	9.74
Ac-c3	A	25	24	576	24.0	Ac-c3-24		1	25	7.5	299	1.82	1.75	32.0	<0.05	0.1	0.30	7.6	0.08	2.9			12.5	1.37	40.1	2.56	0.03	0.22	9.68
Ac-c4	A	1	2	2	0.1	Ac-c4-0.08		0	60		469			39.6	0.03	3.4		29.6	0.16				14.1	2.99	62.6	4.77	0.08	0.45	7.85
Ac-c4	A	1	6	6	0.3	Ac-c4-0.25		0	60		480			35.1	0.04	0.9		24.1	0.26				15.0	3.72	64.4	4.72	0.42	0.41	10.90
Ac-c4	A	1	10	10	0.4	Ac-c4-0.42		0	60		466			40.6	0.05	<0.05		24.1	0.30				14.4	4.00	61.0	4.27	0.81	0.36	12.40
Ac-c4	A	1	24	24	1.0	Ac-c4-1		0	60		425			30.9	0.04	<0.05		15.2	0.28	8.5			13.9	4.26	58.0	3.92	1.52	0.33	14.50
Ac-c4	A	2	8	32	1.3	Ac-c4-1.33		0	60		406			29.4	0.05	0.1		11.0	0.32				13.2	4.23	54.4	3.62	1.84	0.30	15.50
Ac-c4	A	3	4	52	2.2	Ac-c4-2.17		0	60		382			34.7	0.03	0.3		8.1	0.33				13.0	10.50	54.4	3.56	0.37	0.27	15.60
Ac-c4	A	3	12	60	2.5	Ac-c4-2.5		0	60		369			27.6	0.02	<0.05		7.3	0.33				12.0	3.91	49.6	3.20	0.23	0.24	15.10
Ac-c4	A	4	4	76	3.2	Ac-c4-3.17		0	60		356			26.1	0.05	0.1		8.0	0.47				12.9	4.21	54.5	3.41	0.23	0.24	14.60
Ac-c4	A	4	12	84	3.5	Ac-c4-3.5		1	60	7.3	350	1.97	2.43	27.0	0.03	<0.05		6.7	0.29				11.8	3.76	49.0	3.03	0.13	0.21	14.60
Ac-c4	A	5	6	102	4.3	Ac-c4-4.25		0	60		343			31.7	0.05	<0.05		6.5	0.31				12.3	11.00	50.8	3.10	0.08	0.21	14.50

Type	Test	Day	t	hours	Pore flush	ID	VU_ID	Include Phreeqc	Temp	pH	EC	Alk (titr)	Alk (corr)	Cl	Br	NO3	NH4	SO4	F	DOC	UV	SUVA	Na	K	Ca	Mg	Fe	Mn	Si
Units									°C	-	µS/cm	(meq/l)	(meq/l)	mg/l	mg/l	mg/l	mg/l	mg/l	mg/l	mg/l			mg/l	mg/l	mg/l	mg/l	mg/l	mg/l	mg/l
Ac-c4	A	5	24	120	5.0	A-c4-5		0	60	7.1		333		30.3	0.04	0.1		6.9	0.30	4.4			11.8	7.14	46.0	2.77	0.06	0.19	14.30
Ac-c4	A	6	12	132	5.5	A-c4-5.5		0	60			328		30.6	<0.05	0.1		6.5	0.31				11.6	7.59	44.2	2.62	0.05	0.17	13.70
Ac-c4	A	7	6	150	6.3	A-c4-6.25		0	60			323		30.2	0.05	1.1		7.1	0.19				13.3	8.07	51.3	2.97	0.05	0.19	13.40
Ac-c4	A	7	24	168	7.0	A-c4-7		1	60	7.2		318	2.18	30.4	0.06	<0.05		7.1	0.25	4.2			13.5	7.63	50.9	2.86	0.06	0.18	13.20
Ac-c4	A	8	12	180	7.5	A-c4-7.5		0	60			316		30.7	0.05	0.2		7.2	0.19				13.1	7.24	47.0	2.66	0.06	0.17	13.10
Ac-c4	A	9	12	204	8.5	A-c4-8.5		1	60	7.1		321	2.01	31.3	<0.05	1.2		7.3	0.10				11.5	6.74	41.7	2.36	0.04	0.15	13.30
Ac-c4	A	10	24	240	10.0	A-c4-10		1	60	7.3		314	2.11	31.5	0.05	0.5		7.1	0.19	4.4			12.3	6.73	42.7	2.42	0.05	0.16	13.10
Ac-c4	A	14	24	312	13.0	A-c4-13		1	60	7.3		306	2.07	28.0	<0.05	0.1	0.45	7.9	0.05	4.3			12.5	6.45	40.8	2.28	0.06	0.15	12.30
Ac-c4	A	16	24	360	15.0	A-c4-15		1	60	7.2		306	1.92	28.2	<0.05	0.1	0.48	8.0	0.04				12.6	6.78	41.6	2.25	0.04	0.15	12.30
Ac-c4	A	18	24	408	17.0	A-c4-17		0	60			302	1.84	27.0	<0.05	0.1		7.3	0.04	3.7			12.5	6.02	40.6	2.21	0.06	0.15	12.10
Ac-c4	A	21	24	480	20.0	A-c4-20		1	60	7.3		298	1.9	26.9	<0.05	0.1	0.29	7.4	0.05				12.3	5.88	38.8	2.07	0.05	0.14	11.30
Ac-c4	A	23	24	528	22.0	A-c4-22		1	60	7.2		296	1.81	27.9	<0.05	0.1		8.2	0.04	3.6			12.5	5.78	39.7	2.09	0.03	0.14	11.60
Ac-c4	A	25	24	576	24.0	A-c4-24		1	60	7.3		295	1.81	27.8	<0.05	0.1	0.04	7.7	0.05	3.3			12.4	5.36	39.2	2.05	0.02	0.14	11.20
B-hf	B				30.0	B-hf-30		1	20	6.8		215	1.09	28.3	<0.05	0.2		7.9	0.04	1.975			13.6	1.80	27.5	2.52	0.79	0.92	11.00
B-hf	B				35.0	B-hf-35		1	20	7.0		237	1.1	27.9	<0.05	0.2		8.1	0.04	1.975			13.4	1.31	27.1	2.51	0.91	0.92	11.00
B-Hf_av	B				0.0	B-hf_av-0@60		1	20	6.9		227	1.25	27.2	<0.05	0.2		7.8	0.06	1.975			13.6	1.80	24.3	2.11	6.46	0.93	10.40
B-Hf_av	B				10.0	B-hf_av-0@60		1	20	6.9		227	1.25	27.2	<0.05	0.2		7.8	0.06	1.975			13.6	1.80	24.3	2.11	6.46	0.93	10.40
B-Hf_av	B				10.3	B-hf_av-7.2@60		1	20	6.8		215	1.09	28.3	<0.05	0.2		7.9	0.04	1.975			13.6	1.80	27.5	2.52	0.79	0.92	11.00
B-Hf_av	B				35.0	B-hf_av-7.2@60		1	20	6.8		215	1.09	28.3	<0.05	0.2		7.9	0.04	1.975			13.6	1.80	27.5	2.52	0.79	0.92	11.00
B_st_dev	B									0.19	30.20	0.28	0.18	0.50	n/a	0.06	n/a	0.13	0.01	0.54	n/a	n/a	0.48	0.24	5.54				
B-c1	B				0.1	B-c1-0.08		1	5	6.8		301	1.44	0.38	80.8	<0.05	0.5	25.5	0.00				24.2	4.91	33.0	3.72	1.11	0.49	4.16
B-c1	B				0.2	B-c1-0.17		0	5						82.6	<0.05	0.3		24.7	0.01				22.7	4.41	32.1	3.61	0.90	0.48	4.11
B-c1	B				0.3	B-c1-0.25		0	5						80.7	<0.05	0.5		26.1	0.01				23.5	5.00	33.5	3.70	1.14	0.49	4.13
B-c1	B				0.3	B-c1-0.33		0	5						79.5	<0.05	1.4		28.0	0.00				23.5	4.47	33.6	3.74	1.30	0.49	4.11
B-c1	B				0.4	B-c1-0.42		0	5						81.0	0.04	0.4		32.0	0.00				24.7	5.46	33.2	3.84	0.21	0.47	3.81
B-c1	B				0.5	B-c1-0.5		0	5						80.7	0.05	0.2		36.0	0.04				23.8	4.24	34.2	3.85	0.64	0.50	3.91
B-c1	B				1.1	B-c1-1.08		0	5						30.6	<0.05	0.1		13.8	0.04	3.175			19.6	3.10	21.3	2.40	1.60	0.34	4.72
B-c1	B				1.2	B-c1-1.17		1	5	6.9		226	1.56	1.13	29.7	<0.05	2.0		12.1	0.01				20.3	3.39	21.6	2.47	1.45	0.32	4.82
B-c1	B				1.3	B-c1-1.25		0	5						30.0	<0.05	0.5		11.8	0.00				20.2	3.72	21.4	2.58	1.38	0.32	4.91
B-c1	B				1.3	B-c1-1.33		1	5	7.0		226	1.52	1.26	28.5	<0.05	0.2		10.4	0.04				19.3	3.26	21.4	2.47	1.43	0.32	5.17
B-c1	B				1.4	B-c1-1.42		0	5						29.3	<0.05	0.3		10.4	0.01				20.0	3.84	22.2	2.59	0.95	0.32	5.55
B-c1	B				1.5	B-c1-1.5		1	5	7.0		228	1.4	1.25	28.6	0.06	0.2		9.4	0.02				18.1	3.27	21.5	2.44	1.47	0.32	5.86
B-c1	B				2.2	B-c1-2.17		1	5	6.5		225	1.35	1.26	28.0	<0.05	0.1		8.5	0.03	2.375			14.3	3.14	23.9	2.68	1.72	0.36	7.63
B-c1	B				2.3	B-c1-2.33		1	5	6.9		224	1.41	1.26	27.8	0.02	0.1		8.3	0.04				13.7	3.18	24.1	2.71	2.01	0.37	7.93
B-c1	B				2.5	B-c1-2.5		1	5	7.0		236	1.23	1.25	28.0	<0.05	0.1		8.4	0.03				13.3	3.11	24.5	2.68	2.05	0.37	8.03
B-c1	B				3.2	B-c1-3.17		1	5	6.7		220	1.15	1.24	28.2	0.07	0.2		8.4	0.01	2.75			13.2	3.32	24.3	2.69	2.10	0.37	8.82
B-c1	B				3.3	B-c1-3.33		1	5	6.7		219	1.41	1.22	28.1	<0.05	<0.05		8.4	0.03				13.0	3.17	24.0	2.66	2.11	0.37	8.99
B-c1	B				3.5	B-c1-3.5		1	5	6.7		225	1.39	1.17	28.7	<0.05	0.2		8.7	0.03				13.2	3.21	23.4	2.67	2.15	0.36	8.90
B-c1	B				4.2	B-c1-4.17		1	5	6.7		220	1.37	1.38	27.8	<0.05	0.3		8.2	0.05	2.175			14.3	3.37	25.3	2.86	2.51	0.40	9.84
B-c1	B				4.3	B-c1-4.33		0	5						27.7	<0.05	0.4		8.1	0.04				13.8	3.18	24.4	2.75	2.38	0.38	9.62
B-c1	B				4.5	B-c1-4.5		1	5	6.8		222	1.38	1.26	27.8	0.01	1.1		8.3	0.03	1.975			14.2	3.29	24.5	2.80	2.41	0.38	9.77
B-c1	B				5.3	B-c1-5.25		1	5	7.0		221	1.39	1.25	27.9	<0.05	0.2		8.4	0.04	1.975			13.7	3.22	23.9	2.70	2.50	0.38	9.72
B-c1	B				5.5	B-c1-5.5		1	5	6.7		217	1.2	1.34	27.3	<0.05	<0.05		8.0	0.05	1.875			14.0	3.27	24.5	2.73	2.58	0.39	10.10
B-c1	B				6.3	B-c1-6.25		1	5	6.9		219	1.39	1.33	27.5	<0.05	0.3		8.0	0.03	1.875			14.2	3.24	24.6	2.74	2.72	0.39	10.20
B-c1	B				6.5	B-c1-6.5		1	5	6.7		226	1.47	1.33	27.1	0.06	0.1		8.0	0.03	2.275			14.1	3.40	24.0	2.75	2.64	0.39	10.20
B-c1	B				7.3	B-c1-7.25		1	5	6.8		221	1.13	1.21	27.7	<0.05	<0.05		8.1	0.06	2.275			13.4	3.07	23.0	2.57	2.70	0.37	9.91
B-c1	B				7.5	B-c1-7.5		1	5	6.5		216	1.16	1.30	28.1	<0.05	0.1		8.1	0.03				14.0	3.27	24.3	2.68	2.54	0.38	10.10
B-c1	B				8.3	B-c1-8.25		1	5	6.9		223	1.37	1.29	27.9	<0.05	<0.05		8.1	0.06	2.75			14.0	3.10	23.9	2.65	2.67	0.38	10.20
B-c1	B				8.5	B-c1-8.5		1	5	6.9		220	1.3	1.27	27.6	<0.05	0.3		8.1	0.02	2.175			13.8	3.33	24.0	2.65	2.54	0.38	10.40
B-c1	B				9.5	B-c1-9.5		1	5	6.6		215	1.31	1.16	28.6	0.08	0.2		8.3	0.05				13.4	2.86	22.9	2.53	2.57	0.35	9.91
B-c1	B				10.0	B-c1-10		0	5						28.5	<0.05	0.2		8.4	0.05				13.3	2.66	22.5	2.51	0.86	0.35	9.99
B-c1	B				11.0	B-c1-11		1	5	6.6	207	1.26	1.06	28.5	<0.05	0.1		8.4	0.03				13.3	2.66	22.5	2.47	0.43	0.34	9.98
B-c1	B				12.0	B-c1-12		1	5	6.5	209	1.26	0.97	29.0	<0.05	0.2		8.5	0.05				13.5	2.76	21.4	2.45	0.10	0.33	9.65
B-c1	B				13.0	B-c1-13		1	5	6.3	213	1.22	1.02	28.3	<0.05	0.1		8.3	0.04				13.2	2.56	21.6	2.40	0.85	0.34	9.72
B-c1	B				14.0	B-c1-14		1	5	6.8	218	1.27	0.97	28.7	<0.05	0.2		8.4	0.04	1.875			13.4	2.40	20.8	2.43	0.88	0.34	9.73
B-c1	B				15.0	B-c1-15		1	5	6.7	221	1.28	1.05	28.5	<0.05	0.1		8.4	0.04	1.875			13.5	2.29	21.5	2.46	1.99	0.35	9.71
B-c1	B				16.0	B-c1-16		1	5	7.0	219	1.28	1.04	28.7	<0.05	0.1		8.4	0.03	1.975			13.5	2.28	21.9	2.49	1.34	0.35	9.79
B-c1	B				19.0	B-c1-19		1	5	6.9	224	1.34	0.95	28.0	<0.05	0.6		8.7	0.03	1.875			13.3	2.97	21.8	2.47	0.64	0.34	9.68
B-c1	B				20.0	B-c1-20		1	5	7.0	224	1.27	1.00	28.4	<0.05	0.4		8.5	0.04	2.075			13.3	1.69	21.8	2.48	1.17	0.34	9.72
B-c1	B				21.0	B-c1-21		1	5	7.0	221	1.13	1.01	29.4	<0.05	0.2		8.6	0.04	2.075			13.6	1.95	21.8	2.53	1.41	0.34	9.70
B-c1	B				22.0	B-c1-22		1	5	6.9	221	1.34	1.01	29.1	<0.05	<0.05		8.6	0.04	2.275			13.5	1.66	21.8	2.55	1.11	0.34	9.78
B-c1	B				23.0	B-c1-23		1	5	7.0	225	1.29	1.05	29.4	<0.05	0.2		8.6	0.02	2.075			14.0	2.37	22.2	2.56	0.99	0.34	9.78
B-c1	B				26.0	B-c1-26		1	5	7.0	242	1.4	0.95	29.3	<0.05	0.4		8.9	0.06	2.675			13.5	1.71	21.9	2.47	0.40	0.33	9.81
B-c2	B				0.1	B-c2-0.08		1	12	6.7	317	0.64	0.57	58.0	<0.05	0.3		47.6	0.05				23.3	6.76	33.9	3.43	0.13	0.52	5.73
B-c2	B				0.2	B-c2-0.17		0	12						58.5	<0.05	0.3		49.7	0.01				23.6	5.10	33.0	3.49	0.15	0.49	5.40
B-c2	B				0.3	B-c2-0.25		0	12						60.2	<0.05	0.2		52.1	0.00				24.5	5.22	35.5	3.64	0.09	0.51	5.29
B-c2	B				0.3	B-c2-0.33		0	12						60.7	<0.05	0.1		53.7	0.01				24.4	4.89	34.1	3.64	0.060	0.49	4.93
B-c2	B				0.4	B-c2-0.42		0	12						60.1	<0.05	0.3		54.9	0.00				24.1	5.43	33.1	3.58	0.73	0.48	4.82
B-c2	B				0.5	B-c2-0.5		0	12						57.9	<0.05	0.1		56.7	0.04				24.1	4.75	33.0	3.58	0.78	0.48	4.83
B-c2	B				1.1	B-c2-1.08		0	12						35.8	<0.05	0.2		25.2	0.02	3.675			21.3	4.24	23.6	2.61	0.073	0.34	5.37
B-c2	B				1.2	B-c2-1.17		1	12	6.9	215	1.06	0.95	35.7	<0.05	0.5		22.9	0.00				21.6	4.33	23.0	2.60	0.042	0.32	5.51
B-c2	B				1.3	B-c2-1.25		1	12						34.1	<0.05	0.2		22.3	0.01				20.5	4.35	22.3	2.49	0.076	0.34	5.50
B-c2	B				1.4	B-c2-1.42		0	12						30.9	<0.05	<0.05		17.2	0.04				20.5	4.30	21.8	2.46	0.058	0.33	5.57
B-c2	B				1.5	B-c2-1.5		1	12	6.7	214	1.04	0.99	33.1	<0.05	0.1		20.5	0.01				19.9	4.18	21.3	2.38	0.046	0.32	5.73
B-c2	B				2.2	B-c2-2.17		1	12	6.4	212	1.02	1.14	28.9	<0.05	<0.05		11.8	0.03				18.7	3.94	20.6	2.30	0.060	0.31	6.16
B-c2	B				2.3	B-c2-2.33		1	12	6.8	211	1.02	1.04	28.0	0.04	0.9		9.0	0.03				14.6	3.81	21.7	2.40	0.31	0.33	7.32
B-c2	B				2.5	B-c2-2.5		1	12	6.8	238	1.1	1.09	28.0	<0.05	0.1		9.1	0.03	2.875			14.2	4.01	22.1	2.43	0.27	0.33	7.68
B-c2	B				3.2	B-c2-3.17		1	12	6.6	205	0.99	1.05	27.9	<0.05	0.2		8.7	0.03				13.7	4.02	22.2	2.44	0.26	0.33	7.97
B-c2	B				3.3	B-c2-3.33		1	12	6.6	209	1.05	1.03	27.9	<0.05	0.1		8.6	0.03	1.875			13.0	3.92	22.3	2.40	0.22	0.34	8.62
B-c2	B				3.5	B-c2-3.5		1	12	6.7	207	1.01	1.13	30.8	<0.05	0.3		8.5	0.03				13.0	3.88	21.8	2.37	0.17	0.33	8.63
B-c2	B				4.2	B-c2-4.17		1	12	6.6	210	1.06	1.06	27.7	<0.05	1.7		10.2	0.01				15.9	4.56	22.8	2.72	0.28	0.32	8.53
B-c2	B				4.3	B-c2-4.33		0	12						27.8	0.05	0.4		8.7	0.04				14.2	4.02	23.0	2.55	0.38	0.35	9.49

Type	Test	Day	t	hours	Pore flush	ID	VU_ID	Include Phreeqc	Temp	pH	EC	Alk (titr)	Alk (corr)	Cl	Br	NO3	NH4	SO4	F	DOC	UV	SUVA	Na	K	Ca	Mg	Fe	Mn	Si
Units									°C	-	µS/cm	(meq/l)	(meq/l)	mg/l	mg/l	mg/l	mg/l	mg/l	mg/l	mg/l			mg/l	mg/l	mg/l	mg/l	mg/l	mg/l	mg/l
B-c2	B				4.5	B-c2-4.5		1	12	6.8	209	1.11	1.13	28.0	<0.05	0.3		8.7	0.03				14.2	4.09	22.8	2.52	0.24	0.35	9.45
B-c2	B				5.3	B-c2-5.25		1	12	6.8	210	1.03	1.19	27.0	<0.05	0.3		7.9	0.05	1.775			14.0	4.20	22.8	2.52	0.64	0.36	9.81
B-c2	B				5.5	B-c2-5.5		1	12	6.7	208	1	1.18	27.5	<0.05	0.2		8.3	0.03				14.2	4.13	23.0	2.53	0.44	0.36	9.79
B-c2	B				6.3	B-c2-6.25		1	12	6.6	196	1.2	1.20	27.9	<0.05	0.3		8.2	0.02	1.975			14.1	4.00	23.7	2.58	0.55	0.37	9.87
B-c2	B				6.5	B-c2-6.5		1	12	6.7	211	1.01	1.17	27.4	<0.05	0.1		8.0	0.04				13.9	3.95	22.7	2.54	0.48	0.37	9.88
B-c2	B				7.3	B-c2-7.25		1	12	6.8	215	1.04	1.13	27.8	<0.05	0.1		8.4	0.03	1.975			13.6	3.65	22.5	2.54	0.76	0.37	9.75
B-c2	B				7.5	B-c2-7.5		1	12	6.3	211	0.98	1.23	27.7	<0.05	0.1		8.2	0.04				14.1	3.64	23.9	2.65	0.60	0.38	10.10
B-c2	B				8.3	B-c2-8.25		1	12	6.9	219	1.04	1.21	27.3	<0.05	<0.05		8.1	0.02	1.875			13.9	3.31	23.4	2.61	0.79	0.37	10.00
B-c2	B				8.5	B-c2-8.5		1	12	6.9	207	0.99	1.22	27.4	<0.05	0.2		8.3	0.04				14.0	3.39	24.0	2.67	0.67	0.38	10.30
B-c2	B				9.5	B-c2-9.5		1	12	6.7	209	0.98	1.08	28.2	0.09	0.1		8.5	0.04	1.975			13.1	2.92	22.8	2.54	0.54	0.35	9.97
B-c2	B				10.0	B-c2-10		0	12					28.5	<0.05	0.1		8.6	0.06	2.275			13.3	2.77	22.6	2.57	0.05	0.35	9.95
B-c2	B				11.0	B-c2-11		1	12	6.6	217	0.98	1.05	28.5	<0.05	0.1		8.4	0.06	2.175			13.3	2.67	22.6	2.51	0.05	0.33	9.84
B-c2	B				12.0	B-c2-12		1	12	6.6	208	0.99	0.98	28.6	<0.05	0.1		8.5	0.06	1.875			13.3	2.52	21.4	2.51	0.07	0.33	9.73
B-c2	B				13.0	B-c2-13		1	12	6.6	214	1.01	1.03	28.3	<0.05	0.1		8.4	0.08	2.175			13.4	2.49	21.8	2.51	0.53	0.33	9.80
B-c2	B				14.0	B-c2-14		1	12	6.9	216	1.03	0.99	28.6	<0.05	0.2		8.5	0.06	2.075			13.3	2.09	21.7	2.54	0.64	0.33	9.76
B-c2	B				15.0	B-c2-15		1	12	6.8	222	0.99	1.01	29.5	<0.05	0.1		8.9	0.06	1.875			14.1	1.96	22.2	2.63	0.04	0.32	9.81
B-c2	B				16.0	B-c2-16		1	12	7.0	219	1	1.02	28.7	<0.05	0.1		8.4	0.03	1.875			13.6	1.79	22.4	2.61	0.07	0.32	9.87
B-c2	B				19.0	B-c2-19		1	12	6.9	220	1.01	0.91	29.0	<0.05	1.0		8.8	0.06	2.075			13.2	1.41	22.4	2.58	0.10	0.31	9.83
B-c2	B				20.0	B-c2-20		1	12	7.0	219	1.06	1.00	28.8	<0.05	0.4		8.4	0.06	2.175			13.4	1.48	22.7	2.56	0.06	0.30	9.90
B-c2	B				21.0	B-c2-21		1	12	7.0	230	1.02	1.00	29.2	<0.05	0.1		8.8	0.08	2.075			13.6	1.39	22.5	2.61	0.06	0.31	9.81
B-c2	B				22.0	B-c2-22		1	12	7.1	227	1.03	0.98	29.0	<0.05	0.2		8.8	0.08	2.075			13.3	1.47	22.5	2.57	0.04	0.31	9.71
B-c2	B				23.0	B-c2-23		1	12	7.0	221	1.04	1.02	29.0	<0.05	0.1		8.4	0.05	1.975			13.4	1.60	22.8	2.52	0.03	0.31	9.78
B-c2	B				26.0	B-c2-26		1	12	7.1	228	1.07	1.04	29.0	<0.05	0.2		8.6	0.07	2.475			13.4	1.43	23.6	2.47	0.08	0.33	9.98
B-c3	B				0.1	B-c3-0.08		1	25	6.7	210	1.03	0.61	54.8	<0.05	0.2		23.2	0.08				25.0	4.62	22.7	2.51	1.85	0.35	6.37
B-c3	B				0.2	B-c3-0.17		0	25					52.5	<0.05	0.2		22.2	0.06				24.3	4.51	21.0	2.36	1.28	0.32	6.18
B-c3	B				0.3	B-c3-0.25		0	25					45.0	<0.05	0.1		18.6	0.08				22.8	4.30	19.7	2.16	1.06	0.29	6.08
B-c3	B				0.3	B-c3-0.33		0	25					39.5	0.05	0.2		16.4	0.00				22.4	4.10	18.0	1.99	1.43	0.27	6.15
B-c3	B				0.4	B-c3-0.42		0	25					36.9	0.07	0.3		14.4	0.01				22.4	4.26	17.1	2.01	1.06	0.25	6.12
B-c3	B				0.5	B-c3-0.5		0	25					33.5	<0.05	0.1		12.6	0.06				21.7	3.96	17.0	1.90	1.61	0.26	6.20
B-c3	B				1.1	B-c3-1.08		0	25					29.0	<0.05	0.3		9.1	0.01	3.975			19.1	4.36	18.9	2.21	2.01	0.28	6.98
B-c3	B				1.2	B-c3-1.17		1	25	6.8	210	1.09	1.03	28.9	<0.05	0.5		8.9	0.01				18.1	4.30	17.4	2.06	1.50	0.26	6.93
B-c3	B				1.3	B-c3-1.25		0	25					29.1	0.05	0.3		9.3	0.01				18.9	4.30	18.2	2.24	1.82	0.27	6.91
B-c3	B				1.3	B-c3-1.33		1	25	6.7	210	1.05	1.10	28.1	<0.05	0.1		8.4	0.05				17.4	4.16	18.0	2.08	2.18	0.28	7.05
B-c3	B				1.4	B-c3-1.42		0	25					28.2	<0.05	0.1		8.4	0.05				17.1	4.22	18.3	2.09	2.22	0.28	7.21
B-c3	B				1.5	B-c3-1.5		1	25	6.7	206	1.01	1.07	28.1	0.03	0.1		8.2	0.02				16.4	4.25	18.2	2.04	2.41	0.28	7.09
B-c3	B				2.2	B-c3-2.17		1	25	6.5	212	1.02	1.12	27.3	<0.05	0.1		7.9	0.05	2.675			14.1	4.33	20.2	2.25	2.71	0.31	7.64
B-c3	B				2.3	B-c3-2.33		1	25	6.8	210	1.06	1.17	27.9	<0.05	0.2		8.1	0.06				13.9	4.55	21.7	2.36	2.72	0.32	8.08
B-c3	B				2.5	B-c3-2.5		1	25	6.9	215	1.37	1.12	27.3	<0.05	0.1		7.8	0.06				13.3	4.38	20.7	2.28	2.81	0.31	8.01
B-c3	B				3.2	B-c3-3.17		1	25	6.7	209	1.06	1.07	28.5	<0.05	0.4		8.2	0.05	2.175			13.2	4.50	20.9	2.33	2.83	0.31	8.51
B-c3	B				3.3	B-c3-3.33		1	25	6.7	210	1.08	1.05	28.2	0.06	0.1		7.9	0.05				12.8	4.44	20.3	2.29	2.85	0.31	8.56
B-c3	B				3.5	B-c3-3.5		1	25	6.7	206	1.08	1.13	28.7	<0.05	0.1		8.3	0.07				13.8	4.58	21.1	2.43	2.81	0.31	8.91
B-c3	B				4.2	B-c3-4.17		1	25	6.7	210	1.1	1.21	27.7	<0.05	0.3		7.6	0.07	2.275			13.9	4.68	21.8	2.49	2.90	0.33	9.49
B-c3	B				4.3	B-c3-4.33		0	25					28.3	<0.05	0.7		8.0	0.06				13.9	4.56	21.7	2.49	2.96	0.33	9.30
B-c3	B				4.5	B-c3-4.5		1	25	6.8	208	1.1	1.29	27.9	<0.05	0.1		7.9	0.08				14.5	4.73	22.6	2.61	3.00	0.34	9.72
B-c3	B				5.3	B-c3-5.25		1	25	6.9	215	1.09	1.23	27.5	<0.05	0.2		7.8	0.07	2.075			13.8	4.47	22.1	2.52	3.03	0.34	9.68
B-c3	B				5.5	B-c3-5.5		1	25	6.8	213	1.08	1.27	28.3	<0.05	0.3		8.0	0.04				14.6	4.59	22.8	2.62	3.09	0.35	9.92
B-c3	B				6.3	B-c3-6.25		1	25	6.7	212	1.1	1.28	27.5	0.03	0.3		7.9	0.09	2.175			14.1	4.23	23.0	2.60	3.15	0.35	10.00
B-c3	B				6.5	B-c3-6.5		1	25	6.8	212	1.07	1.21	27.8	<0.05	0.1		7.9	0.07				13.7	4.26	22.1	2.55	2.89	0.34	9.87
B-c3	B				7.3	B-c3-7.25		1	25	6.9	216	1.08	1.22	27.8	<0.05	<0.05		8.0	0.07	2.175			13.7	3.90	22.3	2.58	2.95	0.34	9.94
B-c3	B				7.5	B-c3-7.5		1	25	6.4	215	1.04	1.32	27.7	<0.05	<0.05		7.8	0.08				14.2	3.97	23.4	2.64	3.25	0.35	10.30
B-c3	B				8.3	B-c3-8.25		1	25	6.9	215	1.06	1.27	27.7	0.06	0.2		7.7	0.08	2.175			13.9	3.55	23.2	2.65	2.89	0.35	10.20
B-c3	B				8.5	B-c3-8.5		1	25	6.9	210	1.04	1.30	27.8	<0.05	0.2		7.9	0.07				14.1	3.67	23.7	2.67	3.06	0.35	10.40
B-c3	B				9.5	B-c3-9.5		1	25	6.7	205	1	1.11	28.5	<0.05	<0.05		8.0	0.08	2.175			13.0	3.05	21.7	2.48	2.87	0.32	10.10
B-c3	B				10.0	B-c3-10		0	25					28.3	<0.05	0.1		7.9	0.10	2.275			13.3	2.80	22.2	2.50	1.71	0.33	9.99
B-c3	B				11.0	B-c3-11		1	25	6.7	205	0.96	1.05	28.1	<0.05	0.1		7.8	0.08	2.075			13.2	2.65	21.9	2.49	1.02	0.32	9.78
B-c3	B				12.0	B-c3-12		1	25	6.7	207	0.99	1.03	28.2	0.07	0.1		7.9	0.04	2.075			13.4	2.64	20.9	2.50	1.41	0.32	9.66
B-c3	B				13.0	B-c3-13		1	25	6.7	211	0.98	1.05	28.5	0.05	0.1		7.8	0.07	2.375			13.4	2.72	21.3	2.48	1.67	0.32	9.69
B-c3	B				14.0	B-c3-14		1	25	6.9	212	0.98	1.03	28.3	<0.05	0.2		7.6	0.07	2.075			13.3	2.28	21.3	2.45	1.44	0.32	9.82
B-c3	B				15.0	B-c3-15		1	25	6.7	213	1	1.00	29.0	<0.05	0.2		8.2	0.05	1.975			13.5	1.99	21.5	2.50	1.21	0.31	9.72
B-c3	B				16.0	B-c3-16		1	25	6.9	214	1.03	1.01	29.2	<0.05	0.2		8.3	0.08	1.975			13.4	1.88	21.5	2.49	2.03	0.31	9.90
B-c3	B				19.0	B-c3-19		1	25	6.9	210	1.01	0.89	28.9	<0.05	0.9		8.3	0.08	2.075			13.0	1.56	21.3	2.44	0.72	0.30	9.70
B-c3	B				20.0	B-c3-20		1	25	6.9	212	1.02	0.96	28.8	<0.05	0.8		8.1	0.10	2.175			13.3	1.50	21.9	2.49	1.15	0.31	9.91
B-c3	B				21.0	B-c3-21		1	25	7.0	212	1.04	1.01	29.3	<0.05	0.1		8.5	0.05	2.475			13.5	1.60	21.8	2.51	1.55	0.31	9.76
B-c3	B				22.0	B-c3-22		1	25	6.9	220	1.05	1.00	29.1	<0.05	0.1		8.3	0.07	2.375			13.2	1.40	21.7	2.47	1.70	0.31	9.70
B-c3	B				23.0	B-c3-23		1	25	7.0	220	1.02	1.00	29.3	<0.05	0.3		8.5	0.10	2.275			13.5	1.69	22.2	2.47	1.27	0.31	9.71
B-c3	B				26.0	B-c3-26		1	25	6.9	214	1.01	0.96	29.1	<0.05	0.3		8.4	0.07	2.475			13.4	1.52	22.0	2.40	0.58	0.31	9.95
B-c4	B				0.1	B-c4-0.08		1	60	6.2	387			377.5	0.22	0.4		49.5	0.09				23.4	318.00	40.9	3.39	0.23	0.42	12.80
B-c4	B				0.2	B-c4-0.17		0	60					276.3	0.11	0.3		56.5	0.05				24.9	206.00	39.5	3.57	0.45	0.43	13.70
B-c4	B				0.3	B-c4-0.25		0	60					188.4	0.08	0.3		64.4	0.09				26.3	126.00	39.3	3.81	0.89	0.47	14.60
B-c4	B				0.4	B-c4-0.42		0	60					157.7	0.08	0.4		65.3	0.08				25.4	90.70	38.6	3.74	0.88	0.47	14.70
B-c4	B				1.1	B-c4-1.08		0	60					43.2	<0.05	11.6		26.0	0.28	6.875			20.0	11.90	17.7	1.98	1.11	0.23	16.10
B-c4	B				1.2	B-c4-1.17		1	60	6.4	194	0.76	0.57	38.4	<0.05	0.3		20.9	0.02				18.5	10.20	16.3	1.73	1.02	0.21	16.20
B-c4	B				1.3	B-c4-1.25		0	60					35.6	<0.05	0.1		17.4	0.05				17.3	9.52	14.8	1.59	1.00	0.20	16.30
B-c4	B				1.3	B-c4-1.33		1	60	6.3	193	0.75	0.57	36.3	0.05	0.2		18.2	0.06				17.6	9.88	15.3	1.67	0.56	0.20	15.80
B-c4	B				1.5	B-c4-1.5		1	60	6.4	196	0.74	0.65	34.2	<0.05	0.1		14.8	0.02				16.8	10.00	14.6	1.54	0.88	0.21	15.90
B-c4	B				2.2	B-c4-2.17		1	60	6.1	193	0.69	0.74	29.8	<0.05	0.1		8.7	0.05	7.275			15.4	8.04	13.6	1.45	1.17	0.20	14.40
B-c4	B				2.3	B-c4-2.33		1	60	6.5	194	0.69	0.77	30.5	<0.05	0.2		8.7	0.07				15.4	8.54	14.4	1.48	1.35	0.21	14.20
B-c4	B				2.5	B-c4-2.5		1	60	6.5	230	0.76	0.82	30.4	<0.05	0.1		8.6	0.03				15.4	8.73	14.9	1.52	1.47	0.21	13.80
B-c4	B				3.2	B-c4-3.17		1	60	6.6	206	0.66	0.73	30.1	<0.05	0.1		8.3	0.10	3.775			13.7	8.02	14.4	1.51	1.81	0.21	13.00
B-c4	B				3.3	B-c4-3.33		1	60	6.3	187	0.68	0.70	30.5	<0.05	0.1		8.3	0.09				13.5	8.26	14.1	1.49	1.87	0.21	12.70
B-c4	B				3.5	B-c4-3.5		1	60	6.3	186	0.66	0.75	32.1	<0.05	0.2		9.4	0.06				15.0	8.44	15.1	1.68	1.79	0.21	12.50
B-c4	B				4.2	B-c4-4.17		1	60	6.2	185	0.66	0.81	30.0	<0.05	0.4		7.8	0.10	3.375			14.4	8.54	15.0	1.59	2.25	0.22	12.60
B-c4	B				4.3	B-c4-4.33		0	60					31.7	<0.05	0.3		8.0	0.08				14.4	8.39	14.9	1.60	2.24	0.22	12.50

Type	Test	Day	t	hours	Pore flush	ID	VU_ID	Include Phreeqc	Temp	pH	EC	Alk (titr)	Alk (corr)	Cl	Br	NO3	NH4	SO4	F	DOC	UV	SUVA	Na	K	Ca	Mg	Fe	Mn	Si
Units									°C	-	µS/cm	(meq/l)	(meq/l)	mg/l	mg/l	mg/l	mg/l	mg/l	mg/l	mg/l			mg/l	mg/l	mg/l	mg/l	mg/l	mg/l	mg/l
B-c4	B				4.5	B-c4-4.5			1	60	6.4	185	0.69	0.79	29.9	<0.05	<0.05	8.0	0.07				14.1	8.23	14.5	1.55	0.24	0.21	12.20
B-c4	B				5.3	B-c4-5.25			1	60	6.4	185	0.62	0.82	29.2	<0.05	0.3	7.6	0.06	3.175			14.2	8.46	14.7	1.54	2.37	0.22	12.00
B-c4	B				5.5	B-c4-5.5			1	60	6.3	184	0.61	0.83	29.1	<0.05	0.3	7.4	0.06				14.3	8.57	14.6	1.53	2.47	0.22	12.00
B-c4	B				6.3	B-c4-6.25			1	60	6.1	182	0.58	0.77	30.4	<0.05	0.6	7.8	0.04	3.275			14.3	8.49	14.7	1.53	2.62	0.21	11.70
B-c4	B				6.5	B-c4-6.5			1	60	6.3	179	0.59	0.73	30.0	<0.05	<0.05	7.8	0.05				14.0	7.71	13.7	1.49	2.55	0.21	11.60
B-c4	B				7.3	B-c4-7.25			1	60	6.2	185	0.59	0.72	30.1	0.06	0.1	7.7	0.06	3.075			13.8	7.47	13.7	1.48	2.54	0.21	11.00
B-c4	B				7.5	B-c4-7.5			1	60	6.0	181	0.55	0.76	29.8	<0.05	0.1	7.8	0.04				14.1	6.98	14.4	1.49	2.56	0.21	11.10
B-c4	B				8.3	B-c4-8.25			1	60	6.4	199	0.64	0.71	31.5	<0.05	0.1	7.8	0.09	2.975			14.0	7.35	14.3	1.52	2.52	0.21	10.90
B-c4	B				8.5	B-c4-8.5			1	60	6.4	182	0.6	0.77	30.4	<0.05	0.3	7.9	0.07				14.4	6.80	14.8	1.58	2.53	0.22	11.30
B-c4	B				9.5	B-c4-9.5			1	60	6.1	180	0.59	0.64	31.2	<0.05	0.2	8.0	0.10	3.075			13.1	6.72	14.1	1.47	2.26	0.21	10.50
B-c4	B				10.0	B-c4-10			0						30.8	<0.05	0.1	7.9	0.10	3.275			13.2	5.52	15.3	1.58	1.58	0.22	10.60
B-c4	B				11.0	B-c4-11			1	60	6.2	181	0.59	0.64	30.4	<0.05	0.1	7.9	0.13	2.975			13.3	4.85	15.1	1.62	1.16	0.22	10.50
B-c4	B				12.0	B-c4-12			1	60	6.5	184	0.63	0.62	30.4	<0.05	0.1	8.1	0.12	2.775			13.5	4.49	14.8	1.68	1.06	0.21	10.30
B-c4	B				13.0	B-c4-13			1	60	6.3	187	0.63	0.65	30.5	<0.05	0.1	7.8	0.19	2.875			12.9	4.61	15.6	1.71	1.29	0.21	10.30
B-c4	B				14.0	B-c4-14			1	60	6.5	194	0.73	0.72	29.8	<0.05	0.2	7.9	0.22	2.775			13.3	3.57	16.5	1.88	1.51	0.22	10.80
B-c4	B				15.0	B-c4-15			1	60	6.4	199	0.72	0.74	31.7	<0.05	0.2	8.1	0.18	2.875			13.3	4.69	17.4	1.97	1.47	0.21	10.50
B-c4	B				16.0	B-c4-16			1	60	6.8	207	0.81	0.81	31.7	<0.05	0.2	8.2	0.18	2.975			13.6	4.68	18.5	2.10	1.41	0.21	10.40
B-c4	B				19.0	B-c4-19			1	60	6.9	216	0.9	0.89	31.9	<0.05	0.7	8.0	0.13	2.975			13.9	4.41	20.6	2.39	1.08	0.20	10.70
B-c4	B				20.0	B-c4-20			1	60	6.8	217	0.92	0.94	31.2	<0.05	0.5	7.8	0.12	3.075			13.4	4.45	21.1	2.42	1.01	0.19	10.90
B-c4	B				21.0	B-c4-21			1	60	7.0	222	0.92	0.92	31.8	<0.05	0.2	7.9	0.10	3.175			13.6	4.64	20.5	2.43	0.84	0.18	10.60
B-c4	B				22.0	B-c4-22			1	60	6.9	232	0.95	0.92	32.2	<0.05	0.3	8.2	0.09	3.075			13.8	4.51	20.9	2.50	0.71	0.18	10.70
B-c4	B				23.0	B-c4-23			1	60	6.9	223	0.96	0.95	32.2	<0.05	0.2	8.0	0.10	3.275			13.7	4.95	21.1	2.47	0.74	0.17	10.60
B-c4	B				26.0	B-c4-26			1	60	6.9	230	0.93	0.95	32.2	<0.05	0.3	8.2	0.06	3.275			13.6	4.39	21.8	2.52	0.57	0.16	10.60
B-Hf	B				1.5	B-Hf-1.5			1	20	6.9	227	1.25	1.28	27.2	0.03	0.2	7.8	0.06	1.975			11.9	1.00	24.3	2.11	6.46	0.93	10.40
B-Hf	B				30.0	B-Hf-30			1	20	6.8	215	1.09	1.33	28.3	<0.05	0.2	7.9	0.04	1.975			13.6	1.80	27.5	2.52	0.79	0.92	11.00
B-Hf	B				35.0	B-Hf-35			1	20	7.0	237	1.1	1.30	27.9	<0.05	0.2	8.1	0.04	1.975			13.4	1.31	27.1	2.51	0.91	0.92	11.00
B-Hf_av	B				0.0	B-Hf_av0@60			1	20	6.9	227	1.25	1.37	27.2	<0.05	0.2	7.8	0.06	1.975			13.6	1.80	24.3	2.11	6.46	0.93	10.40
B-Hf_av	B				10.0	B-Hf_av0@60			1	20	6.9	227	1.25	1.37	27.2	<0.05	0.2	7.8	0.06	1.975			13.6	1.80	24.3	2.11	6.46	0.93	10.40
B-Hf_av	B				10.3	Hf_av-7.2@60			1	20	6.8	215	1.09	1.33	28.3	<0.05	0.2	7.9	0.04	1.975			13.6	1.80	27.5	2.52	0.79	0.92	11.00
B-Hf_av	B				35.0	Hf_av-7.2@60			1	20	6.8	215	1.09	1.33	28.3	<0.05	0.2	7.9	0.04	1.975			13.6	1.80	27.5	2.52	0.79	0.92	11.00
C_Field	C					C-Inf -17			1	11	7.9	207	1.796	1.67	7.0	0.03	<0.05	6.0	0.07				5.7	0.63	30.5	2.26	0.36	0.07	7.43
C_C0	C				-7.0	C-Inf -7			1	11	7.4	201	1.954	1.64	6.9	0.04	<0.05	6.0	0.06				5.4	0.77	30.2	2.19	0.30	0.07	7.21
C_C0	C				2.5	C0_t=1			1	11	7.3	205	2.077	1.67	7.3	<0.05	<0.05	6.0	0.05				5.7	0.84	29.7	2.21	0.49	0.08	6.51
C_C0	C				2.5	C0_t=3			1	11	7.0	195	1.881	1.75	7.0	<0.05	<0.05	5.9	0.06	0.55	3.8	6.9	5.9	0.93	31.7	2.32	0.26	0.08	6.54
C_C0	C				3.0	C0_t=4			1	11	7.1	199	2.083	1.68	7.1	0.03	<0.05	6.0	0.07				5.8	0.83	30.7	2.26	0.30	0.08	6.61
C_C0	C				7.0	C0_t=8			1	11	7.3	196	1.737	1.57	7.2	0.02	<0.05	6.0	0.07				5.5	0.97	29.0	2.15	0.08	0.07	6.57
C_C0	C				9.0	C0_t=10	106415		1	11	7.2	210	2.209	1.56	7.5	0.09	0.3	6.1	0.06				5.5		29.5	2.18	0.46	0.07	6.57
C_C0	C				10.0	C0_t=11	106409		0	11					6.9	0.02	0.2	5.9	0.07	0.52	3.6	6.9	5.5	0.73	28.8	2.12	0.21	0.07	6.71
C_C0	C				14.0	C0_t=15	106410		1	11	7.5	206	2.229	1.63	7.1	0.03	<0.05	5.9	0.06				5.5		29.3	2.17	0.55	0.08	6.76
C_C0	C				16.0	C0_t=17	106411		1	11	7.3	197	2.188	1.63	7.1	0.03	<0.05	5.9	0.07				5.5	0.84	30.1	2.16	0.04	0.07	6.24
C_C0	C				17.0	C0_t=18	106412		0	11					6.8	0.02	<0.05	5.9	0.06				5.3	0.72	29.4	2.11	0.08	0.07	6.01
C_C0	C				21.0	C0_t=22	106413		1	11	7.1	201	1.802	1.58	7.2	<0.05	<0.05	5.9	0.07	0.58	2.6	4.5	5.4	0.66	29.3	2.13	0.23	0.08	6.04
C_C0	C				23.0	C0_t=24	106414		1	11	7.0	200	1.869	1.66	7.3	0.03	0.1	5.9	0.06	0.55	3.3333333	6.10497548	5.6	0.82	30.8	2.24	0.12	0.08	6.11
C_C0_av	C				0.0	C_C0_av			1	11	7.2	201	2.01	1.63	7.1	0.03	0.1	5.9	0.06				5.6	0.82	29.8	2.19	0.26	0.08	6.42
C_St_dev	C					C_C0_stDev					0.17	5.05	0.19	0.06	0.19	0.02	0.12	0.01											
C_C1	C				0.3	C1_t=1.2	106166		1	5	7.4	230	2.358	2.05	8.9	0.03	<0.05	7.9	0.09				7.1	1.33	37.5	2.82	0.29	0.06	5.91
C_C1	C				0.6	C1_t=1.4	106168		1	5	7.4	221	2.131	2.03	7.9	0.03	<0.05	7.0	0.09				6.7	1.20	36.6	2.74	0.33	0.06	5.78
C_C1	C				0.9	C1_t=1.6	106170		1	5	7.6	231	2.378	2.10	7.8	n.a.	<0.05	7.0	0.07				6.9	1.22	37.5	2.82	0.36	0.06	5.76
C_C1	C				1.4	C1_t=2.2	106190		1	5	7.4	230	2.158	2.10	7.8	0.02	<0.05	6.8	0.08				6.8	1.21	37.7	2.85	0.08	0.07	6.07
C_C1	C				1.8	C1_t=2.4	106192		1	5	7.4	228	2.167	2.06	7.6	0.03	<0.05	6.7	0.08				6.7	1.19	36.8	2.82	0.10	0.06	5.80
C_C1	C				2.2	C1_t=3.1	106205		1	5	7.3	234	2.205	2.09	7.8	n.a.	<0.05	6.9	0.12				6.7	1.19	37.9	2.83	0.11	0.07	6.17
C_C1	C				2.6	C1_t=3.3	106207		1	5	7.4	232	2.201	2.23	7.6	0.04	<0.05	6.7	0.09	2	3	1.5	6.9	1.25	40.0	2.95	0.28	0.07	6.22
C_C1	C				3.2	C1_t=4.1	106221		1	5	7.2	235	2.34	2.05	7.3	0.04	<0.05	6.4	0.11				6.4	1.12	36.8	2.77	0.33	0.06	6.12
C_C1	C				3.6	C1_t=4.3	106223		1	5	7.3	228	2.064	2.18	7.3	0.03	<0.05	6.4	0.11				6.6	1.22	39.0	2.88	0.39	0.07	6.33
C_C1	C				4.2	C1_t=5.1	106227		1	5	7.4	235	2.379	2.03	7.3	0.02	<0.05	6.4	0.07				6.2	1.10	36.6	2.76	0.36	0.06	6.13
C_C1	C				5.2	C1_t=6.1	106253		1	5	7.5	219	2.052	2.14	7.2	n.a.	<0.05	6.3	0.08				6.4	1.13	38.3	2.81	0.40	0.07	6.29
C_C1	C				5.6	C1_t=6.3	106255		1	5	7.5	217	2.102	2.07	7.1	n.a.	<0.05	6.2	0.07	0.82	2.5	3	6.2	1.11	37.1	2.74	0.38	0.07	6.23
C_C1	C				6.3	C1_t=7.1	106269		1	5	7.6	219	2.075	2.06	7.2	n.a.	<0.05	6.2	0.07				6.2	1.14	36.7	2.73	0.36	0.07	6.28
C_C1	C				7.3	C1_t=8.1	106277		1	5	7.6	228	2.077	2.06	7.2	0.03	<0.05	6.1	0.07				6.2	1.13	36.8	2.71	0.61	0.07	6.38
C_C1	C				8.3	C1_t=9.1	106285		1	5	7.6	226	2.077	2.06	7.1	0.02	<0.05	6.0	0.06				6.2	1.13	36.6	2.69	0.39	0.07	6.30
C_C1	C				9.3	C1_t=10.1	106293		1	5	7.4	225	2.107	2.05	7.0	0.02	<0.05	6.0	0.06	0.51	2.9	5.7	6.2	1.13	36.6	2.69	0.39	0.07	6.33
C_C1	C				10.3	C1_t=11.1	106301		1	5	7.6	220	2.225	1.99	7.1	0.03	<0.05	6.1	0.07				6.0	1.09	35.8	2.61	0.36	0.07	6.33
C_C1	C				11.3	C1_t=12.1	106309		1	5	7.6	220	2.103	1.94	7.1	0.03	<0.05	6.1	0.07				5.9	1.05	35.1	2.60	0.36	0.07	6.58
C_C1	C				12.3	C1_t=13.1	106317		1	5	7.5	216	2.065	1.91	7.0	0.03	<0.05	6.1	0.07				5.8	1.05	34.5	2.57	0.35	0.07	6.41
C_C1	C				13.7	C1_t=14.2	106326		0	5													5.7	1.02	33.6	2.50	0.26	0.07	6.33
C_C1	C				14.3	C1_t=15.1	106333		1	5	7.5	219	1.996	1.95	7.4	0.02	<0.05	6.0	0.07	0.55	3.6	6.5	5.9	1.04	35.6	2.61	0.22	0.07	6.08
C_C1	C				15.5	C1_t=16.1	106341		0	5													6.0	1.06	36.7	2.68	0.21	0.07	6.04
C_C1	C				16.5	C1_t=17.1	106345		1	5	7.3	251	2.253	2.20	7.4	0.02	<0.05	6.0	0.06				6.0	1.11	39.9	2.84	0.23	0.08	6.18
C_C1	C				17.5	C1_t=18.1	106349		1	5	7.7	227	227	2.10	7.4	0.03	<0.05	6.0	0.06				5.9	1.06	38.4	2.70	0.23	0.08	6.22
C_C1	C				18.5	C1_t=19.1	106353		1	5	7.5	227	2.147	2.04	7.3	0.03	<0.05	5.9	0.06	0.56	2.8	5.0	5.8	1.06	37.1	2.69	0.22	0.08	5.95
C_C1	C				19.5	C1_t=20.1	106357		1	5	7.4	231	2.211	2.03	7.4	0.03	<0.05	6.0	0.07				5.7	1.01	37.1	2.65	0.23	0.08	6.09
C_C1	C				20.5	C1_t=21.1	106361		1	5	8.1	230	2.488	2.01	7.4	0.03	<0.05	6.0	0.06				5.7	1.01	36.7	2.64	0.21	0.08	5.97
C_C1	C				21.5	C1_t=22.1	106365		1	5	7.6	228	2.206	2.01	7.4	na.	<0.05	6.0	0.07	0.57	2.9	5.1	5.7	1.02	36.7	2.62	0.22	0.08	5.96
C_C1	C				22.5	C1_t=23.1	106369		1	5	7.3	223	2.207	2.03	7.4	0.02	<0.05	6.0	0.06				5.7	1.02	37.2	2.65	0.21	0.08	6.04
C_C1	C				23.5	C1_t=24.1	106373		1	5	7.3	223	2.121	1.95	7.3	0.03	<0.05	6.0	0.07	0.44	2.9	6.6	5.5	0.95	36.0	2.54	0.24	0.08	6.05
C_C2	C				0.3	C2_t=1.2	106172		1	11	7.3	224	2.229	2.12	8.1	0.06	<0.05	7.4	0.10				7.4	1.52	37.6	2.89	0.32	0.06	6.09
C_C2	C				0.6	C2_t=1.4	106174		1	11	7.3	224	2.197	2.03	8.0	0.03	<0.05	7.3	0.09				7.0	1.45	36.2	2.78	0.30	0.06	6.09
C_C2	C				0.9	C2_t=1.6	106176		1	11	7.6	233	2.285	2.07	7.8	0.02	<0.05	7.2	0.09				7.0	1.47	36.9	2.83	0.31	0.06	6.14
C_C2	C				1.4	C2_t=2.2	106184		1	11	7.4	227	2.058	2.07	7.8	0.04	<0.05	7.0	0.09				6.9	1.48	36.6	2.83	0.26	0.06	6.28
C_C2	C				1.8	C2_t=2.4	106196		1	11	7.4	224	2.094	2.06	7.5	0.03	<0.05	6.8	0.09				6.7	1.41	36.2	2.79	0.19	0.06	6.26
C_C2	C				2.2	C2_t=3.1	106209		1	11	7.3	234	2.107	2.15	7.7	0.04	<0.05	7.0	0.10	1.9	2.6	1.4	6.9	1.49	38.1	2.93	0.23	0.06	6.46
C_C2	C				2.6	C2_t=3.3	106211		1	11	7.3	227	2.096	2.19	7.4	0.03	<0.05	6.6	0.10				6.9	1.51	38.8	2.90	0.25	0.06	6.42
C_C2	C				3.2	C2_t=4.1	106225		1	11	7.2	235	2.179	2.11	7.3	0.03	<0.05	6.5	0.19				6.5	1.40	37.6	2.85	0.27	0.06	6.37

Type	Test	Day	t	hours	Pore flush	ID	VU_ID	Include Phreeqc	Temp	pH	EC	Alk (titr)	Alk (corr)	Cl	Br	NO3	NH4	SO4	F	DOC	UV	SUVA	Na	K	Ca	Mg	Fe	Mn	Si
Units									°C	-	µS/cm	(meq/l)	(meq/l)	mg/l	mg/l	mg/l	mg/l	mg/l	mg/l	mg/l			mg/l	mg/l	mg/l	mg/l	mg/l	mg/l	mg/l
C_C2	C			3.6	C2_t=4.3	106227		1	11	7.4	228	2.132	2.14	7.3	0.03	<0.05		6.5	0.20				6.6	1.45	38.1	2.87	0.32	0.06	6.46
C_C2	C			4.2	C2_t=5.1	106241		1	11	7.3	226	2.114	2.04	7.2	0.02	<0.05		6.4	0.08				6.2	1.34	36.6	2.77	0.26	0.06	6.31
C_C2	C			5.2	C2_t=6.1	106257		1	11	7.6	220	2.151	2.08	7.3	0.02	<0.05		6.3	0.08				6.3	1.37	37.2	2.81	0.26	0.06	6.36
C_C2	C			5.6	C2_t=6.3	106259		1	11	7.6	219	2.053	2.12	7.1	n.a.	<0.05		6.2	0.08	0.93	2.5	2.7	6.3	1.38	37.7	2.85	0.33	0.07	6.36
C_C2	C			6.3	C2_t=7.1	106271		1	11	7.6	220	2.018	2.05	7.2	0.03	<0.05	0.04	6.3	0.10				6.2	1.34	36.8	2.73	0.33	0.06	6.34
C_C2	C			7.3	C2_t=8.1	106279		1	11	7.6	224	2.155	2.02	7.1	0.03	<0.05		6.1	0.07				6.1	1.33	36.1	2.73	0.30	0.07	6.36
C_C2	C			8.3	C2_t=9.1	106287		1	11	7.5	224	2.222	2.06	6.9	0.03	<0.05		5.9	0.07				6.1	1.33	36.7	2.73	0.34	0.07	6.44
C_C2	C			9.3	C2_t=10.1	106295		1	11	7.6	222	2.055	1.98	7.0	0.02	<0.05		6.0	0.07				5.9	1.28	35.5	2.64	0.35	0.07	6.43
C_C2	C			10.3	C2_t=11.1	106303		0	11	7.5	217	2.024			<0.05		0.10			0.53	2.9	5.5	5.9	1.27	35.6	2.68	0.28	0.06	6.30
C_C2	C			11.3	C2_t=12.1	106311		1	11	7.7	222	2.145	1.92	7.0	0.03	<0.05		6.0	0.07				5.7	1.23	34.6	2.61	0.27	0.06	6.53
C_C2	C			12.3	C2_t=13.1	106319		1	11	7.4	222	2.138	1.87	7.0	0.02	<0.05		6.0	0.06				5.6	1.20	33.8	2.54	0.24	0.06	6.47
C_C2	C			13.7	C2_t=14.2	106328		0	11						<0.05								5.6	1.19	33.9	2.56	0.19	0.06	6.54
C_C2	C			14.3	C2_t=15.1	106335		1	11	7.4	221	2.103	1.93	7.6	0.03	<0.05	0.07	5.9	0.07	0.66	3.4	5.2	5.8	1.17	35.2	2.61	0.17	0.07	6.01
C_C2	C			15.5	C2_t=16.1	106342		1	11	7.6	219	2.009	1.97	7.4	0.03	<0.05		6.0	0.07				5.8	1.17	35.9	2.64	0.16	0.07	6.01
C_C2	C			16.5	C2_t=17.1	106346		1	11	7.5	235	2.186	2.20	7.4	0.03	<0.05	0.07	6.0	0.06				6.1	1.27	39.6	2.88	0.18	0.08	6.24
C_C2	C			17.5	C2_t=18.1	106350		1	11	7.7	230	2.206	2.12	7.3	0.03	<0.05		5.9	0.06				5.9	1.22	38.3	2.77	0.16	0.07	6.09
C_C2	C			18.5	C2_t=19.1	106354		1	11	7.6	233	2.126	2.06	7.3	0.03	<0.05	0.13	5.9	0.09	0.6	2.5	4.2	5.8	1.19	37.3	2.71	0.14	0.07	6.01
C_C2	C			19.5	C2_t=20.1	106358		1	11	7.6	229	2.302	2.03	7.5	0.03	<0.05		6.1	0.07				5.8	1.18	37.1	2.70	0.09	0.07	6.00
C_C2	C			20.5	C2_t=21.1	106362		0	11					7.5	0.03	<0.05		6.0	0.06				5.7	1.15	37.1	2.67	0.09	0.07	6.09
C_C2	C			21.5	C2_t=22.1	106366		1	11	7.5	229	2.099	1.98	7.3	0.02	<0.05	0.15	6.0	0.08	0.53	2.5	4.7	5.6	1.11	36.2	2.61	0.08	0.07	5.98
C_C2	C			22.5	C2_t=23.1	106370		1	11	7.4	227	2.299	2.07	7.5	0.03	<0.05		6.0	0.09				5.8	1.15	38.0	2.70	0.08	0.08	6.26
C_C2	C			23.5	C2_t=24.1	106374		1	11	7.4	226	2.141	1.96	7.3	0.03	0.1		6.0	0.06	0.45	2.5	5.6	5.5	1.08	36.0	2.59	0.09	0.07	6.03
C_C3	C			0.3	C3_t=1.2	106178		1	25	7.3	229	2.198	2.12	7.4	n.a.	<0.05		7.0	0.09				7.1	2.12	37.1	3.04	0.09	0.06	6.49
C_C3	C			0.6	C3_t=1.4	106180		1	25	7.3	233	2.247	2.02	7.3	0.03	<0.05		7.0	0.10				6.7	2.11	35.7	2.91	0.04	0.06	7.10
C_C3	C			0.9	C3_t=1.6	106182		0	25					7.3	0.03	<0.05		7.0	0.09				6.4	2.03	34.8	2.80	0.04	0.06	7.04
C_C3	C			1.4	C3_t=2.2	106198		1	25	7.5	234	2.478	2.23	7.4	0.04	<0.05	0.04	7.1	0.09				7.0	2.37	38.8	3.11	0.04	0.07	7.24
C_C3	C			1.8	C3_t=2.4	106200		1	25	7.4	235	2.212	2.10	7.2	0.03	<0.05		6.6	0.08				6.4	2.19	36.9	2.97	0.01	0.06	7.11
C_C3	C			2.2	C3_t=3.1	106213		1	25	7.3	229	2.203	2.27	7.4	0.03	<0.05		6.8	0.11				6.9	2.40	39.6	3.15	0.02	0.07	7.31
C_C3	C			2.6	C3_t=3.3	106215		1	25	7.3	230	2.21	2.22	7.3	0.01	<0.05		6.5	0.12	2.1	3.2	1.5	6.6	2.49	38.9	3.09	0.06	0.07	7.33
C_C3	C			3.2	C3_t=4.1	106229		1	25	7.4	230	2.217	2.18	7.2	0.03	<0.05	0.02	6.2	0.22				6.2	2.31	38.4	3.05	0.28	0.07	7.25
C_C3	C			3.6	C3_t=4.3	106231		1	25	7.4	229	2.13	2.22	7.1	0.03	<0.05		6.2	0.11				6.4	2.42	38.7	2.98	0.37	0.07	7.32
C_C3	C			4.2	C3_t=5.1	106245		1	25	7.3	227	2.278	2.03	7.1	0.03	<0.05		6.1	0.09				5.8	2.09	35.9	2.86	0.34	0.06	7.07
C_C3	C			5.2	C3_t=6.1	106261		1	25	7.6	224	2.118	2.07	7.2	n.a.	<0.05		6.1	0.09				5.9	2.08	36.5	2.90	0.57	0.06	7.11
C_C3	C			5.6	C3_t=6.3	106263		1	25	7.6	223	2.139	2.06	7.1	0.02	<0.05		6.0	0.08	1	4.6	4.6	5.8	2.06	36.3	2.85	0.62	0.07	6.92
C_C3	C			6.3	C3_t=7.1	106273		1	25	7.6	224	2.162	2.16	7.1	0.03	<0.05	0.06	6.0	0.09				6.1	2.12	37.7	2.97	0.72	0.07	7.01
C_C3	C			7.3	C3_t=8.1	106281		1	25	7.6	228	2.119	2.09	7.1	0.03	<0.05		6.0	0.09				6.0	2.03	36.5	2.89	0.84	0.07	7.05
C_C3	C			8.3	C3_t=9.1	106289		1	25	7.7	226	2.173	2.05	7.1	0.02	<0.05		5.9	0.08				5.8	1.95	36.0	2.83	0.72	0.07	6.87
C_C3	C			9.3	C3_t=10.1	106297		1	25	7.6	222	2.134	1.98	7.1	n.a.	<0.05		5.9	0.09				5.7	1.88	35.0	2.78	0.49	0.06	6.77
C_C3	C			10.3	C3_t=11.1	106305		0	25	7.6	220	2.235			<0.05		0.11			0.68	4.9	7.2	5.9	1.90	36.5	2.85	0.44	0.07	6.86
C_C3	C			11.3	C3_t=12.1	106313		1	25	7.6	223	2.103	1.93	7.1	0.03	<0.05		5.9	0.08				5.6	1.70	34.5	2.73	0.37	0.07	6.94
C_C3	C			12.3	C3_t=13.1	106321		1	25	7.9	223	2.241	1.94	7.0	0.02	<0.05		5.8	0.07				5.6	1.65	34.5	2.70	0.33	0.07	6.87
C_C3	C			13.7	C3_t=14.2	106330		0	25						<0.05								5.5	1.54	34.1	2.62	0.34	0.07	6.78
C_C3	C			14.3	C3_t=15.1	106337		1	25	7.5	223	2.046	2.02	7.5	0.03	<0.05	0.07	5.8	0.07	0.78	4.8	6.2	5.8	1.54	36.3	2.75	0.36	0.07	6.57
C_C3	C			15.5	C3_t=16.1	106343		1	25	7.7	218	2.069	2.00	7.3	n.a.	<0.05	0.13	5.8	0.07				5.7	1.53	35.7	2.73	0.38	0.07	6.42
C_C3	C			16.5	C3_t=17.1	106347		1	25	7.8	226	2.298	2.26	7.5	0.04	<0.05		5.8	0.07				6.1	1.60	40.0	3.01	0.50	0.08	6.61
C_C3	C			17.5	C3_t=18.1	106351		1	25	7.6	231	2.156	2.25	7.5	0.02	<0.05		5.7	0.07				6.1	1.54	40.0	3.01	0.42	0.08	6.52
C_C3	C			18.5	C3_t=19.1	106355		1	25	7.6	226	2.152	2.11	7.2	0.04	<0.05	0.06	5.5	0.06	0.71	3.2	4.5	5.8	1.43	37.8	2.79	0.32	0.07	6.35
C_C3	C			19.5	C3_t=20.1	106359		1	25	7.6	228	2.267	2.13	7.6	0.03	<0.05		5.8	0.09				5.8	1.41	38.3	2.85	0.44	0.08	6.59
C_C3	C			20.5	C3_t=21.1	106363		1	25	7.5	226	2.13	2.05	7.4	0.03	<0.05		5.6	0.08				5.7	1.33	36.9	2.75	0.35	0.08	6.39
C_C3	C			21.5	C3_t=22.1	106367		1	25	7.7	231	2.198	2.03	7.4	0.03	<0.05	0.23	5.6	0.08	4	7.0		5.6	1.30	36.5	2.72	0.34	0.07	6.24
C_C3	C			22.5	C3_t=23.1	106371		1	25	7.3	231	2.211	2.07	7.4	0.02	<0.05		5.6	0.08	0.56	4.1	7.3	5.8	1.32	37.3	2.80	0.35	0.08	6.55
C_C3	C			23.5	C3_t=24.1	106375		1	25	7.2	227	2.08	1.98	7.3	0.03	<0.05		5.5	0.08				5.4	1.22	36.0	2.65	0.33	0.07	6.30
C_C4	C			0.3	C4_t=1.2	106184		1	60	7.3	243	2.405	2.25	8.3	0.02	<0.05		9.0	0.12				9.3	3.75	38.2	2.92	0.39	0.06	11.75
C_C4	C			0.6	C4_t=1.4	106186		1	60	7.3	261	2.45	2.40	8.2	0.04	<0.05	0.09	12.5	0.17				9.8	4.73	41.4	3.07	0.52	0.06	13.88
C_C4	C			1.4	C4_t=2.2	106202		1	60	7.3	265	2.422	2.45	7.7	0.02	<0.05	0.06	9.5	0.20				9.0	4.88	41.7	3.05	0.12	0.07	13.51
C_C4	C			1.8	C4_t=2.4	106204		1	60	7.2	263	2.35	2.33	7.4	0.03	<0.05		7.0	0.14				8.0	4.36	39.2	2.92	0.35	0.07	12.99
C_C4	C			2.2	C4_t=3.1	106217		1	60	7.1	259	2.295	2.46	7.8	0.04	<0.05		7.2	1.07				8.5	4.73	42.2	3.10	0.35	0.08	13.60
C_C4	C			2.6	C4_t=3.3	106219		1	60	7.1	248	2.327	2.36	7.4	0.03	<0.05		6.5	0.98	4.8	12	2.5	7.8	4.48	40.4	3.04	0.42	0.08	12.80
C_C4	C			3.2	C4_t=4.1	106233		1	60	7.2	245	2.283	2.22	7.2	0.03	<0.05		6.2	0.46				7.1	4.02	38.1	2.77	0.58	0.08	12.01
C_C4	C			3.6	C4_t=4.3	106235		1	60	7.3	240	2.219	2.32	7.2	0.04	<0.05		5.9	0.14				7.2	4.15	39.1	2.85	0.62	0.08	12.31
C_C4	C			5.2	C4_t=6.1	106265		1	60	7.5	228	2.234	2.09	7.1	0.06	<0.05		5.0	0.12				6.3	3.49	35.9	2.60	0.69	0.08	11.39
C_C4	C			5.6	C4_t=6.3	106267		1	60	7.4	226	2.102	2.08	7.1	n.a.	<0.05		4.9	0.12	2.8	10	3.6	6.2	3.35	35.9	2.58	0.52	0.08	11.17
C_C4	C			6.3	C4_t=7.1	106275		1	60	7.5	224	2.153	2.07	7.2	0.03	<0.05		4.9	0.14				6.2	3.36	35.7	2.60	0.54	0.08	10.84
C_C4	C			7.3	C4_t=8.1	106283		1	60	7.6	228	2.288	2.03	7.0	0.03	<0.05		4.9	0.11				6.0	3.14	35.1	2.55	0.48	0.08	10.92
C_C4	C			8.3	C4_t=9.1	106291		1	60	7.7	225	2.245	1.94	7.0	0.03	<0.05		4.9	0.10				5.8	2.88	33.9	2.43	0.42	0.08	10.55
C_C4	C			9.3	C4_t=10.1	106299		1	60	7.6	216	2.066	2.10	7.0	0.03	<0.05		4.9	0.11				6.2	3.09	36.2	2.60	0.50	0.09	10.40
C_C4	C			10.3	C4_t=11.1	106307		1	60	7.5	216	2.074	2.09	7.1	<0.05		0.17			1.9	9.7	5.1	6.1	2.98	36.2	2.61	0.43	0.09	10.36
C_C4	C			11.3	C4_t=12.1	106315		1	60	7.4	221	2.148	1.91	7.1	n.a.	<0.05		5.2	0.10				5.7	2.59	33.7	2.42	0.40	0.08	10.33
C_C4	C			12.3	C4_t=13.1	106323		0	60	7.4				7.1	0.03	<0.05		5.1	0.09				5.8	2.53	33.7	2.42	0.38	0.08	10.09
C_C4	C			13.7	C4_t=14.2	106332		0	60						<0.05								6.1	3.65	50.7	3.45	0.44	0.21	7.06
C_C4	C			14.3	C4_t=15.1	106339		1	60	7.5	385	2.619	3.18	7.4	0.02	0.2	0.20	36.9	0.10	2.5	11	4.4	7.1	4.11	67.4	4.43	0.01	0.44	7.84
C_C4	C			15.5	C4_t=16.1	106344		1	60	7.4	306	2.462	2.50	7.2	0.02	<0.05		22.4	0.08				6.1	2.90	50.8	3.32	0.00	0.29	8.02
C_C4	C			16.5	C4_t=17.1	106348		1	60	7.2	260	2.4	2.32	7.5	0.02	<0.05	0.07	11.7	0.09				6.0	2.38	44.1	2.88	0.06	0.24	7.82
C_C4	C			17.5	C4_t=18.1	106352		1	60	7.4	244	2.222	2.18	7.4	0.01	<0.05		8.2	0.09				5.9	2.18	40.3	2.65	0.17	0.21	7.78
C_C4	C			18.5	C4_t=19.1	106356		1	60	7.4	231	2.134	2.25	7.3	n.a.	<0.05	0.10	6.9	0.09	1.5	6.2	4.1	6.2	2.27	40.6	2.69	0.26	0.20	7.87
C_C4	C			19.5	C4_t=20.1	106360		1	60	7.5	244	2.218	2.09	7.5	0.03	<0.05		6.3	0.11				5.8	2.04	38.0	2.52	0.29	0.19	8.24
C_C4	C			20.5	C4_t=21.1	106364		1	60	7.7	228	2.099	2.00	7.4	0.03	<0.05		5.7	0.09				5.7	1.95	36.3	2.41	0.22	0.19	8.06
C_C4	C			21.5	C4_t=22.1	106368		1	60	7.5	230	2.095	2.00	7.3	n.a.	<0.05	0.12	5.5	0.09	1.3	6.2	4.8	5.7	1.95	36.1	2.43	0.17	0.18	8.28
C_C4	C			22.5	C4_t=23.1	106372		1	60	7.3	227	2.154	1.98	7.6	0.03	<0.05		5.7	0.11				5.8	1.86	36.1	2.39	0.19	0.18	8.20
C_C4	C			23.5	C4_t=24.1	106376		1	60	7.2	225	2	1.91	7.3	n.a.	<0.05		5.3	0.09	1.3	6.4	4.9	5.6	1.75	34.7	2.33	0.18	0.17	8.16

ID	Al	As	B	Ba	Be	Bi	Cd	Co	Cr	Cu	Eu	Ga	Ho	In	La	Li	Mo	Ni	P	Pb	Sb	Sc	Se	Sr	Th
	µg/l	µg/l	µg/l	µg/l	µg/l	µg/l	µg/l	µg/l	µg/l	µg/l	µg/l	µg/l	µg/l	µg/l	µg/l	µg/l	µg/l	µg/l	µg/l	µg/l	µg/l	µg/l	µg/l	µg/l	µg/l
	3	1	4	0	0	3	0.3	1	1	1	0.09	2	0.1	2	0.3	1	1	1	5	1	5	0.07	6	1	2
A-inf-6	12	<1	<4	49	<0.02	<3	<0.3	4	<0.5	1	0.13	<2	<0.1	<2	<0.3	5	1	2	8	5	6	0.08	<6	89	<2
A-inf-9	16	<1	4	51	<0.02	<3	<0.3	4	1	<0.7	0.09	<2	<0.1	<2	<0.3	5	1	2	17	2	<5	<0.07	<6	89	<2
A-inf_av	14.00	<1	4.21	49.80	<0.02	<3	<0.3	4.40	0.59	1.01	0.11	<2	<0.1	<2	<0.3	5	1	2	12	3.84	5.89	0.08	<6	89	<2
A-Stdev	2.40	n/a	n/a	0.99	n/a	n/a	n/a	0.11	n/a	n/a	0.02	n/a	n/a	n/a	n/a	0.12	0.17	0.18	6.51	2.21	n/a	n/a	n/a	0.42	n/a
A-f5	10	<1	<4	47	0	<3	<0.3	2	2	<0.7	0.20	<2	<0.1	<2	<0.3	4	1	<0.8	168	4	<5	0.19	<6	73	6
Ac1-0.083	<3	3	35	44	<0.02	<3	1	4	<0.5	44	<0.09	<2	<0.1	3	<0.3	12	13	201	<5	4	5	<0.07	<6	188	<2
Ac1-0.25	<3	3	27	42	<0.02	<3	<0.3	<0.7	<0.5	11	<0.09	<2	<0.1	<2	<0.3	7	13	35	<5	5	<5	<0.07	<6	220	<2
Ac1-0.42	9	<1	17	32	<0.02	<3	<0.3	<0.7	<0.5	1	<0.09	<2	<0.1	4	<0.3	5	9	10	<5	5	<5	<0.07	<6	186	<2
Ac1-1	7	1	16	27	<0.02	<3	<0.3	<0.7	<0.5	9	0.14	<2	<0.1	<2	<0.3	4	9	10	<5	3	<5	<0.07	<6	162	<2
Ac1-1.33	<3	<1	14	25	<0.02	<3	<0.3	<0.7	<0.5	3	<0.09	<2	<0.1	<2	<0.3	4	7	3	<5	<1	<5	<0.07	<6	148	<2
Ac1-2.17	21	2	13	21	<0.02	<3	<0.3	<0.7	<0.5	2	0.21	<2	<0.1	2	<0.3	3	6	3	<5	3	<5	<0.07	<6	133	<2
Ac1-2.5	14	1	13	21	<0.02	<3	<0.3	<0.7	<0.5	<0.7	0.19	<2	<0.1	<2	<0.3	3	7	3	<5	1	5	<0.07	<6	130	<2
Ac1-3.17	11	<1	11	21	<0.02	<3	<0.3	<0.7	<0.5	<0.7	0.18	<2	<0.1	<2	<0.3	4	4	<0.8	<5	7	7	<0.07	<6	126	<2
Ac1-3.5	15	<1	11	20	<0.02	<3	<0.3	<0.7	<0.5	2	0.10	<2	<0.1	<2	<0.3	4	3	<0.8	<5	5	<5	0.07	<6	128	<2
Ac1-4.25	17	<1	9	19	<0.02	<3	<0.3	<0.7	<0.5	2	0.28	<2	<0.1	<2	<0.3	3	3	<0.8	<5	5	<5	0.07	<6	124	<2
Ac1-4.75	17	<1	9	19	<0.02	<3	<0.3	<0.7	<0.5	2	0.28	<2	<0.1	<2	<0.3	3	3	<0.8	<5	5	<5	0.07	<6	124	<2
Ac1-5	13	<1	8	19	<0.02	<3	<0.3	<0.7	<0.5	4	0.09	<2	<0.1	<2	<0.3	4	4	1	<5	4	6	<0.07	<6	123	<2
Ac1-5.5	16	<1	9	19	<0.02	<3	<0.3	<0.7	<0.5	1	0.18	<2	0	<2	<0.3	4	3	<0.8	<5	6	7	<0.07	<6	119	<2
Ac1-6.25	8	2	6	21	<0.02	<3	<0.3	<0.7	<0.5	<0.7	<0.09	<2	0	<2	<0.3	5	4	2	<5	7	<5	<0.07	<6	126	<2
Ac1-7	13	<1	6	21	<0.02	<3	<0.3	<0.7	<0.5	3	0.20	<2	<0.1	<2	<0.3	4	3	1	<5	5	<5	<0.07	<6	130	<2
Ac1-7.5	15	<1	4	21	<0.02	<3	<0.3	<0.7	<0.5	1	0.22	<2	<0.1	<2	<0.3	5	2	<0.8	<5	3	<5	<0.07	<6	136	<2
Ac1-10	21	<1	5	21	<0.02	<3	<0.3	<0.7	<0.5	2	0.16	<2	0	<2	<0.3	5	2	3	6	2	7	<0.07	<6	141	<2
Ac1-13	<3	1	8	18	0	<3	<0.3	1	1	11	<0.09	<2	<0.1	5	<0.3	4	2	2	57	4	<5	<0.07	<6	115	<2
Ac1-15	<3	2	7	17	0	<3	<0.3	1	<0.5	5	<0.09	<2	<0.1	6	<0.3	5	2	6	12	2	<5	<0.07	<6	112	<2
Ac1-17	15	<1	6	18	<0.02	<3	<0.3	1	<0.5	4	<0.09	<2	<0.1	5	<0.3	5	2	4	9	2	<5	<0.07	<6	116	<2
Ac1-20	12	1	7	17	<0.02	<3	<0.3	1	1	8	0.12	<2	<0.1	3	<0.3	4	2	2	<5	3	<5	<0.07	<6	109	<2
Ac1-22	<3	<1	6	16	<0.02	<3	<0.3	1	1	17	<0.09	<2	<0.1	5	<0.3	4	1	<0.8	12	3	<5	<0.07	<6	110	<2
Ac1-24	12	<1	5	17	<0.02	<3	<0.3	1	<0.5	7	<0.09	<2	<0.1	<2	<0.3	4	2	<0.8	5	4	<5	<0.07	<6	112	<2
Ac2-0.08	<3	<1	33	41	<0.02	<3	1	<0.7	<0.5	2	<0.09	<2	<0.1	<2	<0.3	10	10	5	6	<1	6	<0.07	<6	195	<2
Ac2-0.25	<3	<1	26	37	<0.02	<3	<0.3	<0.7	<0.5	<0.7	0.15	<2	<0.1	<2	<0.3	6	10	1	<5	3	<5	<0.07	<6	190	<2
Ac2-0.42	<3	<1	22	32	<0.02	<3	<0.3	<0.7	<0.5	<0.7	0.11	<2	<0.1	<2	<0.3	6	9	<0.8	<5	5	5	<0.07	<6	178	<2
Ac2-1	11	<1	19	28	<0.02	<3	<0.3	<0.7	<0.5	<0.7	0.09	<2	<0.1	2	<0.3	5	9	<0.8	<5	4	<5	<0.07	<6	157	<2
Ac2-1.33	15	1	19	27	<0.02	<3	<0.3	<0.7	<0.5	1	<0.09	<2	0	<2	<0.3	6	8	<0.8	<5	7	9	<0.07	<6	156	<2
Ac2-2.17	<3	<1	16	23	<0.02	<3	<0.3	<0.7	<0.5	2	0.16	<2	<0.1	<2	<0.3	5	6	<0.8	<5	4	<5	<0.07	<6	131	<2
Ac2-2.5	<3	1	16	21	<0.02	<3	<0.3	<0.7	<0.5	<0.7	0.21	<2	<0.1	7	<0.3	5	4	<0.8	<5	4	<5	<0.07	<6	125	<2
Ac2-3.17	<3	1	15	21	<0.02	<3	<0.3	<0.7	<0.5	<0.7	0.26	<2	0	3	<0.3	5	3	<0.8	<5	6	<5	<0.07	<6	126	<2
Ac2-3.5	11	1	15	20	<0.02	<3	<0.3	<0.7	<0.5	<0.7	0.26	<2	<0.1	<2	<0.3	5	3	<0.8	<5	2	<5	<0.07	<6	123	<2
Ac2-5	12	<1	12	21	<0.02	<3	<0.3	<0.7	<0.5	1	0.18	<2	<0.1	<2	<0.3	5	2	<0.8	<5	<1	<5	<0.07	<6	128	<2
Ac2-5.5	19	1	9	20	<0.02	<3	<0.3	<0.7	<0.5	20	<0.09	<2	<0.1	<2	<0.3	5	2	<0.8	<5	2	<5	<0.07	<6	126	<2
Ac2-6.25	10	<1	11	26	<0.02	<3	<0.3	<0.7	1	1	0.12	<2	0	<2	<0.3	6	2	<0.8	<5	4	<5	<0.07	<6	136	<2
Ac2-7	22	2	6	25	<0.02	<3	<0.3	<0.7	1	9	0.13	<2	0	<2	<0.3	7	3	4	5	5	8	<0.07	<6	153	<2
Ac2-7.5	14	2	6	22	<0.02	<3	<0.3	<0.7	<0.5	2	0.24	<2	<0.1	2	<0.3	6	2	<0.8	<5	4	<5	<0.07	<6	140	<2
Ac2-8.5	<3	<1	5	18	<0.02	<3	<0.3	<0.7	<0.5	4	0.26	<2	<0.1	<2	<0.3	6	2	<0.8	13	<1	<5	<0.07	<6	117	<2
Ac2-10	11	<1	4	21	<0.02	<3	<0.3	<0.7	<0.5	1	0.12	<2	0	5	<0.3	6	2	3	7	5	9	<0.07	<6	136	<2
Ac2-13	13	<1	5	18	<0.02	<3	<0.3	<0.7	<0.5	1	<0.09	<2	<0.1	3	<0.3	5	1	<0.8	<5	5	<5	<0.07	<6	111	<2
Ac2-15	12	2	7	17	<0.02	<3	<0.3	<0.7	<0.5	17	<0.09	<2	<0.1	7	<0.3	5	2	3	24	2	<5	<0.07	<6	115	<2
Ac2-17	<3	<1	5	18	<0.02	<3	<0.3	<0.7	<0.5	2	<0.09	<2	<0.1	3	<0.3	5	2	<0.8	9	5	<5	<0.07	<6	119	<2
Ac2-20	14	<1	4	18	0	<3	<0.3	<0.7	<0.5	2	<0.09	<2	<0.1	7	<0.3	5	2	<0.8	<5	4	<5	<0.07	<6	112	<2
Ac2-24	<3	<1	4	17	0	<3	<0.3	<0.7	<0.5	3	0.09	<2	<0.1	<2	<0.3	5	2	13	6	4	<5	<0.07	<6	116	<2
Ac3-0.08	21	<1	35	64	<0.02	<3	0	<0.7	<0.5	16	<0.09	<2	<0.1	<2	<0.3	7	13	12	6	5	5	<0.07	<6	189	<2
Ac3-0.25	<3	1	31	39	<0.02	<3	<0.3	<0.7	<0.5	2	0.13	<2	<0.1	<2	<0.3	6	13	7	<5	3	<5	<0.07	<6	191	<2
Ac3-0.42	<3	2	29	35	<0.02	<3	<0.3	<0.7	<0.5	1	0.16	<2	<0.1	<2	<0.3	6	13	1	<5	7	<5	<0.07	<6	171	<2
Ac3-1	<3	<1	26	34	<0.02	<3	<0.3	<0.7	<0.5	<0.7	<0.09	<2	<0.1	<2	<0.3	6	12	5	40	4	<5	<0.07	<6	170	<2
Ac3-1.33	<3	2	23	29	<0.02	<3	<0.3	<0.7	<0.5	1	0.25	<2	<0.1	<2	<0.3	6	8	<0.8	<5	3	6	<0.07	<6	153	<2
Ac3-2.17	14	3	14	25	<0.02	<3	<0.3	<0.7	<0.5	<0.7	0.19	<2	<0.1	<2	<0.3	5	4	<0.8	<5	5	<5	<0.07	<6	139	<2
Ac3-2.5	16	<1	13	22	<0.02	<3	<0.3	<0.7	<0.5	<0.7	0.20	<2	0	<2	<0.3	5	2	<0.8	<5	2	<5	<0.07	<6	124	<2
Ac3-3.17	15	2	16	25	<0.02	<3	<0.3	<0.7	1	2	0.16	<2	<0.1	3	<0.3	5	2	<0.8	<5	9	5	0.09	<6	137	<2
Ac3-3.33	8	<1	10	22	<0.02	<3	<0.3	<0.7	<0.5	2	0.27	<2	0	<2	<0.3	5	3	<0.8	<5	2	<5	<0.07	<6	129	<2
Ac3-4.25	13	<1	9	25	<0.02	<3	<0.3	<0.7	<0.5	2	0.27	<2	<0.1	<2	<0.3	5	2	<0.8	<5	4	<5	<0.07	<6	144	<2
Ac3-5	13	2	6	22	<0.02	<3	<0.3	<0.7	<0.5	<0.7	0.09	<2	0	<2	<0.3	5	4	9	<5	6	6	0.09	<6	130	<2
Ac3-5.5	13	2	5	23	<0.02	<3	<0.3	<0.7	<0.5	<0.7	<0.09	<2	<0.1	<2	<0.3	5	3	<0.8	<5	5	<5	<0.07	<6	138	<2
Ac3-6.25	16	2	<4	23	<0.02	<3	<0.3	<0.7	<0.5	<0.7	<0.09	<2	<0.1	<2	<0.3	5	2	<0.8	<5	3	<5	<0.07	<6	140	<2
Ac3-7	9	<1	<4	24	<0.02	<3	<0.3	<0.7	<0.5	<0.7	0.14	<2	<0.1	<2	<0.3	5	2	2	<5	6	<5	<0.07	<6	146	<2
Ac3-7.5	15	<1	<4	22	<0.02	<3	<0.3	<0.7	<0.5	<0.7	0.30	<2	<0.1	<2	<0.3	5	1	<0.8	6	6	<5	<0.07	<6	140	<2
Ac3-8.5	<3	1	<4	20	<0.02	<3	<0.3	<0.7	<0.5	<0.7	0.32	<2	0	<2	<0.3	5	3	<0.8	<5	2	<5	<0.07	<6	123	<2
Ac3-10	12	2	4	21	<0.02	<3	<0.3	<0.7	<0.5	<0.7	0.14	<2	<0.1	<2	<0.3	5	1	1	<5	3	<5	0.08	<6	134	<2
Ac3-13	13	2	5	21	0	<3	<0.3	1	1	7	<0.09	<2	<0.1	9	<0.3	5	1	<0.8	7	3	<5	<0.07	<6	116	<2
Ac3-15	19	2	5	18	0	<3	<0.3	1	2	5	<0.09	<2	<0.1	7	<0.3	5	2	<0.8	11	5	<5	<0.07	<6	119	<2
Ac3-17	16	<1	5	18	<0.02	<3	<0.3	1	<0.5	4	<0.09	<2	<0.1	4	<0.3	5	1	<0.8	8	<1	<5	<0.07	<6	118	<2
Ac3-20	10	2	4	19	0	<3	<0.3	1	1	5	<0.09	<2	<0.1	3	<0.3	5	1	<0.8	8	4	<5	<0.07	<6	113	<2
Ac3-22	4	<1	5	18	0	<3	<0.3	1	1	5	<0.09	<2	<0.1	5	<0.3	5	1	<0.8	6	3	<5	<0.07	<6	116	<2
Ac3-24	13	<1	4	18	0	<3	<0.3	1	1	4	0.10	<2	<0.1	4	<0.3	5	1	<0.8	6	4	<5	<0.07	<6	119	<2

ID	Al	As	B	Ba	Be	Bi	Cd	Co	Cr	Cu	Eu	Ga	Ho	In	La	Li	Mo	Ni	P	Pb	Sb	Sc	Se	Sr	Th
	µg/l	µg/l	µg/l	µg/l	µg/l	µg/l	µg/l	µg/l	µg/l	µg/l	µg/l	µg/l	µg/l	µg/l	µg/l	µg/l	µg/l	µg/l	µg/l	µg/l	µg/l	µg/l	µg/l	µg/l	µg/l
A-c4-0.08	29	1	40	69	<0.02	<3	1	<0.7	1	9	<0.09	<2	<0.1	<2	<0.3	8	11	22	<5	6	10	<0.07	<6	198	<2
A-c4-0.25	21	6	51	49	0	<3	<0.3	<0.7	1	4	0.24	<2	<0.1	<2	<0.3	10	13	10	7	2	<5	<0.07	<6	208	<2
A-c4-0.42	<3	8	61	47	0	<3	<0.3	<0.7	1	<0.7	<0.09	<2	<0.1	<2	<0.3	11	16	3	<5	3	<5	<0.07	<6	198	<2
A-c4-1	5	14	64	46	0	<3	<0.3	<0.7	1	<0.7	0.14	<2	<0.1	<2	<0.3	12	16	3	<5	<1	<5	<0.07	<6	189	<2
A-c4-1.33	5	15	56	43	0	<3	<0.3	<0.7	1	<0.7	0.20	<2	<0.1	<2	<0.3	12	16	9	16	<1	<5	<0.07	<6	178	<2
A-c4-2.17	18	9	37	43	0	<3	<0.3	<0.7	1	<0.7	0.10	<2	0	<2	<0.3	12	11	9	9	<1	<5	<0.07	<6	179	<2
A-c4-2.5	20	8	29	37	0	<3	<0.3	<0.7	1	<0.7	0.19	<2	<0.1	6	<0.3	10	9	<0.8	12	<1	<5	<0.07	<6	163	<2
A-c4-3.17	14	8	20	39	0	<3	<0.3	<0.7	1	<0.7	0.15	<2	0	<2	<0.3	10	7	1	10	<1	8	<0.07	<6	178	<2
A-c4-3.5	<3	8	17	35	0	<3	<0.3	<0.7	1	1	<0.09	<2	<0.1	<2	<0.3	10	6	<0.8	11	<1	<5	<0.07	<6	161	<2
A-c4-4.25	13	5	14	35	0	<3	<0.3	<0.7	1	3	0.19	<2	<0.1	<2	<0.3	9	5	<0.8	10	<1	<5	<0.07	<6	166	<2
A-c4-5	17	8	12	31	0	<3	<0.3	<0.7	1	2	0.11	<2	<0.1	<2	<0.3	9	4	<0.8	14	<1	7	<0.07	<6	151	<2
A-c4-5.5	19	6	9	30	0	<3	<0.3	<0.7	1	2	<0.09	<2	<0.1	<2	<0.3	8	4	2	12	<1	<5	0.08	<6	145	<2
A-c4-6.25	15	7	6	34	0	<3	<0.3	<0.7	1	1	0.12	<2	0	<2	<0.3	9	4	1	8	<1	<5	0.08	<6	168	<2
A-c4-7	20	6	6	33	0	<3	<0.3	<0.7	1	1	0.16	<2	<0.1	2	<0.3	8	4	2	6	<1	<5	<0.07	<6	165	<2
A-c4-7.5	23	5	5	30	0	<3	<0.3	<0.7	1	1	0.29	<2	<0.1	<2	<0.3	8	3	4	18	<1	7	<0.07	<6	154	<2
A-c4-8.5	19	3	6	26	0	<3	<0.3	<0.7	1	1	0.29	<2	<0.1	<2	<0.3	7	3	2	15	<1	<5	0.09	<6	136	<2
A-c4-10	9	6	5	27	0	<3	<0.3	<0.7	1	1	0.12	<2	<0.1	<2	<0.3	7	2	1	15	<1	8	<0.07	<6	140	<2
A-c4-13	19	6	6	25	0	<3	<0.3	1	1	17	<0.09	<2	<0.1	7	<0.3	6	2	<0.8	26	<1	<5	0.07	<6	127	<2
A-c4-15	11	5	5	24	0	<3	<0.3	1	1	9	<0.09	<2	<0.1	7	<0.3	6	2	<0.8	29	<1	<5	<0.07	<6	129	<2
A-c4-17	18	5	5	23	0	<3	<0.3	<0.7	1	6	<0.09	<2	<0.1	3	<0.3	6	2	<0.8	52	<1	<5	<0.07	<6	125	<2
A-c4-20	14	6	6	22	0	<3	<0.3	<0.7	1	9	<0.09	<2	<0.1	2	<0.3	6	2	1	30	<1	<5	<0.07	<6	121	<2
A-c4-22	15	6	5	21	0	<3	<0.3	1	1	6	<0.09	<2	<0.1	6	<0.3	5	2	1	25	<1	<5	<0.07	<6	123	<2
A-c4-24	16	6	5	21	0	<3	<0.3	1	1	5	0.10	<2	<0.1	5	<0.3	5	2	<0.8	25	<1	<5	<0.07	<6	121	<2
B-Inf-1.5	6	<1	6	55	0	<3	<0.3	4	2	<0.7	0.18	<2	<0.1	<2	<0.3	4	1	6	115	8	<5	0.28	<6	71	5
B-Inf-30	16	<1	4	51	0	<3	<0.3	6	1	5	<0.09	<2	<0.1	5	<0.3	5	1	8	37	2	<5	0.74	7	76	<2
B-Inf-35	13	<1	5	51	0	<3	<0.3	5	1	3	<0.09	<2	<0.1	6	<0.3	4	<0.5	8	49	5	<5	0.79	6	75	<2
B-Inf_av-0@60	6	<1	4	55	<0.02	<3	<0.3	4	2	<0.7	0.18	<2	<0.1	<2	<0.3	4	1	6	37	8	<5	0.28	<6	71	5
B-Inf_av-0@60	6	<1	4	55	<0.02	<3	<0.3	4	2	<0.7	0.18	<2	<0.1	<2	<0.3	4	1	6	37	8	<5	0.28	<6	71	5
B-Inf_av-7.2@6	16	<1	4	51	<0.02	<3	<0.3	6	1	5	<0.09	<2	<0.1	5	<0.3	5	1	8	37	2	<5	0.74	7	76	<2
B-Inf_av-7.2@6	16	<1	4	51	<0.02	<3	<0.3	6	1	5	<0.09	<2	<0.1	5	<0.3	5	1	8	37	2	<5	0.74	7	76	<2
B_st_dev	4.71	n/a	0.57	1.98	0.01	n/a	n/a	0.76	0.27	1.52	0.00	n/a	n/a	0.44	n/a	0.08	0.08	1.30	31.24	2.95	n/a	0.26	0.25	2.75	0.00
B-c1-0.08	8	3	64	85	<0.02	<3	0	2	<0.5	81	0.12	<2	<0.1	<2	<0.3	5	3	16	<5	1	6	<0.07	<6	132	<2
B-c1-0.17	34	4	53	86	<0.02	<3	1	2	<0.5	17	0.10	<2	<0.1	<2	<0.3	5	2	12	<5	3	<5	<0.07	<6	128	<2
B-c1-0.25	18	4	56	87	<0.02	<3	0	2	1	26	0.13	<2	<0.1	<2	<0.3	5	2	12	<5	2	9	<0.07	<6	132	<2
B-c1-0.33	24	4	54	88	<0.02	<3	0	2	1	6	<0.09	<2	<0.1	<2	<0.3	5	2	12	<5	3	9	<0.07	<6	134	<2
B-c1-0.42	35	2	55	92	<0.02	<3	<0.3	2	1	12	<0.09	<2	<0.1	<2	<0.3	5	2	8	6	4	19	0.08	<6	135	<2
B-c1-0.5	86	3	53	93	<0.02	<3	0	2	1	5	<0.09	<2	<0.1	<2	0	5	2	8	6		16	0.08	<6	137	<2
B-c1-1.08	48	2	50	53	<0.02	<3	<0.3	1	1	3	<0.09	<2	<0.1	<2	<0.3	4	3	5	16	7	6	0.07	<6	84	<2
B-c1-1.17	134	3	52	55	<0.02	<3	<0.3	1	1	7	<0.09	<2	<0.1	<2	1	4	3	5	<5	11	7	0.13	<6	87	<2
B-c1-1.25	55	3	55	53	<0.02	<3	0	1	1	13	<0.09	<2	<0.1	<2	<0.3	4	3	7	6	6	<5	0.07	<6	89	<2
B-c1-1.33	48	3	48	52	<0.02	<3	<0.3	1	1	4	<0.09	<2	<0.1	<2	<0.3	4	3	5	<5	7	6	<0.07	<6	87	<2
B-c1-1.42	120	1	48	56	0	<3	0	1	1	7	<0.09	<2	<0.1	<2	0	4	3	6	<5	10	6	0.12	<6	90	<2
B-c1-1.5	168	2	44	55	0	<3	<0.3	1	1	6	<0.09	<2	<0.1	<2	0	4	2	5	5	11	<5	0.16	<6	85	<2
B-c1-2.17	98	4	26	58	0	<3	0	1	1	3	<0.09	<2	<0.1	<2	<0.3	4	4	4	<5	9	5	0.11	<6	93	<2
B-c1-2.33	42	4	22	58	<0.02	<3	0	1	1	3	<0.09	<2	<0.1	<2	<0.3	4	4	4	<5	6	<5	<0.07	<6	94	<2
B-c1-2.5	13	4	19	57	<0.02	<3	1	1	<0.5	7	<0.09	<2	<0.1	<2	<0.3	4	4	8	<5	3	<5	0.08	<6	95	<2
B-c1-3.17	30	5	14	58	<0.02	<3	0	1	1	7	<0.09	<2	<0.1	<2	<0.3	4	4	6	<5	4	<5	0.07	<6	94	<2
B-c1-3.33	38	6	12	57	0	<3	<0.3	1	1	5	<0.09	<2	<0.1	<2	<0.3	4	5	5	<5	6	<5	0.08	<6	93	<2
B-c1-3.5	35	6	12	56	0	<3	0	1	1	3	0.10	<2	<0.1	<2	<0.3	4	5	5	<5	6	<5	0.10	<6	93	<2
B-c1-4.17	33	4	11	63	<0.02	<3	2	1	1	2	<0.09	<2	<0.1	<2	<0.3	4	4	36	<5	2	<5	0.09	<6	100	<2
B-c1-4.33	59	3	9	60	<0.02	<3	0	1	1	2	<0.09	<2	<0.1	<2	<0.3	4	4	9	<5	4	<5	0.07	<6	97	<2
B-c1-4.5	39	4	9	60	<0.02	<3	<0.3	1	1	3	0.10	<2	<0.1	<2	<0.3	4	4	5	<5	2	<5	<0.07	<6	99	<2
B-c1-5.25	23	5	7	59	<0.02	<3	<0.3	1	1	2	<0.09	<2	<0.1	<2	<0.3	4	4	4	<5	2	<5	0.07	<6	96	<2
B-c1-5.5	26	4	7	61	<0.02	<3	0	1	1	2	<0.09	<2	<0.1	<2	<0.3	5	3	5	<5	1	<5	0.08	<6	97	<2
B-c1-6.25	19	4	6	60	<0.02	<3	0	1	1	2	<0.09	<2	<0.1	<2	<0.3	5	3	5	<5	2	<5	<0.07	<6	98	<2
B-c1-6.5	63	5	6	60	<0.02	<3	<0.3	1	1	2	<0.09	<2	<0.1	<2	<0.3	5	3	4	<5	4	<5	0.09	<6	97	<2
B-c1-7.25	26	5	5	57	<0.02	<3	<0.3	1	1	1	<0.09	<2	<0.1	<2	<0.3	5	3	4	<5	3	<5	<0.07	<6	93	<2
B-c1-7.5	12	3	6	59	<0.02	<3	0	1	1	3	<0.09	<2	0	<2	<0.3	5	3	3	5	2	<5	<0.07	<6	97	<2
B-c1-8.25	50	3	6	57	<0.02	<3	0	1	1	3	<0.09	<2	<0.1	<2	<0.3	5	3	5	<5	3	<5	0.07	<6	96	<2
B-c1-8.5	8	3	5	57	<0.02	<3	<0.3	1	1	5	<0.09	<2	<0.1	<2	<0.3	5	2	4	<5	<1	<5	<0.07	<6	96	<2
B-c1-9.5	15	3	4	52	<0.02	<3	0	1	1	5	<0.09	<2	<0.1	<2	<0.3	5	2	6	<5	2	<5	<0.07	<6	92	<2
B-c1-10	134	2	5	52	<0.02	<3	<0.3	1	1	2	0.11	<2	<0.1	<2	<0.3	5	2	3	<5	5	<5	0.10	<6	90	<2
B-c1-11	112	1	4	50	<0.02	<3	0	1	1	4	<0.09	<2	<0.1	<2	<0.3	5	2	1	<5	8	<5	0.09	<6	90	<2
B-c1-12	65	1	<4	47	<0.02	<3	0	<0.7	1	3	0.11	<2	0	<2	<0.3	5	2	2	<5	8	<5	<0.07	<6	87	<2
B-c1-13	19	2	5	46	<0.02	<3	0	1	1	3	<0.09	<2	<0.1	<2	<0.3	5	2	3	<5	1	<5	0.09	<6	87	<2
B-c1-14	84	2	5	46	<0.02	<3	0	1	1	3	<0.09	<2	0	<2	<0.3	5	2	2	<5	6	<5	0.09	<6	86	<2
B-c1-15	19	2	5	46	<0.02	<3	0	1	1	4	<0.09	<2	<0.1	<2	<0.3	4	2	2	<5	3	<5	<0.07	<6	88	<2
B-c1-16	12	2	5	45	<0.02	<3	<0.3	1	<0.5	4	<0.09	<2	<0.1	<2	<0.3	5	2	3	15	3	<5	<0.07	<6	88	<2
B-c1-19	12	1	4	40	<0.02	<3	0	2	<0.5	8	<0.09	<2	<0.1	5	<0.3	4	1	2	<5	4	<5	<0.07	<6	86	<2
B-c1-20	7	<1	5	39	<0.02	<3	0	1	1	5	0.13	<2	<0.1	3	<0.3	4	2	2	6	4	<5	0.13	<6	87	<2
B-c1-21	4	<1	5	38	<0.02	<3	1	2	1	7	<0.09	<2	<0.1	4	<0.3	5	2	2	15	4	<5	0.88	<6	87	<2
B-c1-22	9	<1	4	38	<0.02	<3	<0.3	1	1	6	<0.09	<2	0	6	<0.3	5	1	2	8	2	<5	0.88	<6	87	<2
B-c1-23	15	<1	5	38	<0.02	<3	<0.3	1	1	13	<0.09	<2	<0.1	3	<0.3	5	<0.5	5	28	3	<5	0.89	<6	88	<2

© KWR

ID	Al	As	B	Ba	Be	Bi	Cd	Co	Cr	Cu	Eu	Ga	Ho	In	La	Li	Mo	Ni	P	Pb	Sb	Sc	Se	Sr	Th
	µg/l	µg/l	µg/l	µg/l	µg/l	µg/l	µg/l	µg/l	µg/l	µg/l	µg/l	µg/l	µg/l	µg/l	µg/l	µg/l	µg/l	µg/l	µg/l	µg/l	µg/l	µg/l	µg/l	µg/l	µg/l
B-c1-26	13	<1	<4	35	<0.02	<3	0	2	<0.5	9	<0.09	<2	<0.1	4	<0.3	5	2	4	17	<1	<5	0.88	<6	87	<2
B-c2-0.08	4	<1	68	64	<0.02	<3	0	1	1	30	0.09	<2	<0.1	8	<0.3	7	4	24	<5	2	<5	<0.07	<6	131	<2
B-c2-0.17	4	2	69	66	<0.02	<3	0	1	1	39	0.09	<2	<0.1	3	<0.3	7	3	22	<5	5	<5	<0.07	<6	132	<2
B-c2-0.25	35	3	73	75	<0.02	<3	<0.3	1	1	10	<0.09	<2	<0.1	2	<0.3	7	3	18	<5	6	6	<0.07	<6	137	<2
B-c2-0.33	11	3	70	78	<0.02	<3	0	1	1	9	<0.09	<2	<0.1	<2	<0.3	6	3	12	<5	5	8	<0.07	<6	133	<2
B-c2-0.42	12	2	67	82	<0.02	<3	0	1	1	18	<0.09	<2	<0.1	<2	<0.3	6	2	11	<5	4	<5	<0.07	<6	131	<2
B-c2-0.5	7	3	66	82	<0.02	<3	0	<0.7	<0.5	10	<0.09	<2	<0.1	<2	<0.3	6	2	8	<5	2	<5	0.15	<6	131	<2
B-c2-1.08	55	3	60	59	<0.02	<3	<0.3	<0.7	<0.5	10	<0.09	<2	<0.1	<2	<0.3	5	2	4	<5	5	6	<0.07	<6	96	<2
B-c2-1.17	20	3	58	56	<0.02	<3	<0.3	<0.7	<0.5	19	<0.09	<2	<0.1	<2	<0.3	5	2	4	<5	2	<5	<0.07	<6	95	<2
B-c2-1.25	22	3	58	58	<0.02	<3	0	<0.7	<0.5	16	<0.09	<2	<0.1	<2	<0.3	5	2	5	<5	7	<5	<0.07	<6	90	<2
B-c2-1.33	28	2	54	56	<0.02	<3	<0.3	<0.7	<0.5	14	<0.09	<2	<0.1	<2	<0.3	5	2	5	<5	4	6	<0.07	<6	89	<2
B-c2-1.42	31	2	50	56	<0.02	<3	<0.3	<0.7	<0.5	5	<0.09	<2	<0.1	<2	<0.3	5	2	4	<5	4	<5	<0.07	<6	86	<2
B-c2-1.5	44	3	39	53	<0.02	<3	<0.3	1	<0.5	6	<0.09	<2	<0.1	<2	<0.3	5	1	3	<5	3	<5	<0.07	<6	84	<2
B-c2-2.17	21	3	20	56	<0.02	<3	<0.3	<0.7	<0.5	5	<0.09	<2	<0.1	<2	<0.3	5	2	2	<5	1	<5	<0.07	<6	85	<2
B-c2-2.33	26	2	17	56	<0.02	<3	<0.3	<0.7	<0.5	7	<0.09	<2	<0.1	<2	<0.3	5	2	3	<5	3	<5	<0.07	<6	87	<2
B-c2-2.5	19	3	14	56	<0.02	<3	1	<0.7	<0.5	13	<0.09	<2	<0.1	<2	<0.3	5	2	6	<5	2	<5	0.07	<6	88	<2
B-c2-3.17	18	<1	9	56	<0.02	<3	1	<0.7	<0.5	14	<0.09	<2	<0.1	<2	<0.3	5	2	5	<5	5	<5	<0.07	<6	87	<2
B-c2-3.33	17	<1	9	56	<0.02	<3	0	<0.7	<0.5	8	<0.09	<2	<0.1	<2	<0.3	5	2	3	<5	5	<5	<0.07	<6	85	<2
B-c2-3.5	21	1	10	54	<0.02	<3	0	<0.7	<0.5	57	<0.09	<2	<0.1	<2	<0.3	5	2	3	<5	4	<5	<0.07	<6	97	<2
B-c2-4.17	32	<1	8	60	<0.02	<3	<0.3	<0.7	<0.5	4	<0.09	<2	<0.1	<2	<0.3	5	4	2	<5	3	<5	<0.07	<6	92	<2
B-c2-4.33	46	1	7	60	<0.02	<3	0	<0.7	1	3	0.10	<2	<0.1	<2	<0.3	5	4	2	<5	4	<5	<0.07	<6	93	<2
B-c2-4.5	46	<1	7	59	<0.02	<3	1	<0.7	1	7	0.13	<2	<0.1	<2	<0.3	5	4	3	<5	2	<5	<0.07	<6	94	<2
B-c2-5.25	107	<1	7	61	<0.02	<3	<0.3	<0.7	1	2	<0.09	<2	<0.1	<2	<0.3	5	4	3	<5	<1	<5	0.09	<6	92	<2
B-c2-5.5	36	<1	6	60	<0.02	<3	<0.3	<0.7	1	3	<0.09	<2	<0.1	<2	<0.3	5	4	2	<5	<1	<5	0.13	<6	93	<2
B-c2-6.25	34	<1	6	60	<0.02	<3	0	<0.7	1	2	0.13	<2	<0.1	<2	<0.3	5	3	3	<5	1	<5	<0.07	<6	95	<2
B-c2-6.5	26	<1	6	57	<0.02	<3	<0.3	<0.7	1	4	0.08	<2	<0.1	<2	<0.3	5	4	2	<5	<1	<5	<0.07	<6	93	<2
B-c2-7.25	16	<1	7	57	<0.02	<3	<0.3	<0.7	<0.5	6	<0.09	<2	<0.1	<2	<0.3	4	3	3	<5	2	<5	0.14	<6	91	<2
B-c2-7.5	18	<1	7	57	<0.02	<3	0	<0.7	<0.5	8	<0.09	<2	<0.1	<2	<0.3	4	3	2	<5	<1	<5	<0.07	<6	96	<2
B-c2-8.25	6	<1	6	54	<0.02	<3	<0.3	<0.7	<0.5	4	<0.09	<2	<0.1	<2	<0.3	4	3	3	<5	<1	<5	<0.07	<6	95	<2
B-c2-8.5	16	<1	6	55	<0.02	<3	<0.3	<0.7	<0.5	6	<0.09	<2	0	<2	<0.3	4	3	4	<5	<1	<5	<0.07	<6	97	<2
B-c2-9.5	21	<1	5	49	<0.02	<3	0	<0.7	<0.5	6	<0.09	<2	<0.1	<2	<0.3	3	2	3	<5	<1	<5	<0.07	<6	91	<2
B-c2-10	63	<1	4	49	<0.02	<3	0	1	1	4	<0.09	<2	0	<2	<0.3	3	2	1	<5	4	<5	<0.07	<6	91	<2
B-c2-11	67	<1	4	48	<0.02	<3	0	<0.7	1	3	0.13	<2	0	<2	<0.3	3	2	1	<5	4	<5	<0.07	<6	90	<2
B-c2-12	74	<1	4	46	<0.02	<3	<0.3	<0.7	1	3	<0.09	<2	<0.1	<2	<0.3	3	2	1	<5	2	<5	<0.07	<6	87	<2
B-c2-13	99	<1	5	44	<0.02	<3	0	1	1	2	0.11	<2	<0.1	4	<0.3	4	2	1	<5	4	<5	0.09	<6	88	<2
B-c2-14	36	<1	5	42	<0.02	<3	<0.3	1	1	1	<0.09	<2	<0.1	5	<0.3	4	2	1	<5	3	<5	<0.07	<6	88	<2
B-c2-15	28	<1	4	40	<0.02	<3	0	<0.7	<0.5	11	<0.09	<2	<0.1	7	<0.3	4	2	2	<5	3	<5	<0.07	<6	90	<2
B-c2-16	20	<1	<4	39	<0.02	<3	0	1	<0.5	10	<0.09	<2	0	4	<0.3	4	1	2	45	3	<5	<0.07	<6	90	<2
B-c2-19	9	<1	<4	35	<0.02	<3	<0.3	1	<0.5	11	<0.09	<2	<0.1	3	<0.3	4	2	3	21	<1	<5	0.09	<6	88	<2
B-c2-20	35	<1	<4	34	<0.02	<3	<0.3	1	<0.5	14	<0.09	<2	<0.1	7	<0.3	4	1	2	35	4	<5	0.10	<6	89	<2
B-c2-21	29	<1	<4	34	<0.02	<3	<0.3	1	<0.5	9	<0.09	<2	<0.1	5	<0.3	4	2	2	26	3	<5	0.95	<6	89	<2
B-c2-22	23	<1	<4	34	<0.02	<3	0	1	<0.5	11	<0.09	<2	<0.1	4	<0.3	4	2	1	28	4	<5	0.85	<6	89	<2
B-c2-23	22	<1	<4	33	<0.02	<3	<0.3	1	1	15	<0.09	<2	<0.1	3	<0.3	4	1	1	15	2	<5	0.91	<6	89	<2
B-c2-26	15	<1	<4	33	<0.02	<3	0	1	3	1	<0.09	<2	<0.1	7	<0.3	4	2	3	17	<1	<5	0.89	<6	91	<2
B-c3-0.08	7	12	72	70	<0.02	<3	1	3	1	19	0.12	<2	<0.1	<2	<0.3	6	4	24	<5	7	<5	<0.07	<6	95	<2
B-c3-0.17	43	10	72	67	<0.02	<3	1	2	1	6	<0.09	<2	<0.1	<2	<0.3	6	3	17	<5	4	<5	<0.07	<6	88	<2
B-c3-0.25	69	8	72	60	<0.02	<3	0	2	1	6	<0.09	<2	<0.1	<2	<0.3	6	4	12	6	10	19	<0.07	<6	81	<2
B-c3-0.33	80	11	71	57	0	<3	0	2	1	6	<0.09	<2	<0.1	<2	<0.3	6	4	11	7	11	20	0.08	<6	75	<2
B-c3-0.42	53	9	64	52	<0.02	<3	0	2	1	4	<0.09	<2	<0.1	<2	<0.3	5	4	11	<5	8	5	<0.07	<6	74	<2
B-c3-0.5	33	11	64	54	<0.02	<3	0	2	1	3	<0.09	<2	<0.1	<2	<0.3	5	4	11	<5	7	7	0.09	<6	72	<2
B-c3-1.08	170	9	36	59	0	<3	0	2	1	6	<0.09	<2	<0.1	<2	0	5	4	9	<5	15	10	0.16	<6	78	<2
B-c3-1.17	232	9	33	57	0	<3	0	2	2	10	<0.09	<2	<0.1	<2	1	5	4	7	9	21	18	0.19	<6	73	<2
B-c3-1.25	215	10	32	59	0	<3	0	2	1	7	<0.09	<2	<0.1	<2	0	5	3	13	6	18	8	0.17	<6	79	<2
B-c3-1.33	196	10	30	59	0	<3	<0.3	2	1	5	<0.09	<2	<0.1	<2	1	5	4	9	5	16	12	0.27	<6	75	<2
B-c3-1.42	122	11	29	59	0	<3	<0.3	2	1	3	<0.09	<2	<0.1	<2	<0.3	5	4	9	<5	12	<5	0.11	<6	76	<2
B-c3-1.5	70	13	27	59	0	<3	<0.3	2	1	4	<0.09	<2	<0.1	<2	<0.3	5	4	9	<5	11	6	0.10	<6	75	<2
B-c3-2.17	16	13	17	64	<0.02	<3	0	2	1	2	<0.09	<2	<0.1	<2	<0.3	5	4	9	<5	7	<5	0.08	<6	82	<2
B-c3-2.33	44	15	15	66	0	<3	<0.3	2	1	3	<0.09	<2	<0.1	<2	<0.3	6	3	12	<5	8	<5	0.17	<6	86	2
B-c3-2.5	34	14	13	64	<0.02	<3	<0.3	2	1	3	<0.09	<2	<0.1	<2	<0.3	5	3	11	<5	8	<5	0.08	<6	83	<2
B-c3-3.17	34	15	10	65	0	<3	0	2	1	5	<0.09	<2	<0.1	<2	<0.3	5	3	11	<5	7	<5	0.09	<6	84	<2
B-c3-3.33	51	14	9	64	0	<3	<0.3	1	1	3	<0.09	<2	<0.1	<2	<0.3	5	3	8	<5	8	<5	0.08	<6	82	<2
B-c3-3.5	67	15	9	65	0	<3	<0.3	1	1	5	<0.09	<2	<0.1	<2	<0.3	3	3	8	<5	8	<5	0.16	<6	87	2
B-c3-4.17	40	14	9	69	<0.02	<3	0	2	1	3	<0.09	<2	<0.1	<2	<0.3	6	3	7	<5	8	<5	0.08	<6	90	<2
B-c3-4.33	45	13	8	67	<0.02	<3	0	1	1	2	0.10	<2	<0.1	<2	<0.3	6	3	6	<5	9	<5	0.07	<6	90	<2
B-c3-4.5	34	14	8	69	<0.02	<3	0	2	1	1	<0.09	<2	<0.1	<2	<0.3	6	3	7	<5	4	<5	<0.07	<6	95	<2
B-c3-5.25	35	13	6	67	<0.02	<3	<0.3	1	1	2	<0.09	<2	0	<2	<0.3	5	3	7	<5	3	<5	<0.07	<6	91	<2
B-c3-5.5	10	14	7	68	<0.02	<3	0	1	1	5	<0.09	<2	<0.1	<2	<0.3	5	3	6	<5	2	<5	0.08	<6	95	2
B-c3-6.25	14	14	6	66	<0.02	<3	0	1	1	3	0.13	<2	0	<2	<0.3	5	3	5	<5	2	<5	<0.07	<6	95	<2
B-c3-6.5	26	12	6	64	<0.02	<3	0	1	1	3	<0.09	<2	<0.1	<2	<0.3	5	3	5	<5	3	<5	0.08	<6	92	<2
B-c3-7.25	34	13	5	60	<0.02	<3	<0.3	1	1	1	<0.09	<2	<0.1	<2	<0.3	5	2	5	<5	4	<5	0.10	<6	92	<2
B-c3-7.5	10	14	6	62	<0.02	<3	0	1	1	3	<0.09	<2	<0.1	<2	<0.3	5	3	7	<5	2	<5	<0.07	<6	96	<2
B-c3-8.25	19	11	5	58	<0.02	<3	0	1	1	3	<0.09	<2	<0.1	<2	<0.3	5	2	4	<5	3	<5	<0.07	<6	95	<2
B-c3-8.5	33	13	5	59	<0.02	<3	<0.3	1	1	2	<0.09	<2	<0.1	<2	<0.3	5	3	5	<5	4	<5	<0.07	<6	97	<2

ID	Al	As	B	Ba	Be	Bi	Cd	Co	Cr	Cu	Eu	Ga	Ho	In	La	Li	Mo	Ni	P	Pb	Sb	Sc	Se	Sr	Th
	µg/l	µg/l	µg/l	µg/l	µg/l	µg/l	µg/l	µg/l	µg/l	µg/l	µg/l	µg/l	µg/l	µg/l	µg/l	µg/l	µg/l	µg/l	µg/l	µg/l	µg/l	µg/l	µg/l	µg/l	µg/l
B-c3-9.5	65	12	4	51	<0.02	<3	0	1	1	2	0.10	<2	<0.1	<2	<0.3	4	2	4	<5	5	<5	0.09	<6	89	<2
B-c3-10	14	7	6	51	<0.02	<3	<0.3	1	1	2	<0.09	<2	<0.1	<2	<0.3	4	2	3	<5	2	<5	<0.07	<6	90	<2
B-c3-11	5	6	5	47	<0.02	<3	0	1	<0.5	2	0.10	<2	<0.1	<2	<0.3	4	2	3	<5	3	<5	<0.07	<6	88	<2
B-c3-12	6	4	5	45	<0.02	<3	0	2	1	2	<0.09	<2	<0.1	<2	<0.3	4	2	3	<5	2	<5	<0.07	<6	87	<2
B-c3-13	11	5	5	44	<0.02	<3	0	1	1	6	<0.09	<2	0	4	<0.3	4	3	3	20	3	<5	<0.07	<6	87	<2
B-c3-14	9	5	4	42	<0.02	<3	0	1	1	4	<0.09	<2	<0.1	2	<0.3	4	2	2	7	3	<5	<0.07	<6	87	<2
B-c3-15	8	6	5	41	<0.02	<3	0	2	<0.5	4	<0.09	<2	<0.1	4	<0.3	4	3	2	<5	4	<5	<0.07	<6	87	<2
B-c3-16	24	5	5	40	<0.02	<3	0	2	1	4	<0.09	<2	<0.1	5	<0.3	4	7	2	<5	7	<5	<0.07	<6	87	<2
B-c3-19	31	4	4	37	<0.02	<3	0	2	1	3	<0.09	<2	0	<2	<0.3	4	3	2	7	7	<5	<0.07	<6	85	<2
B-c3-20	30	4	5	37	<0.02	<3	<0.3	2	1	3	<0.09	<2	0	5	<0.3	4	2	2	77	6	<5	0.08	<6	87	<2
B-c3-21	34	3	<4	36	<0.02	<3	0	1	1	2	<0.09	<2	<0.1	4	<0.3	4	2	1	26	10	<5	0.95	<6	87	<2
B-c3-22	39	4	5	36	<0.02	<3	<0.3	1	1	2	<0.09	<2	<0.1	4	<0.3	4	2	3	13	7	<5	0.96	<6	86	<2
B-c3-23	10	3	5	34	<0.02	<3	0	1	1	6	<0.09	<2	<0.1	2	<0.3	4	2	2	14	2	<5	0.89	<6	87	<2
B-c3-26	34	2	5	34	<0.02	<3	0	1	1	6	<0.09	<2	<0.1	2	<0.3	4	2	2	134	3	<5	0.91	<6	86	<2
B-c4-0.08	16	15	97	96	<0.02	<3	<0.3	1	1	82	0.11	<2	<0.1	4	<0.3	17	6	13	13	<1	<5	0.08	<6	159	<2
B-c4-0.17	19	19	119	100	0	<3	0	1	1	53	<0.09	<2	<0.1	<2	<0.3	16	5	11	11	<1	<5	0.07	<6	155	<2
B-c4-0.25	6	28	140	104	<0.02	<3	<0.3	<0.7	1	31	<0.09	<2	<0.1	2	<0.3	16	5	10	8	<1	<5	<0.07	<6	155	<2
B-c4-0.42	4	24	141	128	<0.02	<3	0	<0.7	1	28	0.09	<2	<0.1	<2	<0.3	16	5	8	<5	<1	<5	<0.07	<6	153	<2
B-c4-1.08	101	41	77	50	0	<3	<0.3	<0.7	1	10	<0.09	<2	<0.1	<2	<0.3	11	4	3	14	2	<5	0.10	<6	76	<2
B-c4-1.17	90	40	65	44	0	<3	<0.3	1	1	10	<0.09	<2	<0.1	10	<0.3	11	4	3	13	2	<5	0.11	<6	68	<2
B-c4-1.25	101	40	54	41	0	<3	<0.3	1	1	11	<0.09	<2	<0.1	7	<0.3	11	4	3	13	3	<5	0.11	<6	61	<2
B-c4-1.33	79	27	53	41	0	<3	<0.3	1	1	17	<0.09	<2	<0.1	4	<0.3	11	4	3	7	2	6	0.11	<6	64	<2
B-c4-1.5	125	25	44	48	0	<3	<0.3	<0.7	1	7	<0.09	<2	<0.1	<2	<0.3	11	4	2	8	4	7	0.12	<6	60	<2
B-c4-2.17	172	28	15	46	0	<3	<0.3	<0.7	1	3	<0.09	<2	<0.1	<2	0	11	3	1	9	6	<5	0.16	<6	55	<2
B-c4-2.33	115	33	12	45	0	<3	1	1	1	5	<0.09	<2	<0.1	5	<0.3	11	4	6	14	5	<5	0.15	<6	58	<2
B-c4-2.5	109	38	12	45	0	<3	1	1	1	6	<0.09	<2	<0.1	10	<0.3	11	3	6	17	4	5	0.14	<6	60	<2
B-c4-3.17	121	36	9	43	0	<3	1	1	1	4	<0.09	<2	<0.1	4	<0.3	11	3	5	18	4	<5	0.11	<6	58	<2
B-c4-3.33	111	38	9	44	0	<3	0	1	2	5	<0.09	<2	<0.1	7	<0.3	11	3	2	21	3	<5	0.13	<6	57	<2
B-c4-3.5	85	40	9	43	0	<3	<0.3	1	1	17	<0.09	<2	<0.1	10	<0.3	11	3	2	24	3	<5	0.11	<6	65	<2
B-c4-4.17	64	45	9	45	0	<3	<0.3	<0.7	1	5	<0.09	<2	<0.1	<2	<0.3	12	3	1	26	2	<5	0.08	<6	63	<2
B-c4-4.33	162	42	8	45	0	<3	<0.3	<0.7	1	5	0.13	<2	<0.1	<2	<0.3	12	3	1	25	2	<5	0.09	<6	63	<2
B-c4-4.5	73	43	7	45	0	<3	<0.3	<0.7	1	5	<0.09	<2	0	<2	<0.3	12	3	1	22	2	<5	0.09	<6	62	<2
B-c4-5.25	44	41	6	45	0	<3	<0.3	<0.7	1	6	<0.09	<2	0	<2	<0.3	12	2	<0.8	25	2	<5	<0.07	<6	62	<2
B-c4-5.5	18	44	6	44	0	<3	<0.3	<0.7	1	5	<0.09	<2	<0.1	<2	<0.3	12	2	1	29	<1	<5	<0.07	<6	61	<2
B-c4-6.25	49	45	6	44	0	<3	<0.3	<0.7	1	5	0.09	<2	<0.1	<2	<0.3	12	3	<0.8	34	1	<5	<0.07	<6	62	<2
B-c4-6.5	23	44	5	42	0	<3	<0.3	<0.7	1	5	<0.09	<2	<0.1	<2	<0.3	11	3	1	28	2	<5	0.08	<6	59	<2
B-c4-7.25	62	40	5	41	0	<3	<0.3	1	1	4	<0.09	<2	<0.1	4	<0.3	10	4	3	26	2	<5	0.09	<6	59	<2
B-c4-7.5	17	40	5	41	0	<3	<0.3	1	1	7	<0.09	<2	<0.1	3	<0.3	10	3	1	27	1	<5	<0.07	<6	60	<2
B-c4-8.25	15	34	5	40	0	<3	<0.3	<0.7	1	5	<0.09	<2	<0.1	4	<0.3	10	4	1	25	2	<5	<0.07	<6	60	<2
B-c4-8.5	158	33	5	40	0	<3	<0.3	1	1	5	<0.09	<2	0	7	<0.3	10	4	1	25	<1	<5	0.10	<6	62	<2
B-c4-9.5	33	28	5	36	0	<3	<0.3	<0.7	1	6	<0.09	<2	<0.1	3	<0.3	8	4	<0.8	18	2	<5	<0.07	<6	59	<2
B-c4-10	25	15	5	39	0	<3	0	1	1	6	<0.09	<2	<0.1	<2	<0.3	8	4	10	<5	<1	<5	<0.07	<6	62	<2
B-c4-11	25	11	5	37	0	<3	<0.3	<0.7	1	5	0.13	<2	0	<2	<0.3	7	4	7	48	2	<5	<0.07	<6	62	<2
B-c4-12	21	13	5	34	<0.02	<3	<0.3	<0.7	1	7	0.10	<2	0	<2	<0.3	6	4	2	10	<1	<5	0.11	<6	62	<2
B-c4-13	33	19	5	33	0	<3	<0.3	1	1	9	0.10	<2	<0.1	<2	<0.3	5	3	2	13	3	<5	<0.07	<6	64	<2
B-c4-14	110	19	5	34	0	<3	<0.3	<0.7	1	5	0.10	<2	<0.1	3	<0.3	5	3	1	12	3	<5	0.09	<6	67	<2
B-c4-15	7	20	5	31	<0.02	<3	<0.3	1	1	8	<0.09	<2	<0.1	3	<0.3	5	3	2	33	<1	<5	<0.07	<6	70	<2
B-c4-16	6	20	5	30	<0.02	<3	<0.3	1	1	8	<0.09	<2	<0.1	5	<0.3	4	3	<0.8	35	<1	<5	<0.07	<6	74	<2
B-c4-19	6	22	5	28	<0.02	<3	<0.3	<0.7	1	18	<0.09	<2	0	2	<0.3	4	12	1	68	<1	<5	<0.07	<6	81	<2
B-c4-20	8	21	5	28	<0.02	<3	<0.3	1	1	14	<0.09	<2	<0.1	<2	<0.3	3	6	<0.8	173	<1	<5	5.51	<6	81	<2
B-c4-21	5	18	4	27	<0.02	<3	<0.3	1	1	11	<0.09	<2	<0.1	5	<0.3	3	4	1	130	<1	<5	0.83	<6	81	<2
B-c4-22	7	17	5	28	<0.02	<3	<0.3	<0.7	<0.5	11	<0.09	<2	<0.1	3	<0.3	3	4	<0.8	123	<1	<5	0.86	<6	82	<2
B-c4-23	6	17	5	27	<0.02	<3	1	<0.7	1	19	<0.09	<2	<0.1	4	<0.3	3	3	<0.8	84	<1	<5	0.87	<6	81	<2
B-c4-26	16	15	5	26	<0.02	<3	<0.3	<0.7	1	13	<0.09	<2	<0.1	6	<0.3	3	2	<0.8	128	<1	<5	0.85	<6	83	<2
C-Inf_-17	18	<1	8	16	<0.02	<3	<0.3	1	<0.5	<0.7	0.11	<2	0	6	<0.3	2	1	<0.8	78	4	<5	<0.07	<6	87	<2
C-Inf_-7	21	<1	<4	14	<0.02	<3	<0.3	1	<0.5	1	<0.09	<2	<0.1	7	<0.3	2	1	<0.8	77	2	<5	<0.07	<6	87	<2
C0_t=1	17	<1	<4	13	<0.02	<3	<0.3	2	1	9	<0.09	<2	<0.1	10	<0.3	318	5	13	92	3	<5	<0.07	<6	91	<2
C0_t=3	9	<1	<4	16	<0.02	<3	<0.3	1	<0.5	1	<0.09	<2	<0.1	5	<0.3	19	2	3	60	3	<5	<0.07	<6	96	<2
C0_t=4	34	<1	<4	16	<0.02	<3	<0.3	1	1	2	<0.09	<2	<0.1	7	<0.3	6	1	7	67	4	<5	<0.07	<6	93	<2
C0_t=8	17	<1	<4	15	<0.02	<3	<0.3	1	<0.5	3	<0.09	<2	<0.1	7	<0.3	6	2	18	47	3	<5	<0.07	<6	88	<2
C0_t=10	17	<1	<4	14	<0.02	<3	<0.3	1	1	11	<0.09	<2	<0.1	8	<0.3	14	2	6	98	4	<5	<0.07	<6	89	<2
C0_t=11	<3	2	<4	15	<0.02	<3	<0.3	1	<0.5	2	<0.09	<2	<0.1	7	<0.3	2	1	3	234	4	<5	<0.07	<6	88	<2
C0_t=15	23	<1	<4	15	<0.02	<3	<0.3	1	1	9	0.09	<2	<0.1	7	<0.3	316	5	14	119	4	<5	<0.07	<6	88	<2
C0_t=17	17	2	<4	15	<0.02	<3	<0.3	2	<0.5	<0.7	<0.09	<2	<0.1	13	<0.3	6	2	7	41	2	<5	<0.07	<6	88	<2
C0_t=18	19	<1	<4	14	<0.02	<3	<0.3	2	<0.5	1	<0.09	<2	<0.1	9	<0.3	3	2	1	41	5	<5	<0.07	<6	87	<2
C0_t=22	<3	<1	<4	15	<0.02	<3	<0.3	2	<0.5	<0.7	<0.09	<2	<0.1	11	<0.3	3	2	2	61	3	<5	<0.07	<6	87	<2
C0_t=24	9	<1	<4	15	<0.02	<3	<0.3	2	1	1	<0.09	<2	<0.1	2	<0.3	3	2	4	48	6	<5	<0.07	<6	91	<2
C_C0_av	17.92	<1	<4	14.89	<0.02	<3	<0.3	1.42	0.87	4.43	0.09	<2	<0.1	8	<0.3	63	2	7	83	3.73	<5	<0.07	<6	90	<2
C_st_dev	7.30	n/a	n/a	0.86	n/a	n/a	n/a	0.42	0.32	3.94	n/a	n/a	n/a	2.75	n/a	125.59	1.37	5.66	56.30	1.18	n/a	n/a	n/a	2.98	n/a
C1_t=1.2	20	12	27	29	<0.02	<3	<0.3	1	<0.5	30	<0.09	<2	<0.1	2	<0.3	34	3	<0.8	30	4	<5	<0.07	<6	135	<2
C1_t=1.4	44	11	25	26	<0.02	<3	<0.3	1	<0.5	55	<0.09	<2	<0.1	6	<0.3	35	3	1	34	6	<5	<0.07	<6	130	<2
C1_t=1.6	25	10	21	26	<0.02	<3	<0.3	1	<0.5	21	0.16	<2	<0.1	10	<0.3	38	3	<0.8	36	5	<5	<0.07	<6	133	<2
C1_t=2.2	40	9	15	25	<0.02	<3	<0.3	1	<0.5	29	<0.09	<2	<0.1	7	<0.3	60	3	2	19	5	<5	<0.07	<6	133	<2

© KWR

ID	Al	As	B	Ba	Be	Bi	Cd	Co	Cr	Cu	Eu	Ga	Ho	In	La	Li	Mo	Ni	P	Pb	Sb	Sc	Se	Sr	Th
	µg/l	µg/l	µg/l	µg/l	µg/l	µg/l	µg/l	µg/l	µg/l	µg/l	µg/l	µg/l	µg/l	µg/l	µg/l	µg/l	µg/l	µg/l	µg/l	µg/l	µg/l	µg/l	µg/l	µg/l	µg/l
C1_it2.4	11	9	13	26	<0.02	<3	<0.3	<0.7	<0.5	2	0.10	<2	<0.1	5	<0.3	43	2	1	22	4	<5	<0.07	<6	133	<2
C1_it3.1	8	8	12	26	<0.02	<3	<0.3	1	<0.5	1	<0.09	<2	<0.1	4	<0.3	38	2	1	14	5	<5	<0.07	<6	134	<2
C1_it4.1	22	10	11	27	<0.02	<3	<0.3	1	<0.5	3	<0.09	<2	<0.1	5	<0.3	30	2	1	29	2	<5	<0.07	<6	139	<2
C1_it4.3	22	9	9	25	<0.02	<3	<0.3	1	<0.5	6	<0.09	<2	<0.1	7	<0.3	24	2	1	28	4	<5	<0.07	<6	129	<2
C1_it5.1	16	10	9	26	<0.02	<3	<0.3	1	<0.5	2	0.15	<2	<0.1	8	<0.3	22	2	2	24	6	<5	<0.07	<6	135	<2
C1_it5.3	23	11	8	25	<0.02	<3	<0.3	1	<0.5	2	0.10	<2	<0.1	5	<0.3	19	2	<0.8	30	5	<5	<0.07	<6	129	<2
C1_it6.1	16	8	7	25	<0.02	<3	<0.3	<0.7	<0.5	<0.7	0.12	<2	<0.1	8	<0.3	18	2	<0.8	29	1	<5	<0.07	<6	131	<2
C1_it6.3	22	9	6	25	<0.02	<3	<0.3	<0.7	<0.5	<0.7	0.13	<2	<0.1	6	<0.3	16	2	<0.8	34	3	<5	<0.07	<6	126	<2
C1_it7.1	19	8	6	24	<0.02	<3	<0.3	1	<0.5	1	<0.09	<2	<0.1	4	<0.3	16	2	<0.8	36	2	<5	<0.07	<6	127	<2
C1_it8.1	32	8	6	25	<0.02	<3	<0.3	1	<0.5	8	0.10	<2	<0.1	6	<0.3	13	2	1	34	2	<5	<0.07	<6	127	<2
C1_it9.1	37	10	6	25	<0.02	<3	<0.3	2	<0.5	1	<0.09	<2	<0.1	<2	<0.3	12	1	<0.8	56	4	<5	<0.07	<6	127	<2
C1_it10.1	36	8	4	24	<0.02	<3	<0.3	1	<0.5	<0.7	0.14	<2	<0.1	7	<0.3	11	2	1	37	3	<5	<0.07	<6	125	<2
C1_it11.1	26	7	<4	24	<0.02	<3	<0.3	<0.7	<0.5	<0.7	0.12	<2	<0.1	9	<0.3	10	3	<0.8	38	4	<5	<0.07	<6	123	<2
C1_it12.1	28	7	4	23	<0.02	<3	<0.3	1	<0.5	<0.7	0.16	<2	<0.1	9	<0.3	9	3	<0.8	31	4	<5	<0.07	<6	120	<2
C1_it13.1	33	6	<4	23	<0.02	<3	<0.3	1	<0.5	<0.7	<0.09	<2	<0.1	6	<0.3	8	2	<0.8	32	4	<5	<0.07	<6	119	<2
C1_it14.2	23	5	<4	22	<0.02	<3	<0.3	<0.7	<0.5	<0.7	<0.09	<2	<0.1	<2	<0.3	8	2	<0.8	29	3	<5	<0.07	<6	116	<2
C1_it15.1	8	7	15	23	<0.02	<3	<0.3	1	<0.5	<0.7	0.10	<2	<0.1	12	<0.3	7	2	<0.8	26	4	<5	<0.07	<6	120	<2
C1_it16.1	8	7	13	23	<0.02	<3	<0.3	1	<0.5	<0.7	0.14	<2	<0.1	10	<0.3	8	2	<0.8	28	3	<5	<0.07	<6	123	<2
C1_it17.1	5	7	11	25	<0.02	<3	1	1	<0.5	<0.7	0.11	<2	<0.1	5	<0.3	9	2	1	20	4	<5	<0.07	<6	131	<2
C1_it18.1	6	6	9	24	<0.02	<3	1	1	<0.5	<0.7	0.11	<2	<0.1	4	<0.3	9	2	1	23	3	<5	<0.07	<6	125	<2
C1_it19.1	13	6	8	24	<0.02	<3	1	1	<0.5	<0.7	0.13	<2	<0.1	9	<0.3	8	3	1	24	4	<5	0.09	<6	124	<2
C1_it20.1	15	5	7	23	<0.02	<3	<0.3	1	<0.5	<0.7	0.14	<2	<0.1	11	<0.3	8	2	<0.8	24	4	<5	<0.07	<6	122	<2
C1_it21.1	12	5	6	23	<0.02	<3	<0.3	<0.7	<0.5	<0.7	<0.09	<2	<0.1	6	<0.3	7	3	<0.8	22	7	<5	<0.07	<6	122	<2
C1_it22.1	15	4	6	23	<0.02	<3	<0.3	1	<0.5	<0.7	<0.09	<2	<0.1	5	<0.3	7	2	1	26	2	<5	<0.07	<6	122	<2
C1_it23.1	15	6	5	23	<0.02	<3	<0.3	1	<0.5	<0.7	<0.09	<2	<0.1	8	<0.3	6	3	<0.8	25	1	<5	<0.07	<6	123	<2
C1_it24.1	21	6	4	22	<0.02	<3	<0.3	1	<0.5	<0.7	<0.09	<2	<0.1	<2	<0.3	6	2	<0.8	21	2	<5	<0.07	<6	117	<2
C2_it1.2	39	15	25	33	<0.02	<3	<0.3	<0.7	<0.5	15	<0.09	<2	<0.1	5	<0.3	51	3	1	29	4	<5	<0.07	<6	130	<2
C2_it1.4	34	16	24	31	<0.02	<3	<0.3	1	<0.5	32	0.09	<2	<0.1	6	<0.3	53	3	1	35	6	<5	<0.07	<6	134	<2
C2_it1.6	33	17	22	32	<0.02	<3	<0.3	<0.7	<0.5	19	<0.09	<2	<0.1	5	<0.3	51	3	1	36	6	<5	<0.07	<6	136	<2
C2_it2.2	48	14	17	31	<0.02	<3	<0.3	2	<0.5	19	0.11	<2	<0.1	7	<0.3	171	3	1	22	7	<5	<0.07	<6	136	<2
C2_it2.4	28	14	17	30	<0.02	<3	<0.3	<0.7	<0.5	<0.7	<0.09	<2	<0.1	3	<0.3	228	4	<0.8	29	5	<5	<0.07	<6	134	<2
C2_it3.1	25	14	14	31	<0.02	<3	<0.3	1	<0.5	<0.7	0.11	<2	<0.1	5	<0.3	128	3	1	15	5	<5	<0.07	<6	140	<2
C2_it3.3	21	15	13	32	<0.02	<3	<0.3	2	<0.5	1	<0.09	<2	<0.1	4	<0.3	92	2	1	19	3	<5	<0.07	<6	142	<2
C2_it4.1	31	13	11	31	<0.02	<3	<0.3	1	<0.5	1	0.12	<2	<0.1	6	<0.3	69	2	<0.8	25	2	<5	<0.07	<6	137	<2
C2_it4.3	44	15	11	31	<0.02	<3	<0.3	<0.7	<0.5	1	0.11	<2	<0.1	7	<0.3	63	3	1	24	5	<5	<0.07	<6	139	<2
C2_it5.1	20	16	10	30	<0.02	<3	<0.3	1	<0.5	<0.7	<0.09	<2	<0.1	3	<0.3	48	3	<0.8	24	4	<5	<0.07	<6	133	<2
C2_it6.1	34	14	9	30	<0.02	<3	<0.3	<0.7	<0.5	1	0.14	<2	<0.1	4	<0.3	50	3	1	23	6	<5	<0.07	<6	135	<2
C2_it6.3	36	15	8	31	<0.02	<3	<0.3	<0.7	<0.5	<0.7	<0.09	<2	<0.1	10	<0.3	39	2	1	35	5	<5	<0.07	<6	137	<2
C2_it7.1	38	14	7	30	<0.02	<3	<0.3	<0.7	1	<0.7	<0.09	<2	<0.1	<2	<0.3	35	3	1	28	2	<5	<0.07	<6	131	<2
C2_it8.1	30	13	7	30	<0.02	<3	<0.3	1	<0.5	1	<0.09	<2	<0.1	9	<0.3	30	2	<0.8	31	3	<5	<0.07	<6	130	<2
C2_it9.1	44	13	7	30	<0.02	<3	<0.3	<0.7	<0.5	4	<0.09	<2	<0.1	6	<0.3	27	2	<0.8	35	5	<5	<0.07	<6	131	<2
C2_it10.1	50	13	6	29	<0.02	<3	<0.3	<0.7	<0.5	<0.7	0.16	<2	<0.1	3	<0.3	25	3	<0.8	40	6	<5	<0.07	<6	127	<2
C2_it11.1	43	14	6	29	<0.02	<3	<0.3	1	<0.5	<0.7	0.11	<2	<0.1	6	<0.3	24	2	<0.8	36	6	<5	<0.07	<6	127	<2
C2_it12.1	69	12	5	28	<0.02	<3	<0.3	<0.7	<0.5	<0.7	0.14	<2	<0.1	9	<0.3	18	2	<0.8	30	<1	<5	<0.07	<6	124	<2
C2_it13.1	66	11	4	27	<0.02	<3	<0.3	<0.7	<0.5	<0.7	<0.09	<2	<0.1	<2	<0.3	18	2	<0.8	30	<1	<5	<0.07	<6	121	<2
C2_it14.2	65	10	<4	27	<0.02	<3	<0.3	<0.7	<0.5	<0.7	<0.09	<2	<0.1	<2	<0.3	13	2	<0.8	33	5	<5	<0.07	<6	121	<2
C2_it15.1	11	11	15	27	<0.02	<3	<0.3	1	<0.5	<0.7	0.17	<2	<0.1	10	<0.3	16	2	<0.8	27	3	<5	<0.07	<6	123	<2
C2_it16.1	13	10	13	28	<0.02	<3	<0.3	1	<0.5	<0.7	0.10	<2	<0.1	7	<0.3	14	2	<0.8	30	3	<5	<0.07	<6	123	<2
C2_it17.1	12	9	12	30	<0.02	<3	1	1	<0.5	<0.7	0.15	<2	<0.1	6	<0.3	15	1	2	22	2	<5	<0.07	<6	134	<2
C2_it18.1	14	9	9	29	<0.02	<3	1	1	<0.5	<0.7	0.14	<2	<0.1	8	<0.3	13	2	<0.8	26	3	<5	<0.07	<6	131	<2
C2_it19.1	15	9	8	28	<0.02	<3	1	1	<0.5	<0.7	0.13	<2	<0.1	8	<0.3	13	2	1	29	4	<5	<0.07	<6	127	<2
C2_it20.1	33	8	7	28	<0.02	<3	<0.3	1	<0.5	<0.7	<0.09	<2	<0.1	8	<0.3	11	2	<0.8	17	3	<5	<0.07	<6	127	<2
C2_it21.1	46	7	6	37	<0.02	<3	<0.3	1	<0.5	1	<0.09	<2	<0.1	8	<0.3	13	2	<0.8	23	5	<5	<0.07	<6	126	<2
C2_it22.1	44	6	6	27	<0.02	<3	<0.3	1	<0.5	<0.7	<0.09	<2	<0.1	5	<0.3	13	2	<0.8	23	3	<5	<0.07	<6	123	<2
C2_it23.1	47	9	6	28	<0.02	<3	<0.3	1	<0.5	<0.7	0.10	<2	<0.1	10	<0.3	11	3	<0.8	19	4	<5	<0.07	<6	127	<2
C2_it24.1	49	6	5	27	<0.02	<3	<0.3	<0.7	<0.5	<0.7	<0.09	<2	<0.1	5	<0.3	12	2	<0.8	23	2	<5	<0.07	<6	122	<2
C3_it1.2	43	22	34	35	<0.02	<3	<0.3	<0.7	<0.5	13	<0.09	<2	<0.1	7	<0.3	10	3	2	17	3	<5	<0.07	<6	150	<2
C3_it1.4	25	26	38	36	<0.02	<3	<0.3	<0.7	<0.5	14	<0.09	<2	<0.1	3	<0.3	13	3	2	17	4	<5	<0.07	<6	145	<2
C3_it1.6	28	26	35	34	<0.02	<3	<0.3	1	<0.5	19	<0.09	<2	<0.1	5	<0.3	14	4	2	18	3	<5	<0.07	<6	139	<2
C3_it2.2	29	30	33	40	<0.02	<3	<0.3	1	<0.5	11	<0.09	<2	<0.1	5	<0.3	188	4	3	13	3	<5	<0.07	<6	156	<2
C3_it2.4	21	27	30	38	<0.02	<3	<0.3	1	<0.5	1	<0.09	<2	<0.1	5	<0.3	95	3	2	15	6	<5	<0.07	<6	149	<2
C3_it3.1	19	28	27	41	<0.02	<3	<0.3	1	<0.5	1	<0.09	<2	<0.1	4	<0.3	99	3	2	14	4	<5	<0.07	<6	150	<2
C3_it3.3	22	31	25	42	<0.02	<3	<0.3	1	<0.5	1	0.10	<2	<0.1	5	<0.3	71	3	2	18	3	<5	<0.07	<6	158	<2
C3_it4.1	18	32	20	42	<0.02	<3	<0.3	<0.7	<0.5	1	0.10	<2	0	6	<0.3	61	4	1	25	5	<5	<0.07	<6	154	<2
C3_it4.3	22	33	20	43	<0.02	<3	<0.3	1	<0.5	1	0.13	<2	<0.1	9	<0.3	63	4	1	30	1	<5	<0.07	<6	156	<2
C3_it5.1	14	32	16	39	<0.02	<3	<0.3	<0.7	<0.5	<0.7	<0.09	<2	<0.1	8	<0.3	45	3	1	32	3	<5	<0.07	<6	145	<2
C3_it6.1	18	33	13	41	<0.02	<3	<0.3	<0.7	1	<0.7	0.10	<2	<0.1	6	<0.3	39	3	1	48	2	<5	<0.07	<6	147	<2
C3_it6.3	15	29	13	39	<0.02	<3	<0.3	1	<0.5	<0.7	0.10	<2	<0.1	4	<0.3	35	3	3	43	3	<5	<0.07	<6	145	<2
C3_it7.1	18	31	12	41	<0.02	<3	<0.3	1	<0.5	<0.7	<0.09	<2	<0.1	6	<0.3	35	3	4	35	4	<5	<0.07	<6	151	<2
C3_it8.1	30	32	11	39	<0.02	<3	<0.3	2	<0.5	1	0.09	<2	<0.1	7	<0.3	30	6	10	40	4	<5	<0.07	<6	146	<2
C3_it9.1	27	30	8	38	<0.02	<3	<0.3	2	1	1	<0.09	<2	<0.1	10	<0.3	27	6	13	44	4	<5	<0.07	<6	144	<2
C3_it10.1	31	27	7	37	<0.02	<3	<0.3	1	<0.5	<0.7	<0.09	<2	<0.1	7	<0.3	24	4	7	40	3	<5	<0.07	<6	140	<2
C3_it11.1	44	27	6	37	<0.02	<3	<0.3	1	<0.5	<0.7	0.11	<2	<0.1	9	<0.3	24	3	4	42	4	<5	<0.07	<6	145	<2

ID	Al	As	B	Ba	Be	Bi	Cd	Co	Cr	Cu	Eu	Ga	Ho	In	La	Li	Mo	Ni	P	Pb	Sb	Sc	Se	Sr	Th
	µg/l	µg/l	µg/l	µg/l	µg/l	µg/l	µg/l	µg/l	µg/l	µg/l	µg/l	µg/l	µg/l	µg/l	µg/l	µg/l	µg/l	µg/l	µg/l	µg/l	µg/l	µg/l	µg/l	µg/l	µg/l
C3_t=12.1	34	29	6	36	<0.02	<3	<0.3	1	<0.5	<0.7	<0.09	<2	<0.1	7	<0.3	21	3	3	33	3	<5	<0.07	<6	138	<2
C3_t=13.1	24	27	4	35	<0.02	<3	<0.3	<0.7	<0.5	<0.7	0.11	<2	<0.1	7	<0.3	20	3	1	39	6	<5	<0.07	<6	136	<2
C3_t=14.2	45	26	<4	35	<0.02	<3	<0.3	<0.7	<0.5	<0.7	<0.09	<2	<0.1	7	<0.3	18	3	1	40	4	<5	<0.07	<6	133	<2
C3_t=15.1	28	25	15	36	<0.02	<3	<0.3	1	<0.5	<0.7	0.13	<2	0	8	<0.3	18	3	1	41	5	<5	<0.07	<6	138	<2
C3_t=16.1	40	24	12	36	<0.02	<3	<0.3	<0.7	<0.5	<0.7	0.16	<2	<0.1	11	<0.3	16	3	1	43	3	<5	<0.07	<6	136	<2
C3_t=17.1	39	23	11	40	<0.02	<3	1	<0.7	<0.5	<0.7	0.12	<2	<0.1	9	<0.3	16	1	2	38	5	<5	<0.07	<6	151	<2
C3_t=18.1	27	22	9	40	<0.02	<3	<0.3	1	<0.5	<0.7	0.14	<2	<0.1	11	<0.3	15	2	<0.8	49	5	<5	<0.07	<6	151	<2
C3_t=19.1	28	21	7	37	<0.02	<3	0	<0.3	1	<0.5	0.16	<2	<0.1	3	<0.3	14	3	<0.8	43	3	<5	<0.07	<6	140	<2
C3_t=20.1	62	21	7	38	<0.02	<3	<0.3	1	<0.5	<0.7	0.14	<2	<0.1	9	<0.3	14	3	<0.8	43	3	<5	<0.07	<6	142	<2
C3_t=21.1	46	19	6	36	<0.02	<3	<0.3	1	<0.5	<0.7	<0.09	<2	<0.1	7	<0.3	13	2	<0.8	47	3	<5	<0.07	<6	136	<2
C3_t=22.1	41	17	5	36	<0.02	<3	<0.3	2	<0.5	<0.7	<0.09	<2	<0.1	7	<0.3	12	2	<0.8	45	4	<5	<0.07	<6	135	<2
C3_t=23.1	51	19	6	37	<0.02	<3	<0.3	1	<0.5	1	<0.09	<2	<0.1	9	<0.3	12	2	<0.8	50	5	<5	<0.07	<6	137	<2
C3_t=24.1	37	17	4	35	<0.02	<3	<0.3	1	<0.5	<0.7	<0.09	<2	<0.1	<2	<0.3	11	2	<0.8	45	2	<5	<0.07	<6	130	<2
C4_t=1.2	61	67	77	68	<0.02	<3	<0.3	<0.7	1	11	<0.09	<2	<0.1	<2	<0.3	13	6	6	71	<1	<5	<0.07	<6	160	<2
C4_t=1.4	21	114	104	99	<0.02	<3	<0.3	<0.7	<0.5	9	<0.09	<2	<0.1	<2	<0.3	16	8	7	146	3	<5	<0.07	<6	176	<2
C4_t=1.6	24	125	93	106	<0.02	<3	<0.3	<0.7	<0.5	11	0.10	<2	<0.1	<2	<0.3	17	8	8	153	6	<5	<0.07	<6	180	<2
C4_t=2.2	11	130	75	105	<0.02	<3	<0.3	<0.7	<0.5	64	0.12	<2	<0.1	<2	<0.3	103	8	4	123	8	<5	<0.07	<6	177	<2
C4_t=2.4	44	136	61	96	<0.02	<3	<0.3	<0.7	<0.5	9	0.09	<2	<0.1	<2	<0.3	59	6	3	134	9	<5	<0.07	<6	167	<2
C4_t=3.1	43	138	59	104	<0.02	<3	<0.3	<0.7	<0.5	4	0.11	<2	<0.1	<2	<0.3	63	6	2	131	7	<5	<0.07	<6	178	<2
C4_t=3.3	24	128	49	99	<0.02	<3	<0.3	<0.7	<0.5	1	0.11	<2	<0.1	<2	<0.3	44	5	2	140	6	<5	<0.07	<6	171	<2
C4_t=4.1	20	115	37	93	<0.02	<3	<0.3	<0.7	<0.5	9	0.09	<2	<0.1	<2	<0.3	31	5	2	135	4	<5	<0.07	<6	161	<2
C4_t=4.3	23	112	35	95	<0.02	<3	<0.3	<0.7	<0.5	<0.7	0.09	<2	<0.1	<2	<0.3	30	5	5	139	6	<5	<0.07	<6	165	<2
C4_t=6.1	18	90	22	89	<0.02	<3	<0.3	<0.7	<0.5	<0.7	<0.09	<2	<0.1	<2	<0.3	22	5	4	122	4	<5	<0.07	<6	150	<2
C4_t=6.3	21	81	18	87	<0.02	<3	<0.3	<0.7	1	<0.7	0.15	<2	<0.1	<2	<0.3	21	4	3	128	4	<5	<0.07	<6	148	<2
C4_t=7.1	18	79	18	87	<0.02	<3	<0.3	<0.7	<0.5	1	<0.09	<2	<0.1	<2	<0.3	21	5	2	121	3	<5	<0.07	<6	148	<2
C4_t=8.1	36	73	15	86	<0.02	<3	<0.3	<0.7	<0.5	<0.7	<0.09	<2	<0.1	<2	<0.3	20	4	2	117	5	<5	<0.07	<6	145	<2
C4_t=9.1	24	64	12	80	<0.02	<3	<0.3	<0.7	<0.5	<0.7	<0.09	<2	0	<2	<0.3	18	3	1	116	2	<5	<0.07	<6	138	<2
C4_t=10.1	46	61	10	86	<0.02	<3	<0.3	<0.7	1	<0.7	<0.09	<2	0	<2	<0.3	18	4	2	114	4	<5	<0.07	<6	149	<2
C4_t=11.1	23	58	9	83	<0.02	<3	<0.3	<0.7	<0.5	<0.7	0.14	<2	0	<2	<0.3	17	3	1	119	4	<5	<0.07	<6	148	<2
C4_t=12.1	40	51	8	75	<0.02	<3	<0.3	<0.7	<0.5	<0.7	0.09	<2	<0.1	<2	<0.3	15	3	1	101	5	<5	<0.07	<6	136	<2
C4_t=13.1	25	46	6	72	<0.02	<3	<0.3	<0.7	<0.5	<0.7	<0.09	<2	<0.1	<2	<0.3	15	3	1	93	5	<5	<0.07	<6	136	<2
C4_t=14.2	159	56	11	151	<0.02	<3	<0.3	2	1	20	0.12	<2	<0.1	<2	<0.3	31	17	94	101	10	8	<0.07	<6	197	<2
C4_t=15.1	8	23	24	115	<0.02	<3	0	2	<0.5	29	0.23	<2	0	<2	<0.3	18	10	24	51	8	<5	<0.07	<6	243	<2
C4_t=16.1	3	24	15	70	<0.02	<3	<0.3	1	<0.5	4	0.13	<2	<0.1	<2	<0.3	15	5	9	44	3	<5	<0.07	<6	184	<2
C4_t=17.1	12	22	12	63	<0.02	<3	<0.3	<0.7	<0.5	2	<0.09	<2	<0.1	<2	<0.3	14	4	5	42	4	<5	<0.07	<6	157	<2
C4_t=18.1	<3	27	10	65	<0.02	<3	<0.3	<0.7	<0.5	<0.7	0.14	<2	<0.1	<2	<0.3	13	4	4	47	3	<5	<0.07	<6	145	<2
C4_t=19.1	16	27	8	66	<0.02	<3	<0.3	<0.7	<0.5	<0.7	0.12	<2	<0.1	<2	<0.3	13	4	5	55	1	<5	<0.07	<6	147	<2
C4_t=20.1	20	31	8	64	<0.02	<3	<0.3	<0.7	<0.5	<0.7	<0.09	<2	<0.1	<2	<0.3	12	5	5	56	5	<5	<0.07	<6	137	<2
C4_t=21.1	<3	29	7	65	<0.02	<3	<0.3	<0.7	<0.5	<0.7	<0.09	<2	0	<2	<0.3	11	3	3	57	5	<5	<0.07	<6	130	<2
C4_t=22.1	19	31	6	63	<0.02	<3	<0.3	<0.7	<0.5	<0.7	<0.09	<2	<0.1	<2	<0.3	11	3	1	60	<1	<5	<0.07	<6	130	<2
C4_t=23.1	6	30	6	64	<0.02	<3	<0.3	<0.7	<0.5	<0.7	<0.09	<2	<0.1	<2	<0.3	11	3	<0.8	64	3	<5	<0.07	<6	129	<2
C4_t=24.1	4	29	5	61	<0.02	<3	<0.3	<0.7	<0.5	<0.7	<0.09	<2	<0.1	<2	<0.3	10	3	<0.8	65	5	<5	<0.07	<6	124	<2

ID	Ti	Tl	U	V	W	Yb	Zn	Charge balance	Electrical balance	$SI_{Calcite}$	$SI_{Dolomite}$	$SI_{Rhodochrosite}$	$SI_{Siderite}$	SI_{Quartz}	$SI_{K\text{-}feldspar}$	$SI_{Kaolinite}$	$SI_{Gibbsite}$
	µg/l	µg/l	µg/l	µg/l	µg/l	µg/l	µg/l	meq	%								
	0.1	2	4	2	2	0.03	0.3										
A-Inf-6	<0.1	<2	4	<2	<2	0.04	6.4										
A-Inf-9	<0.1	<2	9	<2	<2	0.07	9.2	-0.17	-3.79	-1.18	-3.19	-0.48	-0.60	0.31	-1.36	4.34	1.29
A-Inf_av	<0.1	<2	7	<2	<2	0.05	7.8	-0.21	-4.53	-1.18	-3.19	-0.48	-0.87	0.30	-1.41	4.22	1.24
A-st_dec	n/a	n/a	1.8	n/a	n/a	n/a	1.0										
A-f5	<0.1	<2	8	<2	<2	0.25	35.9										
A-c1-0.083	<0.1	<2	9	<2	<2	0.18	75.2										
A-c1-0.25	<0.1	<2	13	<2	<2	0.23	17.1										
A-c1-0.42	<0.1	<2	15	<2	<2	0.19	7.5										
A-c1-1	<0.1	<2	7	<2	<2	0.16	16.9										
A-c1-1.33	<0.1	<2	16	<2	<2	0.13	11.2										
A-c1-2.17	<0.1	<2	11	<2	<2	0.12	4.9										
A-c1-2.5	<0.1	<2	15	<2	<2	0.13	3.9										
A-c1-3.17	<0.1	<2	13	<2	<2	0.12	6.4										
A-c1-3.5	<0.1	<2	14	<2	<2	0.12	6.2	-0.03	-0.56	-0.54	-2.12	-0.58	-0.24	0.38	-1.04	3.66	0.89
A-c1-4.25	<0.1	<2	14	<2	<2	0.09	7.2										
A-c1-4.25	<0.1	<2	14	<2	<2	0.09	7.2										
A-c1-5	<0.1	<2	8	<2	<2	0.11	12.5	0.11	1.84	-0.80	-2.65	-0.83	-1.54	0.42	-1.22	3.59	0.81
A-c1-5.5	<0.1	<2	12	<2	<2	0.10	7.2										
A-c1-6.25	<0.1	<2	<4	<2	<2	0.11	5.3										
A-c1-7	<0.1	<2	8	<2	<2	0.14	11.5	-0.17	-2.75	-0.71	-2.49	-0.73	-1.85	0.44	-1.16	3.63	0.81
A-c1-7.5	<0.1	<2	9	<2	<2	0.13	5.2										
A-c1-10	<0.1	<2	9	<2	<2	0.14	3.6	0.32	5.17	-0.71	-2.52	-0.69	-1.96	0.45	-0.90	4.07	1.02
A-c1-13	<0.1	<2	13	<2	<2	0.15	12.4	-0.16	-2.68	-0.57	-2.21	-0.52	0.05	0.44	-1.77	2.02	0.01
A-c1-15	<0.1	<2	12	<2	<2	0.14	8.8										
A-c1-17	<0.1	<2	11	<2	<2	0.11	13.9										
A-c1-20	<0.1	<2	10	<2	<2	0.13	11.9										
A-c1-22	<0.1	<2	11	<2	<2	0.14	7.4	-0.57	-9.45	-0.65	-2.39	-0.58	-1.05	0.48	-1.79	2.10	0.01
A-c1-24	<0.1	<2	11	<2	<2	0.13	9.2										
A-c2-0.08	<0.1	<2	15	<2	<2	0.19	75.7										
A-c2-0.25	<0.1	<2	16	<2	<2	0.20	6.6										
A-c2-0.42	<0.1	<2	17	<2	<2	0.20	3.0										
A-c2-1	<0.1	<2	16	<2	<2	0.16	4.0										
A-c2-1.33	<0.1	<2	14	<2	<2	0.17	7.2										
A-c2-2.17	<0.1	<2	15	<2	<2	0.14	6.9										
A-c2-2.5	<0.1	<2	7	<2	<2	0.11	3.0										
A-c2-3.17	<0.1	<2	11	<2	<2	0.13	3.0										
A-c2-3.5	<0.1	<2	10	<2	<2	0.10	2.9	-0.10	-1.69	-0.60	-2.12	-0.68	-1.11	0.24	-1.40	3.56	0.97
A-c2-5	<0.1	<2	9	<2	<2	0.11	9.7										
A-c2-5.5	<0.1	<2	8	<2	<2	0.11	6.0										
A-c2-6.25	<0.1	<2	5	<2	<2	0.13	24.1	0.16	2.61	-0.56	-2.07	-0.69	-1.87	0.34	-1.12	3.66	0.93
A-c2-7	<0.1	<2	8	<2	<2	0.17	31.1										
A-c2-7.5	<0.1	<2	9	<2	<2	0.13	7.6										
A-c2-8.5	<0.1	<2	6	<2	<2	0.11	7.9	-0.61	-10.23	-0.54	-2.04	-0.69	-2.42	0.37	-1.73	2.26	0.19
A-c2-10	<0.1	<2	9	<2	<2	0.14	13.2	0.28	4.68	-0.47	-1.92	-0.61	-1.64	0.38	-0.90	3.75	0.93
A-c2-13	<0.1	<2	9	<2	<2	0.15	4.9	-0.43	-7.37	-0.39	-1.77	-0.45	-1.14	0.38	-0.86	3.81	0.95
A-c2-15	<0.1	<2	9	<2	<2	0.11	12.9										
A-c2-17	<0.1	<2	10	<2	<2	0.13	7.3	-0.30	-4.94	-0.26	-1.54	-0.30	-1.50	0.39	-1.60	2.07	0.08
A-c2-20	<0.1	<2	10	<2	<2	0.13	6.7	-0.34	-5.91	-0.69	-2.40	-0.70	-1.34	0.37	-1.05	4.09	1.11
A-c2-24	<0.1	<2	14	<2	<2	0.11	7.0										
A-c3-0.08	<0.1	<2	16	<2	<2	0.16	204.0										
A-c3-0.25	<0.1	<2	15	<2	<2	0.21	14.2										
A-c3-0.42	<0.1	<2	13	<2	<2	0.18	6.7										
A-c3-1	<0.1	<2	16	<2	<2	0.18	5.3										
A-c3-1.33	<0.1	<2	15	<2	<2	0.15	11.1										
A-c3-2.17	<0.1	<2	14	<2	<2	0.16	3.0										
A-c3-2.5	<0.1	<2	11	<2	<2	0.10	2.9										
A-c3-3.17	<0.1	<2	8	<2	<2	0.11	461.0										
A-c3-3.33	<0.1	<2	8	<2	<2	0.12	15.2										
A-c3-4.25	<0.1	<2	12	<2	<2	0.11	7.8										
A-c3-5	<0.1	2	9	<2	<2	0.11	14.5	-0.05	-0.91	-0.51	-1.78	-0.70	-1.05	0.18	-1.60	3.15	0.82
A-c3-5.5	<0.1	<2	10	<2	<2	0.12	3.4										
A-c3-6.25	<0.1	<2	5	<2	<2	0.12	12.0										
A-c3-7	<0.1	<2	9	<2	<2	0.14	10.0	0.26	4.21	-0.27	-1.32	-0.52	-1.11	0.20	-1.70	2.49	0.47
A-c3-7.5	<0.1	<2	7	<2	<2	0.12	4.4	0.24	3.97	-0.39	-1.56	-0.63	-1.21	0.20	-1.52	3.12	0.79
A-c3-8.5	<0.1	<2	8	<2	<2	0.11	2.8	-0.20	-3.63	-0.36	-1.50	-0.60	-1.73	0.19	-2.45	1.18	-0.18
A-c3-10	<0.1	<2	8	<2	<2	0.10	5.5	-0.04	-0.74	-0.48	-1.74	-0.74	-1.28	0.20	-1.65	3.12	0.79
A-c3-13	<0.1	<2	8	<2	<2	0.13	4.3	-0.12	-2.08	-0.24	-1.27	-0.51	-1.13	0.19	-1.67	2.61	0.54
A-c3-15	<0.1	<2	11	<2	<2	0.13	6.3	-0.04	-0.69	-0.23	-1.27	-0.52	-0.76	0.21	-1.45	2.96	0.70
A-c3-17	<0.1	<2	10	<2	<2	0.14	5.8	-0.12	-2.13	-0.25	-1.30	-0.55	-0.77	0.21	-1.53	2.83	0.63
A-c3-20	<0.1	<2	10	<2	<2	0.13	5.4	-0.12	-2.14	-0.27	-1.36	-0.57	-0.82	0.20	-1.79	2.40	0.43
A-c3-22	<0.1	<2	9	<2	<2	0.12	5.7	-0.13	-2.41	-0.35	-1.53	-0.68	-1.17	0.21	-2.18	1.81	0.12
A-c3-24	<0.1	<2	10	<2	<2	0.15	9.6	-0.07	-1.19	-0.26	-1.37	-0.57	-1.10	0.21	-1.65	2.64	0.54
A-c4-0.08	<0.1	<2	10	<2	<2	0.22	138.0										
A-c4-0.25	<0.1	<2	15	<2	<2	0.21	17.9										
A-c4-0.42	<0.1	<2	16	2	<2	0.20	9.0										
A-c4-1	<0.1	<2	16	3	<2	0.22	6.9										
A-c4-1.33	<0.1	<2	17	3	<2	0.19	15.8										
A-c4-2.17	<0.1	<2	17	2	<2	0.18	5.9										
A-c4-2.5	<0.1	<2	13	<2	<2	0.16	6.5										
A-c4-3.17	<0.1	<2	15	<2	<2	0.20	4.6										
A-c4-3.5	<0.1	<2	13	<2	<2	0.16	6.2	0.46	7.68	0.03	-0.35	-0.49	-0.05	-0.03	-3.86	-1.87	-1.50
A-c4-4.25	<0.1	<2	11	<2	<2	0.18	9.7										
A-c4-5	<0.1	<2	9	<2	<2	0.15	9.7										
A-c4-5.5	<0.1	<2	6	<2	<2	0.13	4.0										
A-c4-6.25	<0.1	<2	6	<2	<2	0.17	5.6										
A-c4-7	<0.1	<2	9	<2	<2	0.15	6.9	0.39	5.91	-0.02	-0.48	-0.62	-0.44	-0.07	-2.69	0.24	-0.40
A-c4-7.5	<0.1	<2	9	<2	<2	0.16	5.3										
A-c4-8.5	<0.1	<2	8	<2	<2	0.13	3.0	-0.14	-2.43	-0.22	-0.89	-0.81	-0.75	-0.07	-2.75	0.41	-0.32
A-c4-10	<0.1	<2	8	<2	<2	0.16	4.5	-0.11	-1.83	0.00	-0.44	-0.57	-0.45	-0.08	-3.10	-0.66	-0.84
A-c4-13	<0.1	<2	11	<2	<2	0.17	8.4	-0.06	-0.96	-0.02	-0.50	-0.60	-0.30	-0.10	-2.87	-0.06	-0.52
A-c4-15	<0.1	<2	10	<2	<2	0.15	6.6	0.14	2.36	-0.14	-0.75	-0.73	-0.61	-0.10	-3.09	-0.34	-0.66
A-c4-17	<0.1	<2	11	<2	<2	0.14	9.5										
A-c4-20	<0.1	<2	12	<2	<2	0.16	5.0	0.00	0.09	-0.07	-0.62	-0.66	-0.42	-0.14	-3.15	-0.40	-0.65
A-c4-22	<0.1	<2	9	2	<2	0.14	6.6	0.11	2.00	-0.18	-0.85	-0.78	-0.82	-0.13	-3.10	-0.12	-0.52
A-c4-24	<0.1	<2	7	<2	<2	0.13	8.2	-0.02	-0.43	-0.09	-0.66	-0.68	-0.77	-0.14	-3.74	-0.29	-0.59
B-Inf-1.5	<0.1	<2	9	<2	<2	0.23	20.2	0.03	0.65	-1.28	-3.35	-0.73	0.39	0.31	-1.81	3.49	0.87
B-Inf-30	<0.1	<2	10	<2	<2	0.20	20.9	0.24	5.64	-1.39	-3.53	-0.89	-0.68	0.33	-1.11	4.48	1.34
B-Inf-35	<0.1	<2	9	<2	<2	0.17	21.0	0.20	4.65	-1.19	-3.13	-0.69	-0.42	0.33	-1.24	4.10	1.15
B-Inf_av-0@60	<0.1	<2	9	<2	<2	0.23	20.2	0.12	2.78	-1.28	-3.35	-0.73	0.39	0.31	-1.55	3.49	0.87
B-Inf_av-0@60	<0.1	<2	9	<2	<2	0.23	20.2	0.12	2.78	-1.28	-3.35	-0.73	0.39	0.31	-1.55	3.49	0.87

ID	Ti	Tl	U	V	W	Yb	Zn	Charge balance	Electrical balance	$SI_{Calcite}$	$SI_{Dolomite}$	$SI_{Rhodochrosite}$	$SI_{Siderite}$	SI_{Quartz}	$SI_{K\text{-}feldspar}$	$SI_{Kaolinite}$	$SI_{Gibbsite}$
	µg/l	µg/l	µg/l	µg/l	µg/l	µg/l	µg/l	meq	%								
B-Inf_av-7.2@60	<0.1	<2	10	<2	<2	0.20	20.9	0.24	5.63	-1.39	-3.53	-0.89	-0.68	0.33	-1.11	4.48	1.34
B-Inf_av-7.2@60	<0.1	<2	10	<2	<2	0.20	20.9	0.24	5.63	-1.39	-3.53	-0.89	-0.68	0.33	-1.11	4.48	1.34
B_st_dev	n/a	n/a	0.46	n/a	n/a	0.02	0.40	0.08	1.97	0.08	0.15	0.09	0.55	0.01	0.29	0.49	0.23
B-c1-0.08	<0.1	2	11	<2	<2	0.11	134.0	-1.06	-14.32	-1.44	-3.77	-1.24	-0.69	0.12	-2.30	2.35	0.49
B-c1-0.17	<0.1	3	12	<2	<2	0.12	98.1										
B-c1-0.25	<0.1	<2	11	<2	<2	0.12	90.2										
B-c1-0.33	<0.1	<2	10	<2	<2	0.12	90.2										
B-c1-0.42	<0.1	<2	12	<2	<2	0.10	86.6										
B-c1-0.5	<0.1	<2	13	<2	<2	0.14	82.8										
B-c1-1.08	<0.1	<2	7	<2	<2	0.13	49.8										
B-c1-1.17	<0.1	<2	8	<2	<2	0.14	59.6	-0.43	-8.50	-1.46	-3.81	-1.26	-0.41	0.19	-0.90	5.00	1.75
B-c1-1.25	<0.1	<2	7	<2	<2	0.12	86.7										
B-c1-1.33	<0.1	<2	7	<2	<2	0.11	66.4	-0.26	-5.46	-1.37	-3.62	-1.16	-0.32	0.22	-1.14	4.23	1.34
B-c1-1.42	<0.1	<2	9	<2	<2	0.15	59.5										
B-c1-1.5	<0.1	<2	7	<2	<2	0.18	58.9	-0.15	-3.34	-1.40	-3.70	-1.20	-0.34	0.27	-0.43	5.43	1.88
B-c1-2.17	<0.1	<2	8	<2	<2	0.14	55.3	-0.09	-2.01	-1.87	-4.64	-1.66	-0.79	0.39	-1.07	4.73	1.42
B-c1-2.33	<0.1	<2	7	<2	<2	0.12	60.1	-0.15	-3.29	-1.45	-3.79	-1.23	-0.30	0.40	-0.78	4.43	1.25
B-c1-2.5	<0.1	<2	8	<2	<2	0.14	95.6	0.02	0.44	-1.40	-3.70	-1.19	-0.25	0.41	-1.15	3.48	0.77
B-c1-3.17	<0.1	<2	9	<2	<2	0.11	84.3	0.09	1.99	-1.73	-4.36	-1.51	-0.57	0.45	-1.05	4.06	1.02
B-c1-3.33	<0.1	<2	8	<2	<2	0.11	73.1	-0.19	-4.21	-1.65	-4.20	-1.43	-0.48	0.46	-0.95	4.28	1.12
B-c1-3.5	<0.1	<2	7	<2	<2	0.13	74.8	-0.22	-4.95	-1.66	-4.22	-1.45	-0.48	0.45	-0.99	4.20	1.09
B-c1-4.17	<0.1	<2	10	<2	<2	0.14	277.0	0.01	0.20	-1.64	-4.17	-1.41	-0.42	0.50	-0.87	4.23	1.06
B-c1-4.33	<0.1	<2	9	<2	<2	0.13	107.0										
B-c1-4.5	<0.1	<2	9	<2	<2	0.11	77.5	-0.12	-2.63	-1.55	-3.99	-1.33	-0.33	0.49	-0.67	4.47	1.18
B-c1-5.25	<0.1	<2	9	<2	<2	0.12	81.5	-0.14	-2.97	-1.36	-3.61	-1.12	-0.11	0.49	-0.64	4.14	1.02
B-c1-5.5	<0.1	<2	8	<2	<2	0.09	82.0	0.14	3.27	-1.71	-4.31	-1.47	-0.46	0.51	-0.95	4.05	0.95
B-c1-6.25	<0.1	<2	10	<2	<2	0.13	79.9	-0.06	-1.21	-1.44	-3.79	-1.21	-0.18	0.51	-0.79	3.96	0.91
B-c1-6.5	<0.1	<2	9	<2	<2	0.11	75.4	-0.14	-2.93	-1.63	-4.15	-1.39	-0.37	0.51	-0.54	4.83	1.34
B-c1-7.25	<0.1	<2	8	<2	<2	0.10	73.6	0.08	1.97	-1.66	-4.21	-1.42	-0.36	0.50	-0.86	4.12	1.00
B-c1-7.5	<0.1	<2	9	<2	<2	0.13	78.9	0.14	3.16	-1.92	-4.75	-1.70	-0.68	0.51	-1.60	3.15	0.51
B-c1-8.25	<0.1	<2	9	<2	<2	0.12	79.7	-0.08	-1.81	-1.46	-3.83	-1.23	-0.19	0.51	-0.39	4.80	1.32
B-c1-8.5	<0.1	<2	9	<2	<2	0.10	75.0	-0.03	-0.64	-1.48	-3.87	-1.25	-0.23	0.52	-1.13	3.22	0.53
B-c1-9.5	<0.1	<2	8	<2	<2	0.10	71.5	-0.15	-3.52	-1.80	-4.50	-1.58	-0.52	0.50	-1.43	3.44	0.66
B-c1-10	<0.1	<2	8	<2	<2	0.12	60.7										
B-c1-11	<0.1	<2	10	<2	<2	0.12	47.8	-0.20	-4.80	-1.82	-4.55	-1.61	-1.32	0.50	-0.57	5.20	1.54
B-c1-12	<0.1	<2	8	<2	<2	0.05	39.7	-0.29	-6.87	-1.94	-4.77	-1.72	-2.03	0.49	-1.01	4.56	1.23
B-c1-13	<0.1	<2	9	<2	<2	0.09	59.9	-0.20	-4.91	-2.15	-5.20	-1.92	-1.33	0.49	-1.91	3.20	0.55
B-c1-14	<0.1	<2	8	<2	<2	0.13	60.5	-0.30	-7.16	-1.65	-4.18	-1.41	-0.80	0.49	-0.48	5.13	1.51
B-c1-15	<0.1	<2	8	<2	<2	0.09	68.5	-0.23	-5.35	-1.73	-4.35	-1.49	-0.54	0.49	-1.29	3.74	0.82
B-c1-16	<0.1	<2	8	<2	<2	0.09	61.4	-0.24	-5.57	-1.42	-3.74	-1.19	-0.41	0.49	-1.07	3.59	0.74
B-c1-19	<0.1	<2	9	<2	<2	0.05	56.2	-0.39	-8.95	-1.51	-3.91	-1.28	-0.79	0.49	-1.27	3.51	0.71
B-c1-20	<0.1	<2	8	<2	<2	0.07	54.3	-0.27	-6.46	-1.43	-3.75	-1.21	-0.48	0.49	-1.44	3.11	0.50
B-c1-21	<0.1	<2	7	<2	<2	0.08	60.7	-0.12	-2.89	-1.48	-3.84	-1.25	-0.43	0.49	-1.62	2.62	0.26
B-c1-22	<0.1	<2	9	<2	<2	0.09	56.2	-0.33	-7.65	-1.51	-3.89	-1.28	-0.58	0.49	-1.46	3.27	0.58
B-c1-23	<0.1	<2	8	<2	<2	0.09	134.0	-0.24	-5.60	-1.42	-3.72	-1.20	-0.54	0.49	-0.95	3.78	0.83
B-c1-26	<0.1	<2	8	<2	<2	0.07	53.8	-0.45	-10.34	-1.39	-3.67	-1.18	-0.90	0.49	-1.15	3.66	0.77
B-c2-0.08	<0.1	2	11	<2	<2	0.09	56.7	-0.07	-1.14	-1.78	-4.39	-1.59	-1.96	0.16	-2.04	2.51	0.53
B-c2-0.17	<0.1	<2	12	<2	<2	0.10	38.9										
B-c2-0.25	<0.1	<2	13	<2	<2	0.12	35.4										
B-c2-0.33	<0.1	3	9	<2	<2	0.11	35.2										
B-c2-0.42	<0.1	<2	12	<2	<2	0.10	44.5										
B-c2-0.5	<0.1	<2	11	<2	<2	0.13	46.6										
B-c2-1.08	<0.1	<2	8	<2	<2	0.11	29.8										
B-c2-1.17	<0.1	2	9	<2	<2	0.08	35.5	-0.11	-2.17	-1.50	-3.78	-1.35	-1.01	0.14	-1.33	3.98	1.28
B-c2-1.25	<0.1	<2	8	<2	<2	0.09	61.7										
B-c2-1.33	<0.1	<2	7	<2	<2	0.09	37.6	-0.05	-1.07	-1.73	-4.24	-1.54	-1.08	0.15	-1.42	4.19	1.38
B-c2-1.42	<0.1	<2	8	<2	<2	0.09	35.8										
B-c2-1.5	<0.1	<2	8	<2	<2	0.09	33.7	0.12	2.78	-1.75	-4.29	-1.57	-1.06	0.19	-1.13	4.67	1.58
B-c2-2.17	<0.1	<2	10	<2	<2	0.08	31.8	0.10	2.44	-2.03	-4.86	-1.85	-1.65	0.26	-1.69	3.86	1.10
B-c2-2.33	<0.1	<2	7	<2	<2	0.10	38.6	0.02	0.47	-1.62	-4.03	-1.44	-1.30	0.29	-0.93	4.46	1.38
B-c2-2.5	<0.1	<2	8	<2	<2	0.10	59.2	-0.01	-0.34	-1.58	-3.96	-1.40	-1.28	0.30	-1.02	4.22	1.24
B-c2-3.17	<0.1	<2	9	<2	<2	0.09	53.7	0.06	1.53	-1.82	-4.45	-1.64	-1.60	0.34	-1.22	4.10	1.15
B-c2-3.33	<0.1	2	8	<2	<2	0.09	38.2	-0.02	-0.58	-1.81	-4.42	-1.62	-1.68	0.34	-1.25	4.05	1.12
B-c2-3.5	<0.1	<2	10	<2	<2	0.08	49.3	0.12	2.69	-1.71	-4.18	-1.56	-1.39	0.33	-0.96	4.31	1.26
B-c2-4.17	<0.1	<2	10	<2	<2	0.07	45.8	0.00	-0.02	-1.78	-4.37	-1.60	-1.29	0.37	-0.85	4.66	1.39
B-c2-4.33	<0.1	<2	10	<2	<2	0.08	46.4										
B-c2-4.5	<0.1	<2	12	<2	<2	0.05	46.8	0.02	0.52	-1.57	-3.93	-1.38	-1.32	0.38	-0.40	5.14	1.63
B-c2-5.25	<0.1	<2	9	<2	<2	0.10	47.6	0.16	4.05	-1.60	-4.00	-1.40	-0.92	0.39	0.02	5.90	1.99
B-c2-5.5	<0.1	<2	10	<2	<2	0.07	47.0	0.18	4.39	-1.71	-4.21	-1.51	-1.20	0.39	-0.59	4.90	1.49
B-c2-6.25	<0.1	<2	10	<2	<2	0.09	41.6	0.00	0.05	-1.72	-4.24	-1.52	-1.13	0.39	-0.76	4.77	1.43
B-c2-6.5	<0.1	<2	9	<2	<2	0.08	45.4	0.16	3.92	-1.71	-4.20	-1.49	-1.16	0.39	-0.74	4.62	1.35
B-c2-7.25	<0.1	<2	9	<2	<2	0.07	42.2	0.09	2.11	-1.60	-3.98	-1.38	-0.84	0.39	-0.87	4.25	1.17
B-c2-7.5	<0.1	<2	11	<2	<2	0.11	42.2	0.25	6.10	-2.10	-4.99	-1.89	-1.47	0.40	-1.55	3.84	0.95
B-c2-8.25	<0.1	<2	8	<2	<2	0.11	44.5	0.17	4.06	-1.48	-3.76	-1.28	-0.72	0.40	-1.19	3.45	0.76
B-c2-8.5	<0.1	<2	9	<2	<2	0.07	45.7	0.23	5.71	-1.49	-3.78	-1.29	-0.82	0.41	-0.71	4.33	1.19
B-c2-9.5	<0.1	<2	11	<2	<2	0.07	39.5	0.10	2.42	-1.72	-4.23	-1.53	-1.12	0.40	-0.95	4.44	1.26
B-c2-10	<0.1	<2	9	<2	<2	0.06	45.5										
B-c2-11	<0.1	<2	9	<2	<2	0.11	39.6	0.07	1.70	-1.82	-4.44	-1.65	-2.24	0.39	-0.65	5.35	1.71
B-c2-12	<0.1	<2	8	<2	<2	0.07	33.3	-0.01	-0.25	-1.84	-4.45	-1.65	-2.12	0.39	-0.64	5.42	1.76
B-c2-13	<0.1	<2	9	<2	<2	0.10	54.4	0.02	0.50	-1.83	-4.43	-1.64	-1.22	0.39	-0.52	5.67	1.88
B-c2-14	<0.1	<2	7	<2	<2	0.11	43.0	-0.04	-0.93	-1.52	-3.81	-1.33	-0.82	0.39	-0.64	4.99	1.54
B-c2-15	<0.1	<2	7	<2	<2	0.07	43.4	0.02	0.51	-1.63	-4.02	-1.46	-2.10	0.39	-0.89	4.74	1.41
B-c2-16	<0.1	<2	7	<2	<2	0.08	38.8	0.02	0.54	-1.42	-3.61	-1.26	-1.72	0.39	-0.84	4.50	1.29
B-c2-19	<0.1	<2	7	<2	<2	0.07	36.0	-0.10	-2.46	-1.51	-3.80	-1.37	-1.64	0.39	-1.41	3.79	0.94
B-c2-20	<0.1	<2	9	<2	<2	0.06	35.3	-0.06	-1.57	-1.39	-3.56	-1.26	-1.72	0.40	-0.68	4.99	1.53
B-c2-21	<0.1	<2	7	<2	<2	0.09	37.7	-0.02	-0.53	-1.41	-3.59	-1.26	-1.78	0.39	-0.80	4.81	1.45
B-c2-22	<0.1	<2	9	<2	<2	0.08	34.9	-0.05	-1.28	-1.30	-3.39	-1.16	-1.83	0.39	-0.80	4.59	1.34
B-c2-23	<0.1	<2	8	<2	<2	0.07	63.7	-0.02	-0.61	-1.39	-3.58	-1.26	-2.02	0.39	-0.86	4.57	1.33
B-c2-26	<0.1	<2	7	<2	<2	0.08	37.8	-0.03	-0.80	-1.27	-3.35	-1.12	-1.54	0.40	-0.96	4.24	1.16
B-c3-0.08	<0.1	<2	6	<2	<2	0.09	111.0	-0.42	-7.38	-1.55	-3.70	-1.41	-0.37	0.03	-2.04	3.12	0.96
B-c3-0.17	<0.1	2	8	<2	<2	0.10	85.5										
B-c3-0.25	<0.1	<2	8	<2	<2	0.09	63.3										
B-c3-0.33	<0.1	<2	5	<2	<2	0.10	63.6										
B-c3-0.42	<0.1	<2	6	<2	<2	0.08	53.7										
B-c3-0.5	<0.1	<2	5	<2	<2	0.09	73.7										
B-c3-1.08	<0.1	<2	6	<2	<2	0.16	66.3										
B-c3-1.17	<0.1	<2	7	2	<2	0.18	66.8	-0.06	-1.48	-1.53	-3.63	-1.40	-0.33	0.06	-0.30	6.31	2.52
B-c3-1.25	<0.1	<2	6	2	<2	0.17	97.2										
B-c3-1.33	<0.1	<2	5	2	<2	0.17	76.0	0.05	1.21	-1.62	-3.83	-1.48	-0.27	0.07	-0.50	6.12	2.42
B-c3-1.42	<0.1	<2	6	<2	<2	0.13	73.0										
B-c3-1.5	<0.1	2	5	<2	<2	0.12	76.8	0.06	1.44	-1.63	-3.86	-1.48	-0.24	0.07	-0.93	5.23	1.97

ID	Ti	Tl	U	V	W	Yb	Zn	Charge balance	Electrical balance	$SI_{Calcite}$	$SI_{Dolomite}$	$SI_{Rhodochrosite}$	$SI_{Siderite}$	SI_{Quartz}	$SI_{K\text{-}feldspar}$	$SI_{Kaolinite}$	$SI_{Gibbsite}$
	µg/l	µg/l	µg/l	µg/l	µg/l	µg/l	µg/l	meq	%								
B-c3-2.17	<0.1	<2	6	<2	<2	0.15	80.8	0.10	2.39	-1.78	-4.16	-1.63	-0.38	0.10	-1.57	4.20	1.42
B-c3-2.33	<0.1	<2	8	<2	<2	0.13	107.0	0.11	2.77	-1.43	-3.48	-1.31	-0.07	0.13	-0.90	4.80	1.70
B-c3-2.5	<0.1	<2	6	<2	<2	0.12	104.0	-0.25	-5.81	-1.25	-3.10	-1.11	0.16	0.12	-1.02	4.41	1.51
B-c3-3.17	<0.1	<2	9	<2	<2	0.12	94.3	0.01	0.21	-1.55	-3.70	-1.42	-0.15	0.15	-0.98	4.76	1.65
B-c3-3.33	<0.1	<2	6	<2	<2	0.14	79.0	-0.03	-0.69	-1.55	-3.70	-1.41	-0.14	0.15	-0.80	5.12	1.83
B-c3-3.5	<0.1	<2	8	<2	<2	0.16	78.6	0.05	1.16	-1.54	-3.67	-1.42	-0.15	0.17	-0.62	5.38	1.95
B-c3-4.17	<0.1	<2	8	<2	<2	0.11	80.6	0.11	2.65	-1.52	-3.62	-1.38	-0.12	0.20	-0.75	4.99	1.72
B-c3-4.33	<0.1	<2	8	<2	<2	0.14	73.5										
B-c3-4.5	<0.1	<2	8	<2	<2	0.11	75.9	0.19	4.47	-1.40	-3.39	-1.27	-0.01	0.21	-0.76	4.73	1.58
B-c3-5.25	<0.1	<2	8	<2	<2	0.11	72.7	0.14	3.32	-1.32	-3.22	-1.17	0.09	0.21	-0.75	4.60	1.52
B-c3-5.5	<0.1	<2	8	<2	<2	0.11	74.0	0.19	4.53	-1.41	-3.40	-1.26	-0.01	0.22	-1.27	3.69	1.05
B-c3-6.25	<0.1	<2	9	<2	<2	0.10	65.2	0.18	4.20	-1.49	-3.58	-1.36	-0.09	0.22	-1.19	4.12	1.27
B-c3-6.5	<0.1	<2	9	<2	<2	0.12	65.1	0.14	3.41	-1.42	-3.43	-1.28	-0.04	0.22	-0.90	4.52	1.47
B-c3-7.25	<0.1	<2	8	<2	<2	0.11	62.2	0.14	3.38	-1.32	-3.22	-1.18	0.07	0.22	-0.79	4.60	1.51
B-c3-7.5	<0.1	<2	11	<2	<2	0.12	64.2	0.28	6.63	-1.81	-4.22	-1.68	-0.40	0.23	-1.52	4.06	1.22
B-c3-8.25	<0.1	<2	8	<2	<2	0.09	57.5	0.21	4.93	-1.31	-3.20	-1.17	0.06	0.23	-1.05	4.12	1.26
B-c3-8.5	<0.1	<2	8	<2	<2	0.13	59.6	0.26	6.17	-1.31	-3.21	-1.18	0.07	0.24	-0.77	4.61	1.50
B-c3-9.5	<0.1	<2	9	<2	<2	0.16	55.8	0.11	2.73	-1.56	-3.71	-1.43	-0.17	0.23	-0.65	5.47	1.93
B-c3-10	<0.1	<2	9	<2	<2	0.09	54.1										
B-c3-11	<0.1	<2	10	<2	<2	0.08	42.5	0.09	2.42	-1.57	-3.73	-1.45	-0.63	0.21	-1.86	3.21	0.82
B-c3-12	<0.1	<2	7	<2	<2	0.08	46.2	0.04	1.00	-1.57	-3.72	-1.43	-0.48	0.21	-1.80	3.36	0.90
B-c3-13	<0.1	<2	8	<2	<2	0.11	52.6	0.07	1.69	-1.57	-3.73	-1.44	-0.41	0.21	-1.52	3.89	1.16
B-c3-14	<0.1	<2	7	<2	<2	0.05	43.0	0.05	1.17	-1.37	-3.33	-1.24	-0.27	0.21	-1.61	3.44	0.93
B-c3-15	<0.1	<2	10	<2	<2	0.08	41.2	0.00	0.08	-1.56	-3.70	-1.44	-0.54	0.21	-1.79	3.62	1.03
B-c3-16	<0.1	<2	8	<2	<2	0.09	40.3	-0.02	-0.43	-1.35	-3.28	-1.23	-0.11	0.22	-1.26	4.30	1.36
B-c3-19	<0.1	<2	8	<2	<2	0.08	58.2	-0.12	-3.11	-1.36	-3.31	-1.25	-0.56	0.21	-1.26	4.50	1.47
B-c3-20	<0.1	<2	7	<2	<2	0.11	35.0	-0.06	-1.57	-1.35	-3.28	-1.24	-0.36	0.22	-1.26	4.49	1.45
B-c3-21	<0.1	<2	8	<2	<2	0.12	37.3	-0.03	-0.68	-1.24	-3.07	-1.13	-0.12	0.21	-1.18	4.42	1.43
B-c3-22	<0.1	<2	8	<2	<2	0.10	37.3	-0.05	-1.25	-1.34	-3.27	-1.23	-0.18	0.21	-1.20	4.70	1.57
B-c3-23	<0.1	<2	8	<2	<2	0.10	56.4	-0.02	-0.49	-1.24	-3.08	-1.14	-0.21	0.21	-1.70	3.35	0.89
B-c3-26	<0.1	<2	8	<2	<2	0.06	37.7	-0.05	-1.24	-1.35	-3.31	-1.24	-0.66	0.22	-1.19	4.60	1.51
B-c4-0.08	<0.1	<2	13	2	<2	0.13	34.0	-0.50	-2.13	-2.03	-4.35	-2.20	-1.77	-0.08	-1.24	1.99	0.48
B-c4-0.17	<0.1	<2	14	<2	<2	0.13	35.5										
B-c4-0.25	<0.1	<2	12	<2	<2	0.13	31.8										
B-c4-0.42	<0.1	3	13	<2	<2	0.13	33.9										
B-c4-1.08	<0.1	<2	5	<2	<2	0.14	24.1										
B-c4-1.17	<0.1	<2	5	<2	<2	0.11	24.8	-0.19	-4.46	-1.72	-3.62	-1.76	-0.39	0.02	-1.62	3.34	1.06
B-c4-1.25	<0.1	2	5	<2	<2	0.12	31.2										
B-c4-1.33	<0.1	<2	6	<2	<2	0.09	27.7	-0.18	-4.51	-1.84	-3.86	-1.88	-0.75	0.01	-1.72	3.41	1.10
B-c4-1.5	<0.1	<2	5	<2	<2	0.15	33.6	-0.09	-2.36	-1.77	-3.72	-1.76	-0.46	0.01	-1.51	3.61	1.20
B-c4-2.17	<0.1	<2	<4	<2	<2	0.16	30.2	0.05	1.53	-2.12	-4.43	-2.10	-0.65	-0.03	-1.59	4.41	1.64
B-c4-2.33	<0.1	<2	<4	<2	<2	0.16	59.6	0.08	2.37	-1.70	-3.59	-1.68	-0.19	-0.04	-1.76	3.25	1.07
B-c4-2.5	<0.1	<2	6	2	<2	0.12	67.3	0.06	1.71	-1.64	-3.48	-1.64	-0.11	-0.05	-1.81	3.17	1.05
B-c4-3.17	<0.1	<2	4	<2	<2	0.15	51.3	0.07	2.04	-1.61	-3.42	-1.60	0.02	-0.08	-1.88	3.01	0.99
B-c4-3.33	<0.1	2	<4	<2	<2	0.12	33.1	0.02	0.57	-1.91	-4.00	-1.89	-0.25	-0.09	-1.94	3.52	1.25
B-c4-3.5	<0.1	2	5	<2	<2	0.11	36.9	0.09	2.57	-1.89	-3.95	-1.90	-0.29	-0.09	-2.06	3.27	1.14
B-c4-4.17	<0.1	<2	5	<2	<2	0.08	30.4	0.15	4.29	-1.99	-4.17	-1.98	-0.28	-0.09	-2.17	3.23	1.11
B-c4-4.33	<0.1	<2	6	2	<2	0.10	30.3										
B-c4-4.5	<0.1	<2	5	<2	<2	0.10	29.7	0.10	2.84	-1.79	-3.76	-1.78	-0.07	-0.10	-2.17	2.92	0.97
B-c4-5.25	<0.1	<2	5	<2	<2	0.10	25.9	0.20	5.81	-1.82	-3.84	-1.80	-0.08	-0.11	-2.40	2.46	0.75
B-c4-5.5	<0.1	<2	5	<2	<2	0.12	25.8	0.22	6.35	-1.93	-4.05	-1.90	-0.17	-0.11	-2.78	1.89	0.46
B-c4-6.25	<0.1	<2	5	<2	<2	0.10	21.2	0.19	5.68	-2.15	-4.50	-2.15	-0.37	-0.12	-2.39	3.13	1.10
B-c4-6.5	<0.1	<2	4	<2	<2	0.08	21.3	0.14	4.31	-1.97	-4.12	-1.94	-0.17	-0.13	-2.77	2.07	0.57
B-c4-7.25	<0.1	<2	4	2	<2	0.11	22.2	0.13	3.85	-2.07	-4.33	-2.04	-0.27	-0.15	-2.42	3.09	1.10
B-c4-7.5	<0.1	<2	6	<2	<2	0.09	22.3	0.21	6.30	-2.28	-4.76	-2.27	-0.49	-0.14	-3.00	2.37	0.74
B-c4-8.25	<0.1	<2	5	<2	<2	0.11	23.0	0.07	1.90	-1.82	-3.82	-1.80	-0.04	-0.15	-3.05	1.45	0.28
B-c4-8.5	<0.1	<2	<4	2	<2	0.08	25.9	0.17	5.00	-1.85	-3.88	-1.83	-0.08	-0.14	-2.02	3.52	1.31
B-c4-9.5	<0.1	<2	5	<2	<2	0.09	25.8	0.05	1.41	-2.16	-4.51	-2.14	-0.42	-0.17	-2.80	2.70	0.93
B-c4-10	<0.1	<2	6	<2	<2	0.06	52.4										
B-c4-11	<0.1	<2	6	<2	<2	0.09	43.1	0.05	1.39	-2.03	-4.24	-2.02	-0.61	-0.17	-3.06	2.26	0.71
B-c4-12	<0.1	<2	5	<2	<2	0.09	42.6	-0.01	-0.29	-1.71	-3.58	-1.71	-0.32	-0.18	-3.20	1.49	0.33
B-c4-13	<0.1	<2	5	<2	<2	0.08	31.8	0.02	0.61	-1.89	-3.95	-1.91	-0.44	-0.18	-2.99	2.28	0.73
B-c4-14	<0.1	<2	5	<2	<2	0.09	29.1	-0.01	-0.26	-1.61	-3.38	-1.64	-0.12	-0.16	-2.52	2.97	1.05
B-c4-15	<0.1	<2	7	<2	<2	0.08	24.0	0.02	0.47	-1.69	-3.53	-1.76	-0.23	-0.17	-3.63	0.75	-0.05
B-c4-16	<0.1	<2	7	<2	<2	0.08	20.8	0.00	0.03	-1.32	-2.79	-1.41	0.10	-0.17	-3.71	0.01	-0.41
B-c4-19	<0.1	<2	8	<2	<2	0.06	19.4	-0.01	-0.17	-1.03	-2.21	-1.19	0.21	-0.16	-3.70	-0.37	-0.61
B-c4-20	<0.1	<2	7	<2	<2	0.08	25.8	0.02	0.43	-1.11	-2.37	-1.31	0.09	-0.15	-3.55	0.10	-0.39
B-c4-21	<0.1	<2	7	<2	<2	0.07	24.8	0.00	-0.08	-0.92	-1.98	-1.13	0.21	-0.17	-3.77	-0.74	-0.79
B-c4-22	<0.1	<2	9	<2	<2	0.09	22.0	-0.03	-0.76	-1.00	-2.14	-1.22	0.05	-0.16	-3.63	-0.24	-0.55
B-c4-23	<0.1	<2	7	<2	<2	0.08	65.6	-0.01	-0.29	-0.99	-2.13	-1.24	0.07	-0.17	-3.67	-0.38	-0.61
B-c4-26	<0.1	<2	8	<2	<2	0.09	24.7	0.02	0.49	-0.99	-2.13	-1.28	-0.05	-0.17	-3.29	0.47	-0.19
C-Inf_-17	<0.1	<2	7	<2	<2	0.15	4.4	-0.13	-3.12	-0.16	-1.29	-0.79	0.14	0.28	-1.18	3.39	0.85
C-Inf_-7	<0.1	<2	8	<2	<2	0.09	4.1	-0.31	-7.49	-0.62	-2.23	-1.25	-0.40	0.27	-1.27	4.09	1.21
C0_t=1	0.6	<2	13	<2	<2	0.12	6.0	-0.40	-9.27	-0.70	-2.39	-1.27	-0.26	0.23	-1.52	3.88	1.15
C0_t=3	0.5	<2	13	<2	<2	0.08	4.7	-0.13	-3.13	-1.01	-3.02	-1.61	-0.88	0.23	-2.02	3.40	0.91
C0_t=4	0.4	2	13	<2	3	0.10	outlier	-0.40	-9.15	-0.89	-2.76	-1.47	-0.67	0.23	-1.37	4.57	1.48
C0_t=8	0.3	<2	11	<2	<2	0.11	12.2	-0.17	-4.30	-0.78	-2.55	-1.39	-1.12	0.23	-1.45	3.89	1.15
C0_t=10	0.3	<2	11	<2	<2	0.07	13.8	-0.65	-14.73	-0.78	-2.54	-1.40	-0.36	0.23	-1000.00	3.94	1.17
C0_t=11	0.2	<2	13	<2	<2	0.07	17.8										
C0_t=15	0.6	<2	13	<2	4	0.07	10.8	-0.60	-13.51	-0.48	-1.94	-1.04	0.02	0.24	-1000.00	4.03	1.20
C0_t=17	<0.1	<2	8	<2	<2	0.09	5.7	-0.56	-12.74	-0.67	-2.35	-1.30	-1.29	0.21	-1.58	3.85	1.15
C0_t=18	0.2	<2	7	<2	<2	0.10	11.6										
C0_t=22	0.3	<2	10	<2	<2	0.09	6.6	-0.23	-5.67	-0.96	-2.92	-1.52	-0.84	0.20	-2.82	2.03	0.25
C0_t=24	1.1	<2	10	<2	<2	0.08	6.6	-0.20	-4.92	-1.03	-3.05	-1.61	-1.21	0.20	-2.16	3.34	0.91
C_C0_av	0.5	<2	11	<2	<2	0.09	9.6	-0.38	-8.92	-0.81	-2.61	-1.38	-0.65	0.22	-1.60	3.97	1.20
C_st_dev	0.29	n/a	2.06	n/a	0.66	0.02	4.31	0.20	4.33	0.18	0.36	0.18	0.45	0.02	440.14	0.71	0.34
C1_t=1.2	0.5	3	16	<2	<2	0.11	20.3	-0.31	-5.90	-0.55	-2.16	-1.31	-0.43	0.27	-1.29	3.69	1.01
C1_t=1.4	0.4	<2	14	<2	<2	0.13	32.1	-0.10	-2.07	-0.60	-2.27	-1.35	-0.42	0.26	-1.02	4.36	1.35
C1_t=1.6	0.6	<2	17	<2	<2	0.11	20.9	-0.28	-5.49	-0.34	-1.76	-1.11	-0.14	0.26	-1.08	3.83	1.09
C1_t=2.2	1.3	<2	14	<2	<2	0.14	15.0	-0.06	-1.19	-0.58	-2.23	-1.28	-1.04	0.29	-0.99	4.32	1.31
C1_t=2.4	0.6	2	13	<2	<2	0.14	0.6	-0.11	-2.20	-0.59	-2.24	-1.35	-0.95	0.27	-1.62	3.16	0.75
C1_t=3.1	0.5	<2	15	<2	<2	0.16	0.5	-0.11	-2.29	-0.67	-2.41	-1.37	-0.98	0.29	-1.78	2.93	0.61
C1_t=3.3	0.5	<2	18	<2	<2	0.12	2.9	0.03	0.64	-0.55	-2.17	-1.28	-0.48	0.30	-1.25	3.74	1.01
C1_t=4.1	0.5	<2	16	<2	<2	0.14	17.1	-0.29	-5.81	-0.75	-2.58	-1.51	-0.58	0.29	-1.49	3.78	1.04
C1_t=4.3	0.6	<2	18	<2	<2	0.14	2.7	0.12	2.44	-0.68	-2.44	-1.40	-0.47	0.30	-1.43	3.55	0.91
C1_t=5.1	0.7	<2	18	<2	<2	0.12	1.1	-0.35	-6.87	-0.55	-2.17	-1.31	-0.34	0.29	-1.26	3.85	1.07
C1_t=6.1	0.5	<2	17	<2	<2	0.11	<0.3	0.09	1.77	-0.49	-2.07	-1.20	-0.25	0.30	-1.28	3.55	0.91
C1_t=6.3	0.6	<2	14	<2	<2	0.09	1.7	-0.03	-0.73	-0.50	-2.07	-1.19	-0.27	0.29	-1.17	3.81	1.05
C1_t=7.1	0.6	<2	15	<2	<2	0.11	<0.3	-0.07	-1.52	-0.40	-1.88	-1.09	-0.19	0.30	-1.14	3.66	0.97
C1_t=8.1	0.9	<2	16	<2	<2	0.09	5.7	-0.03	-0.54	-0.41	-1.89	-1.10	-0.19	0.30	-0.89	4.12	1.20
C1_t=9.1	1.3	<2	14	<2	<2	0.14	0.6	-0.02	-0.32	-0.40	-1.89	-1.10	0.04	0.31	-0.81	4.26	1.26

ID	Ti	Tl	U	V	W	Yb	Zn	Charge balance	Electrical balance	$SI_{Calcite}$	$SI_{Dolomite}$	$SI_{Rhodochrosite}$	$SI_{Siderite}$	SI_{Quartz}	$SI_{K\text{-}feldspar}$	$SI_{Kaolinite}$	$SI_{Gibbsite}$
	µg/l	µg/l	µg/l	µg/l	µg/l	µg/l	µg/l	meq	%								
C1_t=10.1	1.1	<2	15	<2	<2	0.13	<0.3	-0.06	-1.23	-0.60	-2.28	-1.29	-0.35	0.30	-1.02	4.26	1.27
C1_t=11.1	1.1	<2	18	<2	<2	0.11	<0.3	-0.24	-5.08	-0.39	-1.85	-1.07	-0.16	0.30	-0.99	3.95	1.11
C1_t=12.1	1.1	<2	14	<2	<2	0.14	<0.3	-0.16	-3.45	-0.42	-1.91	-1.09	-0.19	0.32	-0.92	4.05	1.14
C1_t=13.1	1.4	<2	15	<2	<2	0.12	<0.3	-0.15	-3.20	-0.53	-2.14	-1.20	-0.30	0.31	-0.97	4.19	1.23
C1_t=14.2	2.1	<2	18	<2	<2	0.11	<0.3										
C1_t=15.1	0.5	<2	14	<2	<2	0.11	0.4	-0.04	-0.90	-0.53	-2.15	-1.21	-0.51	0.29	-1.66	2.91	0.61
C1_t=16.1	0.5	<2	14	<2	<2	0.11	0.9										
C1_t=17.1	0.5	<2	14	<2	<2	0.14	65.9	-0.06	-1.09	-0.64	-2.37	-1.31	-0.66	0.29	-2.01	2.52	0.41
C1_t=18.1	0.6	<2	14	<2	2	0.11	48.7	-0.17	-3.34	-0.25	-1.60	-0.90	-0.25	0.30	-1.58	2.62	0.46
C1_t=19.1	0.8	<2	13	<2	<2	0.14	98.1	-0.11	-2.19	-0.49	-2.06	-1.12	-0.49	0.28	-1.47	3.32	0.82
C1_t=20.1	0.9	<2	13	<2	<2	0.11	0.5	-0.18	-3.65	-0.57	-2.24	-1.21	-0.55	0.29	-1.49	3.47	0.89
C1_t=21.1	1.1	<2	13	<2	<2	0.12	<0.3	-0.48	-9.36	0.16	-0.76	-0.47	0.15	0.27	-1.10	2.90	0.61
C1_t=22.1	1.0	<2	14	<2	<2	0.11	<0.3	-0.20	-4.04	-0.38	-1.85	-1.01	-0.38	0.28	-1.33	3.42	0.87
C1_t=23.1	1.2	<2	13	<2	<2	0.15	<0.3	-0.18	-3.73	-0.67	-2.44	-1.31	-0.70	0.28	-1.60	3.46	0.88
C1_t=24.1	1.3	<2	12	<2	<2	0.10	<0.3	-0.17	-3.64	-0.70	-2.50	-1.33	-0.65	0.28	-1.48	3.75	1.03
C2_t=1.2	1.6	<2	16	<2	<2	0.12	8.9	-0.11	-2.17	-0.58	-2.13	-1.37	-0.43	0.20	-1.00	4.54	1.51
C2_t=1.4	1.5	<2	15	<2	<2	0.10	18.3	-0.17	-3.50	-0.60	-2.17	-1.38	-0.46	0.20	-1.08	4.43	1.45
C2_t=1.6	1.7	<2	15	<2	<2	0.13	11.2	-0.21	-4.24	-0.28	-1.53	-1.06	-0.13	0.20	-0.90	4.15	1.31
C2_t=2.2	2.2	<2	17	<2	<2	0.13	16.4	0.01	0.27	-0.53	-2.01	-1.31	-0.46	0.21	-0.81	4.69	1.57
C2_t=2.4	1.2	<2	15	2	<2	0.12	0.6	-0.04	-0.78	-0.52	-2.01	-1.30	-0.59	0.21	-1.07	4.21	1.33
C2_t=3.1	2.0	<2	17	<2	<2	0.14	0.7	0.04	0.82	-0.60	-2.16	-1.40	-0.58	0.22	-1.12	4.21	1.32
C2_t=3.3	1.8	<2	18	<2	<2	0.13	0.9	0.10	1.95	-0.59	-2.16	-1.40	-0.56	0.22	-1.20	4.05	1.24
C2_t=4.1	1.6	<2	18	<2	<2	0.11	0.5	-0.07	-1.50	-0.69	-2.35	-1.48	-0.61	0.22	-1.15	4.43	1.43
C2_t=4.3	2.2	<2	17	<2	<2	0.11	1.3	0.01	0.18	-0.49	-1.96	-1.29	-0.35	0.22	-0.82	4.63	1.53
C2_t=5.1	1.4	<2	14	<2	<2	0.13	0.3	-0.07	-1.52	-0.61	-2.20	-1.39	-0.54	0.21	-1.29	4.00	1.22
C2_t=6.1	1.8	<2	14	<2	<2	0.17	0.5	-0.07	-1.41	-0.30	-1.58	-1.09	-0.23	0.22	-0.87	4.21	1.32
C2_t=6.3	1.5	<2	15	<2	<2	0.13	0.5	0.07	1.41	-0.31	-1.60	-1.04	-0.15	0.22	-0.85	4.26	1.35
C2_t=7.1	1.9	<2	17	<2	<2	0.15	0.5	0.03	0.73	-0.33	-1.64	-1.11	-0.15	0.22	-0.84	4.30	1.37
C2_t=8.1	1.9	<2	17	<2	<2	0.12	0.6	-0.13	-2.78	-0.31	-1.60	-1.02	-0.17	0.22	-0.94	4.10	1.27
C2_t=9.1	2.0	<2	16	<2	<2	0.14	1.9	-0.16	-3.25	-0.39	-1.76	-1.11	-0.20	0.22	-0.81	4.55	1.49
C2_t=10.1	2.2	<2	16	<2	<2	0.13	0.4	-0.07	-1.60	-0.34	-1.66	-1.04	-0.12	0.22	-0.72	4.55	1.49
C2_t=11.1	2.3	<2	13	<2	<2	0.14	0.4										
C2_t=12.1	6.4	<2	15	<2	<2	0.12	<0.3	-0.22	-4.78	-0.23	-1.44	-0.99	-0.11	0.23	-0.54	4.73	1.57
C2_t=13.1	6.9	<2	12	<2	<2	0.11	<0.3	-0.27	-5.81	-0.54	-2.06	-1.29	-0.46	0.22	-0.72	4.99	1.70
C2_t=14.2	7.0	<2	13	<2	<2	0.10	0.3										
C2_t=15.1	0.8	<2	15	<2	<2	0.10	0.5	-0.17	-3.72	-0.53	-2.04	-1.23	-0.61	0.19	-1.61	3.37	0.93
C2_t=16.1	0.9	<2	13	<2	<2	0.13	0.4	-0.04	-0.81	-0.34	-1.67	-1.05	-0.46	0.19	-1.43	3.32	0.91
C2_t=17.1	1.3	<2	14	<2	2	0.10	114.0	0.01	0.21	-0.37	-1.73	-1.06	-0.48	0.21	-1.43	3.39	0.92
C2_t=18.1	1.4	<2	14	<2	2	0.13	82.5	-0.09	-1.84	-0.18	-1.35	-0.91	-0.32	0.20	-1.33	3.28	0.88
C2_t=19.1	1.8	<2	11	<2	<2	0.12	68.1	-0.07	-1.46	-0.30	-1.60	-1.02	-0.49	0.19	-1.36	3.45	0.97
C2_t=20.1	3.1	<2	11	<2	<2	0.10	<0.3	-0.27	-5.49	-0.27	-1.54	-0.99	-0.65	0.19	-1.03	4.13	1.31
C2_t=21.1	3.2	<2	10	<2	<2	0.13	5.3										
C2_t=22.1	3.7	<2	11	<2	<2	0.13	<0.3	-0.12	-2.48	-0.42	-1.83	-1.13	-0.87	0.19	-0.98	4.48	1.49
C2_t=23.1	4.0	2	12	<2	<2	0.14	<0.3	-0.22	-4.52	-0.46	-1.93	-1.14	-0.91	0.21	-0.93	4.66	1.56
C2_t=24.1	4.2	<2	12	<2	<2	0.15	0.3	-0.19	-3.95	-0.51	-2.02	-1.22	-0.89	0.19	-0.99	4.67	1.58
C3_t=1.2	2.0	<2	14	<2	<2	0.12	7.2	-0.07	-1.49	-0.41	-1.55	-1.24	-0.74	0.03	-1.47	3.72	1.25
C3_t=1.4	1.1	<2	12	<2	<2	0.11	7.7	-0.22	-4.55	-0.41	-1.56	-1.23	-1.14	0.07	-1.59	3.32	1.02
C3_t=1.6	0.9	<2	12	2	<2	0.11	10.1										
C3_t=2.2	0.8	<2	15	<2	<2	0.14	6.0	-0.24	-4.57	-0.14	-1.03	-0.93	-0.89	0.08	-1.44	3.08	0.89
C3_t=2.4	0.5	<2	13	<2	2	0.11	0.7	-0.11	-2.19	-0.31	-1.35	-1.14	-1.49	0.07	-1.64	2.98	0.85
C3_t=3.1	0.5	<2	13	<2	<2	0.13	0.9	0.06	1.22	-0.38	-1.51	-1.18	-1.43	0.08	-1.62	3.11	0.90
C3_t=3.3	0.4	<2	13	<2	<2	0.12	1.0	0.01	0.24	-0.39	-1.52	-1.18	-0.94	0.09	-1.53	3.24	0.96
C3_t=4.1	0.6	<2	16	<2	<2	0.12	<0.3	-0.04	-0.78	-0.29	-1.33	-1.07	-0.16	0.08	-1.66	2.86	0.78
C3_t=4.3	0.7	<2	15	<2	3	0.11	1.1	0.09	1.75	-0.30	-1.37	-1.09	-0.05	0.08	-1.54	3.05	0.87
C3_t=5.1	0.3	<2	16	<2	<2	0.11	<0.3	-0.25	-5.05	-0.40	-1.55	-1.23	-0.16	0.07	-1.85	2.82	0.76
C3_t=6.1	0.3	<2	15	<2	<2	0.10	<0.3	-0.04	-0.94	-0.13	-1.01	-0.96	0.33	0.07	-1.73	2.46	0.58
C3_t=6.3	0.5	<2	17	<2	<2	0.09	<0.3	-0.08	-1.61	-0.13	-1.01	-0.89	0.37	0.06	-1.85	2.28	0.51
C3_t=7.1	0.7	<2	17	<2	<2	0.15	<0.3	-0.01	-0.13	-0.11	-0.97	-0.88	0.44	0.06	-1.74	2.45	0.58
C3_t=8.1	1.1	<2	16	<2	<2	0.11	1.4	-0.03	-0.56	-0.13	-1.01	-0.89	0.49	0.07	-1.53	2.89	0.81
C3_t=9.1	1.2	<2	13	<2	<2	0.11	0.8	-0.12	-2.59	-0.03	-0.80	-0.78	0.54	0.06	-1.62	2.58	0.66
C3_t=10.1	1.3	<2	13	<2	<2	0.10	<0.3	-0.16	-3.38	-0.14	-1.03	-0.95	0.27	0.05	-1.60	2.89	0.82
C3_t=11.1	1.5	<2	16	<2	<2	0.11	<0.3										
C3_t=12.1	1.4	<2	15	<2	<2	0.12	<0.3	-0.17	-3.66	-0.15	-1.06	-0.89	0.14	0.06	-1.57	2.99	0.86
C3_t=13.1	1.2	<2	14	<2	<2	0.10	<0.3	-0.31	-6.49	0.17	-0.42	-0.57	0.41	0.05	-1.75	2.08	0.41
C3_t=14.2	2.3	<2	16	<2	<2	0.09	<0.3										
C3_t=15.1	0.6	<2	13	<2	<2	0.12	14.7	-0.03	-0.55	-0.24	-1.26	-1.00	0.02	0.04	-1.77	2.97	0.87
C3_t=16.1	1.7	<2	12	<2	2	0.13	<0.3	-0.07	-1.54	-0.05	-0.86	-0.80	0.24	0.03	-1.65	2.87	0.83
C3_t=17.1	1.4	2	15	<2	3	0.13	151.0	-0.04	-0.82	0.14	-0.50	-0.61	0.50	0.04	-1.60	2.67	0.72
C3_t=18.1	1.1	<2	14	<2	<2	0.14	4.2	0.09	1.82	-0.09	-0.94	-0.83	0.20	0.03	-1.80	2.73	0.76
C3_t=19.1	1.0	<2	14	<2	<2	0.12	36.8	-0.04	-0.90	-0.11	-1.00	-0.89	0.08	0.02	-1.85	2.74	0.78
C3_t=20.1	3.7	<2	13	<2	<2	0.14	<0.3	-0.14	-2.73	-0.08	-0.94	-0.81	0.24	0.04	-1.46	3.47	1.12
C3_t=21.1	3.3	3	12	<2	<2	0.11	<0.3	-0.08	-1.65	-0.22	-1.22	-0.93	0.02	0.03	-1.66	3.38	1.09
C3_t=22.1	2.8	<2	14	<2	2	0.12	<0.3	-0.17	-3.52	-0.02	-0.81	-0.78	0.21	0.01	-1.74	2.86	0.84
C3_t=23.1	3.0	<2	13	<2	2	0.14	<0.3	-0.14	-2.83	-0.40	-1.57	-1.11	-0.16	0.04	-1.59	3.87	1.33
C3_t=24.1	2.4	<2	13	<2	<2	0.12	<0.3	-0.10	-2.19	-0.54	-1.86	-1.29	-0.31	0.02	-1.82	3.75	1.28
C4_t=1.2	4.1	<2	16	<2	4	0.15	5.9	-0.15	-2.86	0.01	-0.29	-0.93	0.54	-0.12	-2.66	0.91	-0.01
C4_t=1.4	1.1	<2	17	2	3	0.14	5.2	-0.05	-0.96	0.05	-0.23	-0.93	0.66	-0.05	-2.81	0.13	-0.48
C4_t=1.6	0.9	<2	18	<2	3	0.13	6.7	-0.08	-1.36	0.07	-0.18	-0.92	0.78	-0.06	-2.76	0.23	-0.42
C4_t=2.2	0.6	<2	16	3	2	0.14	25.5	0.02	0.44	0.05	-0.23	-0.87	0.04	-0.06	-3.11	-0.45	-0.76
C4_t=2.4	0.7	<2	16	<2	2	0.16	5.9	-0.02	-0.43	-0.08	-0.49	-0.97	0.39	-0.08	-2.60	0.92	-0.05
C4_t=3.1	1.5	<2	16	3	2	0.15	3.4	0.07	1.37	-0.15	-0.63	-1.01	0.30	-0.06	-2.52	1.14	0.04
C4_t=3.3	0.9	<2	16	3	3	0.15	1.7	0.01	0.17	-0.07	-0.47	-0.91	0.47	-0.09	-2.87	0.38	-0.32
C4_t=4.1	0.7	<2	17	<2	2	0.12	30.4	-0.05	-0.92	-0.11	-0.55	-0.93	0.59	-0.11	-3.08	0.17	-0.40
C4_t=4.3	0.6	<2	16	<2	3	0.15	1.4	0.10	1.96	-0.01	-0.35	-0.84	0.83	-0.10	-2.98	0.11	-0.43
C4_t=6.1	0.6	<2	14	<2	<2	0.14	0.5	-0.14	-2.95	0.16	-0.01	-0.63	0.88	-0.14	-3.26	-0.57	-0.74
C4_t=6.3	0.5	<2	16	<2	<2	0.15	<0.3	-0.02	-0.40	0.04	-0.26	-0.75	0.71	-0.15	-3.24	-0.26	-0.57
C4_t=7.1	0.8	<2	15	2	<2	0.11	0.4	-0.06	-1.31	0.14	-0.05	-0.65	0.82	-0.16	-3.34	-0.62	-0.74
C4_t=8.1	1.5	<2	18	<2	<2	0.09	2.9	-0.26	-5.44	0.26	0.18	-0.52	0.89	-0.16	-3.07	-0.21	-0.54
C4_t=9.1	0.6	<2	13	<2	<2	0.11	<0.3	-0.30	-6.59	0.33	0.33	-0.43	0.91	-0.17	-3.33	-0.80	-0.82
C4_t=10.1	1.5	<2	13	<2	<2	0.13	0.9	0.03	0.75	0.23	0.12	-0.52	0.87	-0.18	-3.03	-0.04	-0.43
C4_t=11.1	0.7	<2	15	<2	<2	0.13	0.3	0.02	0.36	0.14	-0.07	-0.61	0.71	-0.18	-3.35	-0.44	-0.63
C4_t=12.1	1.6	<2	15	<2	<2	0.13	<0.3	-0.24	-5.23	0.02	-0.29	-0.74	0.61	-0.18	-3.17	0.24	-0.29
C4_t=13.1	0.9	<2	14	<2	<2	0.10	<0.3										
C4_t=14.2	4.0	<2	23	4	<2	0.19	4.6										
C4_t=15.1	0.2	<2	14	<2	<2	0.26	9.7	0.57	7.88	0.44	0.51	0.11	-0.81	-0.30	-4.05	-1.62	-1.10
C4_t=16.1	0.1	<2	11	2	<2	0.18	2.5	0.04	0.74	0.22	0.06	-0.17	-1.27	-0.29	-4.58	-2.24	-1.42
C4_t=17.1	0.2	<2	13	2	<2	0.14	1.6	-0.08	-1.48	-0.03	-0.44	-0.44	-0.34	-0.30	-4.09	-0.65	-0.62
C4_t=18.1	0.2	<2	11	<2	<2	0.17	0.5	-0.04	-0.80	0.11	-0.17	-0.32	0.25	-0.30	-4.92	-2.61	-1.60
C4_t=19.1	0.1	<2	12	<2	2	0.15	0.5	0.11	2.35	0.09	-0.19	-0.36	0.41	-0.30	-3.98	-0.80	-0.69
C4_t=20.1	0.2	<2	11	<2	<2	0.10	<0.3	-0.13	-2.74	0.18	-0.01	-0.26	0.57	-0.28	-3.87	-0.77	-0.70
C4_t=21.1	0.2	<2	13	<2	<2	0.13	<0.3	-0.10	-2.21	0.34	0.30	-0.09	0.60	-0.29	-4.93	-3.19	-1.89

ID	Ti	Tl	U	V	W	Yb	Zn	Charge balance	Electrical balance	$SI_{Calcite}$	$SI_{Dolomite}$	$SI_{Rhodochrosite}$	$SI_{Siderite}$	SI_{Quartz}	$SI_{K\text{-}feldspar}$	$SI_{Kaolinite}$	$SI_{Gibbsite}$
	µg/l	µg/l	µg/l	µg/l	µg/l	µg/l	µg/l	meq	%								
C4_t=22.1	0.8	<2	13	<2	<2	0.10	<0.3	-0.10	-2.11	0.14	-0.09	-0.30	0.32	-0.28	-3.91	-0.80	-0.72
C4_t=23.1	0.2	<2	13	<2	<2	0.11	<0.3	-0.17	-3.75	-0.04	-0.47	-0.49	0.19	-0.28	-4.44	-1.41	-1.02
C4_t=24.1	0.2	<2	12	<2	<2	0.09	<0.3	-0.09	-2.04	-0.19	-0.75	-0.64	0.04	-0.28	-4.64	-1.56	-1.09

V Chemical analyses in- and effluent – GRAPHS

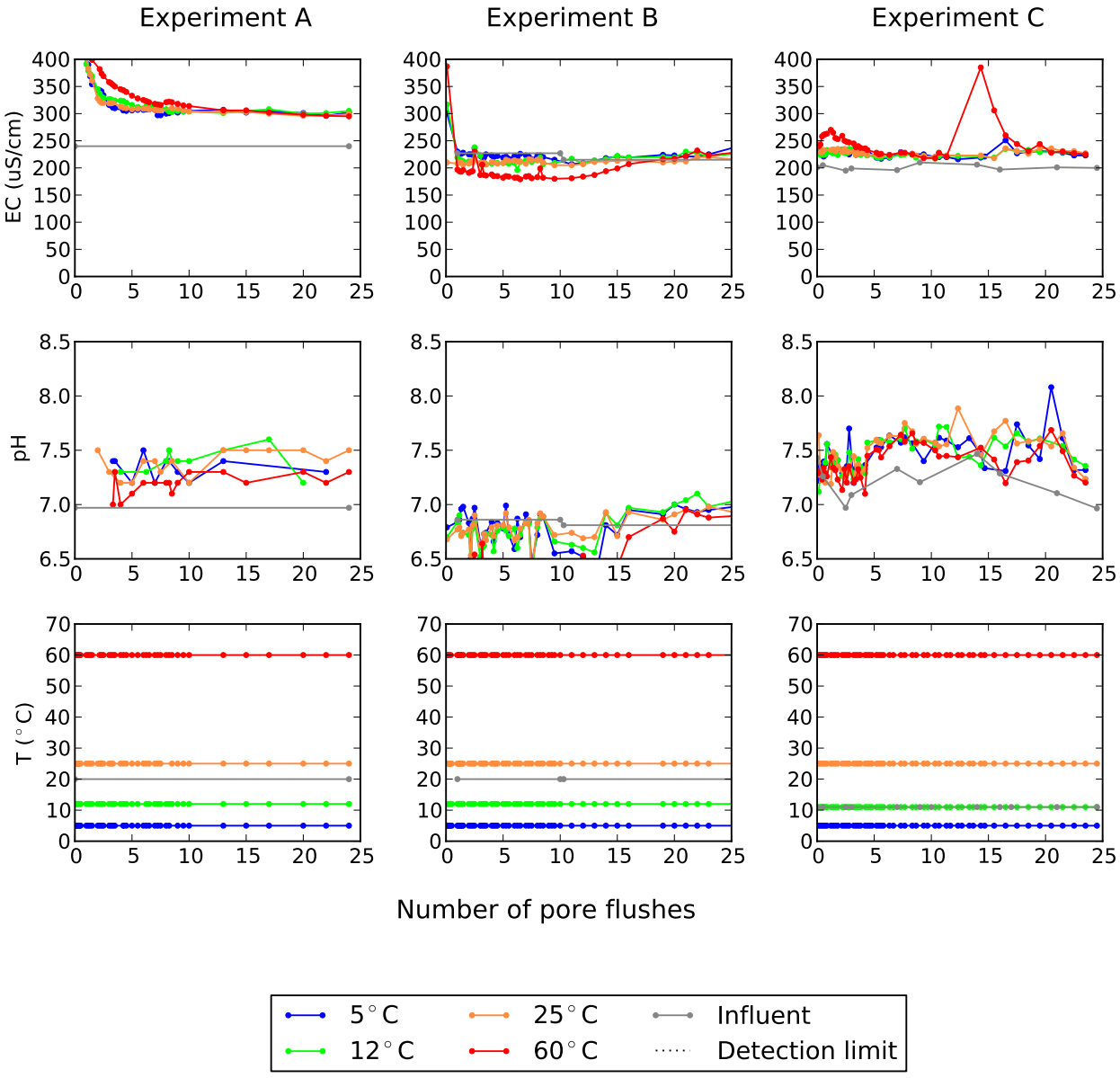

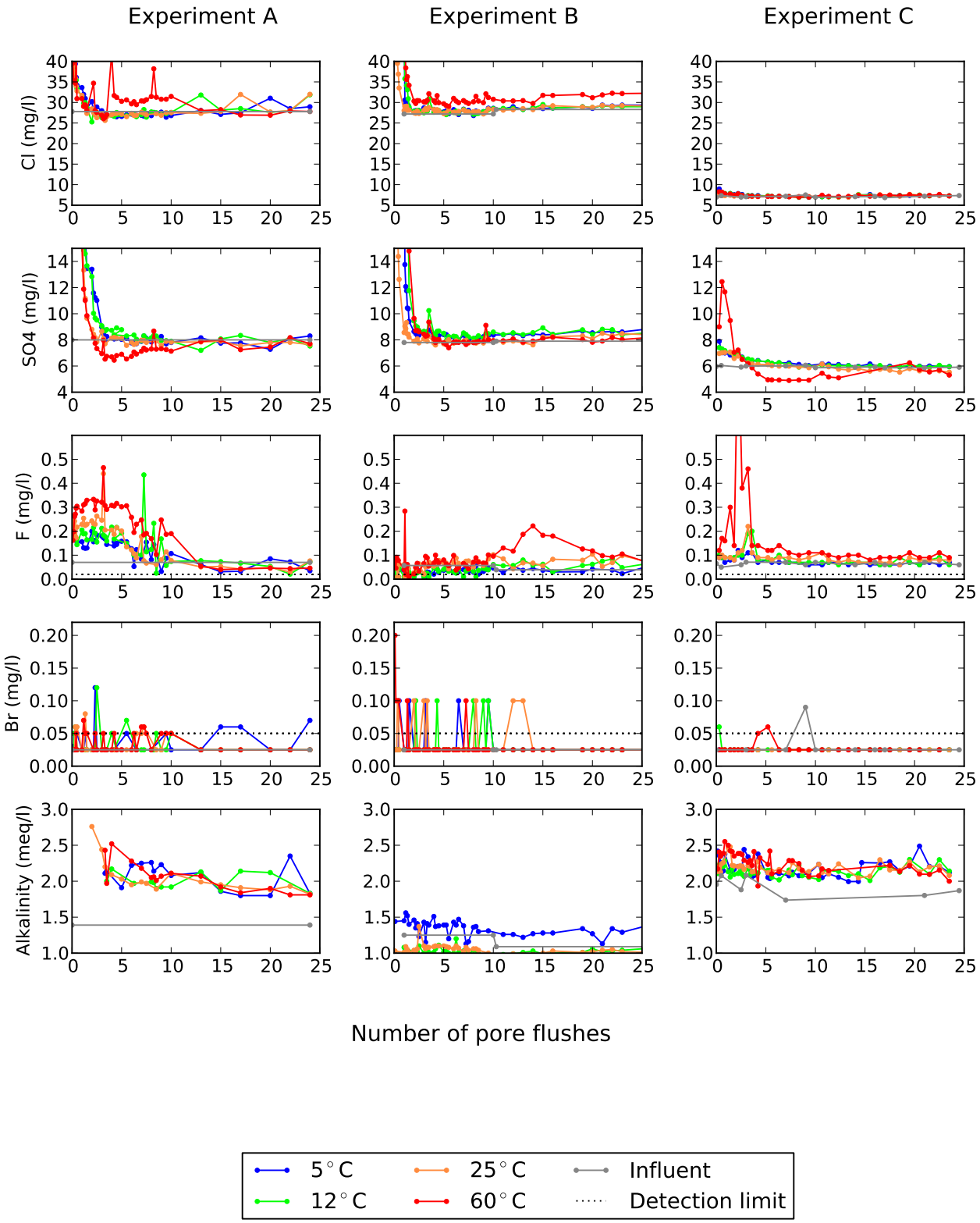
Experiment A
Experiment B
Experiment C
Cl (mg/l)
SO4 (mg/l)
F (mg/l)
Br (mg/l)
Alkalinity (meq/l)
Number of pore flushes
5 °C
12 °C
25 °C
60 °C
Influent
Detection limit

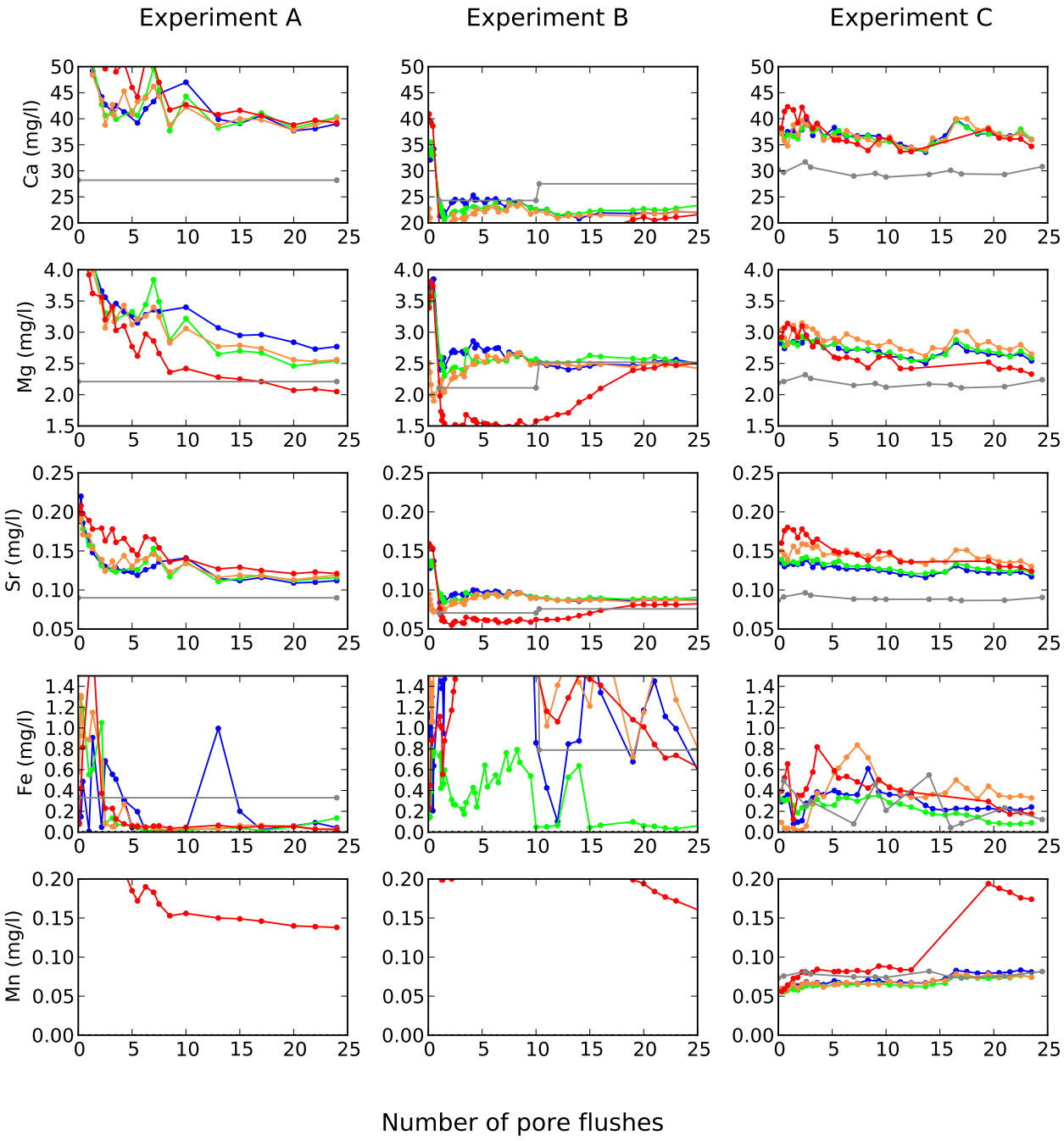
Experiment A
Experiment B
Experiment C
Ca (mg/l)
Mg (mg/l)
Sr (mg/l)
Fe (mg/l)
Mn (mg/l)
Number of pore flushes
5 °C
12 °C
25 °C
60 °C
Influent
Detection limit

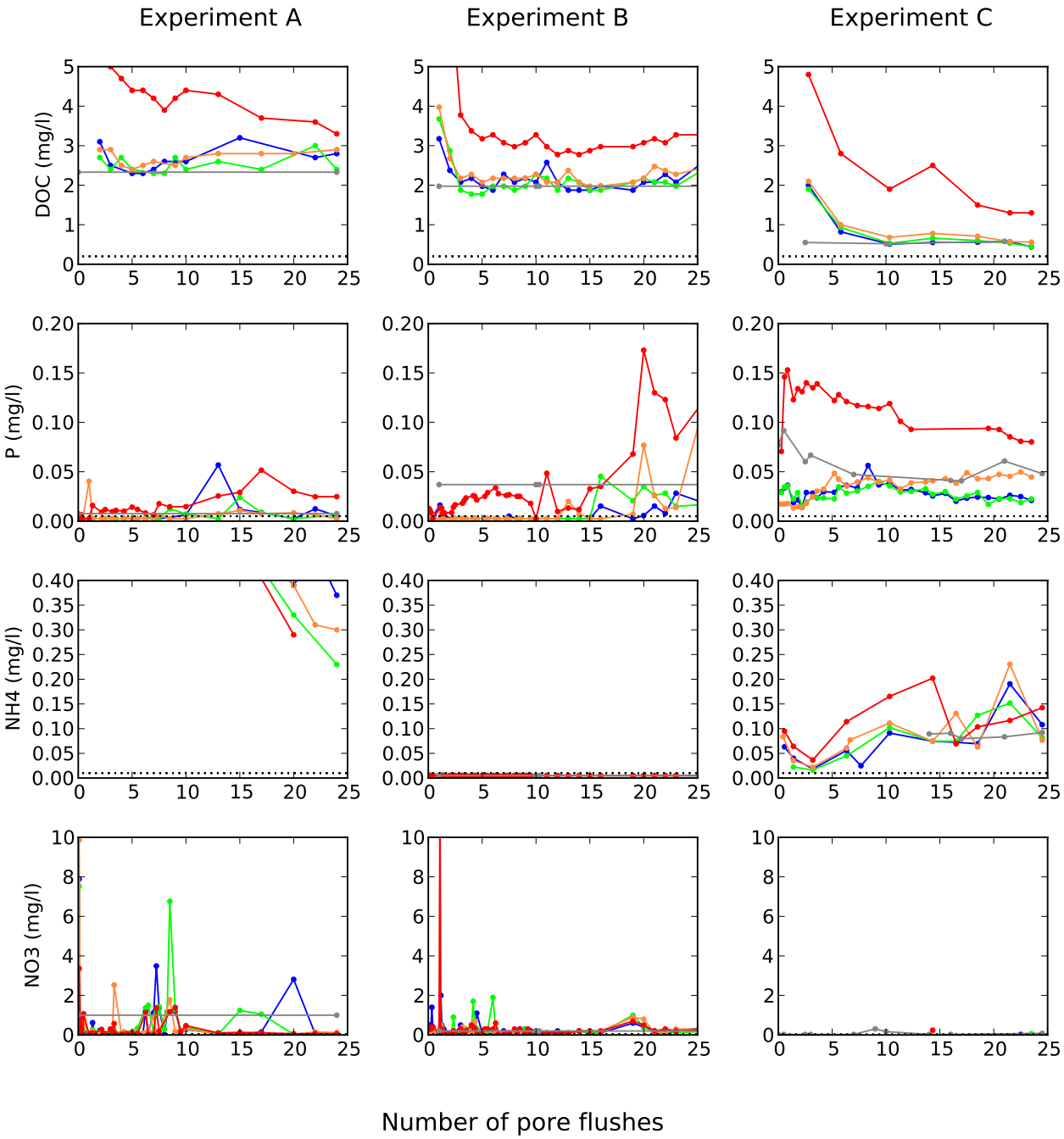
Experiment A
Experiment B
Experiment C
DOC (mg/l)
P (mg/l)
NH4 (mg/l)
NO3 (mg/l)
Number of pore flushes
5 °C
12 °C
25 °C
60 °C
Influent
Detection limit

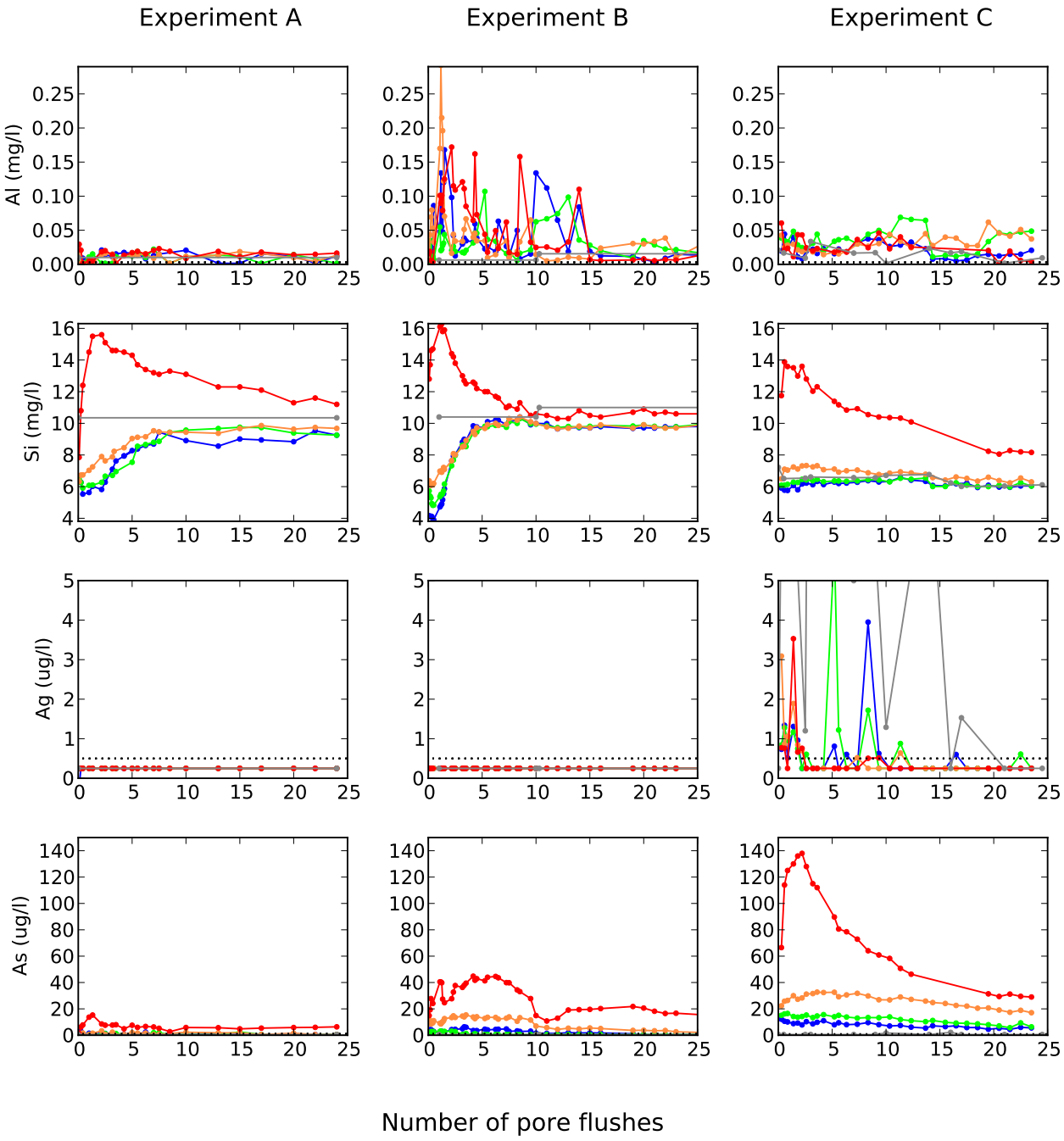
Experiment A
Experiment B
Experiment C
Al (mg/l)
Si (mg/l)
Ag (ug/l)
As (ug/l)
Number of pore flushes
5 °C
12 °C
25 °C
60 °C
Influent
Detection limit

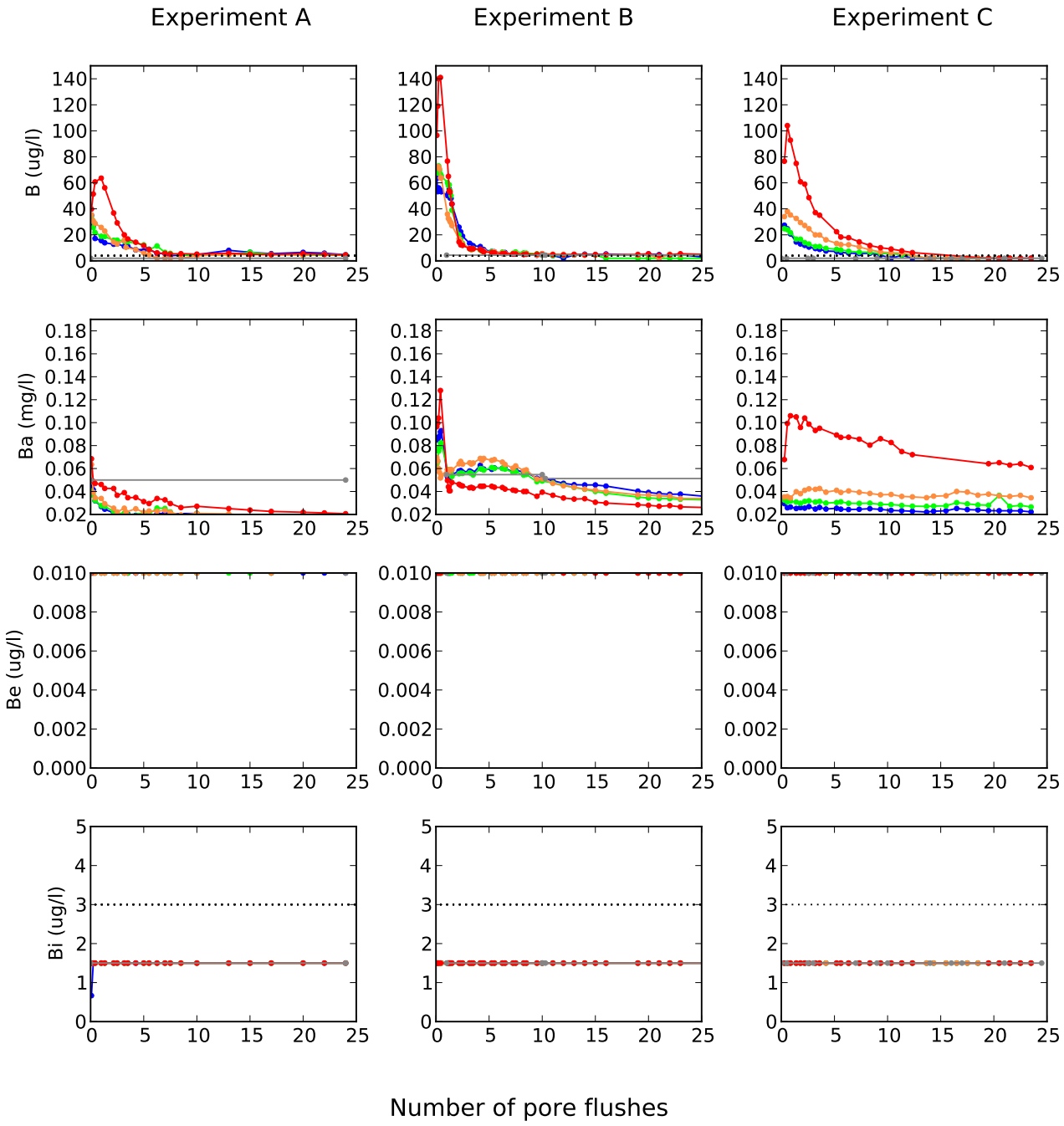
Experiment A
Experiment B
Experiment C
B (ug/l)
Ba (mg/l)
Be (ug/l)
Bi (ug/l)
Number of pore flushes
5 °C
12 °C
25 °C
60 °C
Influent
Detection limit

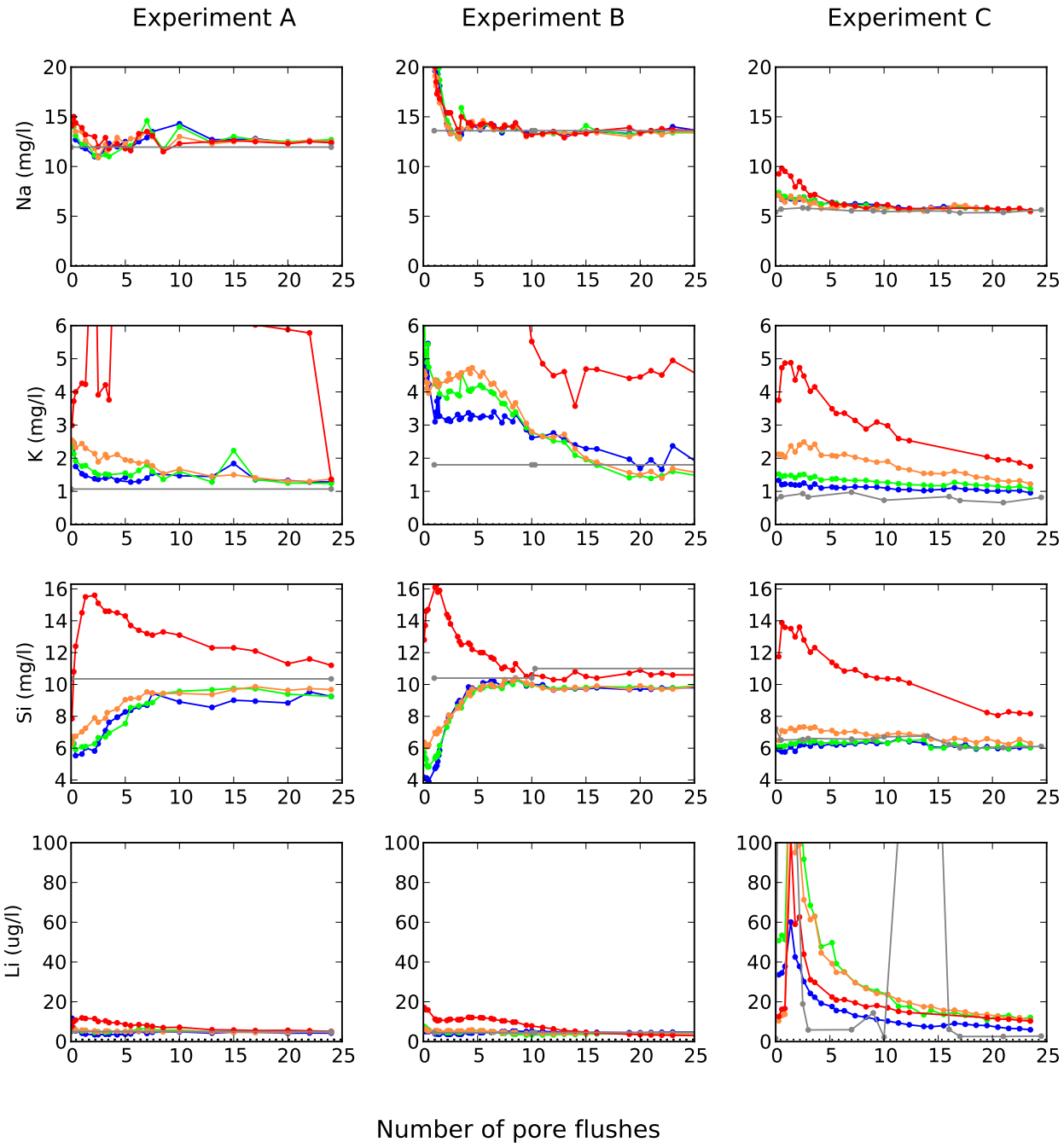
Experiment A
Experiment B
Experiment C
Na (mg/l)
K (mg/l)
Si (mg/l)
Li (ug/l)
Number of pore flushes
5 °C
12 °C
25 °C
60 °C
Influent
Detection limit

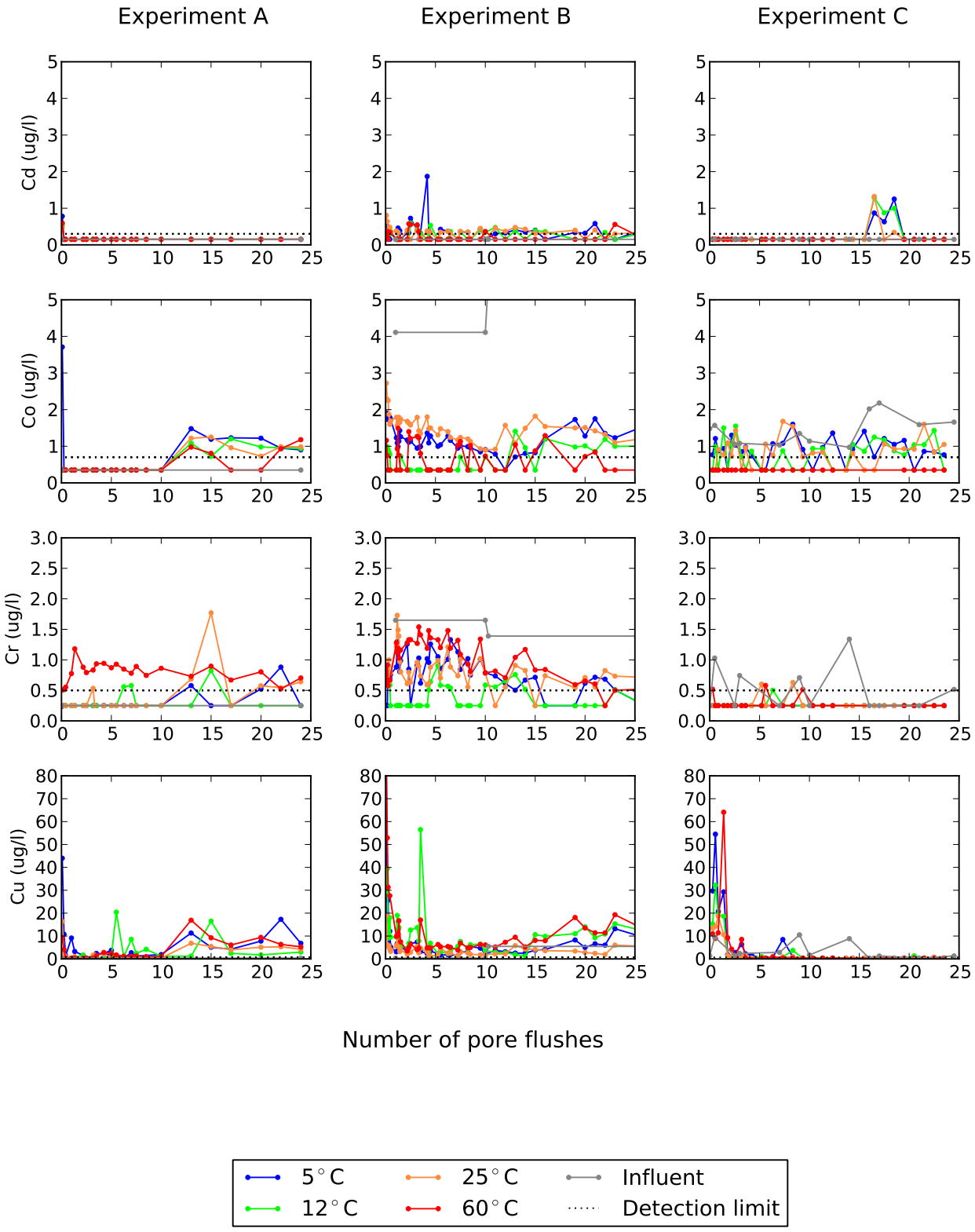
Experiment A
Experiment B
Experiment C
Cd (ug/l)
Co (ug/l)
Cr (ug/l)
Cu (ug/l)
Number of pore flushes
5 °C
12 °C
25 °C
60 °C
Influent
Detection limit

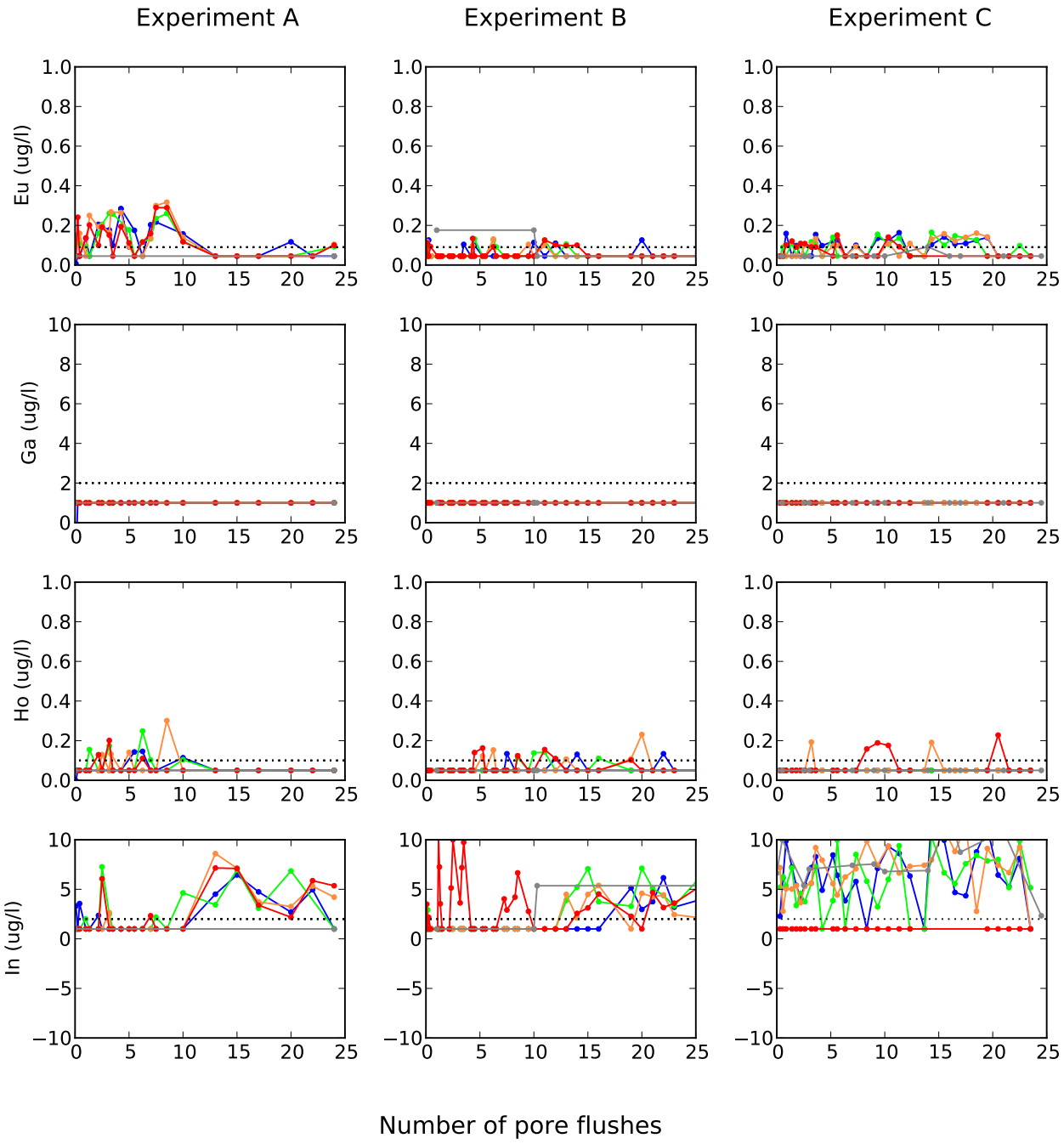
Experiment A
Experiment B
Experiment C
Eu (ug/l)
Ga (ug/l)
Ho (ug/l)
In (ug/l)
Number of pore flushes
5 °C
12 °C
25 °C
60 °C
Influent
Detection limit

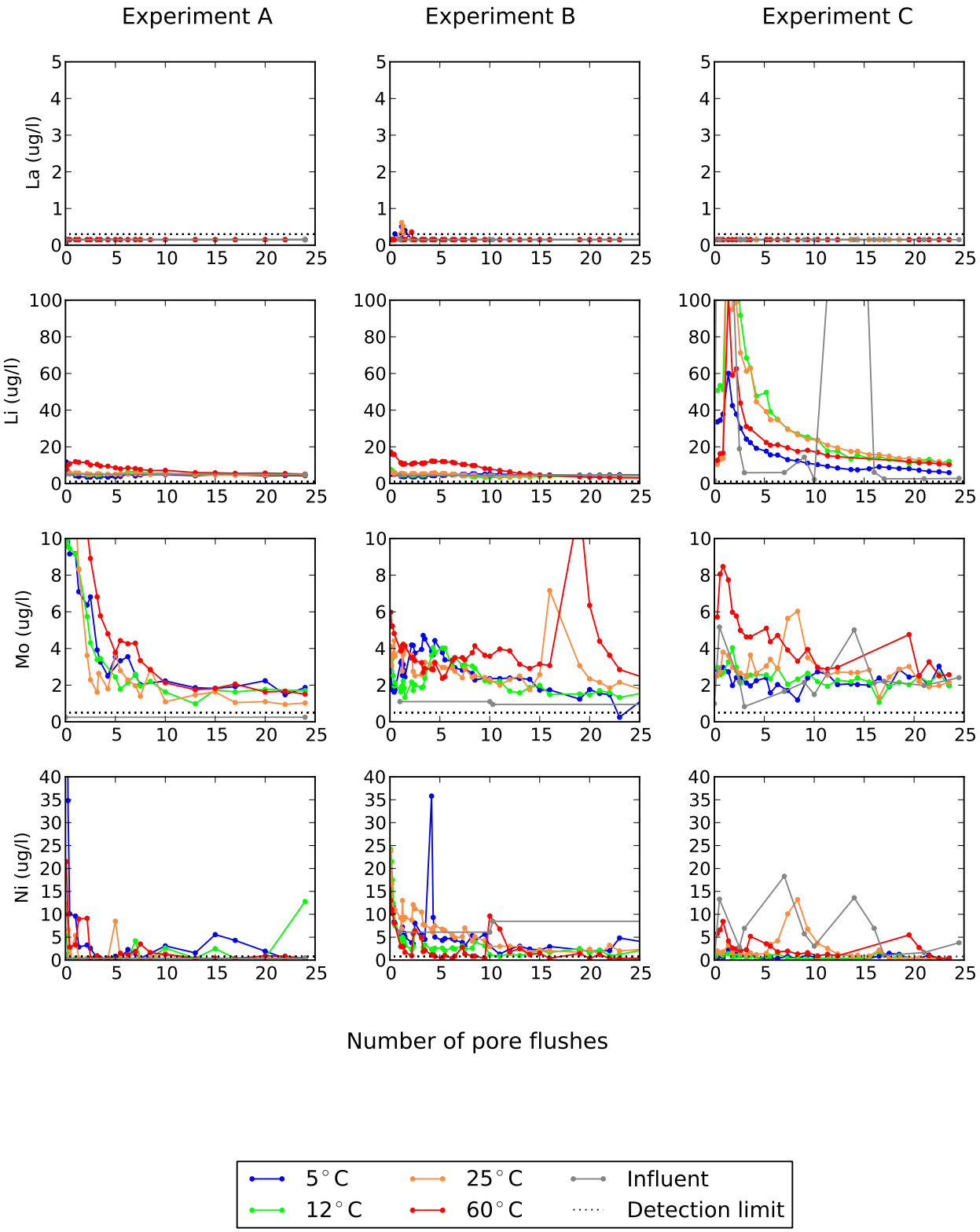
Experiment A
Experiment B
Experiment C
La (ug/l)
Li (ug/l)
Mo (ug/l)
Ni (ug/l)
Number of pore flushes
5 °C
12 °C
25 °C
60 °C
Influent
Detection limit

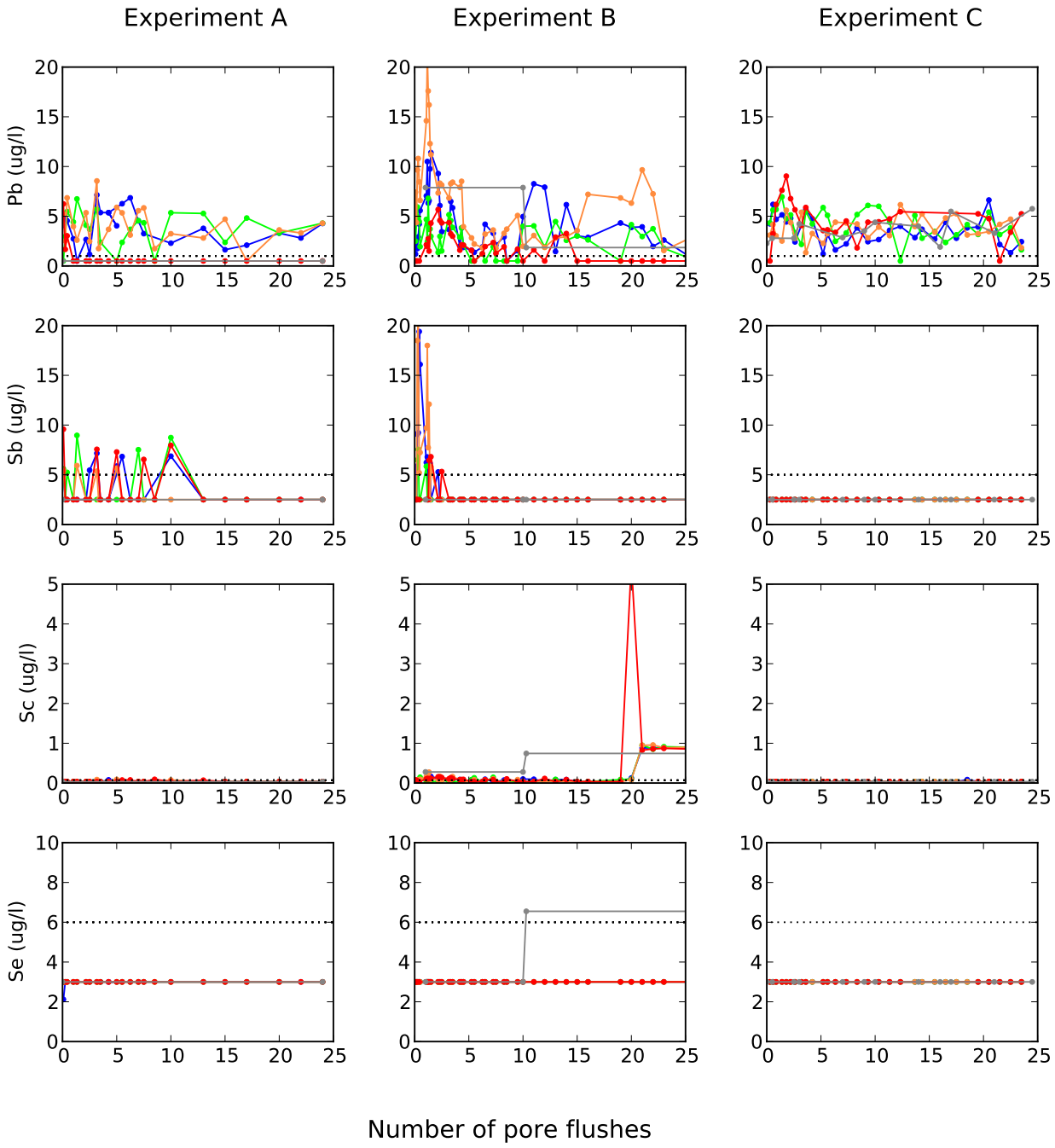
Experiment A
Experiment B
Experiment C
Pb (ug/l)
Sb (ug/l)
Sc (ug/l)
Se (ug/l)
Number of pore flushes
5 °C
12 °C
25 °C
60 °C
Influent
Detection limit

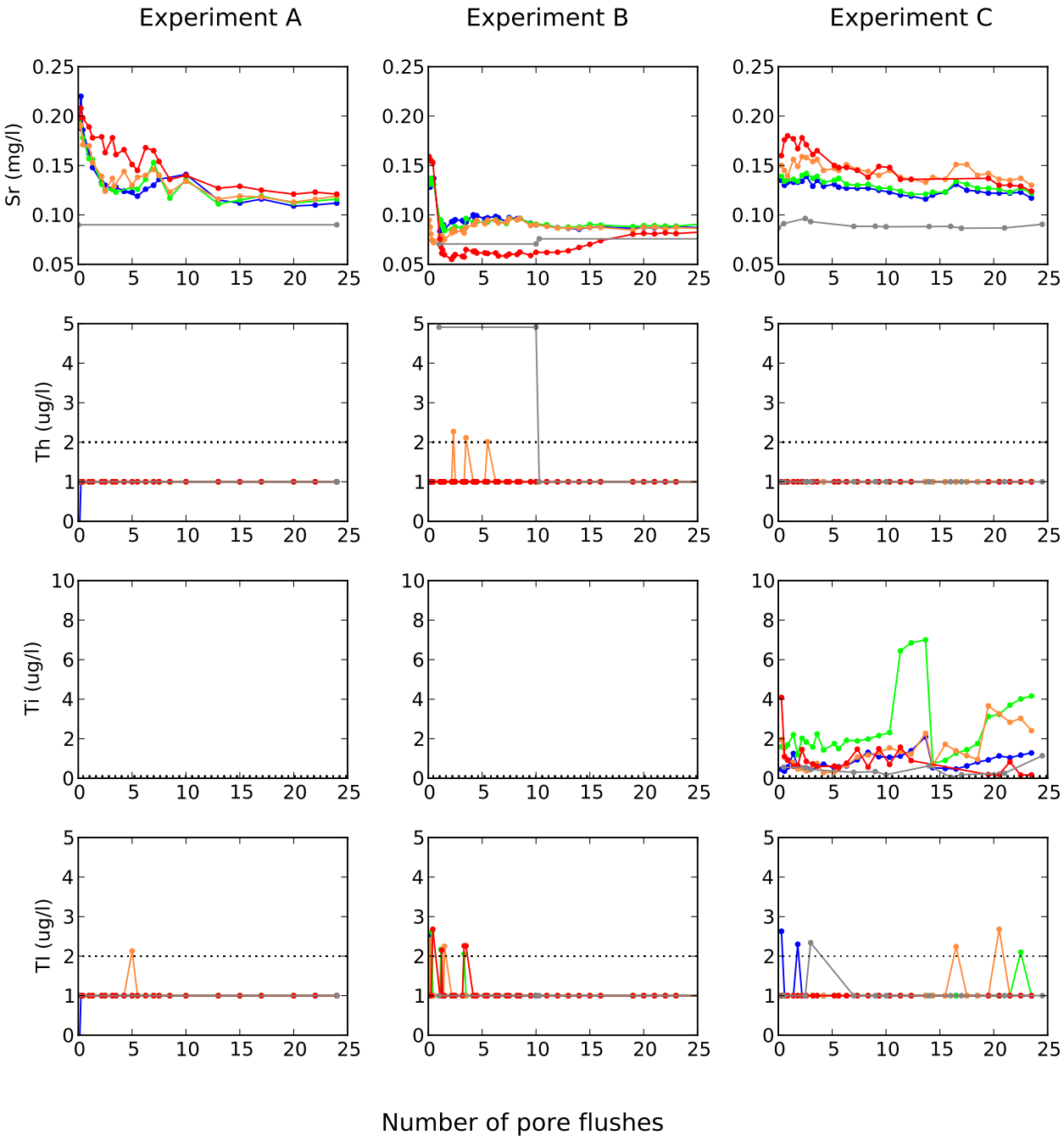
Experiment A
Experiment B
Experiment C
Sr (mg/l)
Th (ug/l)
Ti (ug/l)
Tl (ug/l)
Number of pore flushes
5 °C
12 °C
25 °C
60 °C
Influent
Detection limit

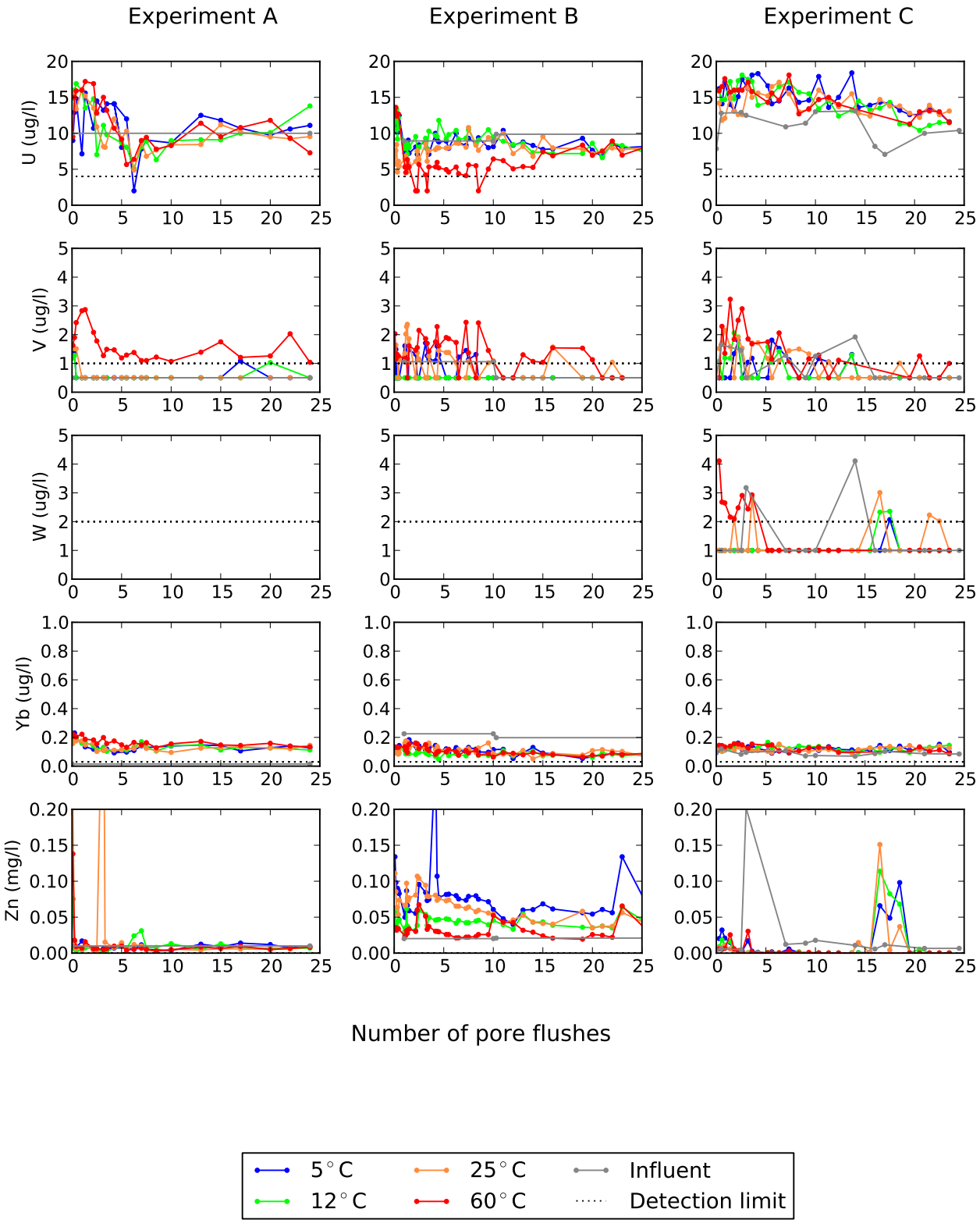
Experiment A
Experiment B
Experiment C
U (ug/l)
V (ug/l)
W (ug/l)
Yb (ug/l)
Zn (mg/l)
Number of pore flushes
5 °C
12 °C
25 °C
60 °C
Influent
Detection limit

VI Statistical analyses

Table VI Relative change of the average leaching concentrations at 5°C, 25°C and 60°C compared to the reference column of 11°C with 1 day residence time. The significance of the relative change is shown at 5% and 1% significance levels based on a two tailed Mann Whitney U-test (respectively shown with orange/red and light blue and dark blue shadings for an increase and decrease).

		Experiment A						Experiment B						Experiment C						Average of 3 exp. And significant in all 3 experiments					
Substance	**D.L.**	**5°C**		**25°C**		**60°C**		**5°C**		**25°C**		**60°C**		**5°C**		**25°C**		**60°C**		**5°C**		**25°C**		**60°C**	
pH	0.1	-6%		24%		21%	**	0%		0%		-5%	**	0%		1%		-1%	**	-2%		8%		5%	
EC	5 µS/cm	-1%		-1%		3%	*	2%	**	-3%	*	-7%	**	1%		1%	*	3%	**	1%		-1%		-1%	
Alkalinity	0.1 meq/l	5%		7%		7%		30%	**	2%	**	-27%	**	3%		2%	**	3%	**	13%		4%		-6%	
Cl	0.1 mg/l	0%		-1%		3%	**	2%		-3%		25%	**	1%		0%		-1%		1%		-1%		9%	
SO4	0.1 mg/l	2%		-4%	*	-10%	**	-11%	*	-21%	**	-2%	**	1%		-3%	*	0%	*	-3%		-9%		-4%	
Br	0.05 mg/l	12%		-4%		-1%		nd.		19%		-2%		-11%		-11%		-8%		0%		1%		-4%	
F	0.02 mg/l	-10%	*	-3%		45%	**	-28%		50%	**	134%	**	-15%	*	0%		77%	**	-18%		16%		85%	**
DOC	0.2 mg/l	8%		2%	*	63%	**	0%		8%	**	64%	**	-3%		14%		173%	**	2%		8%		100%	**
P	0.005 mg/l	85%		2%		267%	**	-42%		-22%		285%	**	7%		38%	**	249%	**	17%		6%		267%	**
Na	0.006 mg/l	6%		4%		4%		-1%		-2%		1%		1%		-2%		6%		2%		0%		4%	
Ca	0.02 mg/l	6%		4%		11%	*	0%		-6%	**	-23%	**	1%		1%		1%		2%		-1%		-3%	
Mg	0.005 mg/l	11%		3%		-12%	*	0%		-5%	**	-24%	**	-1%		5%	**	-4%		4%		1%		-13%	
Sr	0.5 µg/l	4%		7%		18%	**	0%		-4%	**	-22%	**	-3%	*	11%	**	13%	**	1%		4%		3%	**
Li	1 µg/l	-12%	**	-1%		44%	**	11%		7%	*	73%	**	-58%	**	-14%		-42%		-20%		-2%		25%	
K	4 µg/l	-1%	*	13%	*	336%	**	-1%	*	5%		281%	**	-14%	**	40%	**	130%	**	-6%		19%		249%	**
Fe	0.4 µg/l	101%		19%		32%		428%	**	591%	**	424%	**	34%	*	80%	**	77%	**	187%		230%		178%	
Mn	0.06 µg/l	25%	**	-19%	**	-46%	**	6%	**	-6%	**	-37%	**	7%	**	3%	*	77%	**	13%		-7%		-2%	
Al	3 µg/l	11%		17%		53%	**	10%		-11%		17%		-45%	**	-11%		-36%	**	-8%		-2%		12%	
Si	10 µg/l	1%		9%		53%	**	0%		1%		22%	**	-1%	**	8%	**	62%	**	0%		6%		45%	**
Ag	0.5 µg/l	nd.		nd.		nd.		nd.		nd.		nd.		-14%		-35%		-40%		-5%		-12%		-13%	
As	1 µg/l	nd.		65%	**	650%	**	25%	**	265%	**	1164%	**	-36%	**	123%	**	429%	**	-4%		129%	**	605%	**
B	4 µg/l	-1%		-11%		51%		10%		0%		36%		-11%		32%		114%	**	-1%		7%		67%	

Table 3-2, continued

		Experiment A							Experiment B							Experiment C							Average of 3 exp. And significant in all 3 experiments						
Substance	**D.L.**	**5ºC**		**25ºC**		**60ºC**			**5ºC**		**25ºC**		**60ºC**			**5ºC**		**25ºC**		**60ºC**			**5ºC**		**25ºC**		**60ºC**		
Ba	0.2 µg/l	1%		11%		47%	**		7%		5%		-19%	**		-18%	**	29%	**	166%	**		-3%		15%		65%		
Be	0.02 µg/l	-7%		14%		447%	**		10%	*	18%	**	200%	**		nd.		nd.		nd.			1%		11%		216%		
Bi	3 µg/l	nd.		nd.		nd.			nd.		nd.		nd.			nd.		nd.		nd.			nd.		nd.		nd.		
Cd	0.3 µg/l	6%		4%		5%			22%		22%		-19%	**		-7%		-22%		-44%			7%		2%		-20%		
Co	0.7 µg/l	28%		8%		-20%			61%	**	97%	**	-11%			15%		4%		-56%	**		35%		36%		-29%		
Cr	0.5 µg/l	20%		61%		155%	**		77%	**	86%	**	131%	**		-4%		7%		6%			31%		51%		97%		
Cu	0.7 µg/l	66%	*	-11%		57%			-38%	**	-61%	**	16%			61%		-28%		30%			30%		-34%		35%		
Eu	0.09 µg/l	10%		10%		-2%			1%		-8%		4%			5%		-1%		-15%			5%		1%		-5%		
Ga	20 µg/l	nd.		nd.		nd.			nd.		nd.		nd.			nd.		nd.		nd.			nd.		nd.		nd.		
Ho	0.1 µg/l	-2%		5%		-14%			-4%		8%		6%			nd.		18%		48%	*		-2%		10%		13%		
In	2 µg/l	-16%		-4%		-8%			-29%		-18%		6%	**		13%		27%		-83%	**		-11%		2%		-28%		
La	0.3 µg/l	nd.		nd.		nd.			5%	*	4%	*	2%			nd.		nd.		nd.			nd.		nd.		nd.		
Li	1 µg/l	-12%	**	-1%		44%	**		11%		7%	*	73%	**		-58%	**	-14%		-42%			-20%		-2%		25%		
Mo	0.5 µg/l	19%		-5%		57%			7%	*	42%	**	101%	**		-3%		27%	**	70%	**		8%		22%		76%	**	
Ni	0.8 µg/l	352%	*	8%		74%	*		68%	**	71%	**	-19%	**		11%		307%	**	322%	**		143%		129%		126%		
Pb	1 µg/l	-9%		-5%		-84%	**		63%	*	118%	**	-41%	**		-15%		-3%		-4%			13%		37%		-43%		
Sb	5 µg/l	1%		-19%		3%			14%	*	14%		2%			nd.		nd.		nd.			5%		-2%		2%		
Sc	0.07 µg/l	10%		24%	*	33%	*		3%	**	3%	**	114%	**		6%		nd.		nd.			6%		9%		49%		
Se	6 µg/l	nd.		nd.		nd.			nd.		nd.		nd.			nd.		nd.		nd.			nd.		nd.		nd.		
Sr	0.5 µg/l	4%		7%		18%	**		0%		-4%	**	-22%	**		-3%	*	11%	**	13%	**		1%		4%		3%	**	
Th	2 µg/l	nd.		nd.		nd.			nd.		5%	*	nd.			nd.		nd.		nd.			nd.		nd.		nd.		
Tl	2 µg/l	nd.		8%		nd.			-1%		0%		4%			1%		8%		-5%			0%		5%		0%		
U	4 µg/l	16%		6%		15%			-1%		-8%	**	-27%	**		6%		0%		1%			7%		-1%		-4%		
V	1 µg/l	nd.		nd.		28%	*		nd.		1%	*	10%	**		-2%		0%		15%	*		-1%		1%		18%	**	
Yb	0.03 µg/l	3%		-1%		25%	**		20%	**	25%	**	11%	**		-2%		-4%	*	1%			7%		7%		12%		
Zn	0.3 µg/l	4%		77%		-13%			72%	**	31%	**	-25%	**		-10%		-25%		-84%			22%		28%		-41%		

VII Detailed description of carbonate solid solution precipitation

1. Solubility products for carbonate solid solutions

In order to test whether a siderite-calcite solid solution could actually have precipitated, we have to calculate the solubility product and its dependence with temperature. Lipmann [137] derived a model based on equilibrium thermodynamics to describe solid solution solubility and introduced the term ΣΠ or 'total solubility product' [138, 139]:

$$\Sigma\Pi = ([B^+] + [C^+])[A^-]$$

At thermodynamic equilibrium, the equilibrium solubility product, $\Sigma\Pi_{eq}$, as a function of the solid phase fraction, X_{BA}, is given by Lippmann's solidus curve [138, 140]:

$$\Sigma\Pi_{eq,solidus} = a_{BA}K_{BA} + a_{CA}K_{CA} = K_{BA}\gamma_{BA}x + K_{CA}\gamma_{CA}(1-x)$$

Where γ_{BA} and γ_{CA} are the activity coefficients of solid-phase components BA and CA. This relation gives the solubility of a certain solid solution as a function of the fraction of the pure phases. If we want to know whether a solution is saturated with respect to a solid solution using aqueous concentrations, we have to use Lippmann's solutus curve which is given by [138, 139, 141]:

$$\Sigma\Pi_{eq,solutus} = \frac{1}{\frac{x_{B,aq}}{K_{BA}\gamma_{BA}} + \frac{x_{C,aq}}{K_{CA}\gamma_{CA}}}$$

where $x_{B,aq}$ and $x_{C,aq}$ are the aqueous fractions of the contributing cations in the solid-solution $B_xC_{1-x}A$. The activity coefficients for non-ideal solid solutions are calculated with the Guggenheim expansion series [142]:

$$Ln\gamma_{CA} = X_{BA}^2[a_0 - a_1(3X_{CA} - X_{BA}) + ...]$$
$$Ln\gamma_{BA} = X_{CA}^2[a_0 + a_1(3X_{CA} - X_{BA}) + ...]$$

These equations are derived from Guggenheim's expansion series for the excess Gibbs free energy of mixing:

$$G^E = X_{BA}X_{CA}RT(a_0 + a_1(X_{BA} - X_{CA})...)$$

In which R and T are the gas coefficient (8.31 J/mol K) and temperature (K), respectively, a_0 and a_1 are dimensionless fitting parameters (often referred to as the excess free energy (EFE) or Guggenheim parameters) which are derived from laboratory experiments. A highly positive or negative a_0 parameter causes the free energy curve to shift towards one of the solid phases. For many solid solutions, a_0 is sufficient to describe the system, a_1 becomes 0, and we speak of regular solid solutions following the solid-solution model of Hildebrand [143]. If a_1 is required, we speak of a sub-regular solid solution model as described by Thompson and Waldbaum [144]. Glynn [142] compiled a database with EFE parameters to describe carbonates, sulfates, and halides. A selection of calcite based solid solutions is shown in Table 3-4 showing that most carbonates form regular solid solutions (a_1=0).

Table VII-1 Guggenheim parameters for calcite solid solutions (selection from source: [142])

System (main cation & trace)	Fraction of trace, x	Guggenheim parameters (a_1=0)
$(Ca,Mn)CO_3$	Complete	a_0<2
$(Ca,Fe)CO_3$	18%	a_0=2.56
$(Ca,Fe)CO_3$	<=2.5%	a_0=4.18
$(Ca,Mg)CO_3$	2%	a_0=4.05
$Ca,Mg)CO_3$	3.2%	a_0=3.95
$Ca,Mg)CO_3$	4.5%	a_0=4.76
$(Mg,Ca)CO_3$	>10.1%	a_0=2.74
$(Fe,Mn)CO_3$	Complete	a_0<2
$(Fe,Ca)CO_3$	<22.7%	a_0=2.24

In order to visualize the relationship between the siderite-calcite solid solution series (SCSS) and aqueous chemistry, Figure VII-1 plots the solidus and solutus curves for the siderite-calcite solid solution series at 11°C and 60°C. Solubility products and thermodynamic data for calcite and siderite were based on the PHREEQC database [28] and the most recent data for siderite published by Benezeth *et al.* [33]. A Guggenheim a_0 of 2.3 was based on the date of Glynn [142] summarized in Table VII-1.
Included in the figure are the solubility products ($\Sigma\Pi$) for the influent at 11 °C and 60°C, and the effluent samples at 60°C. PHREEQC was used to calculate the $\Sigma\Pi$ (based on Ca^{2+}, Fe^{2+} and CO_3^{2+} activities). Comparing the plotted data with the solutus curve shows that at field temperature, the groundwater is subsaturated with respect to the complete SCSS. When increasing the temperature, the water becomes super saturated with respect to the solid solution series (with $x_{Fe,aqueous}$=16%). Super saturation is due to 1) the reduction of the saturation product (the solutus curve at 60°C is lower than at 11°C) and 2) the increasing $\Sigma\Pi$ due to increasing CO_3 activity with temperature (increasing from $10^{-6.40}$ to $10^{-6.13}$).
The effluent data plot well under the solutus curve and effluents is therefore sub saturated with respect to the SCSS. This implies that precipitation has proceeded beyond saturation with the SCSS which is unlikely. A possible explanation for this is the poor constraint on the a_0 value. Reducing a_0 to 0.3 would make the solutus skim the upper effluent samples, reducing it further to a_0=0 (implying that it would be an ideal solid solution) would make the solutus go through the effluent samples. Another explanation is that the solid solution has more contributing cations than Fe: Mg and Mn both contribute substantially based on the difference between in- and effluent. The vertical tie line between solutus and solidus shows that the solution is in thermodynamic equilibrium with a SCSS containing around 98% Fe and 2% Ca. This implies that precipitation of a SCSS is stochiometrically and not thermodynamically controlled: The fraction of Fe in the solid ($x_{Fe,solid}$ = 21.4%) is nearly identical to the Fe fraction in the solution ($x_{Fe,aqueous}$=16%), which is far less than the Fe fraction expected for a SCSS in thermodynamic equilibrium ($x_{Fe,solid}$=2%) with the aqueous Fe fraction. Also, the Fe fraction for the carbonate present in the aquifer in the XRD analyses (X_{Fe} in ankerite= 34%) is less then expected from the Lipmann curve. This result is consistent with the results from inorganic siderite synthesis at 25 and 70°C by Romanek *et* al. [145] who report that the percentage of CaCO3 in the solid is proportional to the aqueous Ca/Fe ratio of the solution.

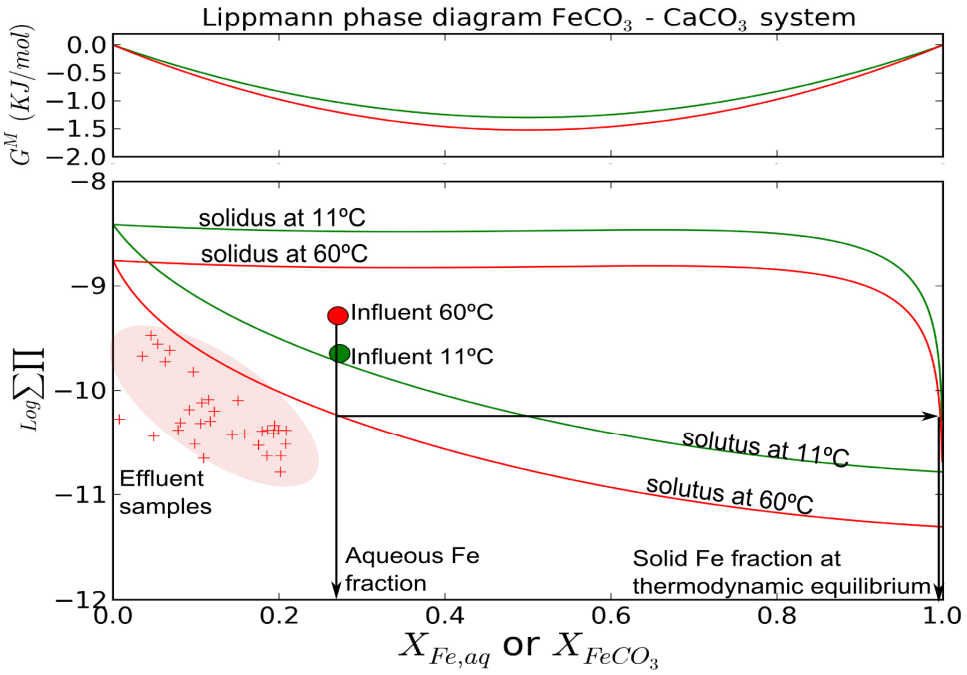

Figure VII-1 Lipmann Diagram for 11°C (green) and 60°C (red) with data from experiment B where precipitation was occurring.

3. Precipitation kinetics for carbonate solid solutions

A final question is whether the residence time in the column is sufficient for a SCSS to have precipitated. Pure siderite precipitation at groundwater temperatures <20°C is reported to be very slow [146]. Slower kinetics of siderite is also given as a reason for the frequently reported super saturation of natural groundwater with respect to siderite [146]. It is noted that the formation of impure siderites, or SCSS, can also cause groundwater to be super saturated with respect to pure siderite and undersaturated with respect to calcite. The kinetics of siderite precipitation is also a topic of interest in oil well construction [147] and water transmission pipes [148], because siderite scaling layer limits corrosion, and, more recently within carbon capture and storage (CCS) studies, because understanding of siderite kinetics contributes to a proper prediction of CO_2 sequestration in deep carbonate aquifers (e.g. [149]).

The kinetics of siderite precipitation as function of temperature have been investigated in more detail by Johnson [150]. Experimental results from this study show that siderite precipitation at temperate groundwater temperatures is extremely slow but increases rapidly with temperature. Experimental data for siderite precipitation experiments under varying temperature were fitted to the following second order growth function:

$$v_{siderite} = 315e^{-11130/T} \qquad (3\text{-}9)$$

where $v_{siderite}$ is the crystal growth rate of siderite (m/s) and T is the temperature (K). Johnson also compared the temperature dependence of both solubility and precipitation rate of siderite with that of calcite as described by a second order growth function by Kazmierczak ([151] in [150]):

$$v_{calcite} = 4.14x10^{-4}e^{-2802/T} \qquad (3\text{-}10)$$

where $v_{calcite}$ is the crystal growth rate of calcite (m/s). Figure VII-2 presents crystal growth velocities for siderite and calcite based on equations 3-9 and 3-10. At low groundwater temperatures (<20 °C, siderite crystal growth rate is 3 orders of magnitude slower than of calcite crystals, whereas at temperatures above 95°C siderite growth proceeds faster than that of calcite. The fast precipitation of siderite is fairly consistent with the findings of Griffioen and Appelo [11] who report the results of ATES column experiments at 90°C that precipitation of Ca-Fe carbonates occurs within 10 hours of residence time. After all Fe was consumed, no further carbonate mineral precipitation was observed even though the water remained strongly super saturated with respect to calcite. A number of possible inhibition mechanisms were described, of which inhibition by humic substances or phosphate was considered most likely [11].

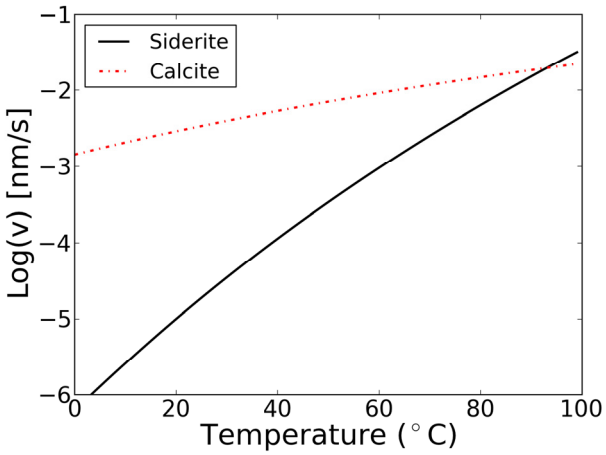

Figure VII-2 Comparison of calcite and siderite crystal growth velocity (v) as a function of temperature. Based on crystal growth equations for siderite in [150] and calcite in [151].

Postbus 1072 3430 BB Nieuwegein The Netherlands P +31 30 606 95 11 F +31 30 606 11 65 E info@kwrwater.nl